

**Pharmacological Investigation on a Herbal Formula
Potentially Used for the Treatment of Diabetes
Mellitus and Atherosclerosis**

CHAN, Yuet Wa

A Thesis Submitted in Partial Fulfillment of the Requirement for the
Degree of Doctoral of Philosophy
in
Chinese Medicine

May 2009

UMI Number: 3392270

All rights reserved

INFORMATION TO ALL USERS

The quality of this reproduction is dependent upon the quality of the copy submitted.

In the unlikely event that the author did not send a complete manuscript and there are missing pages, these will be noted. Also, if material had to be removed, a note will indicate the deletion.



UMI 3392270

Copyright 2010 by ProQuest LLC.

All rights reserved. This edition of the work is protected against unauthorized copying under Title 17, United States Code.



ProQuest LLC
789 East Eisenhower Parkway
P.O. Box 1346
Ann Arbor, MI 48106-1346

Thesis/Assessment Committee

Professor LEUNG WING NANG (Chair)

Professor FUNG KWOK PUI (Thesis Supervisor)

Professor CHE CHUN TAO (Thesis Supervisor)

Professor LIN ZHIXIU (Committee Member)

Professor KO KAM MING (External Examiner)

ABSTRACT

Diabetes Mellitus (DM) is a disorder of glucose metabolism characterized by abnormally high blood sugar level. Type 2 DM is the common form of diabetes which accounts for more than 90% of all DM cases. At the early stage of type 2 DM, the predominant abnormality is reduced insulin sensitivity. As the disease progresses, oxidative stress is found in most diabetic patients. Pancreatic β cell is the primary site of damage under free radical attack due to low antioxidant level in the β cells. When the impairment of insulin secretion worsens, therapeutic replacement of insulin often becomes necessary. In addition, DM chronically causes many complications, including cardiovascular disease, renal failure, retinopathy and foot ulcer, which are harmful to health.

Due to the important role of pancreatic β cells in the pathology of DM, agents that can protect β cell from damage may exert beneficial effects in treating DM and associated complications. Therefore, the aim of this study is to explore the potential of Traditional Chinese Medicines (TCMs) in treating DM and diabetic complications by revealing their protective effects on pancreatic β cell damage. From literature review, 28 TCMs frequently used in treating DM were selected for screening. Water extracts of three TCMs including Radix Astragali, Radix Codonopsis and Cortex Lycii were found to have promising effect on inhibiting β cell death induced by streptozotocin (STZ). After optimizing the ratio of these herbs, a herbal formula, namely SR10, was generated. The weight ratio of Radix Astragali, Radix Codonopsis and Cortex Lycii in SR10 is 3:3:1.

Using rat pancreatic β cell line RIN-m5F as a model, *in vitro* study demonstrated that SR10 significantly inhibited apoptosis induced by STZ as evidenced by inhibiting DNA fragmentation, decreasing externalization of phosphatidylserine (PS),

decreasing sub-G₁ cell cycle and altering expression level of apoptotic proteins. The beneficial effects SR10 in treating type 2 DM was confirmed in animal study. After orally administrated with SR10 for 4 weeks, plasma glucose level of diabetic *db/db* mice was significantly lower than that treated with water. Moreover, plasma insulin level in SR10-treated mice was found to be increased. The anti-oxidative activity of SR10 in scavenging ROS released during hyperglycemia in mice was examined. The results showed that the activities and expression of anti-oxidant enzymes, catalase and superoxide dismutase, were up-regulated when the mice were treated with SR10. The anti-atherosclerotic effect of SR10 was also investigated. Anti-oxidative activity of SR10 was firstly confirmed by its ability to decrease 2,2'-azo-bis-(2-amidinopropane) dihydrochloride-induced rat erythrocyte hemolysis and prolong copper ion-induced human low density lipoprotein oxidation. Vascular smooth muscle cell (VSMC) proliferation and migration are important processes in atherogenesis, the effect of SR10 in inhibiting these events was therefore examined using rat vascular smooth muscle cell line A7r5. The results showed that SR10 attenuated platelet-derived growth factor-induced VSMC proliferation by promoting cell cycle arrest at G₀/G₁ phase as well as inhibited PDGF-BB-induced VSMC migration. Inflammatory responses from macrophages have been demonstrated as a linkage between hyperglycemia and atherosclerosis. SR10 was shown to inhibit the release of various cytokines including interleukin-1 β , interleukin-6 and tumour necrosis factor- α as well as pro-inflammatory mediators nitric oxide and prostaglandin E₂ in culture supernatants. The inhibition of release of these inflammatory mediators was found to be due to inactivation of nuclear factor κ B through the inactivation of MAPK and Akt pathway. In conclusion, SR10 can be potentially used for treating DM and atherosclerosis.

摘要

糖尿病是一種關於葡萄糖新陳代謝的疾病，它的特性為血糖不正常地偏高，而糖尿病引致的醫療及經濟負擔急劇增加。多於九成的糖尿病患者患有常見的二型糖尿病，而這種病主要由於胰島素分泌減少及胰島素出現抵抗而引起的。於發病初期，胰島素敏感性的減少造成了血液裡胰島素份量的增加。在這段時期，我們還可以利用藥物或其他方法來改善胰島素的敏感性或減少肝臟製造葡萄糖，從而減少高血糖的出現。當病情逐漸惡化，大部份糖尿病病人都會有氧化應激，活性氧會從不同的生物化學途徑產生。由於 β 胰島細胞只有少量抗氧化物，當受到自由基的襲擊， β 胰島細胞將會首當其衝受到破壞。在這時候，胰島素的分泌會進一步減少，令病人需要直接注射胰島素。這樣解釋了為什麼很多糖尿病病人在長時間高血糖的情況下都需要依靠注射胰島素以控制病情。另一方面，糖尿病長期患者很多時候都會產生併發症如心血管病、腎衰竭、視網膜病變及足潰瘍。

由於 β 胰島細胞於糖尿病病變中有着重要的角色，任何能夠保護 β 胰島細胞的藥物也會對治療糖尿病及其併發症有重大的益處。所以，本研究的目的就是透過找出傳統中藥對保護 β 胰島細胞的能力，開發傳統中藥治療糖尿病及其併發症的潛能。從文獻分析中找出了二十八種常用作治療糖尿病的傳統中藥，經過生物檢定的篩選後，確定了黃芪、黨參及地骨皮有着減低由鏈尿菌素而引致的 β 胰島細胞的死亡。經過優化這三種中藥的比率後，製造了一個名為 SR10 的中藥方劑。在這方劑中，黃芪、黨參及地骨皮的重量比例為 3:3:1。

試管實驗確立了 SR10 能有效地抑制由鏈尿菌素引起的大鼠 β 胰島細胞 RIN-m5F 進行的細胞程式凋亡，而這效果是透過抑制脫氧核糖核酸的斷裂、

減少及磷脂醯絲氨酸的外露及減低 sub-G₁ 細胞生命週期而引致的。動物實驗進一步確認了 SR10 對治療糖尿病的有效性。糖尿病小鼠被餵食了四個星期的 SR10 後，血糖量明顯比餵食清水的一組為低，小鼠血液裡胰島素的含量也明顯提高，這顯示出小鼠 β 胰島細胞的功能有可能被改善了。SR10 的抗氧化能力對於能否清除在高血糖下產生的活性氧是非常重要的。研究結果顯示 SR10 能提高小鼠過氧化氫酶及超氧化物歧化酶的活性及表達。動脈粥樣硬化是引致糖尿病病人死亡的主要因素之一，所以一種藥物如能同時治療糖尿病及動脈粥樣硬化，將會有着重大好處。所以，我們也測試了 SR10 抑制動脈粥樣硬化的效果。在測試中，透過抑制偶氮二脒基丙烷鹽酸鹽(AAPH)誘導紅血球溶解及延長銅離子誘導低密度脂蛋白氧化的時間，SR10 的抗氧化能力進一步被確認了。血管平滑肌細胞的增生及遷移是動脈粥樣硬化的主要病變過程，我們利用大鼠血管平滑肌細胞 A7r5 來研究 SR10 能否抑制這些過程。結果顯示 SR10 具有這種細胞停留於 G₀/G₁ 細胞生命週期的能力，用以抑制血小板衍生生長因素激活之血管平滑肌細胞增生及遷移。巨噬細胞產生的炎症是連接高血糖與動脈粥樣硬化之間的因數，結果顯示 SR10 有效地抑制這些細胞釋放白細胞介素-1β、白細胞介素-6、腫瘤壞死因子、一氧化氮及前列腺素 E₂，而這些炎症介質的抑制是由於 MAPK 及 Akt 信號通路的失活而引致核因子 κB 的失活。

總括來說，SR10 是對治療糖尿病及動脈粥樣硬化有效的中藥方劑。

ACKNOWLEDGEMENTS

I would like to thank all my colleagues who help me a lot during my study in the past four years. Special thanks to Emma Lam, Johnny Koon, Linda Zhang, Virginia Lau, Frankie Choy, Ho Po Ming, David Lau and Julia Lee. They have provided me countless and valuable suggestions and technical advice. Definitely, I would like to deeply thank my supervisors, Prof. K.P. Fung and Prof. C.T. Che for giving me encouragement, guidance and patience during my study. Last but not least, I would like to thank my parents and family for unlimited support on my study. Thank my parents for giving me wisdom, happiness and health in my life.

PUBLICATION

Chan JY, Leung PC, Che CT, Fung KP. (2008) Protective effects of an herbal formulation of Radix Astragali, Radix Codonopsis and Cortex Lycii on streptozotocin-induced apoptosis in pancreatic β -cells: An implication for its treatment of diabetes mellitus. *Phytotherapy research*. **22**, 190-196.

Chan JY, Lam FC, Leung PC, Che CT, Fung KP. Anti-hyperglycemic and anti-oxidative effects of an herbal formulation of Radix Astragali, Radix Codonopsis and Cortex Lycii in a mouse model of type 2 diabetes mellitus. *Phytotherapy Research*. (in press).

Conference paper:

Chan JY, Che CT, Fung KP. (2008) Protective effects of a herbal formula comprising of Radix Astragali, Radix Codonopsis and Cortex Lycii in Type 2 diabetes by *in vitro* and *in vivo* models. Abstract in *Seventh Meeting of Consortium for Globalization of Chinese Medicine (CGCM)*, Aug. 28-30, Taipei (Student Poster Award was received).

Manuscript:

Chan JY, Koon JC, Leung PC, Che CT, Fung KP. Suppression of low-density lipoprotein oxidation, vascular smooth muscle cell proliferation and migration by a herbal formulation of *Radix Astragali*, *Radix Codonopsis* and *Cortex Lycii*.

LIST OF ABBREVIATIONS

AAPH	2,2'-azo-bis-(2-amidinopropane) dihydrochloride
ALT	Alanine transaminase
AST	Aspartate transaminase
CAT	Catalase
CDK	Cyclin-dependent kinase
CVD	Cardiovascular disease
CK	Creatine kinase
COX-2	Cyclo-oxygenase-2
C _T	Threshold cycle
DM	Diabetes Mellitus
ELISA	Enzyme-linked immunosorbant assay
ERK	Extracellular regulated kinase
FBS	Fetal bovine serum
GAPDH	Glyceraldehyde 3-phosphate dehydrogenase
GLUT	Glucose transporter
GPx	Glutathione peroxidase
GSH	Glutathione
HDL	High density lipoprotein
H ₂ O ₂	Hydrogen peroxide
HPLC	High performance liquid chromatography
IC ₅₀	50% inhibitory concentration
IDDM	Insulin-dependent diabetes mellitus
I κ B	Inhibitor of κ B
IL	Interleukin

iNOS	Inducible nitric oxide synthase
IRS	Insulin receptor substrate
LDH	Lactate dehydrogenase
LDL	Low density lipoprotein
LPS	Lipopolysaccharide
MDA	Malondialdehyde
MTT	(3-(4,5-Dimethylthiazol-2-yl)-2,5-diphenyltetrazolium bromide
NFκB	Nuclear factor kappa B
NIDDM	Non-insulin-dependent diabetes mellitus
NO	Nitric oxide
OGTT	Oral glucose tolerance test
ox-LDL	Oxidized low density lipoprotein
PBS	Phosphate buffer saline
PDGF	Platelet-derived growth factor
PDX	Pancreatic and duodenal homeobox
PI	Propidium iodide
PI-3-K	Phosphoinositol-3-kinase
PKC	Protein kinase C
PON	Paraoxonase
PPAR	Peroxisome proliferators-activated receptor
PS	Phosphatidylserine
RBC	Red blood cell
ROS	Reactive oxygen species
S.D.	Standard deviation
SOD	Superoxide dismutase

STZ	Streptozotocin
TC	Total cholesterol
TCM	Traditional Chinese Medicine
TG	Triglyceride
TLC	Thin layer chromatography
TNF	Tumor necrosis factor
TZD	Thiazolidinedione
VEGF	Vascular endothelial growth factor
VSMC	Vascular smooth muscle cell
WHO	World Health Organization

Units

h	hour
min	minute
s	second
kg	kilogram
g	gram
mg	milligram
µg	microgram
ng	nanogram
L	liter
dL	deciliter
mL	milliliter
µL	microliter
M	molar

mM	millimolar
μ M	micromolar
nM	nanomolar
cm	centimeter
mm	millimeter
nm	nanometer
$^{\circ}$ C	degree Celsius

LIST OF TABLES

Table 1-1	Antioxidant enzyme activities in islets and other tissues of rat
Table 1-2	Pharmacological treatments of hyperglycemia in type 2 DM according to the sites of action
Table 1-3	Thirty-three TCMs commonly used in anti-diabetic compound recipes
Table 1-4	Chemical constituents isolated from TCMs showing hypoglycemic activities
Table 3-1	List of 28 TCMs and their voucher specimen numbers
Table 4-1	Percentage yield of aqueous extracts of 28 TCMs
Table 4-2	Percentage viability of RIN-m5F cells after treatment with STZ (5 mM) in the presence or absence of various concentrations of 28 TCM extracts for 24 hours
Table 4-3	Summary of retention time and percentage of peak area detected by HPLC in two batches of SR10 extracts
Table 6-1	Effects of SR10 treatment on plasma insulin level of <i>db/db</i> mice
Table 6-2	Effects of SR10 treatment on mRNA expression of catalase, superoxide dismutase (SOD) and glutathione peroxidase (GPx) in the islets of <i>db/db</i> mice
Table 8-1	Fold of change in release of IL-1, IL-6 and TNF after treatment with LPS and SR10
Table 9-1	Commonly used herbal formulae for treating diabetes in China

LIST OF FIGURES

- Figure 1-1** A world map showing the prevalence of DM in 2000 and expected prevalence in 2030
- Figure 1-2** Mechanism of action of glucotoxicity in β cells.
- Figure 1-3** Six biochemical pathways along which glucose metabolism can form ROS
- Figure 2-1** Determination of Lag time from a typical profile of Cu^{2+} ions-induced LDL oxidation
- Figure 2-2** A diagram showing the transwell system employed for cell migration assay
- Figure 3-1** Morphology of 28 TCMs
- Figure 3-2** Thin Layer Chromatogram of Cortex Acanthopanax
- Figure 3-3** Thin Layer Chromatogram of Cortex Lycii
- Figure 3-4** Thin Layer Chromatogram of Cortex Phellodendri
- Figure 3-5** Thin Layer Chromatogram of Fructus Corni
- Figure 3-6** Thin Layer Chromatogram of Fructus Ligustri lucidi
- Figure 3-7** Thin Layer Chromatogram of Fructus Lycii
- Figure 3-8** Thin Layer Chromatogram of Fructus Schisandrae chinensis
- Figure 3-9** Thin Layer Chromatogram of Herba Gynostemmae
- Figure 3-10** Thin Layer Chromatogram of Poria.
- Figure 3-11** Thin Layer Chromatogram of Radix Astragali
- Figure 3-12** Thin Layer Chromatogram of Radix Codonopsis
- Figure 3-13** Thin Layer Chromatogram of Radix Notoginseng
- Figure 3-14** Thin Layer Chromatogram of Radix Ophiopogonis
- Figure 3-15** Thin Layer Chromatogram of Radix Panacis quinquefolii

- Figure 3-16** Thin Layer Chromatogram of Radix Platycodonis
- Figure 3-17** Thin Layer Chromatogram of Radix Puerariae
- Figure 3-18** Thin Layer Chromatogram of Radix Rehmanniae
- Figure 3-19** Thin Layer Chromatogram of Radix et Rhizoma Rhei
- Figure 3-20** Thin Layer Chromatogram of Radix Salviae miltiorrhizae
- Figure 3-21** Thin Layer Chromatogram of Radix Trichosanthis
- Figure 3-22** Thin Layer Chromatogram of Rhizoma Alismatis
- Figure 3-23** Thin Layer Chromatogram of Rhizoma Anemarrhenae
- Figure 3-24** Thin Layer Chromatogram of Rhizoma Atractylodis
- Figure 3-25** Thin Layer Chromatogram of Rhizoma Coptidis
- Figure 3-26** Thin Layer Chromatogram of Rhizoma Polygonati
- Figure 3-27** Thin Layer Chromatogram of Rhizoma Polygonati Odorati
- Figure 3-28** Thin Layer Chromatogram of Rhizoma et Radix Polygoni Cuspidati
- Figure 3-29** Thin Layer Chromatogram of Semen Coicis
- Figure 4-1** Effect of SR herbal extract on viability of RIN-m5F cells
- Figure 4-2** Effects of SR10, SR20 and SR30 on viability of RIN-m5F cells
- Figure 4-3** HPLC profiles for two batches of SR10 herbal extracts
- Figure 5-1** Effect of SR10 on DNA fragmentation of RIN-m5F cells induced by STZ
- Figure 5-2** Effect of SR10 on cell cycle distribution of STZ-treated RIN-m5F cells
- Figure 5-3** Effect of SR10 on PS externalization of STZ-treated RIN-m5F cells detected by Annexin V-FITC and propidium iodide (PI)
- Figure 5-4** Western blot analysis of expression levels of apoptosis-related proteins on SR10-treated RIN-m5F cells

- Figure 5-5** Effect of SR10 on nitric oxide production and iNOS expression on SR10-treated RIN-m5F cells
- Figure 5-6** Effect of SR10 on insulin secretion in RIN-m5F cells
- Figure 6-1** Effect of SR10 herbal extract on viability of RIN-m5F cells in medium with high glucose concentration
- Figure 6-2** Effects of SR10 on body weight of *db/db* mice
- Figure 6-3** Effects of SR10 on fasting blood glucose level of *db/db* mice
- Figure 6-4** Effects of SR10 treatment on oral glucose tolerance test in *db/db* mice
- Figure 6-5** Effects of SR10 treatment on anti-oxidant activities in liver tissue extracts and plasma of *db/db* mice
- Figure 6-6** Effects of SR10 treatment on plasma enzyme activities in *db/db* mice
- Figure 7-1** Effect of SR10 on AAPH-induced hemolysis in rat erythrocytes
- Figure 7-2** Effect of SR10 on prolongation of copper ion-induced human LDL oxidation
- Figure 7-3** Effect of SR10 on PDGF-BB-stimulated proliferation of rat VSMCs
- Figure 7-4** Effect of SR10 on PDGF-BB-induced ³H-thymidine incorporation in A7r5 cells
- Figure 7-5** Effect of SR10 on cell cycle distribution of PDGF-BB-treated A7r5 cells
- Figure 7-6** Effect of SR10 on expression of cyclin D1 of PDGF-BB-treated A7r5 cells
- Figure 7-7** Effect of SR10 on PDGF-BB-induced migration of A7r5 cells in a transwell migration assay

- Figure 7-8** Effect of SR10 on plasma concentrations of total cholesterol, triglyceride, HDL-cholesterol, calculated LDL-cholesterol and PON activity in *db/db* mice
- Figure 8-1** Effects of SR10 on nitric oxide release and expression of inducible nitric oxide synthase in mouse macrophages
- Figure 8-2** Effect of SR10 on mRNA expression of IL-1 β , IL-6 and TNF- α in mouse macrophages
- Figure 8-3** Effects of SR10 on PGE₂ release and expression of COX-2 in mouse macrophages
- Figure 8-4** Effects of SR10 on protein expression levels of total and phosphorylated form of ERK, p38 and JNK in mouse macrophages
- Figure 8-5** Effects of SR10 on protein expression levels of total and phosphorylated form of Akt and I κ B- α in mouse macrophages
- Figure 8-6** Effects of SR10 on NF κ B content in nuclear fraction of mouse macrophages
- Figure 9-1** Proposed model for accelerated hyperglycemia when pancreatic β cells were damaged by oxidative stress
- Figure 9-2** Proposed model for the role of antioxidant supplementation in prevention of oxidative stress and vascular disease in diabetes

TABLE OF CONTENTS

ABSTRACT	i
摘要	iii
ACKNOWLEDGEMENT	v
PUBLICATIONS	vi
LIST OF ABBREVIATIONS	vii
LIST OF TABLES	xi
LIST OF FIGURES	xii
TABLE OF CONTENTS	1
CHAPTER 1	6
INTRODUCTION	6
1.1 Definition, classification and epidemiology of Diabetes Mellitus	6
1.1.1 Definition of Diabetes Mellitus.....	6
1.1.2 Classification of Diabetes Mellitus.....	7
1.1.3 Prevalence of Diabetes Mellitus.....	8
1.2 Etiology of Diabetes Mellitus	9
1.2.1 Pancreatic β cell dysfunction	9
1.2.2 Insulin resistance	12
1.3 Diabetic complications	14
1.3.1 Retinopathy	14
1.3.2 Neuropathy	14
1.3.3 Nephropathy	15
1.3.4 Cardiovascular disease.....	15
1.4 Oxidative stress in diabetes and cardiovascular disease	16
1.5 Conventional therapy of type 2 Diabetes Mellitus	19
1.5.1 Insulin sensitizers	20
1.5.2 α -glucosidase inhibitors	20
1.5.3 Secretagogues	21
1.5.4 Exogenous insulin	21
1.6 Traditional Chinese Medicine for Diabetes Mellitus	22
1.7 Project objectives	24
CHAPTER 2	27
MATERIALS AND METHODS	27
2.1 Materials	27
2.1.1 Cell lines	27
2.1.2 Culture media	28

2.1.3	Trypsin-EDTA.....	28
2.1.4	Buffers for biochemical assays	28
2.1.5	Animals.....	30
2.2	Methods	30
2.2.1	Cell proliferation assay (MTT assay)	30
2.2.2	Determination of insulin secretion	31
2.2.3	Determination of insulin in plasma and supernatant	31
2.2.4	Detection of DNA fragmentation	32
2.2.5	Cell cycle analysis by PI staining.....	32
2.2.6	Detection of Phosphatidylserine externalization with Annexin V-FITC and PI	33
2.2.7	Determination of nitric oxide release	33
2.2.8	Western blot analysis.....	33
2.2.9	Detection of mRNA expression level by Reverse Transcription- Polymerase Chain Reaction (RT-PCR).....	35
2.2.10	Basal glycemia test	36
2.2.11	Oral glucose tolerance test (OGTT)	37
2.2.12	Preparation of plasma samples from mice	37
2.2.13	Preparation of liver extract from mice.....	38
2.2.14	Isolation of mouse islets.....	38
2.2.15	Determination of glucose concentration in plasma	38
2.2.16	Determination of total cholesterol concentration in plasma	39
2.2.17	Determination of HDL-C concentration in plasma	39
2.2.18	Determination of triglyceride concentration in plasma	39
2.2.19	Determination of PON activity in plasma.....	39
2.2.20	Determination of Catalase activity in plasma and liver extracts.....	40
2.2.21	Determination of SOD activity in plasma and liver extracts	40
2.2.22	Determination of GSH level in liver extract	41
2.2.23	Determination of MDA in liver extracts.....	41
2.2.24	Measurement of 2,2'-azo-bis-(2-amidinopropane) dihydrochloride (AAPH)-induced RBC hemolysis.....	42
2.2.25	Measurement of LDL peroxidation	43
2.2.26	Measurement of DNA incorporation assay (³ H-thymidine uptake assay)	43
2.2.27	Cell migration assay	44
2.2.28	Measurement of cytokine release by ELISA	45
2.2.29	Extraction of proteins from different subcellular fractions.....	46
CHAPTER 3		47
AUTHENTICATION OF HERBAL MATERIALS		47
3.1 Materials.....		47
3.2 Authentication		54
3.2.1	Cortex Acanthopanax (五加皮).....	54
3.2.2	Cortex Lycii (地骨皮)	55
3.2.3	Cortex Phellodendri (黄柏).....	56
3.2.4	Fructus Corni (山茱萸).....	58
3.2.5	Fructus Ligustri lucidi (女贞子).....	59
3.2.6	Fructus Lycii (枸杞子)	61
3.2.7	Fructus Schisandrae chinensis (五味子).....	62

3.2.8	Herba Gynostemmae (絞股藍).....	63
3.2.9	Poria (茯苓).....	65
3.2.10	Radix Astragali (黃芪).....	66
3.2.11	Radix Codonopsis (黨參).....	68
3.2.12	Radix Notoginseng (三七).....	70
3.2.13	Radix Ophiopogonis (麥冬).....	71
3.2.14	Radix Panacis quinquefolii (西洋參).....	73
3.2.15	Radix Platycodonis (桔梗).....	75
3.2.16	Radix Puerariae (葛根).....	77
3.2.17	Radix Rehmanniae (地黃).....	78
3.2.18	Radix et Rhizoma Rhei (大黃).....	80
3.2.19	Radix Salviae miltiorrhizae (丹參).....	81
3.2.20	Radix Trichosanthis (天花粉).....	82
3.2.21	Rhizoma Alismatis (澤瀉).....	84
3.2.22	Rhizoma Anemarrhenae (知母).....	85
3.2.23	Rhizoma Atractylodis (蒼朮).....	86
3.2.24	Rhizoma Coptidis (黃蓮).....	88
3.2.25	Rhizoma Polygonati (黃精).....	89
3.2.26	Rhizoma Polygonati odorati (玉竹).....	91
3.2.27	Rhizoma et Radix Polygoni Cuspidati (虎杖).....	92
3.2.28	Semen Coicis (薏苡仁).....	94
CHAPTER 4.....		96
SCREENING OF 28 TCMS AND GENERATION OF HERBAL FORMULA.....		96
4.1	Preparation of aqueous extracts of 28 TCMS.....	96
4.2	Screening of 28 herbal extracts on protection of streptozotocin-induced cytotoxicity on RIN-m5F cells.....	97
4.2.1	Screening assay.....	97
4.2.2	Results.....	97
4.3	Generation of a herbal formula SR10.....	99
4.3.1	Selection and combination of effective herbs.....	99
4.3.2	Ratio optimization of 3 effective herbs.....	101
4.4	Batch to batch variations of SR10.....	104
4.4.1	HPLC conditions.....	104
4.4.2	HPLC chromatograms.....	105
CHAPTER 5.....		109
INHIBITORY EFFECTS OF SR10 ON STREPTOZOTOCIN-INDUCED APOPTOSIS ON PANCREATIC β CELLS.....		109
5.1	Introduction.....	109
5.2	Results.....	110
5.2.1	Inhibition of STZ-induced apoptosis on RIN-m5F cells.....	110
5.2.2	Inhibition of nitric oxide production and nitric oxide synthase activity.....	118
5.2.3	Up-regulation of insulin secretion.....	121

5.3	Discussion	123
CHAPTER 6.....		127
ANTI-HYPERGLYCEMIC AND ANTI-OXIDATIVE EFFECTS OF SR10 IN A MOUSE MODEL OF TYPE 2 DM.....		127
6.1	Introduction.....	127
6.2	Experimental results	129
6.2.1	Protective effect of SR10 on hyperglycemia-induced toxicity in rat pancreatic β cells.....	129
6.2.2	Body weights of non-diabetic mice and diabetic mice treated with water or SR10	131
6.2.3	Anti-hyperglycemic effect of SR10 in diabetic mice	133
6.2.4	Increase in insulin release in diabetic mice after SR10 treatment....	135
6.2.5	No significant improvement in glucose tolerance by SR10 treatment	137
6.2.6	Increase of antioxidant enzyme activities in liver extracts and plasma by SR10 treatment.....	139
6.2.7	Increase of antioxidant enzyme expression in islets of <i>db/db</i> mice by SR10	144
6.2.8	Activities of liver, heart and kidney specific enzymes in plasma of <i>db/db</i> mice treated with SR10	146
6.3	Discussion	148
CHAPTER 7.....		151
SUPPRESSION OF LOW DENSITY LIPOPROTEIN OXIDATION, VASCULAR SMOOTH MUSCLE CELL (VSMC) PROLIFERATION AND MIGRATION BY SR10		151
7.1	Introduction.....	151
7.2	Experimental results	153
7.2.1	Inhibition of AAPH-induced RBC hemolysis.....	153
7.2.2	Prolongation of human LDL oxidation.....	155
7.2.3	Inhibition of rat vascular smooth muscle cell (VSMC) proliferation..... ..	157
7.2.4	Cell cycle arrest at G_0/G_1 and inhibition of expression of cyclin D1	160
7.2.5	Suppression of rat VSMC migration	163
7.2.6	Plasma concentrations of total cholesterol, HDL-cholesterol (HDL-C), triglyceride, calculated LDL-cholesterol (LDL-C) and paraoxonase (PON) activity in <i>db/db</i> mice.....	165
7.3	Discussion	170
CHAPTER 8.....		174
INHIBITION OF LIPOPOLYSACCHARIDE-INDUCED INFLAMMATORY RESPONSES OF MACROPHAGES BY SR10		174
8.1	Introduction.....	174
8.2	Experimental results	176
8.2.1	Inhibition of nitric oxide release and nitric oxide synthase expression in macrophages	176

8.2.2	Suppression of release and expression of IL-1, IL-6 and TNF- α	179
8.2.3	Decreased release of PGE ₂ and expression of COX-2 in macrophages	182
8.2.4	Effect of SR10 mediated by MAPK pathway in macrophages.....	184
8.2.5	Effect of SR10 mediated by Akt pathway in macrophages	186
8.2.6	Activation of NF κ B translocation to nucleus in macrophages.....	188
8.3	Discussion	190
CHAPTER 9		194
GENERAL DISCUSSION		194
9.1	Diabetes in Hong Kong	194
9.2	Insulin dependent therapy: a nightmare for type 2 diabetic patients	195
9.3	Antioxidant intervention in animal and human studies	199
9.4	Inflammation: A linkage between DM and atherosclerosis	202
9.5	Treatment of DM by Western medicine and Chinese medicine	205
9.6	Future development of SR10	213
9.7	Conclusions	214
REFERENCES		217

CHAPTER 1

INTRODUCTION

1.1 Definition, classification and epidemiology of Diabetes Mellitus

1.1.1 Definition of Diabetes Mellitus

Diabetes Mellitus (DM), also commonly called diabetes, is a condition of abnormal glucose homeostasis. In 1999, The World Health Organization (WHO) defined DM as a metabolic disorder of multiple etiology characterized by chronic hyperglycemia with disturbances of carbohydrate, fat and protein metabolism resulting from defects in insulin secretion, insulin action, or both (World Health Organization, 1999). The symptoms of DM include increased urination, extreme thirst and unexplained weight loss. Diagnosis of DM is done by measuring fasting plasma glucose level and 2-h post glucose load plasma glucose level. According to WHO, individuals with fasting plasma glucose levels lower than 6.1 mM are considered as normal, while those with 7.0 mM or above are considered as DM. Impaired fasting glucose is referred to fasting plasma glucose level between 6.1 mM and 7.0 mM. Oral glucose tolerance test (OGTT) is performed after overnight fasting of 8 to 14 hours. Glucose solution (75 g in 250 mL to 300 mL water) is orally administered to the testing subject. Then, plasma glucose concentration is determined after 2 h, with value lower than 7.8 mM indicating normal whereas over 11.1 mM indicating diabetic condition. In impaired glucose tolerance, the level is between 7.8 mM and 11.1 mM (World Health Organization, 1999).

1.1.2 Classification of Diabetes Mellitus

DM is formerly classified into insulin-dependent diabetes mellitus (IDDM) and non-insulin-dependent diabetes mellitus (NIDDM). In 1999, WHO re-classified DM into four types depending on their pathogenesis:

Type 1 Diabetes Mellitus

Type 1 DM represents a genetic disorder which accounts for 5-10% of all DM cases. Type 1 DM can be divided into autoimmune/immune-mediated diabetes (Type 1A) and idiopathic diabetes with β cell obstruction (Type 1B). People with type 1 DM must be treated with exogenous insulin to prevent the life threatening ketoacidosis (Koda-Kimble *et al.*, 2001).

Type 2 Diabetes Mellitus

Type 2 DM accounts for over 90% of DM cases. It results from a combination of defects in insulin secretion and insulin response. Patients with type 2 DM are not insulin-dependent in terms of treatment but insulin may be required to control the blood glucose level if this is not achieved by diet or by oral hypoglycemic agents. Chronic hyperglycemia causes microvascular pathology in the retina, renal glomerulus and peripheral nerve which further leads to blindness, end-stage renal disease and neuropathy (World Health Organization, 1999).

Gestational diabetes

Just like type 2 DM, gestational diabetes involved both inadequate insulin and unresponsiveness. About 2-5% of pregnant women develop diabetes but may disappear after delivery. Although the effect is transient, untreated gestational

diabetes can produce damage to the fetus. These include macrosomia, congenital cardiac and central nervous system anomalies, skeletal muscle malformations, and the infant may develop into hypoglycemia (Buchanan *et al.*, 1998).

Other specific types

Other causes of diabetes that do not fit into type 1, type 2, or gestational diabetes. These include genetic defects in β cell function and insulin action, excessive secretion of insulin-antagonistic hormones, chemical-induced impairment of insulin secretion and toxin-induced damage of β cells. This category comprises only 1-2% of DM cases (Harris, 2004).

1.1.3 Prevalence of Diabetes Mellitus

DM has reached epidemic proportions and affects more than 170 millions people worldwide. It is estimated that by the year 2030, this number will almost double. Prevalence in developed and developing countries was 6.2% and 3.5%, respectively, in year 2000 (World Health Organization, 2003). The greatest increase in prevalence is, however, expected to occur in developing countries in Asia and Africa when the people in these countries adapt a more Western-style diet (Figure 1-1). In Hong Kong, according to statistics released by Department of Health in 2007, DM ranks ninth in causes of death in Hong Kong (Hong Kong SAR Government, 2008). The increase in prevalence of DM definitely leads to great economic and medical burden in the future.

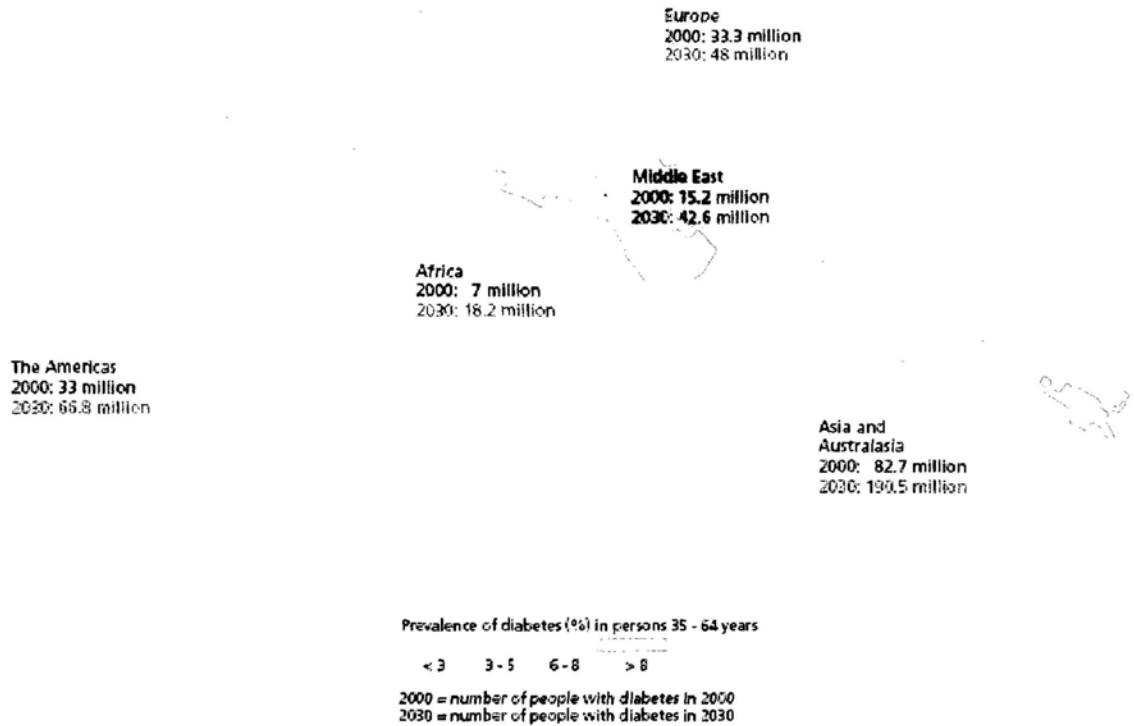


Figure 1-1 A world map showing the prevalence of DM in 2000 and expected prevalence in 2030 (adapted from Wild et al., 2004)

1.2 Etiology of Diabetes Mellitus

DM is a heterogeneous group of disorder. Normoglycemia is maintained by the balanced interplay between insulin action and insulin secretion. Thus, β cell dysfunction and insulin resistance are main causes in the pathophysiology of DM.

1.2.1 Pancreatic β cell dysfunction

For functional pancreatic β cells, glucose is taken up via glucose transporter 2 (GLUT2). Glucose is then phosphorylated by glucokinase and further degraded to

pyruvate and finally leads to the formation of ATP. Through the intermediacy of cell membrane depolarization, ATP delivers the energy needed for release of insulin (Chang *et al.*, 2004). However, in many cases of type 2 DM, insulin secretion is found to be markedly diminished compared with non-diabetic individuals. Glucotoxicity is one of the causes leading to the deterioration of insulin secretion. Chronic hyperglycemia in type 2 DM has been demonstrated to cause the production of reactive oxygen species (ROS). The increased oxidative stress can cause cell death because of low level of antioxidant enzymes in β cells (Robertson *et al.*, 2006) (Figure 1-2). Detailed mechanisms of β cell glucotoxicity will be described in Section 1.4. In addition to glucose, fatty acids can also enhance insulin secretion. However, in hyperglycemia, fatty acid oxidation in β cells is inhibited. The resultant accumulation of long-chain acyl coenzyme A can diminish the insulin secretory process by opening the potassium channels, and reducing ATP formation or inducing generation of nitric oxide in the β cells (Kaneto *et al.*, 2004; Kaneto *et al.*, 2005). Islet amyloid is another factor affecting the function of β cells. Small aggregates of islet amyloid polypeptide (also called amylin) are found in most of type 2 diabetic patients. Amyloid deposits are cytotoxic. Their roles of inhibition of insulin action, inhibition of insulin secretion and inhibition of glucagon secretion have been proposed (Lupi *et al.*, 2008; Höppener *et al.*, 2006).

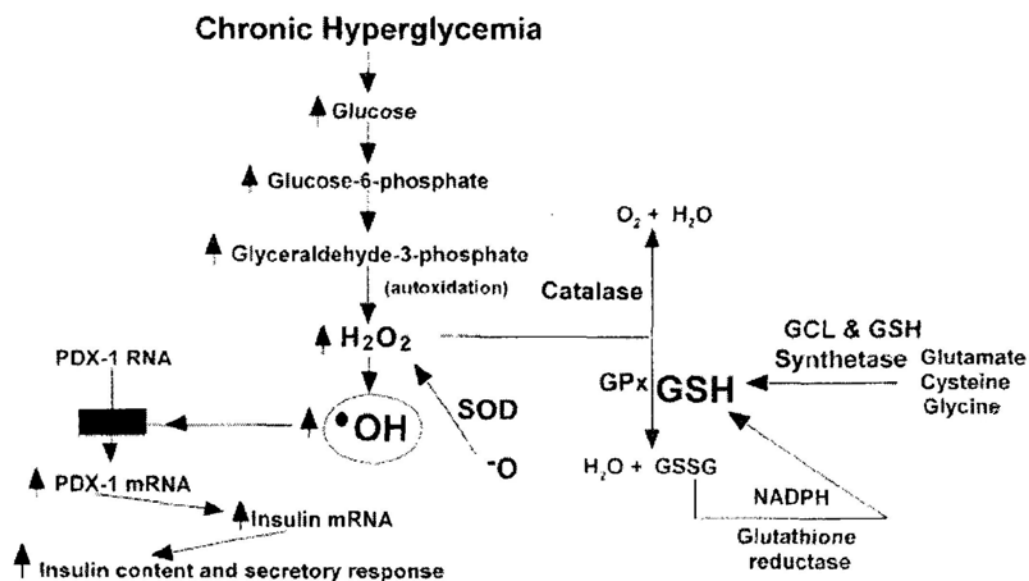


Figure 1-2 Mechanism of action of glucotoxicity in β cells. Hyperglycemia presents excessive high concentrations of glucose to islet glycolytic enzymes that glucose is shunted to alternative pathway, with subsequent formation of superoxide, H₂O₂ and eventually hydroxyl radicals. Hydroxyl radicals interfere with normal processing of PDX-1 mRNA, a necessary transcription factor for insulin gene expression and glucose-induced insulin secretion. Two major defense mechanisms against H₂O₂ formation are catalase, which metabolizes H₂O₂ into water and oxygen, and GPx, which depends on islet GSH to convert H₂O₂ into water and GSSG (adapted from Robertson *et al.*, 2003).

1.2.2 Insulin resistance

Insulin elicits its responses by binding to insulin receptor and activating tyrosine kinase activity. Insulin receptor substrate (IRS) proteins are then tyrosine phosphorylated on several sites which open the multiple pathways of insulin action. Different IRS proteins appear to channel signal transduction into different pathways. However, the phosphoinositol-3-kinase (PI-3-K) pathway, which signals through protein kinase B, is particularly important for metabolic effect of insulin. It participates in glucose transport, glycolysis, lipogenesis and protein synthesis (Carvalho *et al.*, 2003; Musi *et al.*, 2006). Insulin resistance is a condition of reduced ability of insulin to lower plasma glucose level by suppressing hepatic glucose production and stimulating glucose uptake in skeletal muscle and adipose tissue. Insulin resistance is strongly associated with obesity (Guilherme *et al.*, 2008). Increased mass of stored triglyceride leads to large adipocytes that are resistant to insulin response to suppress lipolysis. This results in increased circulating free fatty acid and glycerol, both of which aggravate insulin resistance in skeletal muscle and liver (Petersen *et al.*, 2002; Kraegen *et al.*, 2008; Risérus, 2008). Different cellular mechanisms of insulin resistance have been elucidated:

(i) Adipokines, which are produced and secreted by adipocytes, profoundly influence insulin responses (Dyck *et al.*, 2006). One example is tumor necrosis factor α (TNF- α). TNF- α was found to increase in the fat of obese rodents and human, and produce serine phosphorylation of IRS-1, resulting in reduced insulin receptor kinase activity and insulin resistance (Liang *et al.*, 2008; Murata *et al.*, 2007; Le Marchand-Brustel *et al.*, 2003). Another example is leptin which is produced by adipocyte to inhibit food intake and promote energy expenditure (Meister, 2000). In *ob/ob* or *db/db* mice, insulin resistance is characterized by leptin deficiency and

administration of exogenous leptin has been shown to improve glucose tolerance and insulin sensitivity (Luo *et al.*, 2006).

(ii) Adiponectin (also called Acrp 30 or adipo Q) is secreted by adipocytes and its mRNA expression is decreased in obese human (Swarbrick *et al.*, 2008). Adiponectin signals via AMP kinase, which is implicated in suppression of hepatic gluconeogenesis, glucose uptake in skeletal muscle, fatty acid oxidation and inhibition of lipolysis. Acute treatment of mice with adiponectin decreased insulin resistance, plasma free fatty acids and triglyceride content in muscle, suggesting its role in anti-diabetic response (Vu *et al.*, 2007; Kadowaki *et al.*, 2005).

(iii) Effects on insulin response exerted by tyrosine phosphorylation of insulin receptor and the IRS proteins are opposed by dephosphorylation of these tyrosine side-chains (Gual *et al.*, 2005; Zick, 2005). Phosphotyrosine phosphatase 1B is important in negative regulation of insulin signaling. IRS serine kinases such as c-Jun NH2-terminal kinase and phosphatidylinositol 3'-kinase was shown to reduce the ability of IRS to act as a substrate for tyrosine kinase activity and hence inhibit downstream effector systems (Asano *et al.*, 2007; Tanti *et al.*, 2004).

(iv) Nuclear factor kappa B (NF κ B)-mediated inflammatory signaling pathway is involved in insulin resistance. Phosphorylation of I κ B by its kinase (IKK) leads to I κ B degradation and hence release of NF κ B to the nucleus to affect diverse genes of inflammatory response. Blockage of IKK activity has been shown to ameliorate hyperglycemia and insulin resistance in diabetes. Moreover, genetic disruption of IKK- β returned skeletal muscle insulin resistance to normal (Tilg *et al.*, 2008; Hotamisligil *et al.*, 2005).

1.3 Diabetic complications

Diabetic complications are divided clinically into acute complications and chronic complications. For acute complications, non-ketotic hyperosmolar state is commonly occurred in type 2 diabetic patients. Most prominent features include polyuria, orthostatic hypotension, altered mental state, lethargy, obtundation, seizure and coma (Moore, 2004; Grimaud *et al.*, 2001). Chronic diabetic complications can be divided into vascular and non-vascular complications. Non-vascular complications include gastroparesis, sexual dysfunction and skin changes. Vascular complications, which produce more prominent influence to diabetic patients, include retinopathy, neuropathy, nephropathy and cardiovascular diseases.

1.3.1 Retinopathy

Diabetic retinopathy occurs commonly in elderly diabetic patients. It is classified into two stages. The non-proliferative stage is marked by increased retinal vascular permeability, alternations in regional blood flow and abnormal retinal microvasculature, all of which lead to retinal ischemia. In proliferative stage, the newly formed vessels may appear at the optic nerve and rupture easily, ultimately leading to retinal detachment (Singh *et al.*, 2008; Walker, 2004).

1.3.2 Neuropathy

Peripheral neuropathy can lead to the formation of ulcerations in the feet and lower extremities in diabetic patients, and further lead to more serious complications such as amputation. Lower extremity amputations were 10 times higher amongst diabetic patients than those without diabetes (Boulton, 2008). Factors which influence the predisposition for amputation include ulcerations, autonomic insufficiency leading to

dry, cracked skin with infections, decreased wound healing capacity and immunopathy as a consequence of altered neutrophil function (Pataky *et al.*, 2007; Philbin *et al.*, 2006). In addition to the antimicrobial therapy, ongoing care of the wound or foot ulcer is necessary in order to minimize the risk of amputation.

1.3.3 Nephropathy

Due to the enormous increasing number of patients with renal failure resulting from diabetes and the high mortality of these patients receiving dialysis, diabetic nephropathy become one of the most problematic renal diseases. One of the changes in glomeruli of this disorder is mesangial expansion. Moreover, apoptosis has been demonstrated in tubular epithelial cells which may contribute to atrophy of tubular epithelium and tubulointerstitial fibrosis. Thus, both space-occupation by mesangial matrix and cell loss via apoptosis account for glomerular sclerosis with decreased capillaries in diabetic nephropathy (Dalla *et al.*, 2001; Schena *et al.*, 2005; Fioretto *et al.*, 2007).

1.3.4 Cardiovascular disease

Cardiac complications are a major cause of morbidity and mortality in the diabetic population. Diabetic people are 2 to 4 times more likely to have heart diseases compared to the normal population and 75% of diabetes related deaths are due to heart diseases (Sowers *et al.*, 2001; Mazzone *et al.*, 2008). Cardiac involvement in diabetes include coronary atherosclerosis, diabetic cardiomyopathy and autonomic neuropathy. The presence of accelerated atherosclerosis in both type 1 and type 2 diabetes have been well documented (Yamagishi *et al.*, 2006). In addition, for unknown reasons, diabetic patients develop congestive cardiac failure more readily

and have significantly worse prognosis than their non-diabetic counterpart once they develop coronary disease. Several mechanisms may be involved in the generation of diabetic heart diseases, including defective glucose transport, cellular overload of fatty acid metabolites, altered calcium metabolism in cardiomyocytes and structural alterations in the form of microangiopathy, interstitial and perivascular fibrosis (Yamagishi *et al.*, 2006).

1.4 Oxidative stress in diabetes and cardiovascular disease

Oxidative stress is important in the pathogenesis of diabetes and cardiovascular disease. In humans, the evidence concerning the role of antioxidants and free radicals in diabetes is limited. But, antioxidant vitamin deficiency and increased lipid peroxidation have been observed in patients with diabetes and atherosclerosis compared to control subjects (Riccioni *et al.*, 2007). It has been speculated that as pancreatic β cells and arterial endothelial cells have low antioxidant enzyme activities (Table 1-1), they might be more sensitive to free radical-mediated damage (Tiedge *et al.*, 1998).

Table 1-1 Antioxidant enzyme activities in islets and other tissues of rat. Data are expressed as Mean \pm Standard Deviation. SOD, superoxide dismutase; GPx, glutathione peroxidase. (Adapted from Tiedge *et al.*, 1998)

	Cu/Zn SOD	Mn SOD	Catalase	GPx
Liver	100 \pm 7	100 \pm 12	100 \pm 9	100 \pm 8
Kidney	104 \pm 12	105 \pm 12	64 \pm 9	118 \pm 7
Skeletal muscle	42 \pm 5	50 \pm 6	4 \pm 1	31 \pm 7
Fat	49 \pm 5	84 \pm 14	32 \pm 5	67 \pm 7
Islet	31 \pm 3	25 \pm 2	1 \pm 0	21 \pm 1

Reactive Oxygen species (ROS) have been formed from glucose metabolism via various biochemical pathways (Figure 1-3). Under physiological conditions, glucose primarily undergoes glycolysis and oxidative phosphorylation. Under pathological conditions of hyperglycemia in diabetes, excessive glucose levels can swamp the glycolytic process and inhibit glyceraldehyde catabolism, which cause glucose, fructose-1,6-bisphosphate, and glyceraldehyde-3-P to be shunted to other pathways including enolization and ketoaldehyde formation, PKC activation, dicarbonyl formation and glycation, sorbitol metabolism, hexosamine metabolism and oxidative phosphorylation (Robertson, 2004).

Given the involvement of oxidative stress in diabetes, many compounds with anti-oxidative function have been tested for their efficacy in preventing and treating DM.

These compounds include nicotinamide, desferrioxamine, N-acetylcysteine and vitamin E (Wright *et al.*, 2008; Levy *et al.*, 2007; Hamer *et al.*, 2007).

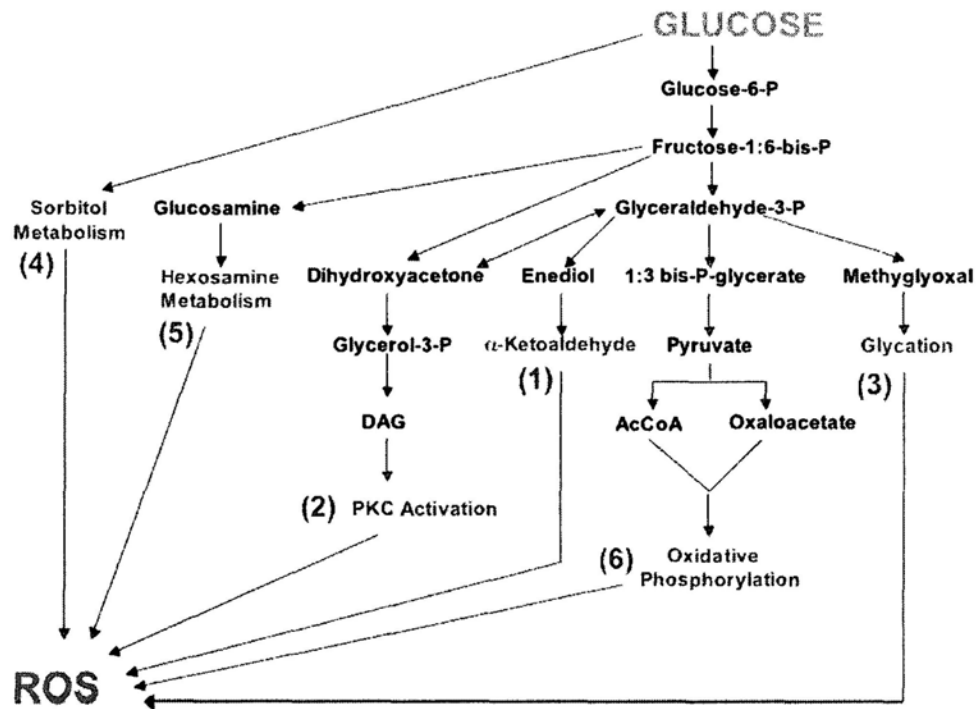


Figure 1-3 Six biochemical pathways along which glucose metabolism can form ROS. Under physiological conditions, glucose primarily undergoes glycolysis and oxidative phosphorylation. Under pathological conditions of hyperglycemia, excessive glucose levels swamp the glycolytic process and inhibit glyceraldehydes catabolism, which cause glucose, fructose-1,6-bisphosphate and glyceraldehydes-3-P to be shunted to other pathways (adapted from Robertson, 2004).

1.5 Conventional therapy of type 2 Diabetes Mellitus

When diet restriction and exercise fail to control or improve type 2 DM, oral anti-diabetic agents are required to maintain normal glycemic level. These drugs target on different organs and achieve glycemic control by different modes of action including inhibition of intestinal absorption of carbohydrates, stimulation of insulin release, suppression of hepatic gluconeogenesis and improvement of insulin sensitivity in peripheral tissues (Stumvoll *et al.*, 2005). Before 1996, only insulin and insulin secretion stimulator, sulfonylurea, were available for the treatment of type 2 DM. Currently, treatment options for type 2 DM consist of insulin sensitizers, α -glucosidase inhibitors, secretagogues and insulin (Stumvoll *et al.*, 2005). The target sites and action mechanisms of these drugs are summarized in Table 1-2.

Table 1-2 Pharmacological treatments of hyperglycemia in type 2 DM according to the sites of action

Anti-diabetic drugs	Target tissues	Action mechanisms
Pramlintide	Gastrointestinal tract	Delay of gastric emptying Inhibition of glucagon release
α -glucosidase inhibitors	Gastrointestinal tract	Inhibition of glucose absorption
Sulfonylureas	Pancreatic β cell	Stimulation of insulin release
Meglitinides	Pancreatic β cell	Stimulation of insulin synthesis and release Inhibition of β cell death
Metformin	Liver	Inhibition of glucose production
Thiazolidinediones	Skeletal muscle and adipose tissue	Increase in muscle insulin sensitivity Suppression of free fatty acid release Modulation of adipokine release

1.5.1 Insulin sensitizers

Drugs that enhance insulin sensitivity are primarily thiazolidinediones (TZDs). Rosiglitazone and pioglitazone are now being used in clinics (Doggrell, 2008; Deeks *et al.*, 2007). These drugs not only reduce glycemia, but also enhance vascular function and ameliorate the dyslipidemia and inflammation of type 2 DM. Their action is associated with stimulation of insulin receptor expression through the activation of peroxisome proliferators-activated receptor-gamma (PPAR- γ), a transcription factor that is found mainly in adipose tissues (Hauner, 2002). TZDs can be used in patients with reduced renal function, and they are better tolerated without significant gastrointestinal side effects. Major adverse effects of TZDs include hepatotoxicity, weight gain, peripheral edema and haemodilution (Lee, 2003; Henry, 1997).

Another kind of insulin sensitizer is metformin. Metformin is an anti-hyperglycemic drug which works by inhibiting hepatic glucose output. It has lesser beneficial effects on insulin resistance and vascular function but also lesser side effects of weight gain and hypoglycemia. Major concerns in using this drug are the causing of gastrointestinal disturbances including diarrhea, abdominal discomfort and loss of appetite (Garber *et al.*, 1997).

1.5.2 α -glucosidase inhibitors

At least two kinds of α -glucosidase inhibitors, namely acarbose and miglitol, have been developed to delay the intraluminal production of monosaccharide (Hanefeld *et al.*, 2008). They competitively inhibit α -glucosidase that are located on the brush-border of the mucosa of the small intestine and digest disaccharides into absorbable monosaccharides, and thereby slowing down carbohydrate digestion and lowering

postprandial hyperglycemia. Because α -glucosidase inhibitors lower only postprandial but not fasting plasma glucose level, the efficacy of these agents is limited to a 0.5% to 1% decrease in HbA1c value (Yee *et al.*, 1996; Scott *et al.*, 2000). For the adverse effects, α -glucosidase inhibitors often induce gastrointestinal effects such as flatulence, diarrhea and abdominal pain, which are due to fermentation of unabsorbed carbohydrates in the intestine. Moreover, acarbose, when taken in high dose, could induce hepatic damage (Coniff *et al.*, 1995).

1.5.3 Secretagogues

All secretagogues cause the release of insulin by closing the energy-sensitive potassium channel in the cell membrane of β cells, leading to β cell depolarization, influx of calcium and then increased exocytosis and release of insulin (Zimmerman, 1997). Sulphonylureas are primary drugs of this category. Examples of sulphonylureas include chlorpropamide, tolazamide, tolbutamide, glipizide, glyburide and glimepiride. The most common side effects of sulphonylureas are hypoglycemia and weight gain. They would also induce syndrome of inappropriate anti-diuretic hormone secretion by enhancing the release of anti-diuretic hormone (So *et al.*, 2002; Kabadi *et al.*, 2003).

1.5.4 Exogenous insulin

Insulin is the only therapeutic agent for type 1 DM. For severe type 2 diabetic patients, insulin therapy is required when they have failed on an adequate trial of diet, exercise and oral anti-diabetics. Insulin administration significantly reduces blood glucose concentration by suppressing hepatic glucose production, increasing postprandial glucose utilization and improving abnormal lipoprotein composition in

patients with insulin resistance (Nelson *et al.*, 2006). Moreover, it may decrease glucotoxicity by reducing hyperglycemia to improve insulin sensitivity and β cell secretory function (Giorgino *et al.*, 2005). Common adverse effect of insulin is hypoglycemia which is caused by over-insulinization, skipped meals, exercise, defective counter-regulatory hormonal response or alcohol (Amiel *et al.*, 2008). Insulin may also cause lipohypertrophy and allergic reactions at the injection sites (Fineberg *et al.*, 2007).

1.6 Traditional Chinese Medicine for Diabetes Mellitus

Thousands years of experience has been accumulated in the practice of Chinese medicine for diabetic therapy. It categorizes DM as XiaoKeZhen (消渴症) which is attributed to *yin* deficiency with dryness and *heat*. Chinese doctors treat DM through a holistic care rather than only by lowering blood glucose. A general therapeutic rule is to promote blood circulation to remove blood stasis, to activate vital energy circulation, to clear away *heat* in the body, to invigorate liver and kidney to activate *yang*, and to invigorate the spleen and stomach to strengthen the body (Dai, 2000; Xu *et al.*, 2000). A recent paper reviews 86 natural medicines (82 originate from plants and 4 from animals) which are commonly used for diabetic treatment with regard to their origin, anti-diabetic active components and pharmacological results (Li *et al.*, 2004). Table 1-3 showed a list of 33 TCMs most commonly used in anti-diabetic compound recipes.

Table 1-3 Thirty-three TCMs commonly used in anti-diabetic compound recipes.

TCMs frequently used in anti-diabetic compound recipes		
Radix Astragali (黃芪)	Rhizoma Coptidis (黃蓮)	Fructus Schisandrae (五味子)
Radix Rehmanniae (地黃)	Fructus Lycii (枸杞子)	Herba Gynostemmae (絞股藍)
Radix Rehmanniae preparata (熟地黃)	Cortex Lycii (地骨皮)	Radix Salviae miltiorrhizae (丹參)
Radix Trichosanthis (天花粉)	Poria (茯苓)	Rhizoma Phragmitis (蘆根)
Radix Puerariae (葛根)	Rhizoma Atractylodis (蒼朮)	Rhizoma Alismatis (澤瀉)
Radix Ginseng (人參)	Rhizoma Anemarrhenae (知母)	Semen Cuscutae (菟絲子)
Radix Panacis quinquefolii (西洋參)	Radix Ophiopogonis (麥冬)	Herba Epimedii (淫羊藿)
Rhizoma Polygonati (黃精)	Fructus Ligustri lucidi (女貞子)	Radix Clematidis (威靈仙)
Rhizoma Polygonati odorati (玉竹)	Fructus Mori (桑椹)	Radix Notoginseng (三七)
Fructus Cointi (山茱萸)	Folium Mori (桑葉)	Herba Dendrobii (石斛)
Hirudo (水蛭)	Cortex Mori (桑白皮)	Concha Ostreae (牡蠣)

Different classes of compounds with hypoglycemic effect were isolated from various TCMs, including terpenoids, polysaccharides, flavonoids, alkaloids, etc (Chen, 1987; Wu *et al.*, 1992; Gu *et al.*, 1997; Yin *et al.*, 2000). Examples of chemical constituents isolated from TCM with anti-diabetic activity are listed in Table 1-4. These compounds are effective in relief of symptoms such as lowering blood glucose but they cannot replace the roles of herbs in compound recipes. Chinese medicines are effective not only to treat DM but also at the same time to treat diabetic complications. So far, Chinese doctors have put forward many prescriptions with different medical emphasis subjecting to various symptoms of DM. Some classical prescriptions with outstanding curative effect have been used for hundreds of years. Examples include Xiao Ke Fang (消渴方), Liu Wei Di Huang Wan (六味地黃丸) and Yu Nu Jian (玉女煎) (Chen *et al.*, 1993; Kuchinski, 1999).

Table 1-4 Chemical constituents isolated from TCMs showing hypoglycemic activities.

Chemical categories	Bioactive compounds	Medicinal herbs
Terpenoids	Triterpenoids: ginsenoside oleanolic acid tormentic acid ursolic acid Diterpenoids: stevioside, salvin, salvicin Monoterpenoids: catalpol, rehmanniosides	<i>B. baselloides</i> <i>L. lucidum</i> <i>E. japonica</i> <i>C. officinalis</i> <i>S. japonica</i> <i>R. glutinosa</i>
Polysaccharides	Panaxan Laminaran Coixan	
Flavonoids	Swerchirin Hyperin	<i>S. chirayita</i> <i>T. cordata</i>
Peptides	α -methylenecyclopropylglycin S-allyl cysteine sulfoxide	<i>L. chinensis</i> <i>A. sativum</i>
Alkaloids	Berberine Vindoline	<i>C. chinensis</i> <i>C. roseus</i>
Sterols	Charantin	<i>M. charantia</i>
Fatty acids	Linoleic acid Trihydroxylicjeric acid	<i>B. mori</i> <i>B. alba</i>

1.7 Project objectives

Type 2 DM affects about one-tenth of the world population and shows increasing trend in prevalence. In Hong Kong, DM causes great concern in the health of elderly and youth due to more “Western” style in diet and lack of sufficient exercise. One of the serious consequences of DM is diabetic complication. Due to high morbidity and

mortality, atherosclerosis has aroused wide studies among various complications. Different causes have been proposed in the pathogenesis of DM. One of them, oxidative stress, plays an important role in DM. Under oxidative stress, pancreatic β cells become a major site of cell injury due to its low antioxidant enzyme activity. Apoptosis of β cells by hyperglycemia explains why many non-insulin dependent diabetic patients may shift to insulin-dependent when hyperglycemia exists chronically. Oxidative stress is also important in the induction of accelerated atherosclerosis of diabetic patients. Inflammation and vascular smooth muscle cell proliferation and migration are closely related to free radical generation, and are closely linked between DM and atherosclerosis. In therapy of type 2 DM, many Western drugs are now available commercially. However, they have limitations such as insufficient efficacy and existence of side effects. In making therapeutic choices in the management of type 2 DM, the major goal of protecting patients from the long-term complications of the disease must be considered. For this aspect, Chinese medicine that consider different systems of the body as a whole, may have advantages over Western medicine.

This study aims at evaluating the potency of TCMs in treating DM and the associated complications. Using various biochemical assays, effective TCM(s) for protecting pancreatic β cell death will be screened from 28 TCMs. The short-listed herbs will be combined to form a herbal formula. Then, different biological activities of the formula will be investigated using *in vitro* and *in vivo* models. They include (i) anti-apoptotic effect on pancreatic β cells; (ii) anti-hyperglycemic effect in diabetic *db/db* mice; (iii) anti-oxidative effect on β cells and LDL on cell membrane; (iv) anti-atherosclerotic effect in vascular smooth muscle cells; (v) anti-inflammatory effect in

macrophages. It is hoped that a herbal formula possessing therapeutic actions in both DM and atherosclerosis will be developed.

CHAPTER 2

MATERIALS AND METHODS

2.1 Materials

2.1.1 Cell lines

RIN-m5F (ATCC number CRL-11605): it is an insulinoma cell line isolated from rat pancreatic β cells. The cells were maintained in RPMI-1640 medium supplemented with 10% fetal bovine serum (FBS, purchased from Invitrogen, USA), 100 U/mL penicillin and 100 μ g/mL streptomycin. They were incubated at 37°C humidified incubator supplied with 5% CO₂. Sub-cultivation was performed two to three times per week when the cells was grown to 80-90% confluence.

A7r5 (ATCC number CRL-1444): it is a vascular smooth muscle cell line derived from embryonic rat aorta. The cells were maintained in Dulbeccos Modified Eagle's Medium supplemented with 10% FBS, 100 U/mL penicillin and 100 μ g/mL streptomycin. They were incubated at 37°C humidified incubator supplied with 5% CO₂. Sub-cultivation was performed one to two times per week when the cells was grown to 80-90% confluence.

RAW264.7 (ATCC number TIB-71): it is a mouse macrophage cell line isolated from Balb/c ascites. The cells were maintained in Dulbeccos Modified Eagle's Medium supplemented with 10% FBS, 100 U/mL penicillin and 100 μ g/mL streptomycin. They were incubated at 37°C humidified incubator supplied with 5% CO₂. Sub-cultivation was performed two to three times per week when the cells was grown to 80-90% confluence.

2.1.2 Culture media

Roswell Park Memorial Institute tissue culture medium 1640 (RPMI 1640) and Dulbeccos Modified Eagle's Medium (DMEM) were purchased from Invitrogen (USA). A pack of medium powder with phenol red, L-glutamine and HEPES was dissolved in 1 L of distilled water. Sodium bicarbonate (Sigma, USA) was added (2 g for RPMI 1640 medium and 3.7 g for DMEM) and the pH value was adjusted to 7.2. The medium was then sterilized by filtration using 0.22 μm bottle-top filter (Millipore, USA). Sterilized medium was stored at 4°C until use.

2.1.3 Trypsin-EDTA

Trypsin-EDTA solution containing 0.25% trypsin and 1 mM EDTA-tetrasodium in Hank's Buffered Salt Solution (HBSS) was purchased from Invitrogen (USA).

2.1.4 Buffers for biochemical assays

Phosphate Buffered Saline (PBS)

PBS was prepared by dissolving 8 g NaCl, 0.2 g KCl, 0.24 g KH_2PO_4 and 1.44 g Na_2HPO_4 in 1 L of distilled water. The pH was adjusted to 7.4 using HCl. The solution was sterilized by autoclave and was stored at 4°C until use.

Lysis buffer for preparing fragmented DNA

The buffer contains 3% NP-40, 20 mM EDTA, 50 mM Tris-Cl at pH 7.5.

Tris-EDTA (TE) buffer for preparing fragmented DNA

TE buffer was composed of 0.1 mM EDTA, 10 mM Tris-Cl at pH 7.5.

Insulin secretion buffer

Insulin secretion buffer was composed of 20 mM HEPES, 115 mM NaCl, 5 mM NaHCO₃, 4.7 mM KCl, 2.6 mM CaCl₂, 1.2 mM KH₂PO₄, 1.2 mM MgSO₄. The pH value of the solution was adjusted to 7.4. Before adding to the cells, dexamethone and glucose was added to make up to final concentrations of 500 nM and 5.5 mM, respectively.

Lysis Buffer for Total Protein Extraction

Lysis buffer was composed of 2% SDS, 10% glycerol and 0.0625 M Tris-HCl (pH 6.8).

10X SDS Running Buffer

10X SDS running buffer was prepared by dissolving 30.3 g of Tris base, 144 g of glycine and 10 g of SDS in 1 L of distilled water. The concentrated stock solution was then diluted to 1X SDS running buffer by distilled water.

10% Ammonium Persulfate (APS)

10% APS was prepared by dissolving 10% (w/v) APS (Bio-Rad, USA) in distilled water and was stored at -20°C.

2X SDS Loading Dye

2X SDS loading dye was prepared by mixing 10% (v/v) glycerol, 0.4% (w/v) SDS, 0.05% (w/v) bromophenol blue, 20 mM EDTA in 0.5 M Tris-HCl (pH 7.5) and 5% (v/v) 2-mercaptoethanol.

Electroblotting Buffer (E-Blot Buffer)

E-Blot buffer was prepared by mixing 66.7 mL of 10X Tris-glycine (30.3 g of Tris base and 144 g of glycine in 1 L of distilled water, pH 8.3), 100 mL of methanol and 500 mL of distilled water.

Phosphate Buffered Saline-Tween-20 (PBS-T)

PBS-T was prepared by mixing 1 mL of Tween-20 with 1 L of PBS.

2.1.5 Animals

Female, 4-5 weeks C57BL/KsJ-m^{+/+}Lepr^{db} mice (diabetic, +db/+db; non-diabetic, m/+db) were supplied by the Laboratory Animal Services Centre (LASEC) of The Chinese University of Hong Kong (CUHK). The mice were fed with standard chow and sterile water *ad lib* in a 12-h light/dark cycle. All animal experiments were performed according to the protocols approved by Animal Research Ethics Committee of CUHK (Ref No. 07/084/MIS).

2.2 Methods

2.2.1 Cell proliferation assay (MTT assay)

After appropriate treatment, the medium in each well of 96-well culture plate was discarded. Then, 40 μ L of MTT solution (5 mg/mL in PBS) was added to each well and the cells were incubated at 37°C, 5% CO₂ humidified incubator for 4 h. MTT solution was then removed and 100 μ L of dimethyl sulfoxide (DMSO) was added to dissolve the crystals. Absorbance at 540 nm was then read using microplate reader (Bio-Rad).

2.2.2 Determination of insulin secretion

RIN-m5F cells (5×10^5 cells/well) were seeded in each well of 6-well plate. After incubation for 24 h, the cells were treated with streptozotocin (STZ, 5 mM) in the presence or absence of SR10 for further 24 h. Then, the medium was removed and the cells were washed twice with insulin secretion buffer. Cells of each well were then incubated with 1 mL insulin secretion buffer at 37°C for 2 h. After that, the supernatant was collected and diluted for 3-fold for determination of insulin content using Ultra Sensitive Rat Insulin ELISA kit (Crystal Chem, USA).

2.2.3 Determination of insulin in plasma and supernatant

Insulin concentration in supernatant and plasma was determined using Ultra Sensitive Rat Insulin ELISA kit. To each well of antibody pre-coated microplate, 95 μ L Sample Diluent was dispensed. Then, 5 μ L of each sample was added to each well and the plate was incubated at 4°C for 2 h. After that, the wells were washed with Wash Buffer for five times. Anti-insulin enzyme conjugate (100 μ L) was added per well and the plate was incubated at room temperature for 30 min. The wells were washed with Wash Buffer for seven times. Enzyme Substrate Solution (100 μ L) was added to each well and the plate was left to stand for 40 min in dark. The enzyme reaction was stopped by adding 100 μ L Enzyme Reaction Stopping Solution per well. Absorbance at 450 nm was measured using microplate reader. The absorbance was corrected by the reading at 630 nm. Insulin concentration was calculated from the standard curve of insulin standard.

2.2.4 Detection of DNA fragmentation

2×10^5 cells were seeded into each well of a 6-well culture plate and were incubated at 37°C, 5% CO₂ humidified incubator overnight. After appropriate treatment, cells were harvested, washed with PBS and centrifuged at 800 \times g for 3 min. Cell pellet was then lysed with 400 μ L DNA lysis buffer. The lysate was added with 20 μ L of proteinase K solution (10 mg/mL) and then incubated at 56°C for 2 h. After that, the lysate was mix vigorously with 150 μ L saturated NaCl. The mixture was centrifuged at 5000 \times g for 20 min. The supernatant was isolated and mixed with 1 mL cold ethanol. The mixture was centrifuged at 10000 \times g at 4°C for 20 min. Then, the pellet was rinsed with cold 70% ethanol, air-dried and dissolved in 20 μ L TE buffer. The mixture was incubated at 37°C for 1.5 h. Dissolved DNA was subjected to 1.5% agarose gel electrophoresis and DNA bands were visualized under UV illumination.

2.2.5 Cell cycle analysis by PI staining

2×10^5 cells were seeded into each well of a 6-well culture plate. The cells were incubated in complete medium for 24 h and in medium with 1% FBS for another 24 h for synchronization. After appropriate drug treatment, the cells were collected and washed with PBS. Cells were then fixed with 1 mL of 70% ethanol at 4°C overnight. After fixation, ethanol was removed. Cells were then resuspended in 0.4 mL PBS containing propidium iodide (43 μ g/mL) and RNase A (1mg/mL), and incubated in dark at 37°C for 30 min. After incubation, cell cycles were analyzed using FACSCanto flow cytometer (Becton Dickinson).

2.2.6 Detection of Phosphatidylserine externalization with Annexin V-FITC and PI

TACS™ Annexin V-FITC kit (Trevigen, Inc.) was used to examine early apoptosis and necrosis/late apoptosis. Cells (2×10^5) were seeded in 6-well culture plate and incubated overnight. After appropriate treatment, cells were harvested and washed twice with PBS. 1×10^5 cells were used for the assay. Each sample was added with 100 μ L of Annexin V incubation reagent containing 10 μ L of 10X binding buffer, 10 μ L of PI, 1 μ L of Annexin V-FITC conjugate and 79 μ L of distilled water. The mixture was incubated at room temperature for 15 min. After incubation, 400 μ L of 1X binding buffer was added to each sample and the samples were analyzed by FACScanto flow cytometer (Becton Dickinson).

2.2.7 Determination of nitric oxide release

Nitric oxide (NO) production was detected by the formation of nitrite in the culture medium. Cells (0.5×10^6) per well were seeded in 24-well plates. After 24 h incubation, the culture medium in each well was replaced by appropriate concentrations of STZ or SR10. After 24 h incubation, media were collected, centrifuged for 5 min at 14,000 \times g, and 100 μ L of supernatant was incubated with 100 μ L of Griess reagent (Sigma Chemical Company) for 15 min. The absorbance was read at 540 nm using a microplate reader. Nitrite concentration was calculated using sodium-nitrite as standard.

2.2.8 Western blot analysis

Total protein extraction

Cells (2×10^6) were seeded in a 100-mm tissue culture dish and incubated overnight. After appropriate treatment, cells were collected and were washed twice with PBS. Lysis buffer (2% SDS, 10% glycerol, 0.0625 M Tris-HCl, pH 6.8) was added and the samples were allowed to stand on ice for 30 min. Then, the samples were boiled for 10 min and were subjected to centrifugation at $1,5000 \times g$ for 10 min at 4°C . After centrifugation, supernatant was collected and stored at -20°C .

Determination of protein concentration

Protein content in each sample was determined by bicinchoninic acid (BCA) protein assay. Bovine serum albumin (BSA) was used to establish the protein standard curve. Both testing samples and BSA standard were done in triplicate. BCA reaction mixture was made by mixing BCA solution and $\text{CuSO}_4 \cdot 5\text{H}_2\text{O}$ solution (v/v 50:1). In each well of 96-well plate, 2 μL protein sample or BSA standard was mixed with 200 μL BCA reaction mixture and incubated at 37°C for 30 min. After incubation, absorbance at 540 nm was measured by microplate reader (Bio-Rad). Protein amount of each sample was determined from BSA standard curve.

Western hybridization

Whole cell extract (25 μg) was analyzed by 8-12% SDS-polyacrylamide gel electrophoresis (SDS-PAGE) and transferred to polyvinylidene fluoride (PVDF) membrane using Semi-Dry blotter (Bio-Rad). After blocking with PBS-T containing 10% (w/v) non-fat milk powder for 1 h, the membranes were incubated at 4°C overnight with primary antibodies. After probing, the membrane was washed with PBS-T for 15 min for 3 times and probed with appropriate secondary antibody at room temperature for 1 h. The membrane was washed again with PBS-T for 3 times and it was ready for Enhanced Chemiluminescence (ECL) detection. ECL detection reagent 1 and reagent 2 (GE Healthcare) were mixed in the ratio of 1:1. After

incubated with ECL reagent, the signal developed on the membrane was captured by X-ray film (Super Rx, Fuji) with appropriate exposure time. The film was then developed by a film processor (M35 X-OMAT, Kodak) and the band intensity was analyzed by ImageQuant software (Molecular Dynamics).

2.2.9 Detection of mRNA expression level by Reverse Transcription-Polymerase Chain Reaction (RT-PCR)

RNA isolation

Total RNA was purified from culture cells using RNeasy Mini kit (Qiagen) according to the manufacturer's protocol. In brief, cells (2×10^5) grown in 6-well culture plate was lysed with 350 μ L RLT buffer. Cell lysates were passed 5 times through 20-gauge needle. Then, 350 μ L of 70% ethanol was added to the lysates. The mixtures were transferred to RNeasy spin columns and centrifuged for 15 s at 8000 \times g. Buffer RW1 (700 μ L) was added to the columns and they were centrifuged at 8000 \times g for 15 s. After that, 500 μ L RPE buffer was added to the columns and they were centrifuged again at 8000 \times g for 15 s. This step was repeated once. RNA was collected by adding 40 μ L RNase-free water to the column and then centrifuged at 8000 \times g for 1 min. RNA concentration was measured at 260 nm using UV spectrophotometer.

cDNA synthesis by reverse transcription

First strand cDNA was synthesized using Taqman® Reverse Transcription Reagent Kit according to the manufacturer's protocol. Reverse transcription mixture contained 5 μ L of 10X RT buffer, 11 μ L of 25 mM $MgCl_2$, 10 μ L of 10 mM dNTP, 2.5 μ L of random hexamer, 1 μ L of RNase inhibitor, 0.5 μ L of reverse transcriptase (50 U/ μ L) and 20 μ L of total RNA (1 μ g). Reaction was carried out at 25°C for 10

min, 37°C for 1 h and then at 95°C for 5 min. Synthesized cDNA was stored at -20°C until used.

Polymerase Chain Reaction (PCR)

PCR amplification was carried out using the reagents supplied by Invitrogen. Reaction mixture contained 2 µL of 10X PCR buffer, 1 µL of 10mM dNTP, 0.5 µL of *Taq* DNA polymerase, 1 µL of 10mM primer mix (forward and reverse primer), 5 µL of cDNA template and 10.5 µL of distilled water. PCR was performed in GeneAmp® PCR system 9700 (Applied Biosystem). The samples were denatured at 94°C for 5 min before running the cycles of 1 min at 94°C, 1 min at 50°C and 1 min at 72°C. Finally, extension was made at 72°C for 10 min. PCR products were analyzed using agarose gel electrophoresis. The signals were detected using UVI gel documentary system.

2.2.10 Basal glycemia test

At day 0, diabetic mice (+*db/db*) were divided into three groups (water, low dosage of SR10 and high dosage of SR10) and one group of non-diabetic lean mice (*m/+db*) was used as normal control. Eight mice were included in each group. After overnight fasting, blood was collected from tail vein of each mouse and plasma glucose level was determined by glucose oxidase method (Biosystem, USA). In chronic treatment, powder of SR10 was dissolved in distilled water (0.2 mL) and administered by force feeding once daily for 4 weeks. For low dosage group, the mice were fed with 464 mg/kg of SR10. For high dosage group, the mice were fed with 927 mg/kg of SR10. For both water group and non-diabetic mice, they were fed with 0.2 mL water. Plasma glucose levels were determined once per week in overnight fasting mice. Plasma insulin of each mouse was determined before and after 4-week treatment

using Ultra Sensitive Rat Insulin ELISA Kit (Crystal Chem Incorporation, USA) according to the manufacturer's instructions. The experiments were repeated for 3 times ($n = 8$ for each experiment) and the data were expressed as the Mean \pm Standard Deviation (S.D.) of total 24 mice.

2.2.11 Oral glucose tolerance test (OGTT)

On the day of OGTT, first blood sample (-30 min) was collected from tail vein of overnight-fasted mice followed immediately by force-feeding with water (water control group and non-diabetic control group) or 200 mg/kg metformin (Sigma Chemical Company) (positive control group) or SR10 (low dosage and high dosage treatment groups) according to their assigned groups (8 mice in each group). Second blood sample (0 min) was taken 30 min after the treatment and immediately followed by force-feeding of 2 g/kg glucose solution. Blood samples were then collected at 30 min, 60 min and 90 min after glucose challenge. The mice were kept fasting until last blood sample was taken. The experiments were repeated for three times under the same condition. The data were expressed as the Mean \pm S.D. of total 24 mice.

2.2.12 Preparation of plasma samples from mice

Whole blood was collected in centrifuge tube pre-coated with 5 μ L of 1250 U/mL heparin from tail tip of mice. Blood sample was then immediately centrifuged at 4000 \times g for five minutes for separation of plasma from blood cells. Plasma as supernatant was collected.

2.2.13 Preparation of liver extract from mice

After the mice were sacrificed, one gram of liver tissue was removed from each mouse and homogenated in 10 mL homogenizing buffer (50 mM Tris-HCl, 0.1 mM EDTA, pH 7.6). The homogenates were centrifuged at $10,000 \times g$ for 10 minutes and the supernatants (i.e. liver extracts) were collected for performing assays.

2.2.14 Isolation of mouse islets

Pancreases of the mice were isolated, cut into fine pieces and put into Hank's balanced salt solution (Invitrogen, USA) containing 25 mg collagenase A (Roche, USA). The tissues were shaken in 37°C water bath for about 10 min until no tissue clump could be seen. Extra Hank's balanced salt solution was added to stop the digestion and the tissue digest was allowed to stand for few minutes. Supernatant was collected and examined under dissection microscope. Islets were selected by hand picking. Two thousand islets were collected from each mouse and three mice of each treatment group were randomly selected for islets preparation.

2.2.15 Determination of glucose concentration in plasma

The glucose concentration in plasma was measured by glucose oxidase method. One milliliter glucose assay solution (Biosystems) was pre-warmed at 37°C. Then, 5 μ L plasma sample was added and the absorbance at 500 nm was measured after 5 min incubation at 37°C. The absorbance was converted to actual glucose level by calibration with 5.6 mM glucose standard.

2.2.16 Determination of total cholesterol concentration in plasma

An aliquot of 1 mL of assay reagent (Biosystems) was added to 10 μ L sample or standard. The mixture was incubated at room temperature for 10 min. Then, the absorbance at 500 nm was read within 30 min. Cholesterol concentration was calculated by comparing the absorbance of the standard at concentration of 200 mg/dL.

2.2.17 Determination of HDL-C concentration in plasma

An aliquot of 0.2 mL of plasma sample was added to 0.5 mL Reagent A of HDL-C determination kit (Biosystems). The mixture was allowed to stand at room temperature for 10 min, followed by centrifugation at 6000 \times g for 10 min. Supernatant or standard (100 μ L) was added to 1 mL of Reagent A and the mixture was incubated at 37°C for 10 min. Then, absorbance at 500 nm was read using microplate reader. HDL-C concentration was calculated by comparing the absorbance of the standard at concentration of 15 mg/dL.

2.2.18 Determination of triglyceride concentration in plasma

An aliquot of 1 mL of assay reagent (Biosystems) was added to 10 μ L sample or standard. The mixture was incubated at 37°C for 5 min. Then, the absorbance at 500 nm was read. Triglyceride concentration was calculated by comparing the absorbance of the standard at concentration of 200 mg/dL.

2.2.19 Determination of PON activity in plasma

Plasma sample was diluted 5-fold with freshly prepared reaction buffer (1.9 mM CaCl₂, 3.6 mM NaCl, 90 mM Tris-HCl, pH 8.5). Paraoxon was dissolved in reaction

buffer at concentration 1.2 mM as substrate. Then, the substrate (580 μ L) was added to 20 μ L diluted plasma sample. Absorbance at 405 nm was measured at room temperature every 1 min for total 10 min. Comparison of PON activity between control group and treatment group was made by comparing the rate of reaction (slope of the reaction curve) of each sample.

2.2.20 Determination of Catalase activity in plasma and liver extracts

Catalase activity assay was performed according to the manufacturer's instructions (Sigma Chemical Company, USA). Activities were measured in the plasma or liver extracts as remaining hydrogen peroxide substrate after the action of catalase. In brief, 25 μ L liver extract or 50 μ L of plasma was added with 1X Assay Buffer to make the final volume to be 75 μ L. The reaction was started by adding 25 μ L of the Colorimetric Assay Substrate Solution. The mixture was incubated at room temperature for 5 minutes. Then, 900 μ L of the Stop Solution was added to stop the reaction. After that, 10 μ L aliquot of the reaction mixture was added with 1mL of the Color Reagent. Color development was quantified by measuring the absorbance at 520 nm after 15 min incubation at room temperature. Cellular protein contents in liver extracts were measured using BCA protein assay and all enzyme activities in the liver extracts were normalized to cellular protein content.

2.2.21 Determination of SOD activity in plasma and liver extracts

Superoxide dismutase (SOD) activity assay was performed according to the manufacturer's instructions (Biochemika). In brief, 20 μ L of liver extract or plasma samples were added with 200 μ L of WST Working Solution and 20 μ L of Enzyme Working Solution into a 96-well plate. After incubating the plate at 37°C for 20 min,

absorbance at 450 nm was read using a microplate reader. SOD activity was calculated in terms of inhibition rate (%).

2.2.22 Determination of GSH level in liver extract

Tissue glutathione (GSH) was quantified according to the manufacturer's instructions (Sigma Chemical Company, USA). In brief, 10 μ L liver extract or GSH standards were added with 150 μ L Working Mixture [6 U/mL of glutathione reductase, 1.5 mg/mL of dithionitrobenzoic acid (DTNB) solution] to a 96-well plate and incubated at room temperature for 5 min. Sulfosalicylic acid (5%) was used as a reagent blank. Fifty microliters of NADPH solution (0.16 mg/mL) was added to the mixtures. Absorbance was measured once per minute for totally 6 min. The reagent blank value was subtracted from every measurement. From the standard curve, $\Delta A_{412}/\text{min}$ equivalent to 1 nmole of GSH was calculated. The amount of GSH in liver homogenate samples were calculated as follows:

$$\text{nmoles GSH/mL} = \Delta A_{412}/\text{min}(\text{sample})/\Delta A_{412}/\text{min} (1 \text{ nmole})$$

$$\Delta A_{412}/\text{min} (\text{sample}) = \text{slope generated by sample}$$

$$\Delta A_{412}/\text{min} (1\text{nmole}) = \text{slope calculated from standard curve for 1 nmole of GSH}$$

2.2.23 Determination of MDA in liver extracts

An aliquot of 0.5 mL liver homogenate was added with 0.5 mL of thiobarbituric acid (TBA) reagent (0.67% TBA in 50% acetic acid), 225 μ L of H₂O, 25 μ L of butylated hydroxytoluene (BHT, 90 mM in isopropanol) and 250 μ L of FeCl₃ (4 mM). The mixture was incubated at 90°C for 30 min. After cooling, 2 mL butanol was added and the mixture was centrifuged at 5000 \times g for 30 min. The top layer in pink colour

was taken out for absorbance measurement at 532 nm (subtracted by absorbance at 453 nm). MDA concentration was calculated against MDA standard curve.

2.2.24 Measurement of 2,2'-azo-bis-(2-amidinopropane) dihydrochloride (AAPH)-induced RBC hemolysis

Preparation of red blood cell suspension

Blood was collected from adult Sprague-Dawley (SD) rat from thoracic aorta by heparinized tube. RBCs were obtained by centrifugation at 1500 \times g for 10 min and were washed twice with 0.15 M NaCl solution. After centrifugation, 20% RBC suspension was obtained by resuspending RBC in four times volume of 0.15 M NaCl solution.

Measurement of RBC lysis

RBC lysis reaction was set up in microcentrifuge tubes, each containing 10% RBC suspension, 100 mM of AAPH and various concentrations of testing drug in a total volume of 1 mL. Control was set up by using PBS instead of testing drug. RBC and testing drug were added firstly and the reaction was initiated by adding 100 mM of AAPH. The mixtures were then incubated in oscillator at 37°C for 200 min. After incubation, the mixtures were diluted with PBS or distilled water by 20-fold, respectively. The diluted mixtures were centrifuged at 1500 \times g for 10 min. Supernatant (200 μ L) of each mixture was transferred to 96-well plate for measurement at 540 nm using microplate reader. Percentage inhibition of RBC hemolysis was calculated by the following equation:

$$\text{Inhibition \%} = \left(\frac{DW_{\text{sample}} - \text{PBS}_{\text{sample}}}{DW_{\text{sample}}} - \frac{DW_{\text{control}} - \text{PBS}_{\text{control}}}{DW_{\text{control}}} \right) \times 100\%$$

2.2.25 Measurement of LDL peroxidation

The reaction was set up in quartz cuvette, each containing 75 μg of human LDL, 5 μM of copper (II) chloride and various concentrations of testing drug in a total volume of 1 mL. LDL and the testing drug were added to the cuvette firstly and the reaction was initiated by adding copper (II) chloride. Conjugated dienes formation was continually monitored at 37°C by measuring UV absorption at 234 nm in 5-min intervals for total 24 h. The lag time for the formation of conjugated dienes was determined to be the intercept of the slopes for the lag and propagation phases, and was compared with control (using PBS instead of testing drug). Figure 2-1 shows an example for determining the lag time of LDL oxidation.

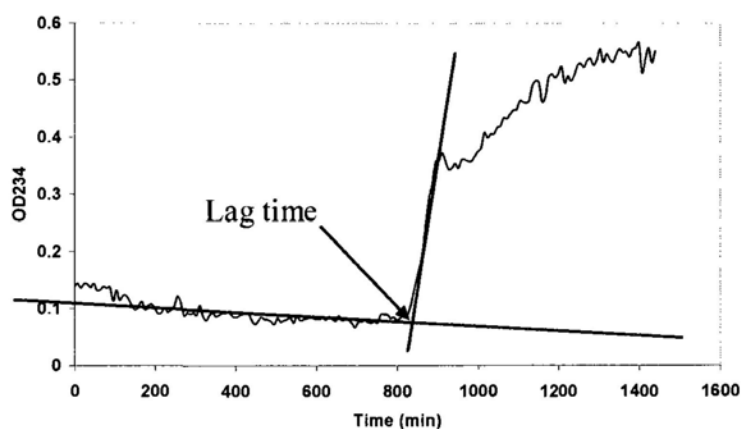


Figure 2-1 Determination of Lag time from a typical profile of Cu^{2+} ions-induced LDL oxidation.

2.2.26 Measurement of DNA incorporation assay (^3H -thymidine uptake assay)

0.5×10^4 cells were seeded into each well of a 96-well culture plate. The cells were incubated in complete medium for 24 h and in medium with 1% FBS for another 24

h for synchronization. After appropriate drug treatment, cells in each well were added with 0.5 μCi of ^3H -thymidine in 25 μL of PBS and incubated at 37°C for 6 h. Then, the cells were subjected once to freeze and thaw cycle. After that, DNA in the cells was harvested on microfilter with a cell harvester. The radioactivity of ^3H -thymidine on the filter was counted by a microplate scintillation counter (Beckman Coulter).

2.2.27 Cell migration assay

To examine cell migration activity, transwell system was employed (Costar) (Fig. 2-2). The system included a 24-well plate with transwell insert put on the top of the well. In the upper compartment, cells (1.5×10^4) were seeded in each well in 100 μL plain medium containing none or various concentrations of SR10. In the lower chamber, 600 μL of plain medium with or without 25 ng/mL PDGF-BB was added. After 3 h incubation, cells in the transwell were fixed in 1% paraformaldehyde and stained in hematoxylin. Non-migrated cells in the upper compartment were scraped away. Migrated cells on lower surface of the filter were counted under microscope with power of 200X and 5 regions were counted per well.

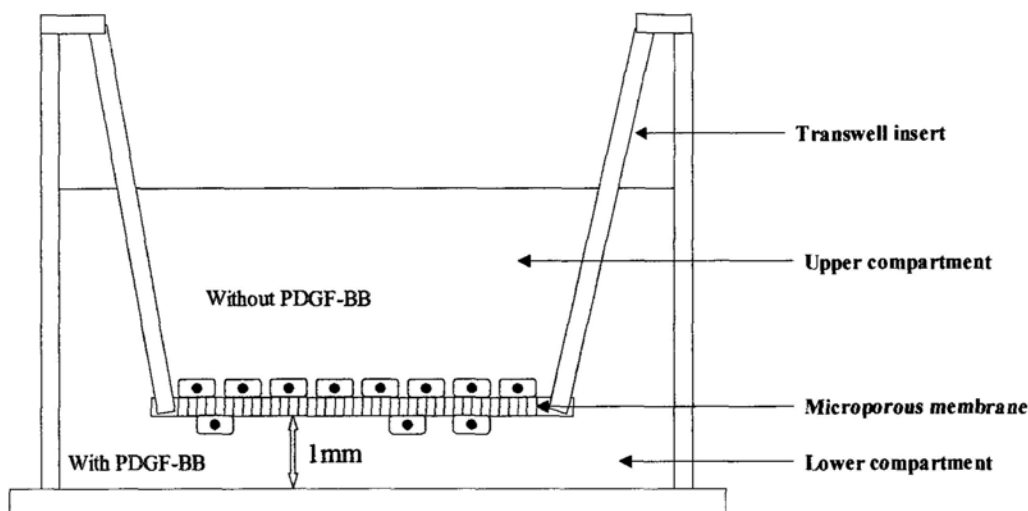


Figure 2-2 A diagram showing the transwell system employed for cell migration assay.

2.2.28 Measurement of cytokine release by ELISA

Amount of cytokines in plasma or cell culture supernatant were measured by ELISA kit. It was carried out according to the manufacturer's protocol. Briefly, 100 μL of capture antibody diluted in coating buffer (0.1 M sodium bicarbonate, pH 6.5) was added to each well of a 96-well ELISA plate and incubated overnight at 4°C. After incubation, the wells were washed 3 times with wash buffer (PBS with 0.05% Tween-20). The plate was blocked with assay diluent (10% FBS in PBS) and incubated at room temperature for 1 h. The plate was then washed with wash buffer for 3 times. After washing, 100 μL of standard, plasma or 200 μL of medium supernatant were added into each well. The plate was incubated at room temperature for 3 h. The wells were then washed with wash buffer for 5 times. Detecting reagent (detection antibody + avidin-HRP reagent, 100 μL) was added and incubated for 1 h

room temperature. Then, the wells were washed with wash buffer for 5 times. Substrate solution (100 μ L) was added and the plate was incubated for 30 min at room temperature in dark. Finally, 50 μ L of stop solution (2N sulphuric acid) was added to each well and absorbance at 450 nm was recorded using microplate reader (Bio-Rad).

2.2.29 Extraction of proteins from different subcellular fractions

Extraction of subcellular proteins was done with ProteoExtract Subcellular Proteome Extraction Kit (Calbiochem, USA) according to the protocol supplied by the manufacturer. Cells (5×10^6) were seeded in 25 cm² culture flask. After appropriate treatment, medium was removed from the flask. The cells were washed twice with 2 mL ice-cold Wash buffer by gentle agitation at 4°C for 5 min. The buffer was removed and 1 mL ice-cold Extraction Buffer I with 5 μ L protease inhibitor cocktail was added. The cells were gently agitated at 4°C for 10 min. The supernatant was collected as cytosolic fraction. Another 1 mL ice-cold Extraction Buffer II with 5 μ L protease inhibitor cocktail was added to the cells and incubated for 30 min at 4°C with gentle agitation. The supernatant was removed, and 500 μ L ice-cold Extraction Buffer III with 5 μ L protease inhibitor cocktail and 1.5 μ L Benzonase nuclease was added to the cells. The cells were incubated for 10 min at 4°C and then the supernatant was collected as nuclear fraction.

CHAPTER 3

AUTHENTICATION OF HERBAL MATERIALS

3.1 Materials

Twenty-eight TCMs were purchased from a local supplier in Sheung Wan, Hong Kong. Morphological authentication was done by Dr. Cao Hui (National Engineering Research Center for Modernization of TCM, Zhuhai, Guangdong, China). Thin Layer Chromatography (TLC) analysis of each herb was performed according to the procedures cited in *Chinese Pharmacopoeia* (edition in year 2000) with minor modifications. Reference herbs and reference compounds were purchased from National Institute for the Control of Pharmaceutical and Biological Products (NICPBP) or Sigma-Aldrich, Inc. For all of these TCMs, herbarium voucher specimens were deposited at the museum of the Institute of Chinese Medicine, The Chinese University of Hong Kong, with voucher specimen numbers shown in Table 3-1. Morphology of these herbs was shown in Figure 3-1.

Table 3-1 List of 28 TCMs and their voucher specimen numbers.

TCM	Voucher specimen number
Cortex Acanthopanax	2005-2637
Cortex Lycii	2005-2601
Cortex Phellodendri	2005-2595
Fructus Corni	2005-2586
Fructus Ligustri lucidi	2005-2590

Fructus Lycii	2005-2600
Fructus Schisandrae chinensis	2005-2591
Herba Gynostemmae	2005-2603
Poria	2005-2588
Radix Astragali	2005-2580
Radix Codonopsis	2005-2597
Radix Notoginseng	2005-2636
Radix Ophiopogonis	2005-2589
Radix Panacis quinquefolii	2005-2583
Radix Platycodonis	2005-2602
Radix Puerariae	2005-2582
Radix Rehmanniae	2005-2581
Radix et Rhizoma Rhei	2005-2594
Radix Salviae miltiorrhizae	2005-2592
Radix Trichosanthis	2005-2599
Rhizoma Alismatis	2005-2593
Rhizoma Anemarrhenae	2005-2605
Rhizoma Atractylodis	2005-2604
Rhizoma Coptidis	2005-2587
Rhizoma Polygonati	2005-2584
Rhizoma Polygonati odorati	2005-2585
Rhizoma et Radix Polygoni cuspidati	2005-2596
Semen Coicis	2005-2598

Cortex Acanthopanax

Cortex Lycii

Cortex Phellodendri

Fructus Corni

Fructus Ligustri lucidi

Fructus Lycii

Fructus Schisandrae chinensis Herba Gynostemmae

Poria

Radix Astragali

Radix Codonopsis

Radix Notoginseng

Radix Ophiopogonis

Radix Panacis quinquefolii

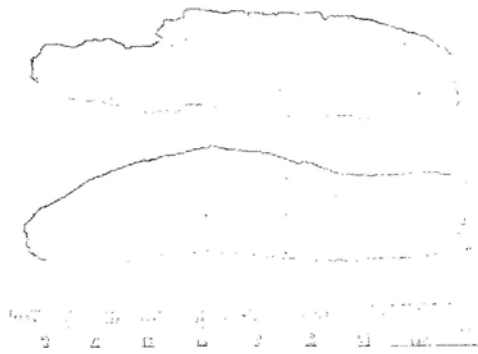
Radix Platycodonis

Radix Puerariae

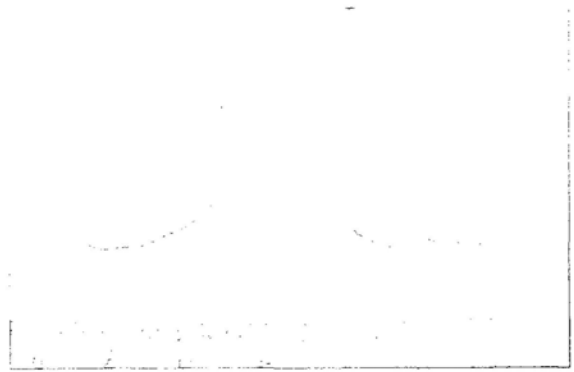


Radix Rehmanniae

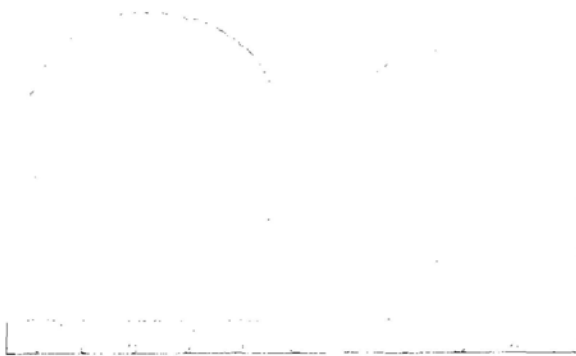
Radix et Rhizoma Rhei



Radix Salviae miltiorrhizae



Radix Trichosanthis



Rhizoma Alismatis



Rhizoma Anemarrhenae



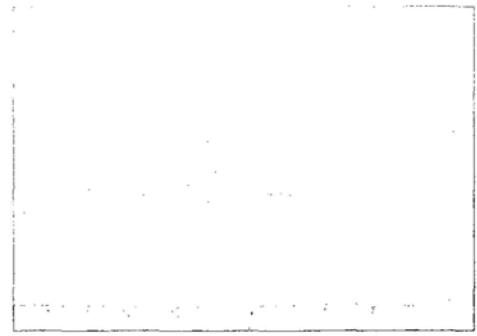
Rhizoma Atractylodis



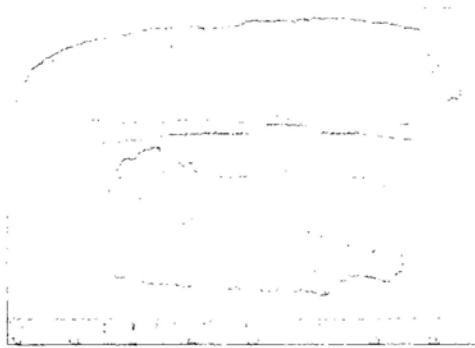
Rhizoma Coptidis



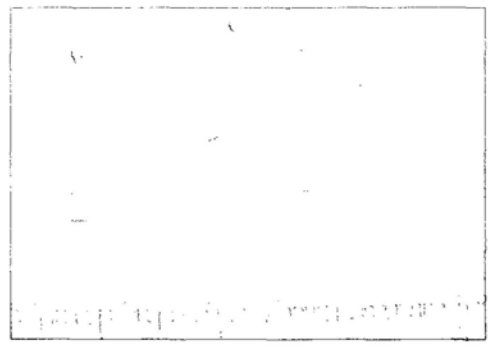
Rhizoma Polygonati



Rhizoma Polygonati odorati



**Rhizoma et Radix
Polygoni cuspidati**



Semen Coicis

Figure 3-1 Morphology of 28 TCMs.

3.2 Authentication

3.2.1 Cortex Acanthopanax (五加皮)

General description and characteristics of the herb

It is the dried root bark of *Acanthopanax gracilistylus* W. W. Smith (Fam. Araliaceae). It is collected in summer and autumn. It is shown as irregular quills, 5-15 cm long, 0.4-1.4 cm in diameter, about 2 mm thick. The outer surface is grayish-brown with slightly twisted longitudinal wrinkles and transverse lenticel-like scars. The inner surface is grayish-yellow with fine longitudinal striations. The texture is light and fragile. The odor is slightly aromatic. The taste is slightly pungent and bitter. The herb is used to relieve rheumatic condition, tonify the liver and the kidney, strengthen the tendons and bones.

Thin Layer Chromatographic analysis

Methodology

2 g of testing herb heated at 45°C with 20 mL methanol for 2 h. The solution was filtered and evaporated to dryness. The residue was dissolved in 0.5 mL methanol as the testing solution. A solution using 2 g of Cortex Acanthopanax reference herb (NICPBP catalog number 121523) was prepared in the same manner as the reference solution. TLC was carried out using silica gel 60 F₂₅₄ as the stationary phase and a mixture of chloroform-methanol (7:3) as the mobile phase. The solutions were applied separately to the plate. After developed and dried in air, the plate was sprayed with 10% sulfuric acid in ethanol and heated at 105°C to make the spots distinct.

Results

TLC profile of Cortex Acanthopanax was shown in Figure 3-2. The spots in the chromatogram obtained from the testing solution corresponded in color and position to the spots in the chromatogram obtained from the reference solution.

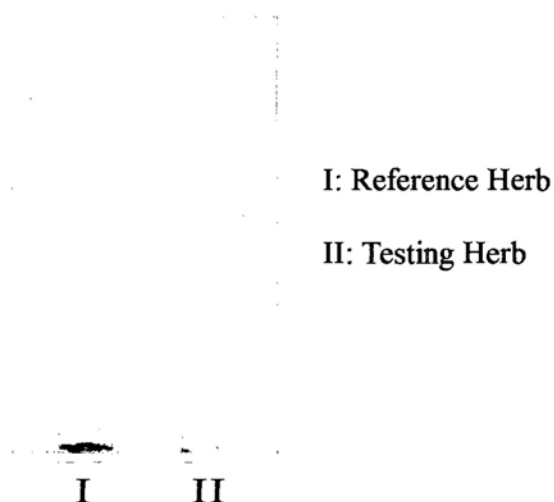


Figure 3-2 Thin Layer Chromatogram of Cortex Acanthopanax.

3.2.2 Cortex Lycii (地骨皮)

General description and characteristics of the herb

It is the dried root bark of *Lycium chinense* Mill. or *Lycium barbarum* L. (Fam. Solanaceae). It is collected in early spring or late autumn. It is quilled or channeled, 3-10 cm long, 0.5-1.5 cm wide, 1-3 mm thick. The outer surface is grayish-yellow, rough and easily exfoliated. The inner surface is yellowish-white with fine longitudinal striations. The texture is light and fragile. The odor is slight. The taste is sweetish and then bitter. It is known to reduce *heat* in blood, to relieve consumptive fever and to remove *heat* from the lung.

Thin Layer Chromatographic analysis

Methodology

1 g of testing herb was heated under reflux with 30 mL ethanol for 1 h. The solution was filtered and evaporated to dryness. The residue was dissolved in 3 mL ethanol as testing solution. A solution using 1 g of Cortex Lycii reference herb (NICPBP catalog number 121087) was prepared in the same manner as the reference solution. TLC was carried out using silica gel 60 F₂₅₄ as the stationary phase and a mixture of

toluene-ethyl acetate-formic acid (5:2.5:0.5) as the mobile phase. The solutions were applied separately to the plate. After developed and dried in air, the plate was examined under UV light at 365 nm.

Results

TLC profile of Cortex Lycii was shown in Figure 3-3. The spots in the chromatogram obtained from the testing solution corresponded in position to the spots in the chromatogram obtained from the reference solution.

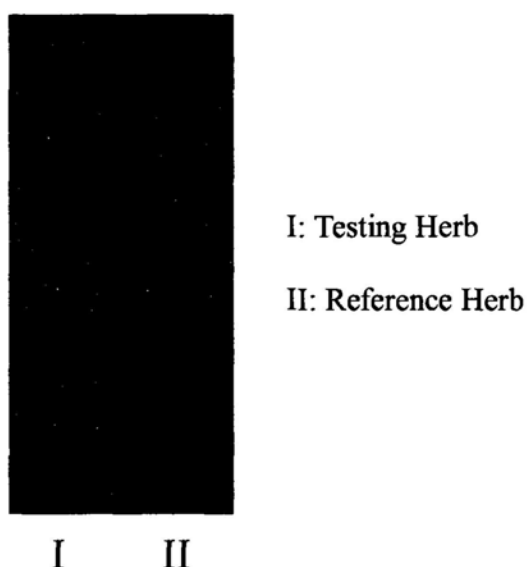


Figure 3-3 Thin Layer Chromatogram of Cortex Lycii.

3.2.3 Cortex Phellodendri (黃柏)

General description and characteristics of the herb

It is the dried bark of *Phellodendron amurense* Rupr. (Family Rutaceae) or *Phellodendron chinense* Schneid. (Family Rutaceae) It is tabular channeled. The length and width are varied with 1-6 mm thickness. The outer surface is yellowish-brown, longitudinally furrowed. The inner surface is dark yellow with fine longitudinal ridges. The texture is light and hard. The odor is slight. The taste is very

bitter. It is used to remove *damp-heat*, to quench *fire*, to counteract toxicity and to relieve consumptive fever.

Thin Layer Chromatographic analysis

Methodology

0.1 g of testing herb was heated under reflux with 10 mL methanol for 30 min. The solution was filtered as the testing solution. A solution using 0.1 g of Cortex Phellodendri Amurensis reference herb (NICPBP catalog number 120937) was prepared in the same manner as the reference solution. Berberine hydrochloride (NICPBP catalog number 110713, purity $\geq 98\%$) was dissolved in methanol (0.5 mg/mL) as the standard solution. TLC was carried out using silica gel 60 F₂₅₄ as the stationary phase and a mixture of ethyl acetate-acetone-formic acid-water (10:6:1:1) as the mobile phase. The solutions were applied separately to the plate. After developed and dried air, the plate was examined under UV light at 365 nm.

Results

TLC profile of Cortex Phellodendri was shown in Figure 3-4. The spot in the chromatogram obtained from the testing solution corresponded in position to the spot in the chromatogram obtained from the reference solution and standard solution.

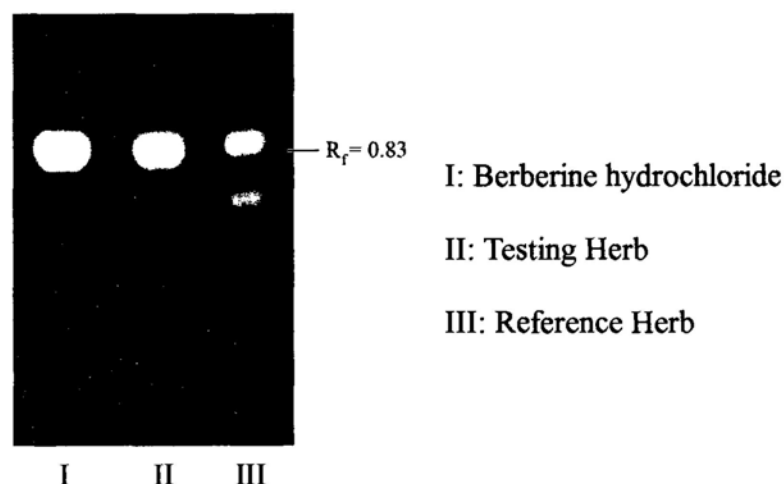


Figure 3-4 Thin Layer Chromatogram of Cortex Phellodendri.

3.2.4 Fructus Corni (山茱萸)

General description and characteristics of the herb

It is the dried ripe sarcocarp of *Cornus of ficinalis* Sieb. et Zucc. (Fam. Cornaceae). It is collected in late autumn and early winter. It is irregularly flaky, 1-1.5 cm long and 0.5-1 cm wide. It is externally purplish-red, shrunken and lustrous, with a rounded scar of persistent calyx at the apex and a scar of fruit stalk at the base. The texture is soft. The odor is slight. The taste is sour, astringent and slightly bitter. It is used to replenish the liver and kidney, to restrain seminal emission and to relieve collapse.

Thin Layer Chromatographic analysis

Methodology

0.5 g of testing herb was sonicated with 10 mL ethyl acetate for 15 min. The solution was filtered and evaporated to dryness. The residue was dissolved in 1 mL dehydrated ethanol as the testing solution. Ursolic acid (Sigma-Aldrich catalog number 89797, purity $\geq 98.5\%$) was dissolved in dehydrated ethanol (1 mg/mL) to produce the standard solution. TLC was carried out using silica gel 60 F₂₅₄ as the stationary phase and a mixture of toluene-ethyl acetate-formic acid (20:4:0.5) as the

mobile phase. The solutions were applied separately to the plate. After developed and dried in air, the plate was examined under UV light at 365 nm. Then, the plate was sprayed with 10% sulfuric acid in ethanol and heated at 105°C to make the spots distinct.

Results

TLC profile of Fructus Corni was shown in Figure 3-5. The spot in the chromatogram obtained from the testing solution corresponded in position to the spot in the chromatogram obtained from the standard solution.

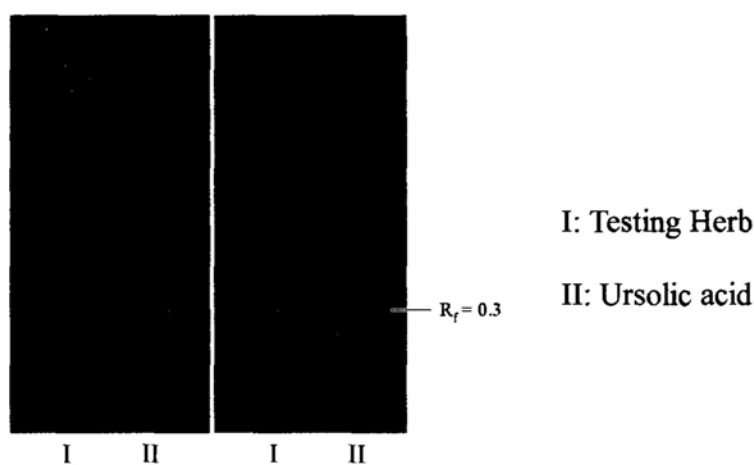


Figure 3-5 Thin Layer Chromatogram of Fructus Corni.

3.2.5 Fructus Ligustri lucidi (女貞子)

General description and characteristics of the herb

It is the dried ripe fruit of *Ligustrum lucidum* Ait. (Fam. Oleaceae). It is collected in winter. It is ovoid, 6-8.5 mm long, 3.5-5.5 mm in diameter. It is externally blackish-purple, shrunken, with a fruit stalk scar or persistent calyx and a short fruit stalk at the base. The texture is light. The odor is slight. The taste is sweet but slightly bitter and astringent. It is used to replenish the liver and kidney, to improve vision and to promote hair growth.

Thin Layer Chromatographic analysis

Methodology

0.5 g of testing herb was heated under reflux with 20 mL methanol for 30 min. The solution was filtered and evaporated to dryness. The residue was dissolved in a mixture of ethanol-chloroform (3:2) as the testing solution. Oleanolic acid (NICPBP catalog number 110709, purity $\geq 98\%$) was dissolved in ethanol (1 mg/mL) to produce the standard solution. TLC was carried out using silica gel 60 F₂₅₄ as the stationary phase and a mixture of hexane-acetone-ethyl acetate (5:2:1) as the mobile phase. The solutions were applied separately to the plate. After developed and dried in air, the plate was sprayed with 10% sulfuric acid in ethanol and heated at 105°C to make the spots distinct.

Results

TLC profile of Fructus Ligustri lucidi was shown in Figure 3-6. The spot in the chromatogram obtained from the testing solution corresponded in color and position to the spot in the chromatogram obtained from the standard solution.

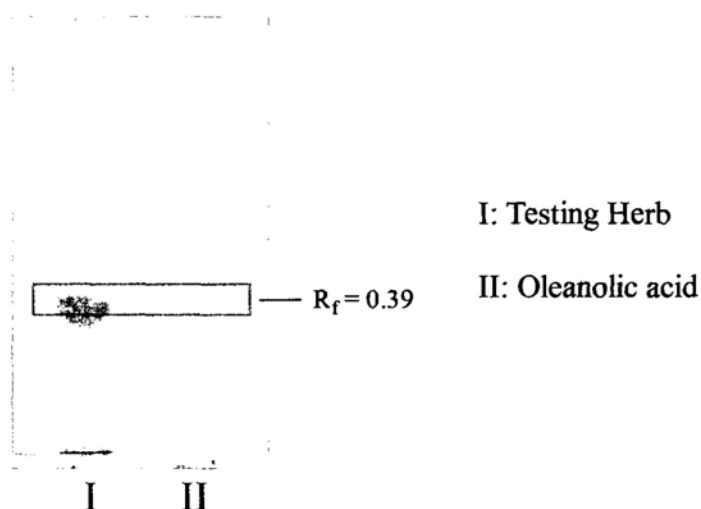


Figure 3-6 Thin Layer Chromatogram of Fructus Ligustri lucidi.

3.2.6 Fructus Lycii (枸杞子)

General description and characteristics of the herb

It is the dried ripe fruit of *Lycium barbarum* L. (Fam. Solanaceae). It is collected in summer and autumn. It is ellipsoid, 6-20 mm long, 3-10 mm in diameter. It is externally dark red, with a protrudent style scar at the apex and a white fruit stalk scar at the base. The texture is soft and viscous. The odor is slight. The taste is sweet.

Thin Layer Chromatographic analysis

Methodology

0.5 g of testing herb was boiled with 35 mL of water for 15 min. The solution was filtered and extracted with 15 mL of ethyl acetate. The ethyl acetate fraction was evaporated to dryness. The residue was dissolved in 0.5 mL ethyl acetate as the testing solution. A solution using 0.5 g of Fructus Lycii reference herb (NICPBP catalog number 121072) was prepared in the same manner as the reference solution. TLC was carried out using silica gel 60 F₂₅₄ as the stationary phase and a mixture of ethyl acetate-chloroform-formic acid (3:2:1) as the mobile phase. The solutions were applied to the plate. After developed and dried in air, the plate was examined under UV light at 365 nm.

Results

TLC profile of Fructus Lycii was shown in Figure 3-7. The spots in the chromatogram obtained from the testing solution corresponded in position to the spots in the chromatogram obtained from the reference solution.

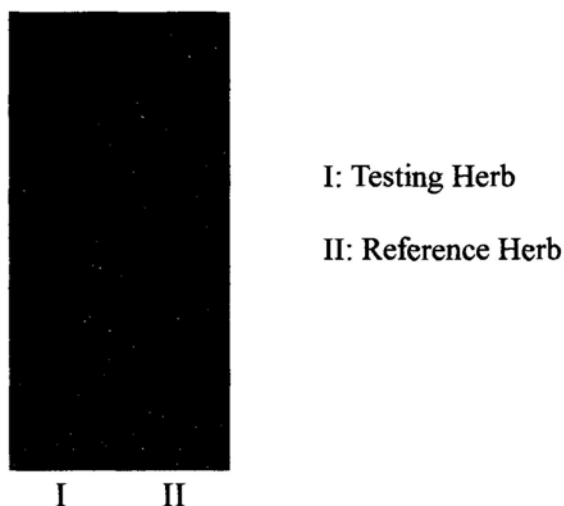


Figure 3-7 Thin Layer Chromatogram of Fructus Lycii.

3.2.7 Fructus Schisandrae chinensis (五味子)

General description and characteristics of the herb

It is the dried ripe fruit of *Schisandra chinensis* (Turcz.) Barll. (Fam. Magnoliaceae). It is collected in autumn. It is irregularly spheroidal, 5-8 mm in diameter. It is externally purplish-red, shrunken, oily with soft pulp. The odor is aromatic. The taste is pungent and slightly bitter. It is used to replenish *qi*, to promote production of body fluids, to tonify the kidney and to induce sedation.

Thin Layer Chromatographic analysis

Methodology

1 g of testing herb was heated under reflux with 20 mL chloroform for 30 min. The solution was filtered and evaporated to dryness. The residue was dissolved in 1 mL chloroform as the testing solution. A solution using 1 g of Fructus Schisandrae chinensis reference herb (NICPBP catalog number 120922) was prepared in the same manner as the reference solution. Deoxyschizandrin (NICPBP catalog number 110764, purity $\geq 98\%$) was dissolve in chloroform (1 mg/mL) to produce the standard solution. TLC was carried out using silica gel 60 F₂₅₄ as the stationary phase

and a mixture of petroleum ether (30-60°C)-ethyl acetate-formic acid (15:5:1) as the mobile phase. The solutions were applied to the plate. After developed and dried in air, the plate was examined under UV light at 254 nm.

Results

TLC profile of Fructus Schisandrae chinensis was shown in Figure 3-8. The spot in the chromatogram obtained from the testing solution corresponded in position to the spots in the chromatogram obtained from the reference solution and standard solution.

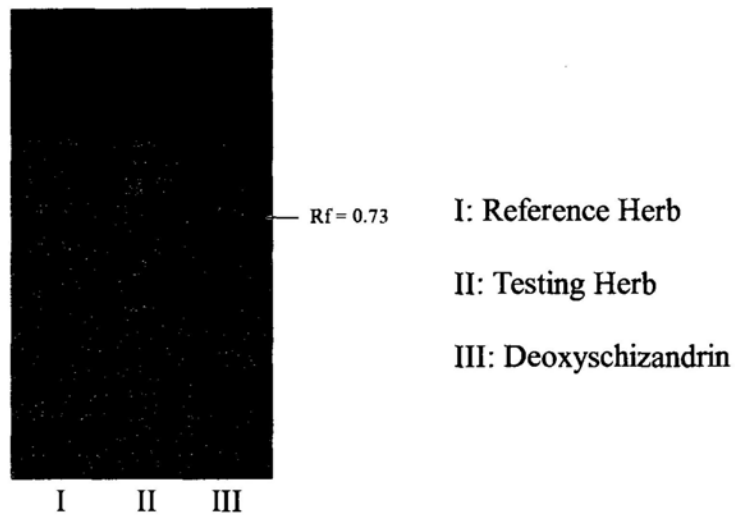


Figure 3-8 Thin Layer Chromatogram of Fructus Schisandrae chinensis.

3.2.8 Herba Gynostemmae (絞股藍)

General description and characteristics of the herb

It is whole herb of *Gynostemma pentaphyllum* (Thunberg). Stem and branches slender, angular-sulcate, glabrous or sparsely pubescent. Leaves membranous or papery, pedately 3-9-foliolate, usually 5-7-foliolate, pubescent or glabrous; leaflets ovate-oblong or lanceolate, median 3-12 × 1.5-4 cm, lateral smaller, apex acute or shortly acuminate, base attenuate, margin crenate, hispid on both surfaces, lateral veins 6-8 pairs; petiolule 1-5 mm.

Thin Layer Chromatographic analysis

Methodology

5 g of testing herb was heated under reflux with 50 mL of 75% ethanol for 3 h. The solution was filtered and evaporated to dryness. The residue was dissolved in 1 mL dehydrated ethanol as the testing solution. Panaxadiol (NICPBP catalog number 110701, purity $\geq 98\%$) and panaxatriol (NICPBP catalog number 110702, purity $\geq 95\%$) were dissolved in ethanol (2 mg/mL) to produce two standard solutions. TLC was carried out using silica gel 60 F₂₅₄ as the stationary phase and a mixture of chloroform-ethyl acetate-methanol (20:10:1) as the mobile phase. The solutions were applied to the plate. After developed and dried in air, the plate was sprayed with 10% sulfuric acid in ethanol and heated at 105°C to make the spots distinct.

Results

TLC profile of Herba Gynostemmae was shown in Figure 3-9. The spots in the chromatogram obtained from the testing solution corresponded in color and position to the spots in the chromatogram obtained from the standard solutions.

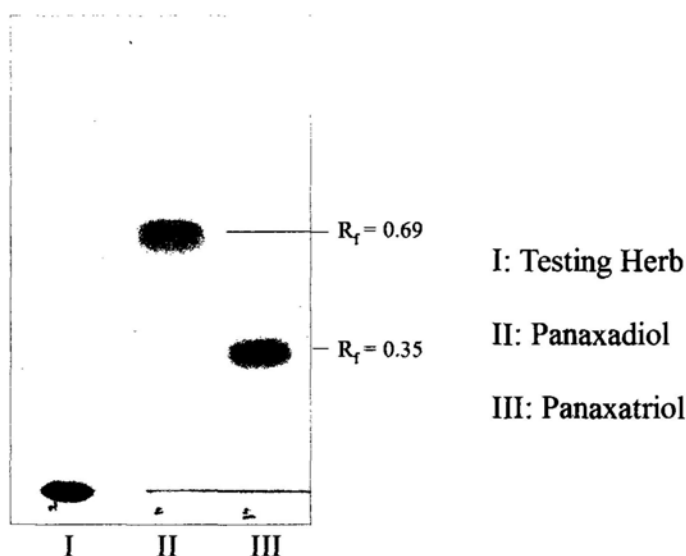


Figure 3-9 Thin Layer Chromatogram of Herba Gynostemmae.

3.2.9 Poria (茯苓)

General description and characteristics of the herb

It is the dried sclerotium of the fungus, *Poria cocos* (Schw.) Wolf (Fam. Polyporaceae). It is collected mostly in July to September. It is irregular-shaped and varied in size. The outer skin is thin and rough, in brown color. The texture is hard and compact. The odor is slight. The taste is weak.

Thin Layer Chromatographic analysis

Methodology

2 g of testing herb was sonicated with 5 mL acetone for 30 min. The solution was filtered as testing solution. A solution using 2 g of Poria reference herb (NICPBP catalog number 121117) was prepared in the same manner as the reference solution. TLC was carried out using silica gel 60 F₂₅₄ as the stationary phase and a mixture of chloroform-acetone-formic acid (20:6:0.5) as the mobile phase. The solutions were applied to the plate. After developed and dried in air, the plate was examined under UV light at 254 nm. Then, the plate was sprayed with 10% sulfuric acid in ethanol and heated at 105°C to make the spots distinct.

Results

TLC profile of Poria was shown in Figure 3-10. The spots in the chromatogram obtained from the testing solution corresponded in color and position to the spots in the chromatogram obtained from the reference solution.

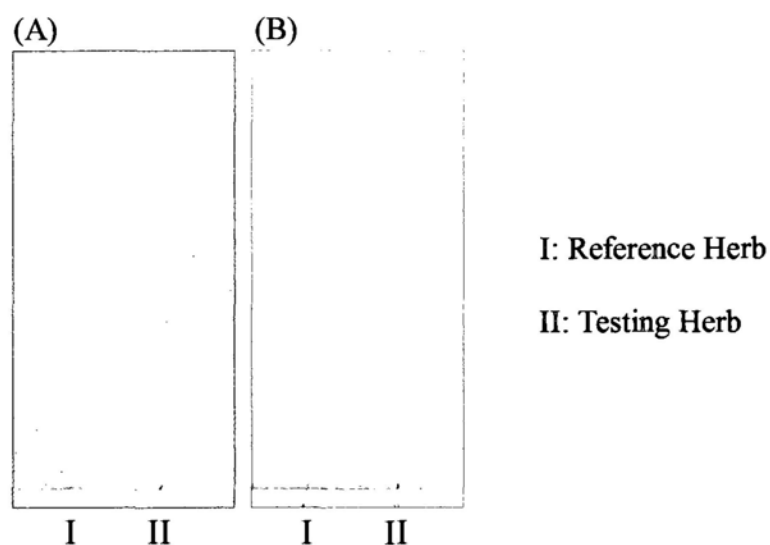


Figure 3-10 Thin Layer Chromatogram of Poria. (A) Examination under UV 254 nm. (B) Examination under visible light.

3.2.10 Radix Astragali (黃芪)

General description and characteristics of the herb

It is the dried root of *Astragalus membranaceus* (Fisch.) Bge. var. *mongholicus* (Bge.) Hsiao or *Astragalus membranaceus* (Fisch.) Bge. (Fam. Leguminosae). It is collected in spring or autumn. It is cylindrical, 30-90 mm long, 1-3.5 cm in diameter. It is externally pale brownish-yellow with irregular longitudinal wrinkles. The texture is hard, highly fibrous and starchy with radiated striations and fissures. The odor is weak. The taste is slightly sweet. It is used to reinforce *qi*, to strengthen the superficial resistance, to induce urination, to promote drainage of pus and growth of new tissue.

Thin Layer Chromatographic analysis

Methodology

3 g of the testing herb was heated in 20 mL methanol under reflux for 1 h. The solution was filtered and the filtrate was applied to a prepared neutral aluminum

oxide column (100-120 mesh, 5 g, 10-15 mm in internal diameter) and was eluted with 100 mL of 40% methanol. The eluate was collected and evaporated to dryness. The residue was dissolved in 30 mL water and extracted twice with 20 mL water-saturated n-butanol. The n-butanol fraction was combined and washed twice with 20 mL water. Butanol fraction was evaporated to dryness. The residue was dissolved in 0.5 mL methanol as testing solution. Astragaloside IV (NICPBP catalog number 110781, purity $\geq 98\%$) was dissolved in methanol (1 mg/mL) to produce the standard solution. TLC was carried out using silica gel 60 F₂₅₄ as the stationary phase and a mixture of chloroform-methanol-water (20:5:2) as the mobile phase. The solutions were applied to the plate. After developed and dried in air, the plate was examined under UV light at 365 nm. Then, the plate was sprayed with 10% sulfuric acid in ethanol and heated at 105°C to make the spots distinct.

Results

TLC profile of Radix Astragali was shown in Figure 3-11. The spot in the chromatogram obtained from the testing solution corresponded in color and position to the spot in the chromatogram obtained from the standard solution.

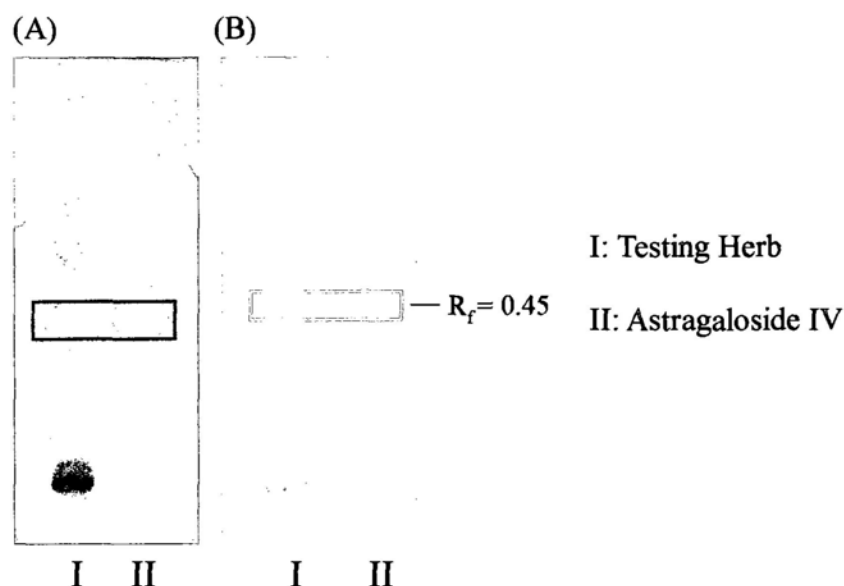


Figure 3-11 Thin Layer Chromatogram of Radix Astragali. (A) Examination under UV 365 nm. (B) Examination under visible light.

3.2.11 Radix Codonopsis (黨參)

General description and characteristics of the herb

It is the dried root of *Codonopsis pilosula* (Franch.) Nannf., *Codonopsis pilosula* Nannf. var. *modesta* (Nannf.) L. T. Shen or *Codonopsis tangshen* Oliv. (Fam. Campanulaceae). It is collected in autumn. It is cylindrical, slightly curved, 10-35 cm long, 0.5-2.5 cm in diameter. It is externally yellowish-brown. Dense transverse annulations occurs below the root stock with distinct longitudinal wrinkles. The texture is slightly hard. The odor is aromatic. The taste is sweet. It is used to reinforce *qi* and to invigorate the function of spleen and lung.

Thin Layer Chromatographic analysis

Methodology

1 g of testing herb was sonicated with 25 mL methanol for 30 min. The solution was filtered and evaporated to dryness. The residue was dissolved in 2 mL water and

applied to a C18 SEP-PAK cartridge (500 mg, column equilibrated with 10 mL methanol and then 10 mL of 20% methanol). It was eluted with 5 mL of 20% methanol followed by 5 mL methanol. The methanol eluate was collected and concentrated to 1 mL as testing solution. A solution using 1 g of Radix Codonopsis reference herb (NICPBP catalog number 121057) was prepared in the same manner as the reference solution. TLC was carried out using silica gel 60 F₂₅₄ as the stationary phase and a mixture of n-butanol-acetic acid-water (7:1:0.5) as the mobile phase. The solutions were applied separately to the plate. After developed and dried in air, the plate was examined under UV light at 365 nm. Then, the plate was sprayed with 10% sulfuric acid in ethanol and heated at 105°C to make the spots distinct.

Results

TLC profile of Radix Codonopsis was shown in Figure 3-12. The spots in the chromatogram obtained from the testing solution corresponded in color and position to the spots in the chromatogram obtained from the reference solution.

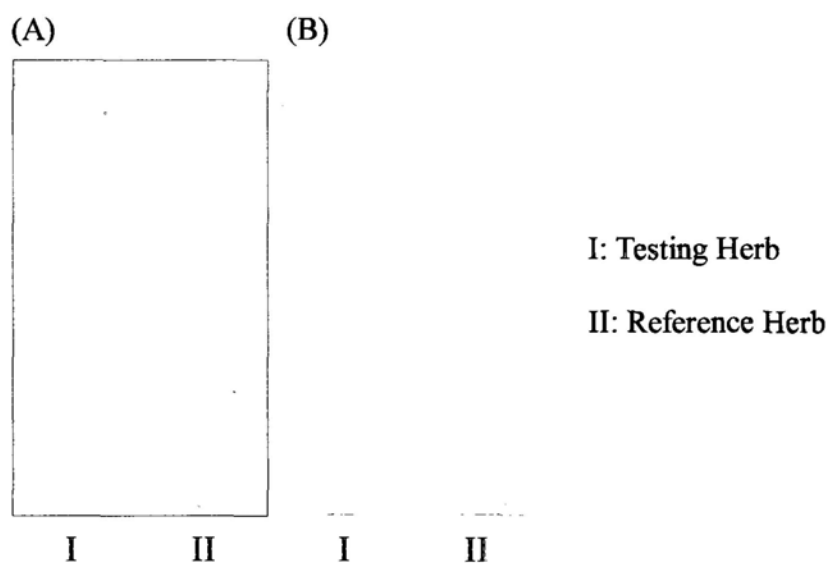


Figure 3-12 Thin Layer Chromatogram of Radix Codonopsis. (A) Examination under UV 365nm. (B) Examination under visible light.

3.2.12 Radix Notoginseng (三七)

General description and characteristics of the herb

It is the dried root of *Panax notoginseng* (Burk.) F. H. Chen (Fam. Araliaceae). It is collected in autumn. It is subconical, 1-6 cm long, 1-4 cm in diameter. It is externally grayish-brown with longitudinal wrinkles. The texture is heavy and compact. The odor is slight. The taste is bitter and then sweetish.

Thin Layer Chromatographic analysis

Methodology

0.5 g of testing herb was added with 5 drops of water and 5 mL of water-saturated n-butanol. The solution was shaken for 10 min and allowed to stand for 2 h. Another 15 mL n-butanol-saturated water was added and let stand to fractionate. The butanol fraction was isolated and evaporated to dryness. The residue was dissolved in 1 mL methanol as testing solution. Ginsenoside Rb1 (NICPBP catalog number 110704, purity \geq 98%), Ginsenoside Re (NICPBP catalog number 110754, purity \geq 98%), Ginsenoside Rg1 (NICPBP catalog number 110703, purity \geq 98%) and Notoginsenoside R1 (NICPBP catalog number 110745, purity \geq 98%) were dissolved in methanol (0.5 mg/mL), respectively, to produce four standard solutions. TLC was carried out using silica gel 60 F₂₅₄ as the stationary phase and the lower layer of a mixture of chloroform-ethyl acetate-methanol-water (15:40:22:10, standing for 2 h under 10°C) as the mobile phase. The solutions were applied to the plate. After developed and dried in air, the plate was examined under UV light at 365 nm. Then, the plate was sprayed with 10% sulfuric acid in ethanol and heated at 105°C to make the spots distinct.

Results

TLC profile of Radix Notoginseng was shown in Figure 3-13. The spot in the

chromatogram obtained from the testing solution corresponded in color and position to the spot in the chromatogram obtained from the standard solutions.

(B)

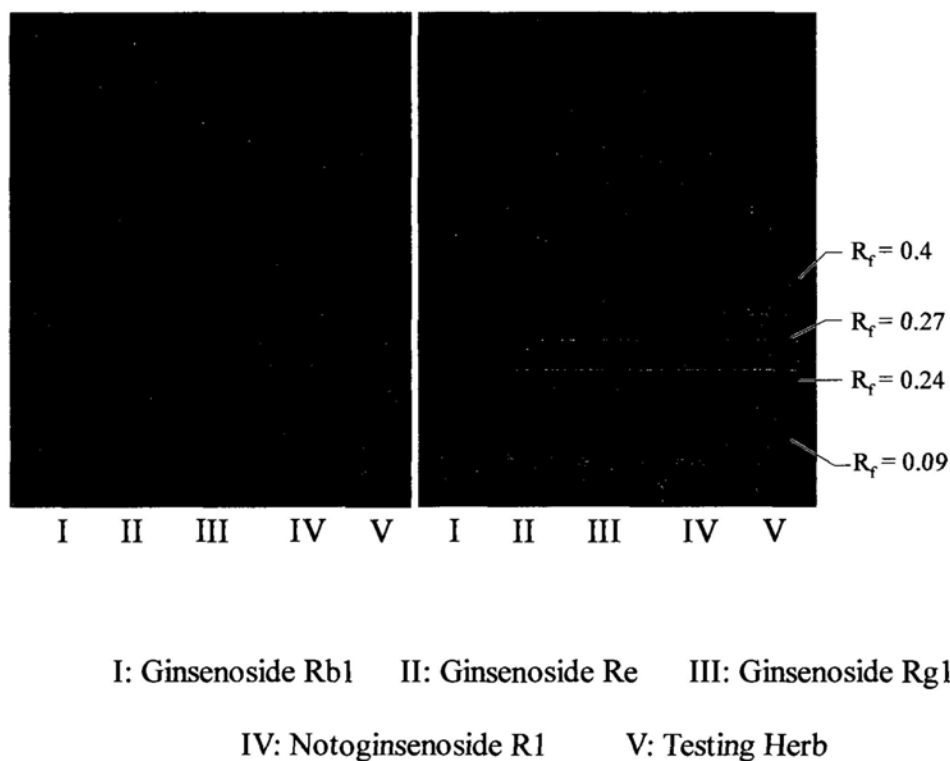


Figure 3-13 Thin Layer Chromatogram of Radix Notoginseng.

3.2.13 Radix Ophiopogonis (麥冬)

General description and characteristics of the herb

It is the dried root tuber of *Ophiopogon japonicus* (Thunb.) Ker-Gawl. (Fam. Liliaceae). It is collected in summer. It is fusiform, 1.5-3 cm long, 3-6 mm in diameter. It is externally yellowish-white with longitudinal and fine wrinkle. The texture is tough. The odor is slightly aromatic. The taste is sweet and bitter. It is used to nourish *yin*, to promote production of body fluids, to moisten the lung and to

anchor the mind.

Thin Layer Chromatographic analysis

Methodology

2 g of testing herb was macerated with 20 mL of a mixture of chloroform-methanol (7:3) for 3 h and sonicated for 30 min. The solution was filtered and evaporated to dryness. The residue was dissolved in 0.5 mL chloroform as the testing solution. A solution using 2 g of Radix Ophiopogonis reference herb (NICPBP catalog number 121013) was prepared in the same manner as the reference solution. TLC was carried out using silica gel 60 F₂₅₄ as the stationary phase and a mixture of toluene-methanol-glacial acetic acid (80:12.5:0.1) as the mobile phase. The solutions were applied to the plate. After developed and dried in air, the plate was examined under UV light at 365 nm. Then, the plate was sprayed with 10% sulfuric acid in ethanol and heated at 105°C to make the spots distinct.

Results

TLC profile of Radix Ophiopogonis was shown in Figure 3-14. The spots in the chromatogram obtained from the testing solution corresponded in color and position to the spots in the chromatogram obtained from the reference solution.

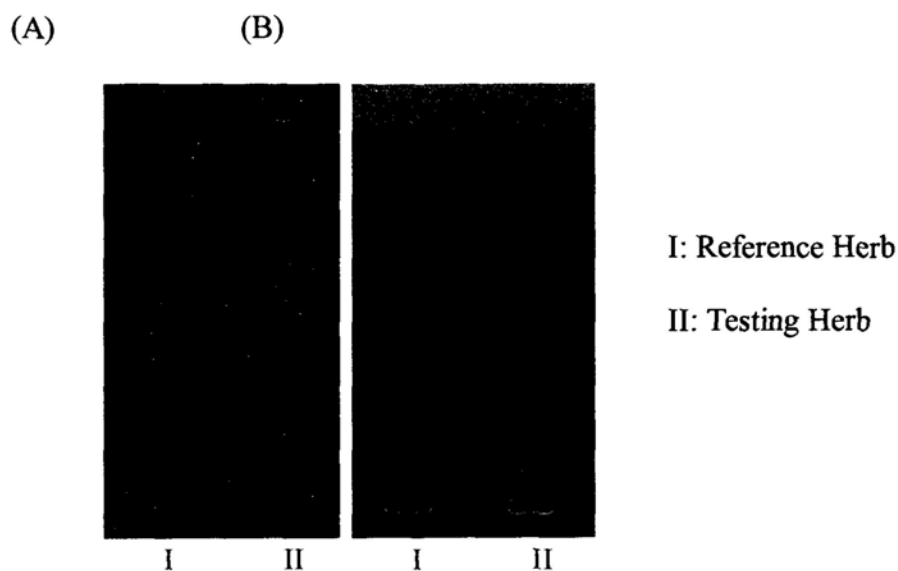


Figure 3-14 Thin Layer Chromatogram of Radix Ophiopogonis. (A) Examination under UV 365nm. (B) Examination under visible light.

3.2.14 Radix Panacis quinquefolii (西洋参)

General description and characteristics of the herb

It is the dried root of *Panax quinquefolium* L. (Fam. Araliaceae). All the commercial supplies are obtained from cultivated forms. It is collected in autumn. It is cylindrical or conical, 3-12 cm long, 0.8-2 cm in diameter. It is externally pale yellowish-brown or yellowish-white. It exhibits transverse-striations and linear lenticel-like protrudings. It showed fine and dense longitudinal wrinkles and rootlet scars. The texture is heavy and hard with even fracture. The odor is slight and characteristic. The taste is slightly bitter and sweet. It is used to tonify *qi* and nourish *yin*, to remove *heat* and to promote production of body fluids.

Thin Layer Chromatographic analysis

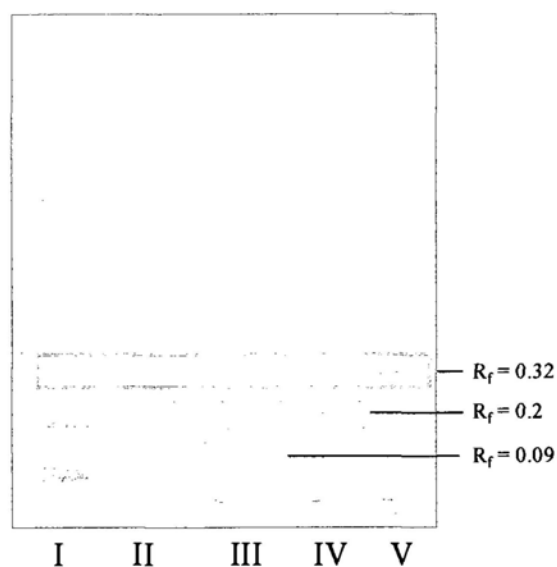
Methodology

1 g of testing herb was ground into powder and heated under reflux with 25 mL

methanol for 1 h. The solution was filtered and evaporated to dryness. The residue was dissolved in 20 mL water. The solution was extracted by shaking twice with 10 mL ethyl ether. Water layer was extracted again with 15 mL water-saturated n-butanol for three times. Butanol fractions were combined and washed with 10 mL water twice. Butanol layer was collected and evaporated to dryness. The residue was dissolved in 1 mL methanol as the testing solution. A solution using 1 g of *Radix Panacis quinquefolii* reference herb (NICPBP catalog number 120997) was prepared in the same manner as the reference solution. Ginsenoside Rb1 (NICPBP catalog number 110704, purity $\geq 98\%$), Ginsenoside Re (NICPBP catalog number 110754, purity $\geq 98\%$) and Ginsenoside Rg1 (NICPBP catalog number 110703, purity $\geq 98\%$) were dissolved in methanol (2 mg/mL), respectively, to produce three standard solutions. TLC was carried out using silica gel 60 F₂₅₄ as the stationary phase and the lower layer of a mixture of chloroform-ethyl acetate-methanol-water (15:40:22:10, standing for 2 h under 10°C) as the mobile phase. Two microliter of each of the solutions was applied to the plate. After developed and dried in air, the plate was sprayed with a 10% solution of sulfuric acid in ethanol and heated at 105°C to make the spots distinct.

Results

TLC profile of *Radix Panacis quinquefolii* was shown in Figure 3-15. The spots in the chromatogram obtained from the testing solution corresponded in color and position to the spots in the chromatogram obtained from the reference solution and standard solutions.



I: Reference Herb II: Testing Herb III: Ginsenoside Rb1
 IV: Ginsenoside Re V: Ginsenoside Rg1

Figure 3-15 Thin Layer Chromatogram of *Radix Panacis quinquefolii*.

3.2.15 *Radix Platycodonis* (桔梗)

General description and characteristics of the herb

It is the dried root of *Platycodon grandiflorum* (Jacq.) A. DC. (Fam. Campanulaceae). It is collected in spring and autumn. It is cylindrical and tapering downwards, slightly twisted, 7-20 cm long, 0.7-2 cm in diameter. It is externally white or pale yellowish-white. It is longitudinally twisted-furrowed with transverse lenticel-like scars and with transverse striations at the upper part. The texture is fragile with uneven fracture. The odor is slight. The taste is slightly sweet and then bitter. It is used to relieve cough, to ease sore throat, to promote phlegm expectoration and drainage of pus.


Thin Layer Chromatographic analysis

Methodology

20 mL of the mixture of 7% ethanolic sulfuric acid water (1:3) was added to 1 g of testing herb and heated under reflux for 3 h. The extract was filtered and the filtrate was extracted twice with 20 mL chloroform. Chloroform extracts were combined and washed with 30 mL water. Chloroform fraction was dehydrated with anhydrous sodium sulfate and then filtered. The filtrate was evaporated to dryness. The residue was dissolved in 1 mL methanol as the testing solution. A solution using 1 g of Radix Platycodonis reference herb (NICPBP catalog number 121028) was prepared in the same manner as the reference solution. TLC was carried out using silica gel 60 F₂₅₄ as the stationary phase and a mixture of chloroform-ether (1:1) as the mobile phase. Ten microliter of each of the solutions was applied to the plate. After developed and dried in air, the plate was sprayed with 10% solution of sulfuric acid in ethanol and heated at 105°C to make the spots distinct.

Results

TLC profile of Radix Platycodonis was shown in Figure 3-16. The spots in the chromatogram obtained from the testing solution corresponded in color and position to the spots in the chromatogram obtained from the reference solution.



I II
I: Testing Herb II: Reference Herb

Figure 3-16 Thin Layer Chromatogram of Radix Platycodonis.

3.2.16 Radix Puerariae (葛根)

General description and characteristics of the herb

It is the dried root of *Pueraria thomsonii* Benth. (Fam. Leguminosae). It is collected in autumn and winter. It is cylindrical, 12-15 cm long, 4-8 cm in diameter. It is externally yellowish-white. The texture is heavy, hard and starchy. Transversely cut surface shows pale brown concentric rings formed by fibers. Longitudinally cut surface shows several longitudinal striations formed by fibers. The odor is slight. The taste is slightly sweet. It is used to release muscles, to encourage production of body fluids, to induce eruptions and to elevate spleen-yang to arrest diarrhea.

Thin Layer Chromatographic analysis

Methodology

0.8 gram of test herb was ground into powder and macerated in 10 mL methanol for 2 h. The solution was filtered and evaporated to dryness. The residue was dissolved in 0.5 mL methanol as the testing solution. Puerarin (NICPBP catalog number 110752, purity $\geq 98\%$) was dissolved in methanol (1 mg/mL) to produce the standard

solution. TLC was carried out using silica gel 60 F₂₅₄ as the stationary phase and a mixture of chloroform-methanol-water (7:2.5:0.25) as the mobile phase. Ten microliter of each of the solutions was applied to the plate. After developed and dried in air, the plate was examined under UV light at 254 nm.

Results

TLC profile of Radix Puerariae was shown in Figure 3-17. The spot in the chromatogram obtained from the testing solution corresponded in color and position to the spot in the chromatogram obtained from the standard solution.

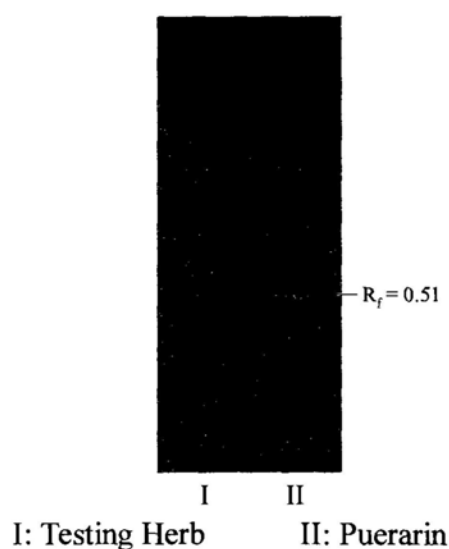


Figure 3-17 Thin Layer Chromatogram of Radix Puerariae.

3.2.17 Radix Rehmanniae (地黃)

General description and characteristics of the herb

It is the fresh root tuber of *Rehmannia glutinosa* Libosch. (Fam. Scrophulariaceae). It is collected in autumn. It is spat-shaped, 8-24 cm long, 2-9 cm in diameter. It is externally pale reddish-yellow with curved longitudinal wrinkles and bud scars. The texture is fleshy, fracture shows pale yellow-white bark with orange-red oil dots. The odor is slight. The taste is slightly sweet and bitter.

Thin Layer Chromatographic analysis

Methodology

2 gram of testing herb was cut into small pieces and heated under reflux with 20 mL methanol for 30 min. The solution was filtered and evaporated to dryness. The residue was dissolved with 1 mL methanol as the testing solution. A solution using 1 g of Radix Rehmanniae reference herb (NICPBP catalog number 121180) was prepared in the same manner as the reference solution. TLC was carried out using silica gel 60 F₂₅₄ as the stationary phase and a mixture of chloroform-methanol-water (14:8:1) as the mobile phase. Five microliter of each of the solutions was applied to the plate. After developed and dried in air, the plate was sprayed with anisaldehyde TS and heated at 105°C to make the spots distinct.

Results

TLC profile of Radix Rehmanniae was shown in Figure 3-18. The spots in the chromatogram obtained from the test solution corresponded in color and position to the spots in the chromatogram obtained from the reference solution.



I: Reference Herb II: Testing Herb

Figure 3-18 Thin Layer Chromatogram of Radix Rehmanniae.

3.2.18 Radix et Rhizoma Rhei (大黃)

General description and characteristics of the herb

It is the dried root and rhizome of *Pheum palmatum* L., *Rheum tanguticum* Maxim. ex Balf. or *Rheum officinale* Baill. (Fam. Polygonaceae). It is collected in late autumn. It is conical, ovoid or irregular pieces, 3-17 cm long, 3-10 cm in diameter. It is externally yellowish-brown with brownish-black patches of cork. The texture is compact with reddish-brown fracture. The odor is aromatic. The taste is bitter and slightly astringent.

Thin Layer Chromatographic analysis

Methodology

0.1 g of the testing herb was cut into small pieces and soaked with 20 mL of methanol for 1 h. After filtration, 5 mL of the filtrate was evaporated to dryness. The residue was dissolved in 10 mL of water and then 1 mL of hydrochloric acid was added. The mixture was heated under reflux for 30 min. The mixture was extracted twice with 20 mL ether. The ether extracts were combined and evaporated to dryness. The residue was dissolved in 1 mL chloroform as testing solution. Rhein (NICPBP catalog number 110757, purity $\geq 98\%$) was dissolved in methanol (1 mg/mL) to produce the standard solution. TLC was carried out using silica gel 60 F₂₅₄ as the stationary phase and a mixture of petroleum ether-ethyl acetate-formic acid (15:5:1) as the mobile phase. Four microliter of each of the solutions was applied to the plate. After developed and dried in air, the plate was examined under UV at 365 nm and visible light.

Results

TLC profile of Radix et Rhizoma Rhei was shown in Figure 3-19. The spot in the chromatogram obtained from the testing solution corresponded in color and position

to the spot in the chromatogram obtained from the standard solution.

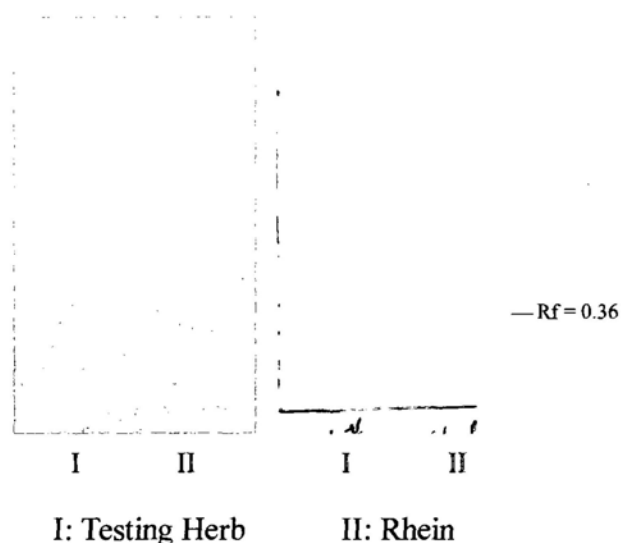


Figure 3-19 Thin Layer Chromatogram of Radix et Rhizoma Rhei.

3.2.19 Radix Salviae miltiorrhizae (丹参)

General description and characteristics of the herb

It is the dried root of *Salvia miltiorrhiza* Bge. (Fam. Labiatae). It is collected in spring or autumn. It is long cylindrical, slightly curved and branched with rootlets, 10-20 cm long, 0.3-1 cm in diameter. It is externally brownish-red, rough and longitudinally wrinkled. The texture is hard. The odor is slight. The taste is slightly bitter and astringent.

Thin Layer Chromatographic analysis

Methodology

1 g of testing herb was ground into powder and sonicated with 5 mL ether for 1 hour. After filtration, the filtrate was evaporated to dryness. The residue was dissolved in 1 mL ethyl acetate as the testing solution. Tanshinone IIA (NICPBP catalog number 110766, purity $\geq 98\%$) was dissolved in ethyl acetate (2 mg/mL) to produce the standard solution. TLC was carried out using silica gel 60 F₂₅₄ as the stationary phase

and a mixture of hexane-ethyl acetate (19:1) as the mobile phase. Five microliter of each of the solutions was applied to the plate. After developed and dried in air, the plate was examined under visible light.

Results

TLC profile of Radix Salviae miltiorrhizae was shown in Figure 3-20. The spot in the chromatogram obtained from the testing solution corresponded in color and position to the spot in the chromatogram obtained from the standard solution.

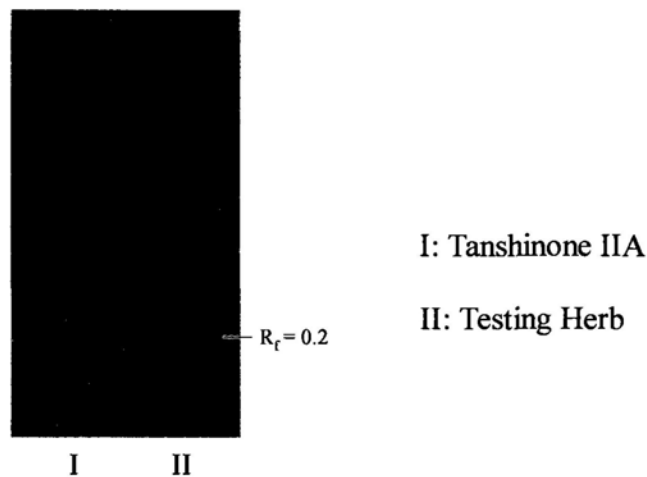


Figure 3-20 Thin Layer Chromatogram of Radix Salviae miltiorrhizae.

3.2.20 Radix Trichosanthis (天花粉)

General description and characteristics of the herb

It is the dried root of *Trichosanthes kirilowii* Maxim. or *Trichosanthes rosthornii* Harms (Fam. Cucurbitaceae). It is collected in autumn and winter. It is irregular cylindrical, 8-16 cm long, 1.5-5.5 cm in diameter. It is externally yellowish-white with longitudinal wrinkles and rootlet scars. The texture is compact and starchy. The odor is slight. The taste is slightly bitter. It is used to remove *heat*, to promote production of body fluids and to facilitate the drainage of pus.

Thin Layer Chromatographic analysis

Methodology

5 g of testing herb was ground into powder and sonicated with 15 mL of 75% ethanol for 30 min. The solution was filtered and the filtrate was used as the testing solution. L-citrulline (NICPBP catalog number 110875, purity $\geq 95\%$) was dissolved in 75% ethanol (1 mg/mL) to produce the standard solution. TLC was carried out using silica gel 60 F₂₅₄ as the stationary phase and a mixture of n-butanol-dehydrated ethanol-glacial acetic acid-water (8:2:2:3) as the mobile phase. Six microliter of test solution and 1 μ L of the standard solution were applied to the plate. After developed and dried in air, the plate was sprayed with ninhydrin TS and heated at 105°C to make the spots distinct.

Results

TLC profile of Radix Trichosanthis was shown in Figure 3-21. The spot in the chromatogram obtained from the testing solution corresponded in color and position to the spot in the chromatogram obtained from the standard solution.

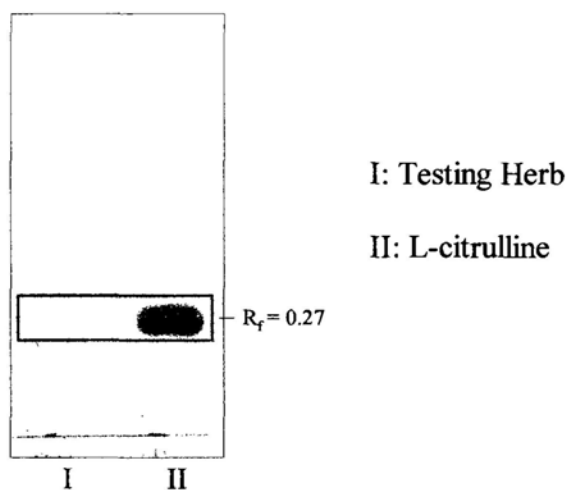


Figure 3-21 Thin Layer Chromatogram of Radix Trichosanthis.

3.2.21 Rhizoma Alismatis (澤瀉)

General description and characteristics of the herb

It is the dried tuber of *Alisma orientalis* (Sam.) Juzep. (Fam. Alismataceae). It is collected in winter. It is subspherical, 2-7 cm long, 2-6 cm in diameter. It is externally yellowish-white with irregular shallow furrows. The texture is compact, starchy with numerous small pores. The odor is slight. The taste is slightly bitter. It is used to cause urination and to remove *damp-heat*.

Thin Layer Chromatographic analysis

Methodology

0.5 g of testing herb was ground into powder and sonicated with 20 mL methanol for 20 min. The solution was filtered and evaporated to dryness. The residue was dissolved in 1 mL methanol as the testing solution. A solution using 0.5 g of Rhizoma Alismatis reference herb (NICPBP catalog number 121081) was prepared in the same manner as the reference solution. TLC was carried out using silica gel 60 F₂₅₄ as the stationary phase and a mixture of toluene-ethyl acetate-methanol (8:1:1) as the mobile phase. The solutions were applied separately to the plate. After developed and dried in air, the plate was sprayed with 10% molybdato-phosphoric acid in ethanol and heated at 110°C to make the spots distinct.

Results

TLC profile of Rhizoma Alismatis was shown in Figure 3-22. The spots in the chromatogram obtained from the testing solution corresponded in color and position to the spots in the chromatogram obtained from the reference solution.

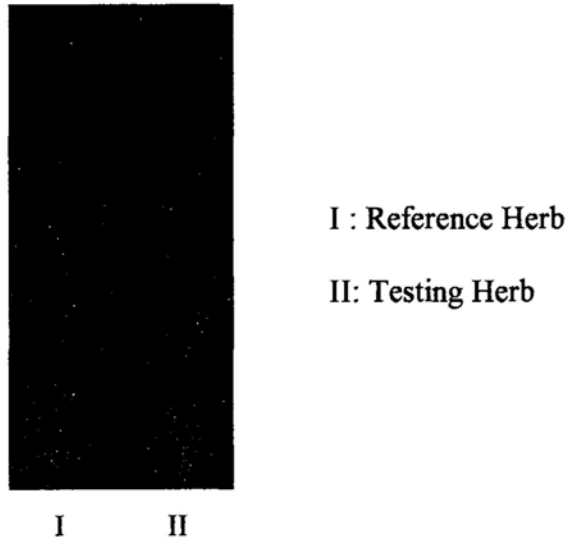


Figure 3-22 Thin Layer Chromatogram of Rhizoma Alismatis.

3.2.22 *Rhizoma Anemarrhenae* (知母)

General description and characteristics of the herb

It is the dried rhizome of *Anemarrhena asphodeloides* Bge. (Fam. Liliaceae). It is collected in spring or autumn. It is spat-shaped, 3-15 cm long, 0.8-1.5 cm in diameter. It is externally yellowish-brown. The upper part exhibits a concave groove. The lower part raised and shriveled. The texture is hard. The odor is slight. The taste is slightly sweet and bitter. It is used to remove *heat* and quench *fire*, to promote production of body fluids and to relieve dryness syndrome.

Thin Layer Chromatographic analysis

Methodology

2 g of testing herb was heated under reflux with 20 mL ethanol for 40 min. One milliliter of hydrochloric acid (37%) was added to 10 mL supernatant and heated under reflux for 1 hour. The solution was concentrated to 5 mL and added with 10 mL water. The solution was extracted with 20 mL toluene and toluene fraction was evaporated to dryness. The residue was dissolved in 2 mL toluene as the testing

solution. Sarsasapogenin (NICPBP catalog number 110744, purity $\geq 98\%$) was dissolved in toluene (5 mg/mL) to produce the standard solution. TLC was carried out using silica gel 60 F₂₅₄ as the stationary phase and a mixture of toluene-acetone (9:1) as the mobile phase. The solutions were applied to the plate separately. After developed and dried in air, the plate was sprayed with a mixture of 8% solution of vanillin in ethanol and sulfuric acid (0.5:5) and heated at 100°C to make the spots distinct.

Results

TLC profile of Rhizoma Anemarrhenae was shown in Figure 3-23. The spot in the chromatogram obtained from the testing solution corresponded in color and position to the spot in the chromatogram obtained from the standard solution.

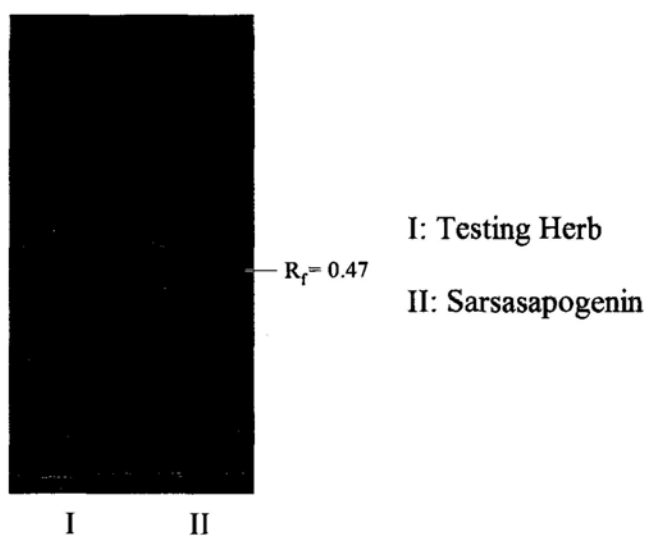


Figure 3-23 Thin Layer Chromatogram of Rhizoma Anemarrhenae.

3.2.23 Rhizoma Atractylodis (蒼朮)

General description and characteristics of the herb

It is the dried rhizome of *Atractylodes lancea* (Thunb.) DC. or *Atractylodes chinensis* (DC.) Koidz. (Fam. Composite). It is collected in spring and autumn. It is nodular-

cylindrical, 3-10 cm long, 1-2 cm in diameter. It is externally grayish-brown, wrinkled, transversely twisted-lined. The texture is compact, scattered with many cavities. The odor is characteristic. The taste is sweet, pungent and bitter. It is used to remove *dampness*, to invigorate the function of the spleen and to improve eyesight.

Thin Layer Chromatographic analysis

Methodology

0.5 g of testing herb was sonicated with 2 mL n-hexane for 15 min. The solution was filtered as the testing solution. A solution using 0.5 g of Rhizoma Atractylodis reference herb (NICPBP catalog number 120932) was prepared in the same manner as the reference solution. TLC was carried out using silica gel 60 F₂₅₄ as the stationary phase and a mixture of petroleum ether (60-90°C)-ethyl acetate (20:1) as the mobile phase. The solutions were applied separately to the plate. After developed and dried in air, the plate was sprayed with 5% solution of p-dimethylaminobenzaldehyde in an ethanol solution containing 10% sulfuric acid and heated at 105°C to make the spots distinct.

Results

TLC profile of Rhizoma Alismatis was shown in Figure 3-24. The spots in the chromatogram obtained from the testing solution corresponded in color and position to the spots in the chromatogram obtained from the reference solution.

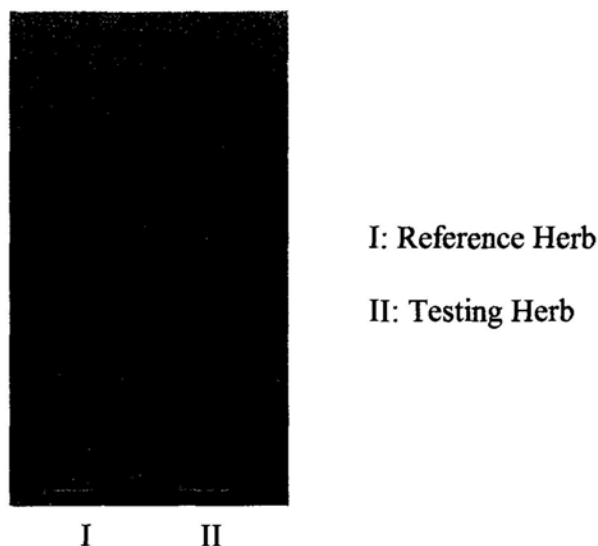


Figure 3-24 Thin Layer Chromatogram of Rhizoma Atractylodis.

3.2.24 Rhizoma Coptidis (黃蓮)

General description and characteristics of the herb

It is the dried rhizome of *Coptis chinensis* Franch., *Coptis deltoidea* C. Y. Cheng et Hsiao or *Coptis teeta* Wall. (Fam. Ranunculaceae). It is cylindrical, slightly curved, 4-8 cm long, 0.5-1 cm in diameter. It is externally grayish-yellow, rough, with irregular nodular protrudings. The texture is hard. The odor is slight. The taste is very bitter. It is used to remove *damp-heat*, to quench *fire* and to counteract toxicity.

Thin Layer Chromatographic analysis

Methodology

0.1 g of test herb was heated under reflux with 5 mL methanol for 15 min. The solution was filtered as the testing solution. A solution using 0.1 g of Rhizoma Coptidis reference herb (NICPBP catalog number 120913) was prepared in the same manner as the reference solution. Berberine hydrochloride (NICPBP catalog number 110713, purity $\geq 98\%$) was dissolved in methanol (0.5 mg/mL) to produce the standard solution. TLC was carried out using silica gel 60 F₂₅₄ as the stationary phase

and a mixture of ethyl acetate-acetone-formic acid-water (10:6:1:1) as the mobile phase. The solutions were applied separately to the plate. After developed and dried in air, the plate was examined under UV light at 365 nm.

Results

TLC profile of Rhizoma Coptidis was shown in Figure 3-25. The spot in the chromatogram obtained from the testing solution corresponded in position to the spot in the chromatogram obtained from the reference solution and standard solution.

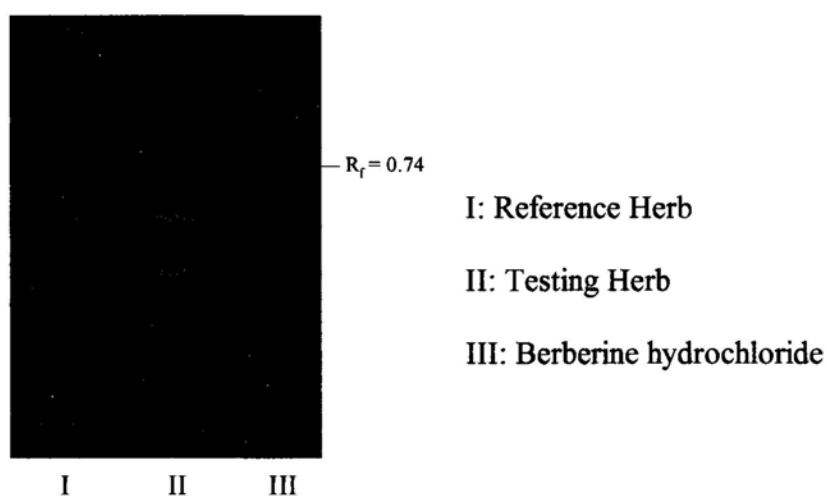


Figure 3-25 Thin Layer Chromatogram of Rhizoma Coptidis.

3.2.25 Rhizoma Polygonati (黄精)

General description and characteristics of the herb

It is the dried rhizome of *Polygonatum kingianum* Coll. et Hemsl., *Polygonatum sibiricum* Red., or *Polygonatum cyrtonema* Hua (Fam. Liliaceae). It is collected in spring or autumn. It is fleshy tuberculated, up to more than 10 cm long, 3-6 cm wide, 2-3 cm thick. It is externally yellowish-brown with ring-shaped nodes. The texture is hard and tenacious. The odor is slight. The taste is sweet. It is used to reinforce *qi*, to nourish *yin*, to invigorate the function of spleen and to moisten the lung.

Thin Layer Chromatographic analysis

Methodology

3 g of testing herb was heated under reflux with 50 mL methanol for 4 h. Methanol was discarded and the residue was heated under reflux with 20 mL water. The solution was filtered and the filtrate was added with appropriate amount of ethanol to make to 65% ethanol. White precipitate was observed and the solution was refrigerated overnight. After filtration, the precipitate was added with 10 mL 1M sulfuric acid and boiled for 2 h. Then, 30 mL water was added to the solution and barium carbonate was used to adjust the pH to 6-7. After filtration, the filtrate was added with SP sepharose and incubated overnight. Then, the solution was centrifuged to remove the sepharose and the supernatant was concentrated to 1 mL as testing solution. Galacturonic acid (NICPBP catalog number 111640, purity \geq 98%) and mannose (NICPBP catalog number 140651, purity \geq 98%) was dissolved in water (5 mg/mL) separately as standard solutions. TLC was carried out using silica gel 60 F₂₅₄ as the stationary phase and a mixture of n-butanol-acetone-water (4:5:1) as the mobile phase. The solutions were applied separately to the plate. After developed and dried in air, the plate was sprayed with aniline phthalate solution and heated at 105°C to make the spots distinct.

Results

TLC profile of Rhizoma Polygonati was shown in Figure 3-26. The spot in the chromatogram obtained from the testing solution corresponded in color and position to the spots in the chromatogram obtained from the standard solutions.

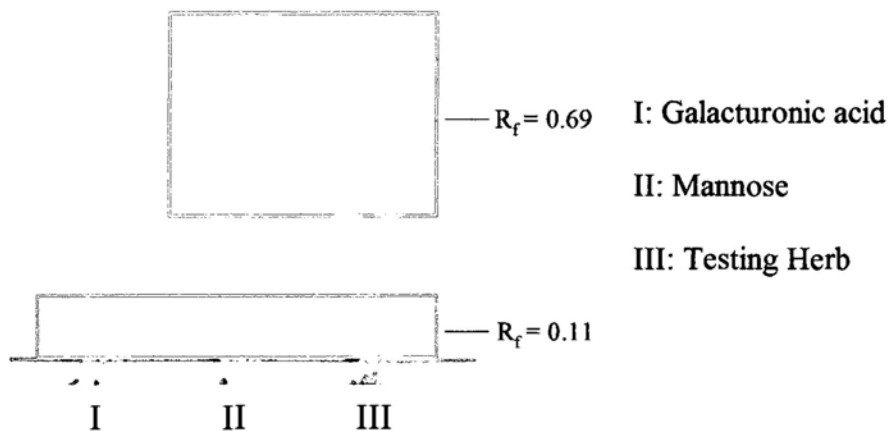


Figure 3-26 Thin Layer Chromatogram of Rhizoma Polygonati.

3.2.26 Rhizoma Polygonati odorati (玉竹)

General description and characteristics of the herb

It is the dried rhizome of *Polygonatum odoratum* (Mill.) Druce (Fam. Liliaceae). It is collected in autumn. It is long cylindrical, 4-18 cm long, 0.3-1.6 cm in diameter. It is externally yellowish-white, translucent with longitudinally wrinkles. The texture is slightly soft. The odor is slight. The taste is sweet. It is used to nourish *yin*, to promote production of body fluid and to relieve dryness syndrome.

Thin Layer Chromatographic analysis

Methodology

The method in preparing testing solution and standard solutions as well as the method of detection for Rhizoma Polygonati odorati was the same as that of Rhizoma Polygonati (Section 3.2.25).

Results

TLC profile of Rhizoma Polygonati Odorati was shown in Figure 3-27. The spot in the chromatogram obtained from the testing solution corresponded in color and position to the spots in the chromatogram obtained from the standard solutions.

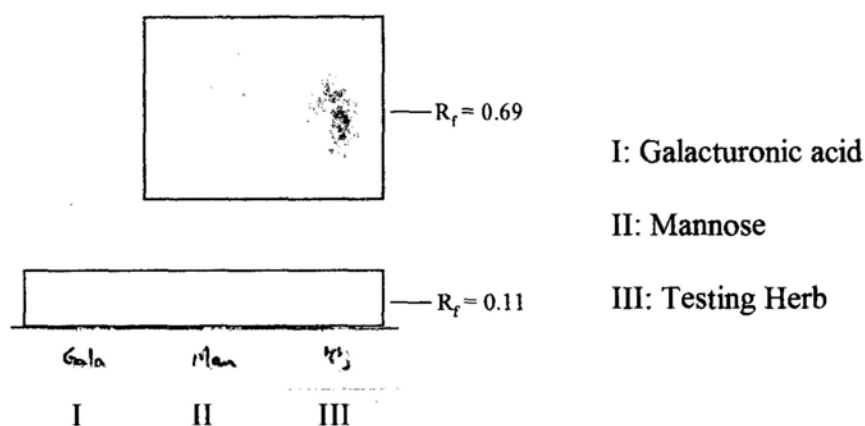


Figure 3-27 Thin Layer Chromatogram of Rhizoma Polygonati Odorati.

3.2.27 Rhizoma et Radix Polygoni Cuspidati (虎杖)

General description and characteristics of the herb

It is the dried rhizome and root of *Polygonum cuspidatum* Sieb. Et Zucc. (Fam. Polygonaceae). It is collected in spring or autumn. It is mostly in irregular thick slices, 1-7 cm long and 0.5-2.5 cm in diameter. It is externally brown, with longitudinal wrinkles and rootlet scars. In transversely cut surface, the bark is relatively thin but the wood is broad, brownish-yellow with radial rays. The pith in rhizome is septated or hollowed. The texture is hard. The odor is slight. The taste is slightly bitter and astringent.

Thin Layer Chromatographic analysis

Methodology

1 g of testing herb was sonicated with 25 mL methanol for 15 min. The solution was filtered and evaporated to dryness. The residue was added with 20 mL sulfuric acid (2.5 M), heated in water bath for 30 min and cooled down. The mixture was extracted twice with 20 mL chloroform. Chloroform fractions were collected, pooled

together and evaporated to dryness. Residue was dissolved with 1 mL chloroform as the testing solution. A solution using 1 g of Rhizoma et Radix Polygoni Cuspidati reference herb (NICPBP catalog number 120980) was prepared in the same manner as the reference solution. Emodin (Sigma-Aldrich catalog number E7881, purity \geq 90%) and physcion (BioChemika catalog number 17797, purity \geq 98%) were dissolved in methanol (1 mg/mL), respectively, to produce two standard solutions. TLC was carried out using silica gel 60 F₂₅₄ as the stationary phase and a mixture of petroleum ether (30-60°C)-ethyl acetate-formic acid (15:5:1) as the mobile phase. The solutions were applied separately to the plate. After developed and dried in air, the plate was examined under UV light at 365 nm. Then, the plate was put in saturated ammonia for few minutes until the spots turned red.

Results

TLC profile of Rhizoma et Radix Polygoni Cuspidati was shown in Figure 3-28. The spot in the chromatogram obtained from the testing solution corresponded in color and position to the spots in the chromatogram obtained from the reference solution and standard solutions.

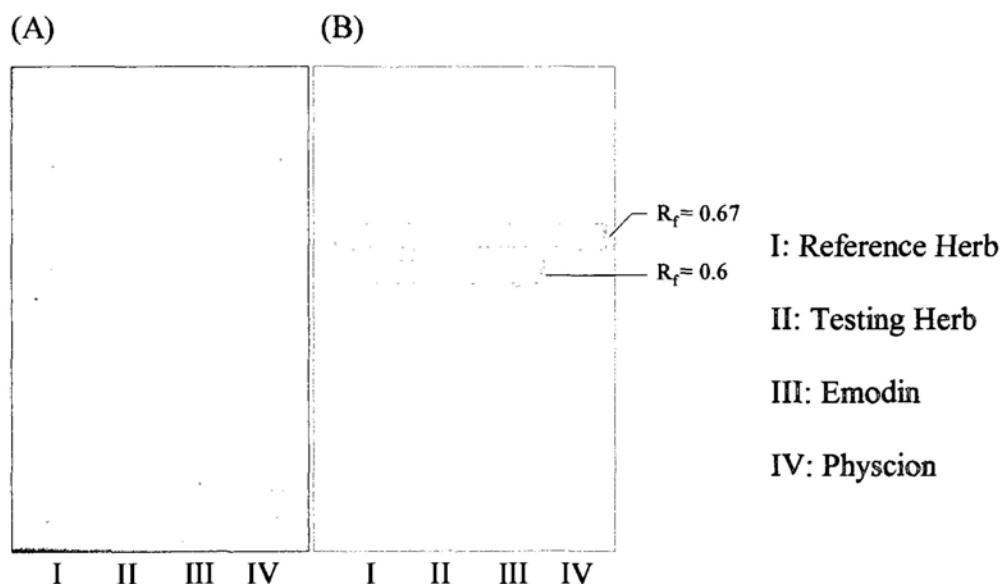


Figure 3-28 Thin Layer Chromatogram of Rhizoma et Radix Polygoni Cuspidati.
 (A) Examination under UV 365nm. (B) Examination under visible light.

3.2.28 Semen Coicis (薏苡仁)

General description and characteristics of the herb

It is the dried ripe kernel of *Coix lacryma-jobi* L. var. mayuen (Roman.) Stapf (Fam. Gramineae). It is collected in autumn. It is broad ovoid, 4-8 mm long, 3-6 mm wide. It is externally milky white. One end is obtusely rounded, the other end is relatively broad and slightly dented with one pale brown dotted hilum. The texture is hard and starchy. The odor is slight. The taste is slightly sweet.

Thin Layer Chromatographic analysis

Methodology

1 g of testing herb was sonicated with 10 mL of petroleum ether (60-90°C) for 30 min. The solution was filtered and evaporated to dryness. The residue was dissolved in 0.5 mL petroleum ether as the testing solution. A solution using 1 g of Semen Coicis reference herb (NICPBP catalog number 121254) was prepared in the same

manner as the reference solution. TLC was carried out using silica gel 60 F₂₅₄ as the stationary phase and a mixture of petroleum ether-ethyl acetate-acetic acid (10:3:0.1) as the mobile phase. The solutions were applied separately to the plate. After developed and dried in air, the plate was examined under UV light at 365 nm.

Results

TLC profile of Semen Coicis was shown in Fig. 3-29. The spots in the chromatogram obtained from the testing solution corresponded in position to the spots in the chromatogram obtained from the reference solution.

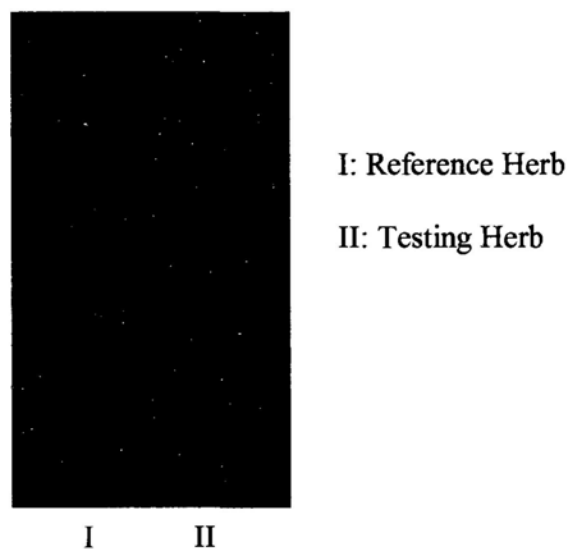


Figure 3-29 Thin Layer Chromatogram of Semen Coicis.

CHAPTER 4

SCREENING OF 28 TCMS AND GENERATION OF HERBAL FORMULA

4.1 Preparation of aqueous extracts of 28 TCMS

5 g of each of 28 TCMS was cut into small pieces and boiled in 50 mL of water for 2 h under reflux. The procedure of boiling was repeated and two batches of aqueous extracts were combined together. After lyophilization, the powders were stored at -20°C until use. Percentage yield of each TCM aqueous extract was listed in Table 4-1.

Table 4-1 Percentage yield of aqueous extracts of 28 TCMS

	<u>Yield of aqueous extract (%)</u>
Cortex Acanthopanax	13.42
Cortex Lycii	8.63
Cortex Phellodendri	14.31
Fructus Corni	34.31
Fructus Ligustri lucidi	9.35
Fructus Lycii	73.12
Fructus Schisandrae chinensis	27.63
Herba Gynostemma	20.14
Poria	5.19
Radix Astragali	34.24
Radix Codonopsis	44.80
Radix Notoginseng	14.22
Radix Ophiopogonis	69.71
Radix Panacis quinquefolii	21.41
Radix Platycodonis	44.06
Radix Puerariae	15.88
Radix Rehmanniae	29.37
Radix et Rhizoma Rhei	31.43
Radix Salviae miltiorrhizae	45.89
Radix Trichosanthis	24.33
Rhizoma Alismatis	18.91
Rhizoma Anemarrhenae	56.40
Rhizoma Atractylodis	59.58
Rhizoma Coptidis	36.32
Rhizoma Polygonati	59.90
Rhizoma Polygoni cuspidati	24.22
Rhizoma Polygonati odorati	59.54
Semen Coicis	16.56

4.2 Screening of 28 herbal extracts on protection of streptozotocin-induced cytotoxicity on RIN-m5F cells

4.2.1 Screening assay

2×10^4 RIN-m5F cells were seeded in each well of 96-well culture plate. After overnight incubation, 5 mM streptozotocin (STZ, dissolved in citrate buffer, pH4.5) was added to the cells together with various concentrations (0.78 $\mu\text{g}/\text{mL}$ to 100 $\mu\text{g}/\text{mL}$) of herbal extracts. Treatment with streptozotocin alone was assigned as STZ control. Cells without streptozotocin and herbal extracts was assigned as negative control. The cells were further incubated for 24 h. Then, MTT assay was performed to measure the cell viability.

4.2.2 Results

Percentages of viable RIN-m5F cells after treatment with STZ in the presence or absence of TCM extracts were shown in Table 4-2. The percentage cell viability of negative control was set as 100% whereas percentage cell viability of other treatments were calculated compared to negative control. Results showed that cell viability of streptozotocin alone was about 50% and only three herbs (Cortex Lycii, Radix Astragali and Radix Codonopsis) exhibited significant increase in cell viability when compared to streptozotocin control. Effective concentration of Cortex Lycii is between 0.78 to 3.13 $\mu\text{g}/\text{mL}$ while that of Radix Astragali and Radix Codonopsis is between 6.25 to 100 $\mu\text{g}/\text{mL}$.

Table 4-2 Percentage viability of RIN-m5F cells after treatment with STZ (5 mM) in the presence or absence of various concentrations of 28 TCM extracts for 24 hours. Negative control without the addition of STZ and TCM extracts was set as 100% cell viability. The data were expressed as Mean \pm S.D. Eight replicates were performed for each treatment. Mann-Whitney test was carried out to compare the difference between STZ and STZ with herbal treatment. Statistically significant increase of cell viability was indicated by asterisk (* $p < 0.05$).

	Negative control	STZ (5 mM) + Herbal extracts ($\mu\text{g/ml}$)									
		STZ (5mM)	0.78	1.56	3.13	6.25	12.5	25	50	100	
Cortex Acanthopanax	100.00	54.63 \pm 3.14	51.30 \pm 4.53	47.89 \pm 6.78	46.10 \pm 4.52	43.42 \pm 6.78	32.90 \pm 4.31	25.10 \pm 5.34	20.59 \pm 3.11	23.88 \pm 4.19	
Cortex Lycii	100.00	51.53 \pm 7.67	64.19 \pm 6.65 *	62.42 \pm 7.89 *	67.29 \pm 3.45 *	23.02 \pm 3.02	15.76 \pm 4.56	20.10 \pm 4.11	22.58 \pm 3.69	38.51 \pm 2.24	
Cortex Phellodendri	100.00	48.47 \pm 6.32	51.17 \pm 3.54	50.74 \pm 6.17	45.89 \pm 7.66	43.01 \pm 5.98	9.02 \pm 3.85	11.10 \pm 2.95	14.17 \pm 3.80	23.01 \pm 3.69	
Fructus Corni	100.00	52.29 \pm 4.11	54.17 \pm 8.23	49.00 \pm 6.42	49.77 \pm 3.54	53.98 \pm 4.18	55.40 \pm 5.65	59.60 \pm 3.99	54.30 \pm 4.11	48.55 \pm 6.07	
Fructus Ligustri lucidi	100.00	43.90 \pm 4.80	45.36 \pm 5.02	39.76 \pm 4.53	42.90 \pm 3.24	42.76 \pm 6.21	24.22 \pm 3.80	12.27 \pm 4.31	15.94 \pm 3.88	22.01 \pm 3.64	
Fructus Lycii	100.00	51.53 \pm 4.52	48.14 \pm 5.97	50.46 \pm 7.84	46.48 \pm 6.25	46.04 \pm 3.52	32.40 \pm 2.40	40.19 \pm 5.56	45.15 \pm 5.33	38.51 \pm 6.48	
Fructus Schisandrae chinensis	100.00	51.32 \pm 3.74	48.18 \pm 5.16	46.21 \pm 6.77	44.35 \pm 3.10	42.33 \pm 5.69	31.04 \pm 3.55	23.39 \pm 3.39	19.80 \pm 2.58	21.48 \pm 3.67	
Herba Gynostemma	100.00	55.72 \pm 3.91	54.78 \pm 6.94	53.15 \pm 5.31	55.05 \pm 5.63	51.24 \pm 4.88	51.42 \pm 5.47	49.65 \pm 3.37	49.58 \pm 6.53	52.11 \pm 5.20	
Poria	100.00	50.10 \pm 6.48	51.90 \pm 5.75	52.45 \pm 5.29	49.74 \pm 4.75	50.60 \pm 3.38	50.26 \pm 4.49	53.44 \pm 5.22	55.09 \pm 6.75	54.49 \pm 5.63	
Radix Astragali	100.00	55.36 \pm 3.18	56.13 \pm 6.57	51.09 \pm 5.52	56.78 \pm 6.99	69.37 \pm 8.24 *	69.37 \pm 6.02 *	79.19 \pm 10.57 *	80.14 \pm 9.45 *	83.96 \pm 10.02 *	
Radix Codonopsis	100.00	51.97 \pm 5.55	53.59 \pm 7.82	55.22 \pm 6.31	53.05 \pm 4.66	62.54 \pm 6.90 *	59.29 \pm 7.87 *	70.40 \pm 9.24 *	78.52 \pm 6.91 *	85.13 \pm 10.30 *	
Radix Notoginseng	100.00	52.23 \pm 4.91	51.21 \pm 4.32	55.51 \pm 3.68	53.89 \pm 5.91	49.58 \pm 3.89	51.11 \pm 3.20	51.02 \pm 6.37	54.64 \pm 7.02	49.94 \pm 2.14	
Radix Ophiopogonis	100.00	52.93 \pm 2.85	50.94 \pm 3.78	49.43 \pm 5.0	51.20 \pm 3.11	47.65 \pm 6.10	50.91 \pm 3.23	46.18 \pm 4.03	47.60 \pm 3.81	48.45 \pm 6.46	
Radix Panacis quinquefolii	100.00	49.74 \pm 6.02	47.63 \pm 3.64	46.50 \pm 5.37	49.02 \pm 4.91	48.61 \pm 6.31	47.22 \pm 3.62	48.56 \pm 4.70	48.61 \pm 3.44	46.42 \pm 2.78	
Radix Platycodonis	100.00	45.80 \pm 3.60	46.29 \pm 6.99	45.19 \pm 4.54	49.37 \pm 5.07	51.25 \pm 5.40	50.92 \pm 7.02	45.84 \pm 5.83	44.78 \pm 6.57	48.16 \pm 4.69	
Radix Puerariae	100.00	50.89 \pm 6.53	51.44 \pm 3.23	50.21 \pm 6.25	48.38 \pm 4.04	56.94 \pm 4.19	56.57 \pm 6.68	50.94 \pm 8.29	45.41 \pm 3.28	30.28 \pm 1.50	
Radix Rehmanniae	100.00	55.36 \pm 2.22	56.13 \pm 6.40	51.09 \pm 3.83	58.78 \pm 2.49	56.50 \pm 6.03	56.50 \pm 4.50	56.10 \pm 7.22	58.79 \pm 4.13	50.71 \pm 6.93	
Radix et Rhizoma Rhei	100.00	42.44 \pm 3.08	44.50 \pm 6.29	43.47 \pm 2.22	46.55 \pm 5.09	43.36 \pm 3.13	25.51 \pm 3.48	23.20 \pm 4.21	33.38 \pm 6.15	24.90 \pm 3.66	
Radix Salviae miltorrhizae	100.00	46.55 \pm 5.88	45.84 \pm 3.61	44.77 \pm 4.48	47.78 \pm 3.90	51.30 \pm 4.77	47.98 \pm 5.45	20.27 \pm 3.83	12.76 \pm 3.61	17.68 \pm 2.14	
Radix Trichosanthis	100.00	42.33 \pm 2.52	41.17 \pm 5.23	39.30 \pm 3.30	41.28 \pm 5.05	44.60 \pm 5.46	41.09 \pm 5.31	40.94 \pm 3.64	41.96 \pm 6.35	46.25 \pm 3.85	
Rhizoma Alismatis	100.00	48.95 \pm 4.75	51.88 \pm 2.14	51.24 \pm 3.38	46.35 \pm 3.60	49.44 \pm 4.69	49.11 \pm 3.99	51.24 \pm 4.37	54.31 \pm 5.90	53.24 \pm 6.37	
Rhizoma Anemarrhenae	100.00	53.85 \pm 6.51	56.50 \pm 4.86	51.14 \pm 5.30	51.48 \pm 2.18	57.00 \pm 3.65	54.01 \pm 5.02	45.55 \pm 6.94	39.98 \pm 5.66	39.97 \pm 3.84	
Rhizoma Atractylodis	100.00	45.99 \pm 4.11	44.46 \pm 3.53	40.32 \pm 6.21	43.70 \pm 4.22	42.69 \pm 2.15	40.74 \pm 3.90	42.43 \pm 6.05	46.60 \pm 4.81	39.48 \pm 5.55	
Rhizoma Coptidis	100.00	52.27 \pm 6.36	53.32 \pm 4.00	50.93 \pm 7.19	51.17 \pm 3.86	45.78 \pm 4.46	33.29 \pm 3.34	9.27 \pm 1.77	12.76 \pm 1.23	18.41 \pm 2.12	
Rhizoma Polygonati	100.00	51.11 \pm 3.48	53.15 \pm 4.56	54.42 \pm 3.88	51.50 \pm 5.36	54.61 \pm 2.43	53.49 \pm 6.58	55.12 \pm 3.40	53.95 \pm 5.11	53.57 \pm 4.79	
Rhizoma Polygoni cuspidati	100.00	52.96 \pm 1.96	51.12 \pm 3.58	48.48 \pm 3.33	50.92 \pm 5.59	46.89 \pm 3.90	35.75 \pm 2.14	35.35 \pm 3.29	32.91 \pm 1.53	33.69 \pm 3.63	
Rhizoma Polygonati odorati	100.00	49.17 \pm 2.49	52.31 \pm 5.13	44.85 \pm 6.43	53.34 \pm 4.40	49.95 \pm 5.65	51.72 \pm 7.18	55.67 \pm 6.67	52.64 \pm 6.13	53.89 \pm 7.25	
Semen Coicis	101.00	46.86 \pm 4.85	46.69 \pm 7.68	49.67 \pm 5.84	47.11 \pm 7.71	53.43 \pm 8.68	50.63 \pm 4.51	51.39 \pm 7.30	49.96 \pm 3.71	54.27 \pm 10.52	

4.3 Generation of a herbal formula SR10

4.3.1 Selection and combination of effective herbs

From the results shown in Table 4-2, greatest inhibition of β cell toxicity for Cortex Lycii was found at the concentration 3.13 $\mu\text{g/mL}$ whereas for Radix Astragali and Radix Codonopsis, greatest inhibitions were both found at 100 $\mu\text{g/mL}$. Therefore, the ratio of effective concentration of Radix Astragali : Radix Codonopsis : Cortex Lycii is 30:30:1. According to this ratio, an aqueous herbal formula, namely SR, was produced by boiling the raw herb of Radix Astragali, Radix Codonopsis and Cortex Lycii in water in the ratio 30:30:1. The effect of SR on STZ-induced toxicity on RIN-m5F was examined and the result was shown in Figure 4-1. Results showed that percentage of viable cells after STZ treatment is 45.1%. When SR herbal extract was treated together, the percentage of cell viability was increased significantly to 54.4%, 66.7% and 66.7% at concentrations 25 $\mu\text{g/mL}$, 50 $\mu\text{g/mL}$ and 100 $\mu\text{g/mL}$, respectively.

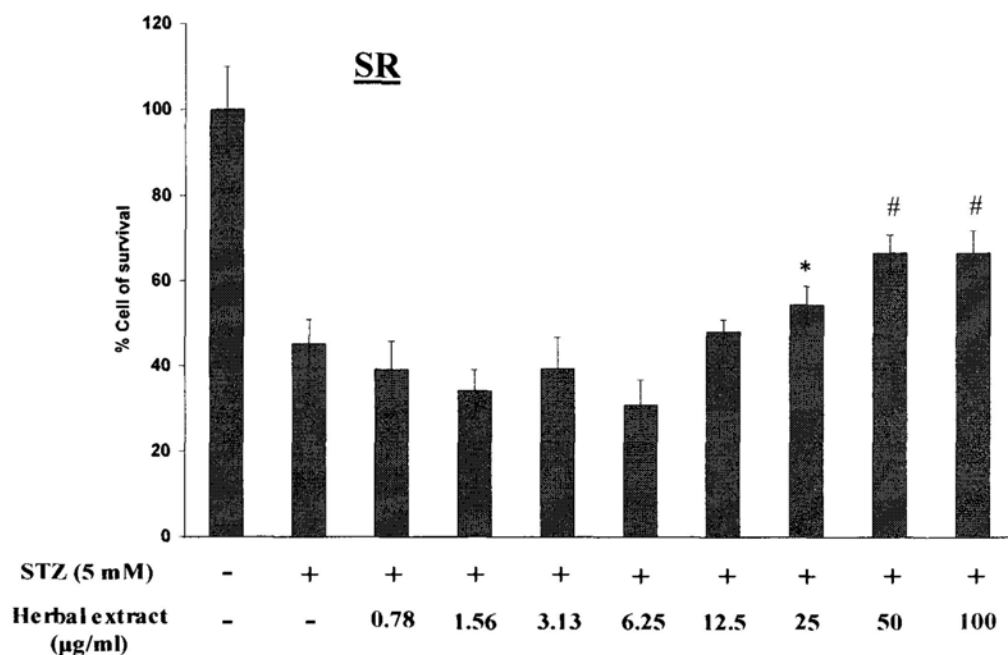


Figure 4-1 Effect of SR herbal extract on viability of RIN-m5F cells. An aqueous herbal formula SR was prepared by extracting the mixture of Radix Astragali, Radix Codonopsis and Cortex Lycii in water in the ratio 30:30:1. The cells were treated with STZ (5 mM) in the presence or absence of various concentrations of SR for 24 h. MTT assay was performed to determine the percentage of viable cells. Percentage viability of negative control (without STZ and SR) was set as 100%. The data were expressed as Mean \pm S.D. with 8 replicates for each treatment. By Mann-Whitney test, significant increase in cell viability when compared to STZ (5 mM) control was indicated by # $p < 0.01$ or * $p < 0.05$.

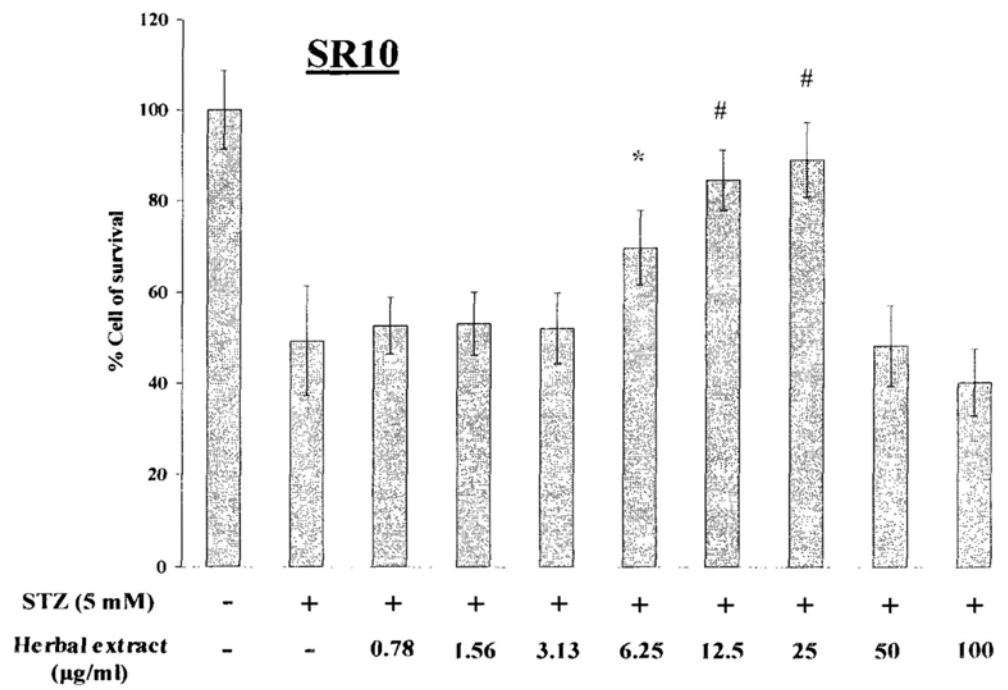
4.3.2 Ratio optimization of 3 effective herbs

For a herbal formula, the ratio of component herbs may produce various effects. Thus, in this part, the ratio of three herbs in the formula SR was modified in order to maximize the protective effect on β cell toxicity. In the formula SR, the amount of Radix Astragali and Radix Codonopsis is 30-fold higher than that of Cortex Lycii. Thus, it may be a reasonable trial to increase the ratio of Cortex Lycii. Another rationale to increase the amount of Cortex Lycii is because Cortex Lycii was reported by Chinese Pharmacopoeia to have hypoglycemic effect on its own. Therefore, other three formulae with increased amount of Cortex Lycii were generated, namely SR10, SR20 and SR30, respectively. The weight ratio of raw herb of Radix Astragali, Radix Codonopsis and Cortex Lycii in making these formulae are 30:30:10 (SR10), 30:30:20 (SR20) and 30:30:30 (SR30), respectively. Again, the inhibitory effects of these formulae on cytotoxicity of RIN-m5F cells induced by STZ were tested and the results were shown in Figure 4-2.

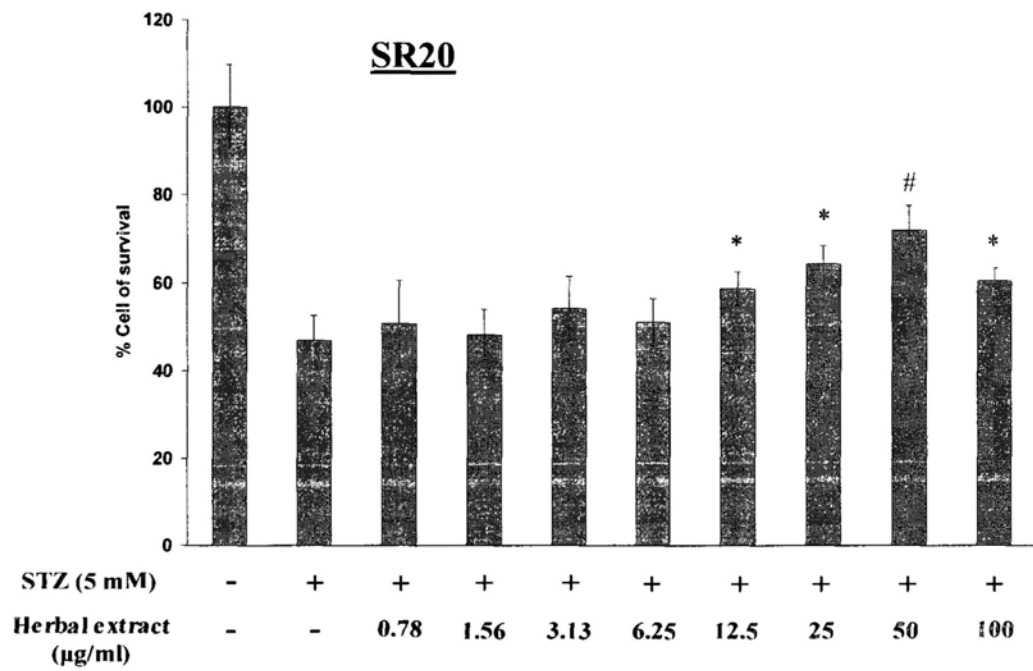
For SR10, it was shown that percentage of cell viability significantly increased from 49.3% in STZ control to 69.8%, 84.5% and 89.1% at concentrations 6.25 $\mu\text{g/mL}$, 12.5 $\mu\text{g/mL}$ and 25 $\mu\text{g/mL}$, respectively. For SR20, significant increases of percentage viable cells were found at concentrations 12.5 $\mu\text{g/mL}$, 25 $\mu\text{g/mL}$, 50 $\mu\text{g/mL}$ and 100 $\mu\text{g/mL}$ when compared to STZ control which showed 46.9% of cell viability. For SR30, cell viability was found to be significantly increased from 42.8% (STZ control) to 62.5% and 63.8% at concentrations 12.5 $\mu\text{g/mL}$ and 25 $\mu\text{g/mL}$, respectively.

From the results in Figure 4-2, it is concluded that SR10 at concentration 12.5 $\mu\text{g/mL}$ and 25 $\mu\text{g/mL}$ exhibited higher protective effects on RIN-m5F cells against STZ-induced ROS-mediated death than SR20 or SR30.

(A)



(B)



(C)

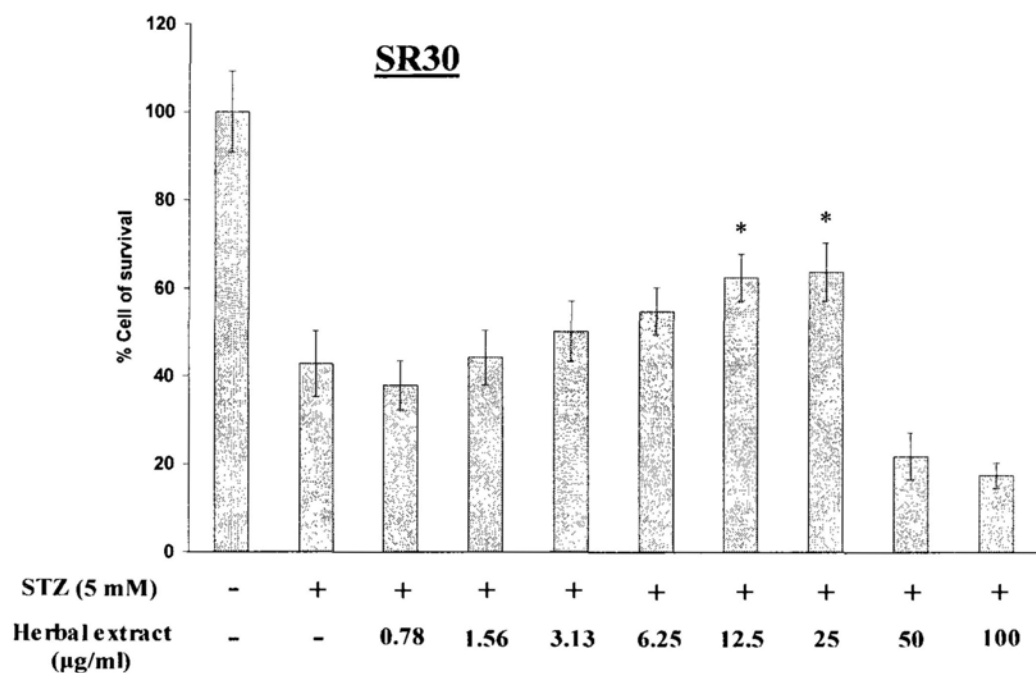


Figure 4-2 Effects of SR10, SR20 and SR30 on viability of RIN-m5F cells. The cells were treated with STZ (5 mM) in the presence or absence of various concentrations of SR10 (A), SR20 (B) or SR30 (C) for 24 h. MTT assay was performed to determine the percentage of viable cells. Percentage of cell viability of negative control (without STZ and herbal extracts) was set as 100%. The data were expressed as Mean \pm S.D. with 8 replicates for each treatment. By Mann-Whitney test, significant increase in cell viability when compared to STZ (5 mM) was indicated by # $p < 0.01$ or * $p < 0.05$.

4.4 Batch to batch variations of SR10

In order to characterize SR10 in terms of different biological activities, second batch of SR10 was prepared in large scale. Totally, 857.1 g of Radix Astragali, 857.1 g of Radix Codonopsis and 285.7 g of Cortex Lycii were boiled in 20 L of distilled water. Then, the procedures mentioned in Section 4.1 were followed. Final percentage yield of this batch of SR10 was 23.7% (yield of first batch of SR10 is 24.5%). To examine the batch to batch variations, HPLC was performed on both batches of SR10. This part was performed by Dr. Linda Zhang of Jinan University, Guang Zhou, China.

4.4.1 HPLC conditions

Sample: SR10 extract was dissolved in 30% methanol and then filtered through 0.45 μm membrane to produce an test solution for HPLC analysis.

Instrument: Agilent 1200 High Performance Liquid Chromatography System
(Data analysis by Agilent ChemStation)

Column: Agilent ZORBAX SB-Aq, 4.6 mm x 250 mm, 5 HM

Sample injection volume: 10 μL

Mobile phase: H₂O : Methanol with gradient profile

Time program:	B: Methanol
0-20 min	% B 2.00-15.00
20-35 min	% B 15.00-50.00
35-45 min	% B 50.00-70.00
45-55 min	% B 70.00-95.00
55-70 min	% B 95.00

Flow rate: 0.8 mL/min

Time course: 70 min

Detection mode: UV at 254 nm

4.4.2 HPLC chromatograms

HPLC profiles for two batches of SR10 herbal extracts were shown in Figure 4-3. The percentage areas of major peaks shown in the profile were determined and summarized in Table 4-3. Both retention time and percentage area of each major peak in batch 1 corresponded well to that in batch 2. Moreover, screening assay shown in Section 4.2 was performed on batch 2 extract to confirm that the quality of batch 2 extract (in terms of biological activity) was same as that batch 1.

Batch 1

VIAU/1.1. WABN02915409.001, (ANALYSIS FILE) 2006 US 03 10 34 75FFZJ000102.D

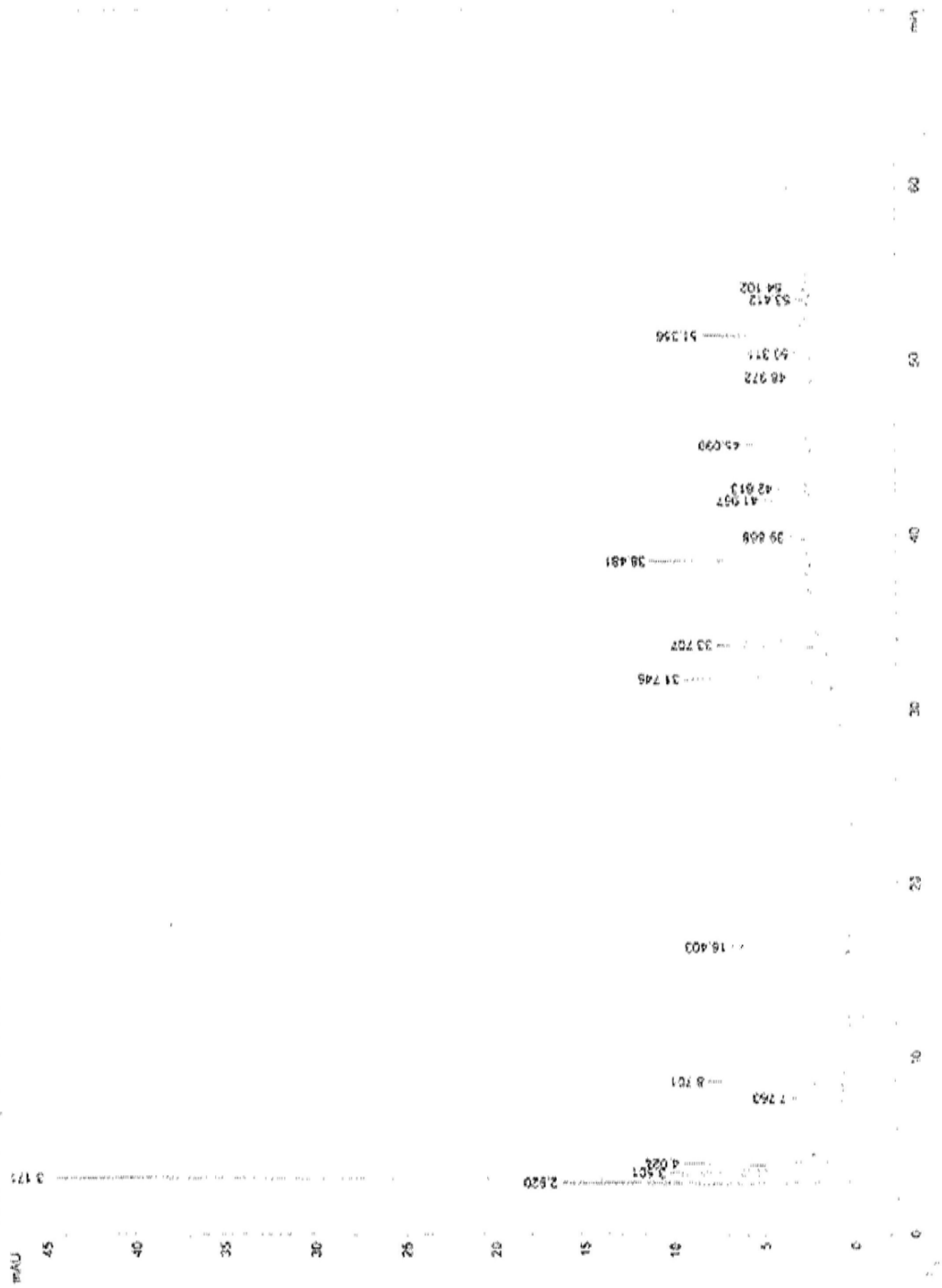




Figure 4-3 HPLC profiles for two batches of SR10 herbal extracts.

Table 4-3 Summary of retention time and percentage of peak area detected by HPLC in two batches of SR10 extracts.

Peak Number	Retention time	% peak area for batch 1 extract	% peak area for batch 2 extract
1	2.765-2.920	4.196	8.9226
2	3.075-3.171	26.2015	23.8161
3	3.475-3.501	6.0952	5.9586
4	4.024-4.026	3.4524	3.1598
5	7.736-7.760	2.7991	3.4101
6	8.673-8.701	8.1762	8.1882
7	16.368-16.403	8.3731	9.3503
8	31.698-31.745	5.3349	3.3035
9	33.707-33.663	7.2265	8.2497
10	38.481-38.490	4.8794	3.0319
11	39.868-39.882	0.7152	1.2390
12	41.967-42.008	1.5597	1.1953
13	42.613-42.655	0.9510	0.6342
14	45.099-45.136	2.2701	2.1598
15	48.961-48.972	0.7042	0.9824
16	50.290-50.311	0.5709	1.1175
17	53.389-53.412	0.4153	0.7073
18	54.078-54.102	0.7279	1.2273

CHAPTER 5

INHIBITORY EFFECTS OF SR10 ON STREPTOZOTOCIN-INDUCED APOPTOSIS ON PANCREATIC β CELLS

5.1 Introduction

In Type 2 DM, hyperglycemia is the outcome of both insulin resistance and insulin insufficiency. Furthermore, high glucose is a secondary factor that further damages the pancreatic β cells. Oxidative stress has been shown to be responsible, at least in part, for the β cell dysfunction caused by hyperglycemia (Wu *et al.*, 2004). Diabetic patients are exposed to oxidative stress, and diabetic complications seem to be mediated by oxidative stress. Increased blood glucose level promotes protein glycation through the Maillard reaction, which consecutively produces Schiff bases, Amadori products and advanced glycation end products (Schmidt *et al.*, 1994; Wolff *et al.*, 1991). In this process, reactive oxygen species (ROS) are formed and β cells are vulnerable to oxidative stress when compared with other tissues due to the fact that relatively low level of antioxidant enzymes is found in β cells (Lenzen *et al.*, 1996). ROS cause β cell death via induction of apoptosis (Brownlee, 2001). Although the toxicity of glucose has been studied extensively, the molecular mechanisms connecting glucotoxicity and β cell loss in DM have only begun to be unraveled.

In this part of study, rat pancreatic β cell line, RIN-m5F, was used as a cellular model. By different biochemical assays, the inhibitory effect of SR10 on apoptosis of RIN-m5F cells induced by streptozotocin (STZ) in these cells was demonstrated.

5.2 Results

5.2.1 Inhibition of STZ-induced apoptosis on RIN-m5F cells

Suppression of DNA fragmentation

Genomic DNA was prepared from STZ-treated RIN-m5F cells which were incubated in the absence (lane 2) or presence (lane 3-6) of various concentrations of SR10. DNA integrity was then assessed by agarose gel electrophoresis (Figure 5-1). From the result, a typical laddering pattern was observed when RIN-m5F cells were treated with 5 mM of STZ (lane 2). This laddering pattern was not found in negative control without STZ (lane 1). However, the contents of DNA fragmentation in the STZ-treated cells decreased gradually when SR10 in increasing concentrations from 3.13 $\mu\text{g/mL}$ to 25 $\mu\text{g/mL}$ (lane 3-6) were added.

STZ (5 mM)	-	+	+	+	+	+
SR10 (µg/ml)	-	-	3.125	6.25	12.5	25

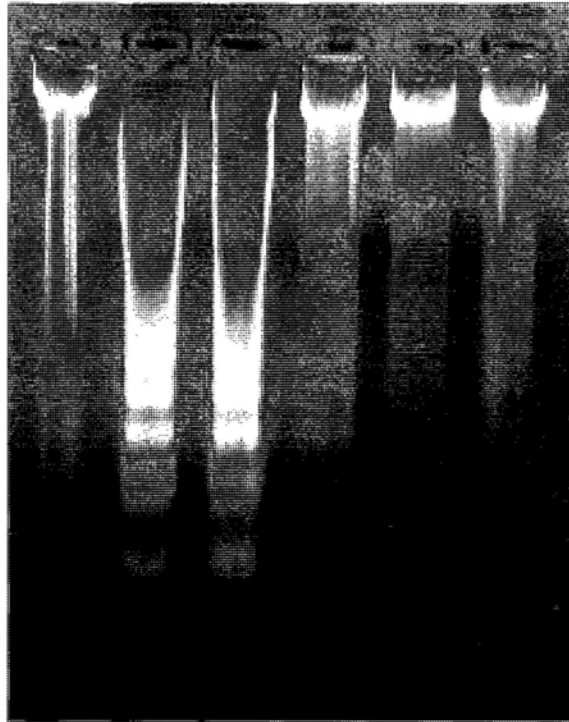


Figure 5-1 Effect of SR10 on DNA fragmentation of RIN-m5F cells induced by STZ. RIN-m5F cells were treated with medium alone (lane 1), 5 mM STZ alone (lane 2) or 5 mM STZ together with various concentrations of SR10 (lane 3-lane 6) for 24 h. After treatment, genomic DNA was extracted and analyzed by agarose gel electrophoresis. The figure is a representative of three independent trials with similar results.

Decrease of sub-G₁ phase

The appearance of sub-G₁ peak in cell cycle analysis is a typical indication of apoptosis. By flow cytometry, different phases of cell cycle were analyzed. As shown in Figure 5-2, when RIN-m5F cells were treated with 5 mM STZ, the percentage of sub-G₁ phase increased from 1.49% (negative control) to 33.52%. Treatment of cells with various concentrations of SR10 decreased the percentage of sub-G₁ cell cycle significantly to 28.90%, 15.15%, 14.32% and 9.87%, respectively.

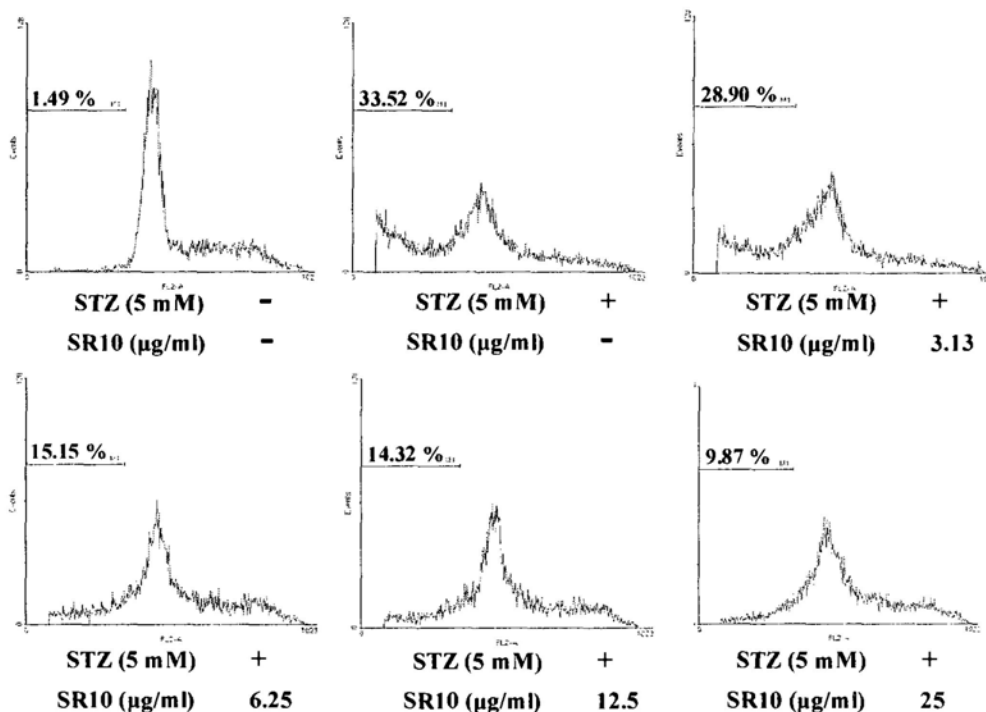


Figure 5-2 Effect of SR10 on cell cycle distribution of STZ-treated RIN-m5F cells. Cell cycle patterns of negative control, STZ control (5 mM STZ alone) and STZ together with SR10 treatment were assessed by PI staining using flow cytometry. A distinct sub-G₁ phase was detected in the treatment of 5 mM STZ. This proportion was decreased when increasing concentrations of SR10 were added to the cells. The figure is a representative of three independent trials with similar results.

Inhibition of Phosphatidylserine (PS) externalization

As shown in Figure 5-3, majority of cells in negative control were localized in the lower left quadrant indicating the presence of viable cells without apoptotic or necrotic stimulation. When the cells were treated with 5 mM STZ, certain proportion of the cells was observed in lower right quadrant (33.4%), indicating the presence of PS externalisation which is an important step in apoptosis. Upon treatment of SR10 for 24 h, there was a shift of proportion from lower right quadrant to lower left quadrant. The percentage of apoptotic cells decreased from 33.4% to 3.1% when the cells were treated with 25 µg/mL of SR10.

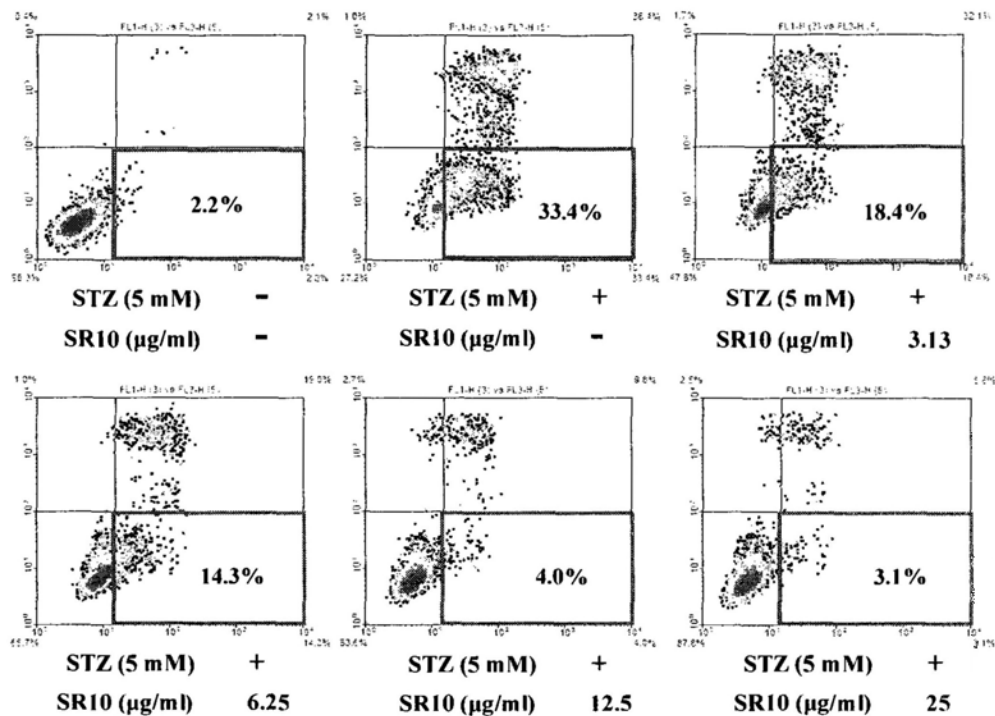


Figure 5-3 Effect of SR10 on PS externalization of STZ-treated RIN-m5F cells detected by Annexin V-FITC and propidium iodide (PI). Cells treated with 5 mM STZ in the presence or absence of SR10 were incubated with FITC labeled Annexin-V and PI. After washing, the cells were subjected to flow cytometric analysis. Numbers at the corners represent the percentage of cells found in each quadrant. The figure is a representative of three independent trials with similar results.

Change in expression level of apoptosis-related proteins

Caspase 3, caspase 9 and bcl-2 are major regulatory proteins associated with the network of apoptosis. Western blot analysis was applied to detect the activation of caspase 3 and caspase 9 proteins and the level of anti-apoptotic protein bcl-2. As shown in Figure 5-4, the expression level of caspase 3 precursor (pro-caspase 3), caspase 9 precursor (pro-caspase 9) and apoptotic suppressor bcl-2 were significantly decreased after 5 mM STZ treatment for 24 hours when compared with negative control. When SR10 was added, the decreased expressions of these proteins were suppressed. Western blot analysis of cytochrome c also showed a release of this protein to cytosol when RIN-m5F cells were treated with STZ alone. When SR10 was added, cytochrome c release was significantly decreased. Similar band intensity of β -actin showed even loading of protein in each sample.

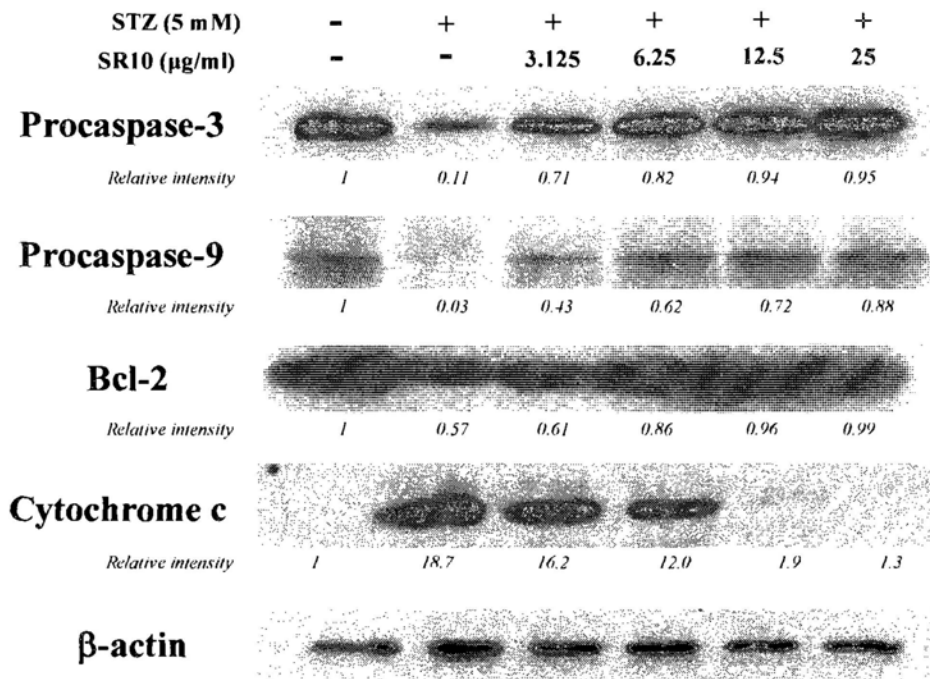
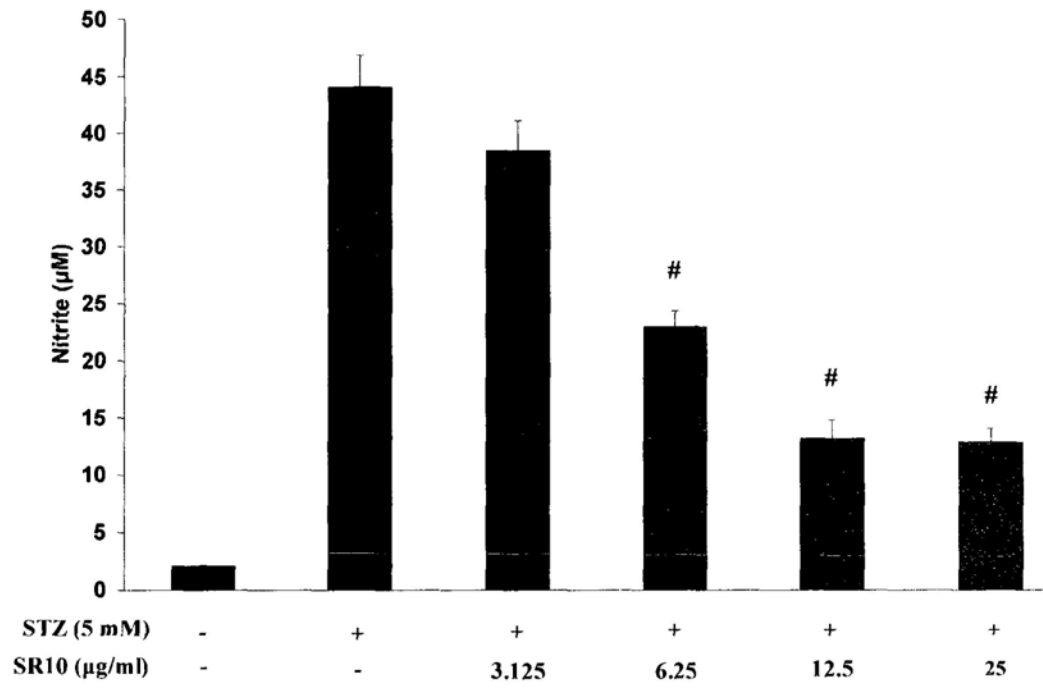


Figure 5-4 Western blot analysis of expression level of apoptosis-related proteins on SR10-treated RIN-m5F cells. Cells without STZ treatment was used as negative control (lane 1). Cells treated with 5 mM STZ were added with various concentrations of SR10 (lane 3-lane 6) or without SR10 (lane 2). Total cellular proteins or cytosolic protein fraction was collected after 24 h treatment. Expression level of procaspase-3, procaspase-9, bcl-2, cytochrome c and β-actin were detected by Western blot analysis. The figure is a representative of 3 independent trials with similar results.

5.2.2 Inhibition of nitric oxide production and nitric oxide synthase activity

STZ is known to stimulate nitric oxide (NO) production in pancreatic β cells via induction of inducible nitric oxide synthase (iNOS). We therefore examined iNOS expression and NO production. From Figure 5-5A, it could be seen that 5 mM STZ caused large amount of NO release in RIN-m5F cells when compared to negative control. When various concentrations of SR10 were added in increasing concentrations (from 3.13 $\mu\text{g/mL}$ to 25 $\mu\text{g/mL}$), the NO production decreased in a dose-dependent manner (from 38 μM to 13 μM). To investigate the expression of iNOS, Western blot analysis was performed (Figure 5-5B). After normalization by β -actin, STZ significantly induced the expression of iNOS (lane 2) when compared to negative control (lane 1). This STZ-induced iNOS expression was suppressed by SR10 in a dose-dependent manner (lane 3-6).

(A)



(B)

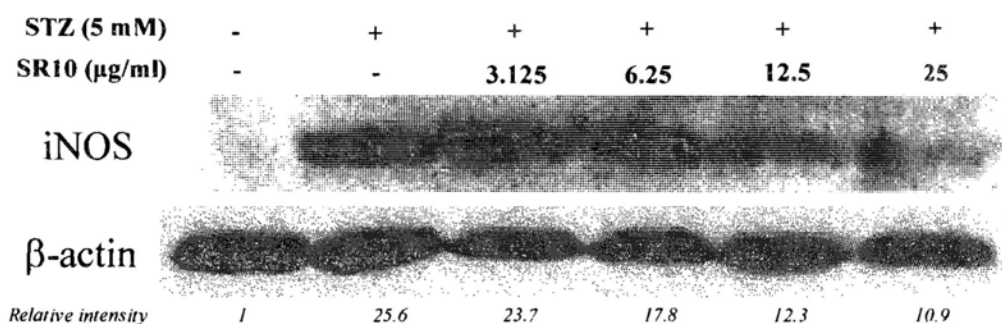


Figure 5-5 Effect of SR10 on nitric oxide production and iNOS expression on SR10-treated RIN-m5F cells. RIN-m5F cells were treated with 5 mM STZ in the presence or absence of the indicated concentrations of SR10. (A) Following 24 h incubation, nitrite concentration (indication of nitric oxide synthesis) was measured in culture medium. Results of four replicates were expressed as Mean \pm S.D. of three independent experiments. The data was statistically significant when # $p < 0.01$ compared to 5 mM STZ alone by Mann-Whitney test. (B) Protein expression level of iNOS by different SR10 treatment on RIN-m5F cells was analyzed by Western blot. The figure is a representative of three independent trials with similar results.

5.2.3 Up-regulation of insulin secretion

Insulin secretion in RIN-m5F cells were stimulated by insulin secretion buffer. After 24 h of incubation with STZ alone or STZ together with SR10 extracts, the concentration of insulin released in culture supernatant was determined by ELISA. From the result shown in Figure 5-6, insulin secretion was significantly suppressed when STZ (5 mM) was added to the cells (47.2% of negative control). However, when SR10 extracts were added, insulin secretion was up-regulated when compared to STZ treatment. Insulin released was increased from 47.2% to 64.2%, 80.9% and 85.7% when 6.25 µg/mL, 12.5 µg/mL and 25 µg/mL of SR10 were added, respectively.

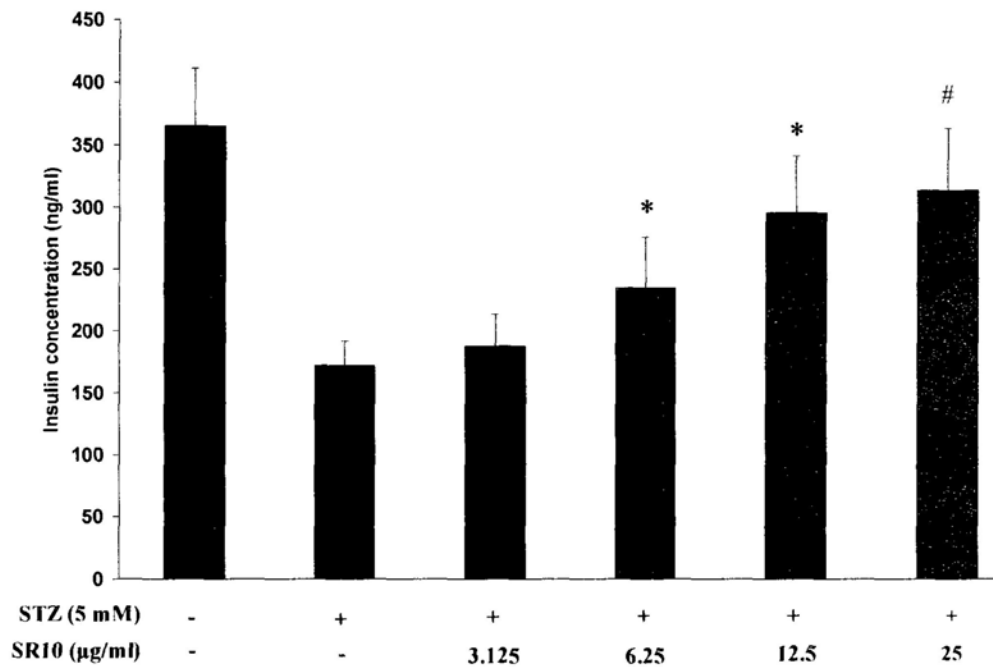


Figure 5-6 Effect of SR10 on insulin secretion in RIN-m5F cells. The concentration of insulin released in the culture supernatant was determined by ELISA. Results of 4 replicates were expressed as Mean \pm S.D. of three independent experiments. The data was statistically significant when * $p < 0.05$ or when # $p < 0.01$ compared to 5 mM STZ alone by Mann-Whitney test.

5.3 Discussion

Pancreatic β cells play a critical role in the pathogenesis of DM. In advanced stages of type 2 DM, chronic hyperglycemia is toxic to the β cells and the functions of β cells often degenerate to such a degree that insulin therapy becomes necessary. This glucotoxicity is a gradual process characterized by increasing β cell dysfunction culminating in irreversible β cells loss by apoptosis (Kaneto *et al.*, 1996). In general, the apoptosis cascade is triggered by various kinds of stimuli such as DNA damage, cell cycle perturbation, metabolic imbalance, as well as oxidative stress. Oxidative stress in DM could be due to an increased production of ROS, especially from enhanced glycation, and decreased enzymatic and non-enzymatic anti-oxidant defense systems (Sakurai *et al.*, 1988; Baynes, 1991). ROS participate in the toxic actions then lead to necrosis or apoptosis of the insulin-producing cells.

In this study, the anti-diabetic effect of SR10 was examined. SR10 is a novel herbal preparation comprising three herbs, Radix Astragali, Radix Codonopsis and Cortex Lycii extracted at weight ratio of 3:3:1 (Section 4.3.2). All these herbs have been frequently used in TCM for treating DM (Li *et al.*, 2004). There may be hundreds of chemical constituents in formula SR10 and the interaction of these constituents are not well known. However, certain chemical compounds in these three herbs have been identified and they exhibited therapeutic effects in DM and diabetic complications. These compounds include linoleic acid present in Cortex Lycii (Aminot-Gilchrist *et al.*, 2004) and astragaloside IV present in Radix Astragali (Yu *et al.*, 2006).

Streptozotocin, a potent diabetogenic compound, selectively causes pancreatic β cell death. In the present study, we have demonstrated that death of rat pancreatic β cells, RIN-m5F cells, induced by STZ was suppressed by incubation of SR10 at

concentrations 12.5 $\mu\text{g/mL}$ and 25 $\mu\text{g/mL}$. As shown in Figure 4-2A, SR10 at concentrations 50 $\mu\text{g/mL}$ and 100 $\mu\text{g/mL}$ did not enhance cell survival rate when compared with 5 mM STZ alone. This may be due to toxic effect of high concentration of SR10 because it was found that 50 $\mu\text{g/mL}$ and 100 $\mu\text{g/mL}$ SR10 produced 20-30% toxicity to the cells without the presence of STZ. However, no cytotoxicity was observed when SR10 with concentration 25 $\mu\text{g/mL}$ or below was added to the cells. The data in this part of study suggested that the induced viability of RIN-m5F cells in the presence of SR10 was due to inhibition of apoptosis. The higher resistance to STZ-induced death was demonstrated by reduced DNA fragmentation (Figure 5-1), reduced proportion of sub- G_1 cell cycle (Figure 5-2) and inhibition of PS externalization (Figure 5-3). The destruction of β cells is mediated by an altered expression level of anti-apoptotic or pro-apoptotic proteins. In many cell types including pancreatic cells, the onset of apoptosis is regulated by the relative abundance of bcl-2. On the other side, ROS production induced by STZ would lead to mitochondrial membrane potential changes and hence the release of cytochrome c, which triggers the initiation of apoptosis.

The rapid induction of ROS concentration near the mitochondrial membrane would lead to the increase of its permeability due to the peroxidation of the mitochondrial membrane lipids (Hunt *et al.*, 1991). As a result, the mitochondrial membrane potential ($\Delta\psi_m$) decreased and led to the release of cytochrome c (Figure 5-4) from the mitochondria, which triggered the initiation of apoptosis. Many genes contribute to the regulation of apoptosis, activation of caspase cascade is one of the checkpoints. Our results showed that the precursor form of caspase-3 and caspase-9 was significantly decreased (Figure 5-4), which implied an activation of cleavage of caspases. The activated caspase-9 could further activate the downstream effectors

involved in the cascade, such as procaspase-3. As a result, procaspase-3 was finally activated which triggered chromosomal DNA fragmentation and finally apoptosis. This cascade of apoptosis was significantly observed when 5 mM STZ was added to RIN-m5F cells. However, when SR10 was added to the cells, the appearance of this pattern was inhibited, i.e. suppression of procaspase-3 and procaspase-9 cleavage, decrease of bcl-2 down-regulation and decrease of cytochrome c release was observed in SR10 treatments.

Excessive production of nitric oxide and the subsequent increase in local oxidative stress are suggested mechanisms in the destruction of pancreatic β cells and the development of DM. Relevant for β cells failure in type 2 DM is that culture in high glucose in vitro causes IL-1 β production in human islets of Langerhans leading to β cells apoptosis (Maedler *et al.*, 2002). The molecular mechanisms underlying the effects of cytokines on β cells are not yet clear. However, cytokine-induced production of intracellular NO and expression of inducible nitric oxide synthase (iNOS) has been associated with β cells death. Blocking NO production with iNOS inhibitors significantly abolishes pancreatic β cell death induced by cytokines (Hadjivassiliou *et al.*, 1998). In our study, STZ induced markedly increase in NO production and iNOS expression whereas the addition of SR10 abolished the effect (Figure 5-5). This may be an indication that SR10 could alleviate oxidative stress and thus has a curative effect on oxidative stress-induced DM. Thus, in later part of study, the anti-oxidative and anti-diabetic effects of SR10 will be examined in animal model.

From Figure 5-6, the data showed that SR10 up-regulated insulin secretion. When compared with cell viability (Figure 4-2A), SR10 showed similar up-regulation in both cell viability and insulin secretion at the same concentrations. This indicated

that the up-regulation of insulin secretion by SR10 might be due to increased β cell viability. No indication was found that SR10 could increase insulin production/release in individual islets.

CHAPTER 6

ANTI-HYPERGLYCEMIC AND ANTI-OXIDATIVE EFFECTS OF SR10 IN A MOUSE MODEL OF TYPE 2 DM

6.1 Introduction

Both type 1 and type 2 DM involve abnormalities in pancreatic β cells. Type 1 DM is characterized by the death while type 2 DM is characterized by the accelerated apoptosis in β cells. Glucose in abnormally high concentrations forms reactive oxygen species (ROS) and thus chronic hyperglycemia leads to oxidative stress that can play an important role in development of β cell dysfunction (Wu *et al.*, 2004; Baynes *et al.*, 1991). Four major molecular mechanisms have been proposed in hyperglycemia-induced oxidative stress, viz activation of protein kinase C (PKC) via de novo synthesis of the lipid second messenger diacylglycerol (DAG), increased hexosamine pathway flux, increased advanced glycation end product (AGE) formation, and increased polyol pathway flux (Hunt *et al.*, 1991; Kaneta *et al.*, 1996). ROS generated in DM are involved to some extent in complications of the patients. For example, ROS can stimulate oxidation of low density lipoprotein (LDL), leading to the formation of oxidized LDL (ox-LDL). Ox-LDL, which is not recognized by the LDL receptor, can be taken up by scavenger receptors in macrophages leading to foam cell formation and atherosclerotic plaques.

Research interest in the protective role of anti-oxidants isolated from natural plant has been aroused in the past tens of years. These anti-oxidants can protect against oxidative damage caused by free radicals which lead to various kinds of diseases such as degenerative diseases and carcinogenesis (Reynolds *et al.*, 2007). Examples of anti-oxidants include vitamins A, C and E, glutathione (GSH), α -lipoic acid,

carotenoids, trace elements like copper, zinc and selenium, coenzyme Q₁₀ and cofactors like folic acid, uric acid, albumin, and vitamins B₁, B₂, B₆ and B₁₂ (Karihtala *et al.*, 2007; Faure *et al.*, 2003).

This part of study was carried out to investigate the effect of SR10 on blood glucose level and anti-oxidant level in diabetic mice. Before *in vivo* study, the protective effect of SR10 on hyperglycemia-induced β cell toxicity was examined using RIN-m5F cells. Cell toxicity was induced by incubating the cells with high glucose (33.3 mM) culture medium for 7 days. After confirming the protective effect of SR10 in hyperglycemic condition, animal study was applied. *db/db* mouse model is a well-known animal model for investigating type 2 DM (Kaneto *et al.*, 2004). This animal exhibits symptoms typical of human type 2 DM, such as obesity, hyperinsulinemia, hyperglycemia and glucose tolerance. Studies with this animal model of type 2 DM have established that pharmacological protection of β cells against oxidative stress could ameliorate the severity of diabetic progression (Kaneto *et al.*, 2004). In order to examine if SR10 could exhibit its anti-diabetic effect through inhibiting the ROS-induced damage in β cells of the host, plasma glucose, activities of anti-oxidant enzymes such as catalase and superoxide dismutase in plasma and liver, as well as tissue malondialdehyde (MDA) and GSH in liver were determined in *db/db* mice treated with or without SR10. Furthermore, mRNA expression of antioxidant enzymes in pancreatic islets were also examined.

6.2 Experimental results

6.2.1 Protective effect of SR10 on hyperglycemia-induced toxicity in rat pancreatic β cells

2×10^4 RIN-m5F cells were seeded in each well of 96-well culture plate. After overnight incubation, the medium was replaced with high glucose medium (containing 33.3 mM of glucose) in the absence or presence of various concentrations (0.78 $\mu\text{g/mL}$ to 100 $\mu\text{g/mL}$) of herbal extracts. Control cells were incubated with normal medium (containing 5.5 mM of glucose). The cells were further incubated for 7 days. On every other day, fresh medium and herbal extract were replaced in each well. Then, MTT assay was performed to measure the cell viability.

Figure 6-1 showed the results that cells treated with SR10 at concentrations 12.5 $\mu\text{g/mL}$, 25 $\mu\text{g/mL}$ and 50 $\mu\text{g/mL}$ exhibited significantly higher viability when compared to the cells treated with high glucose medium alone.

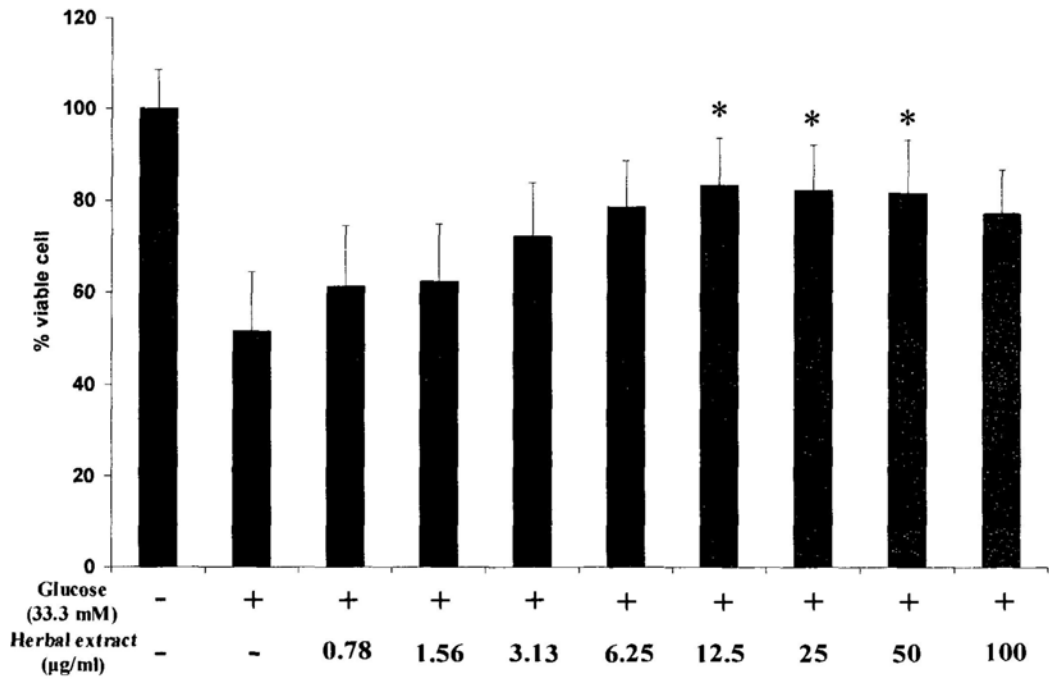


Figure 6-1 Effect of SR10 herbal extract on viability of RIN-m5F cells in medium with high glucose concentration. The cells were treated with high glucose medium (containing 33.3 mM glucose) in the presence or absence of various concentrations of SR10 for 7 days. MTT assay was performed to determine the percentage of viable cells. Percentage viability of negative control (with normal medium and without SR10 treatment) was set as 100%. The data were expressed as Mean \pm S.D. with 8 replicates for each treatment. By Mann-Whitney test, significant increases in cell viability of SR10-treated samples when compared to high glucose control were indicated by * $p < 0.05$.

6.2.2 Body weights of non-diabetic mice and diabetic mice treated with water or SR10

Body weights of mice were measured at Day 0, Day 7, Day 14, Day 21 and Day 28. The results were shown in Figure 6-2. Results showed that there was a gradual increase in body weights for all groups in 28 days. Diabetic *+db/+db* mice (water control group and both low dosage and high dosage SR10 treatment groups) showed obviously higher body weight than normal non-diabetic *m/+db* mice. However, no significant difference was found between water control group and SR10 treatment groups at both low and high dosages in diabetic mice.

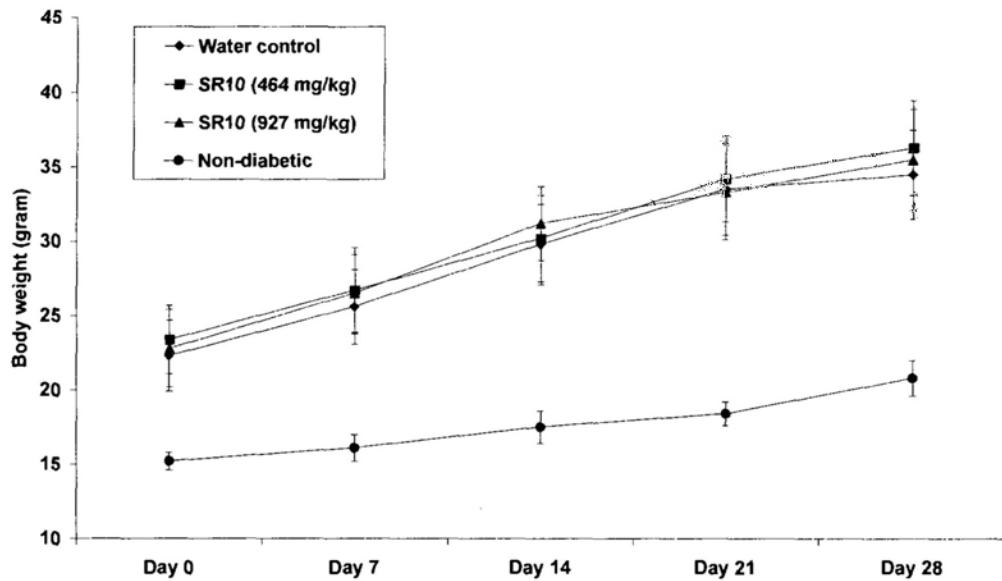


Figure 6-2 Effects of SR10 on body weight of *db/db* mice. The body weights of non-diabetic group, water control group and SR10 treatment group (n = 24 in each group) were measured once per week. Data were expressed as Mean \pm S.D. Diabetic mice showed obviously higher body weight than non-diabetic group but no significant difference was found between water control group and SR10 treatment groups.

6.2.3 Anti-hyperglycemic effect of SR10 in diabetic mice

Figure 6-3 shows that diabetic control mice (i.e. water control) exhibited almost 3-fold increase in blood glucose concentration throughout 4-week treatment period (from 155 mg/dL to 450 mg/dL). However, when the diabetic mice were treated with SR10 for 4 weeks, the rise of blood glucose concentration was significantly suppressed. For low dosage group (464 mg/kg), blood glucose concentration increased from 160 mg/dL to 375 mg/dL. For high dosage group (927 mg/kg), blood glucose level increased to 350 mg/dL after treatment period. The blood glucose concentrations of normal non-diabetic mice were maintained below 140 mg/dL throughout the treatment period. For high dosage group, a significant difference in blood glucose level was detected from day 14 to day 28 when compared to the water control group.

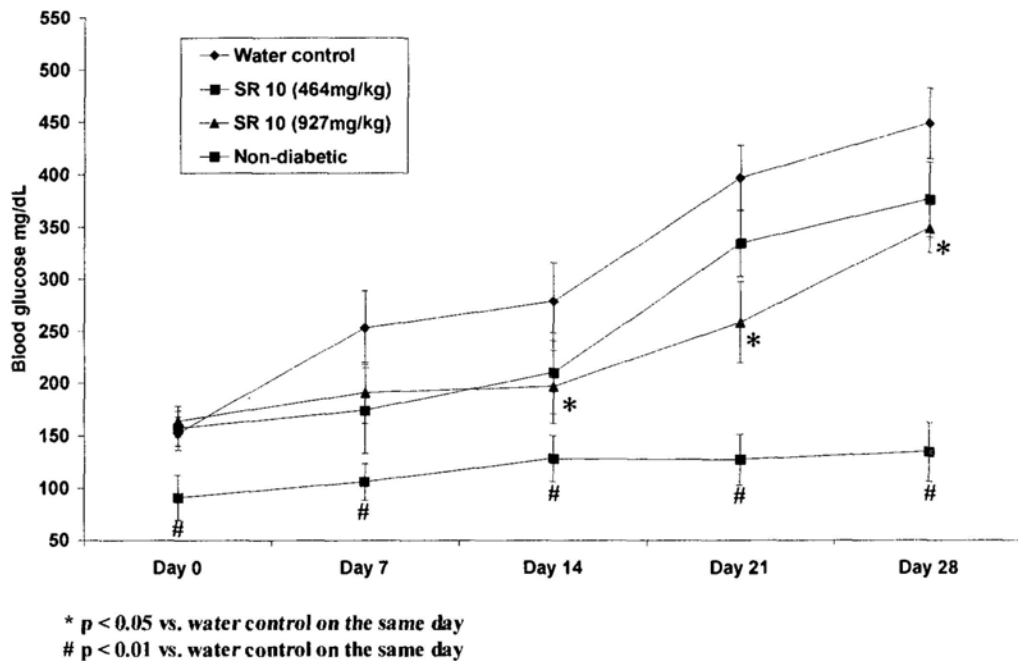


Figure 6-3 Effects of SR10 on fasting blood glucose level of *db/db* mice. For non-diabetic group, water control group and SR10 treatment groups (n = 24 in each group), the blood glucose concentrations were measured on Day 0, Day 7, Day 14, Day 21 and Day 28. Data were expressed as Mean \pm S.D. P values were generated by One-way Analysis of Variance (ANOVA) using the Dunnett's Test for multiple comparisons to water control. Statistical significance was indicated by * p < 0.05 or # p < 0.01 when compared to water control group on same day.

6.2.4 Increase in insulin release in diabetic mice after SR10 treatment

Change of plasma insulin levels in *db/db* mice with different treatment were shown in Table 6-1. Before treatment period, no significant difference in blood insulin level was observed in all of the four groups of mice. After 4-week treatment with SR10, the plasma insulin level of water control group increased from 2.15 ng/mL to 11.27 ng/mL. In both low and high dosage groups, significantly higher plasma insulin levels were observed (15.06 ng/mL in low dosage group and 17.57 ng/mL in high dosage group) when compared to water control group. In non-diabetic mice, the blood insulin content remained more or less constant during the treatment period.

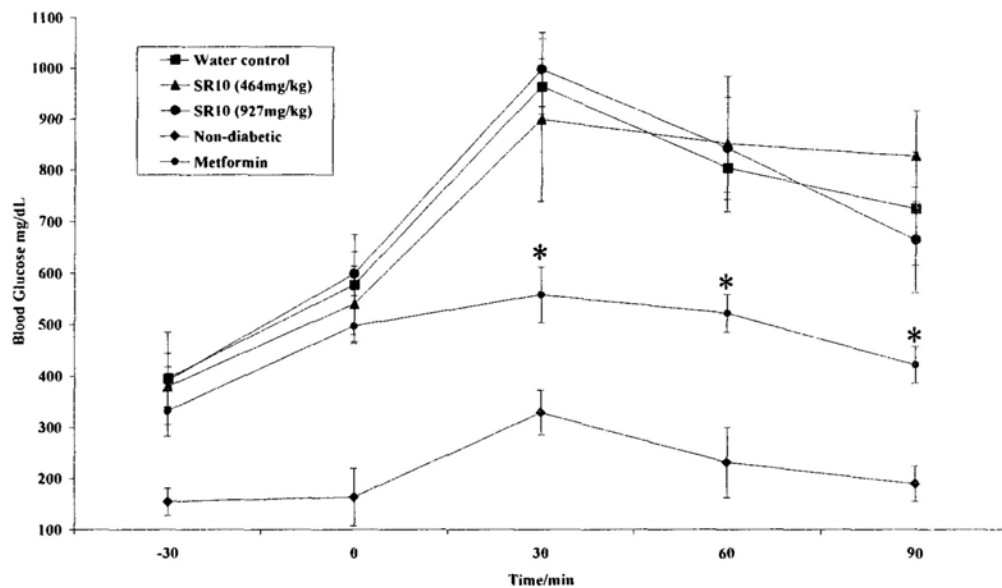
Table 6-1 Effects of SR10 treatment on plasma insulin level of *db/db* mice. For all groups of mice (n = 24 in each group), the mean plasma insulin concentrations were measured before and after 4 weeks treatment period at low and high dosages of SR10. Data was expressed as mean \pm standard deviation. *P* values were generated by One-way Analysis of Variance (ANOVA) using the Dunnett's Test for multiple comparisons to water control. Statistical significance was indicated by * $p < 0.05$ when compared to water control group on same day.

Group	Dosage (mg/kg)	Plasma insulin (ng/mL)	
		Before treatment	After 4 weeks treatment
Water control	-	2.15 \pm 0.38	11.27 \pm 2.21
SR10 (low dosage)	464	2.23 \pm 0.46	15.06 \pm 2.31 *
SR10 (high dosage)	927	2.02 \pm 0.50	17.57 \pm 3.37 *
Non-diabetic	-	1.32 \pm 0.22	1.65 \pm 0.38 *

* $p < 0.05$ compared with water control after treatment

6.2.5 No significant improvement in glucose tolerance by SR10 treatment

Glucose tolerance of *db/db* mice was evaluated by oral glucose tolerance test (OGTT) after consumption of water, metformin or SR10. As shown in Figure 6-4, oral administration of 2 g/kg glucose to non-diabetic mice increased blood glucose level to the peak of 330 mg/dL at 30 min and almost returned to baseline level at 90 min. For water control diabetic mice, the blood glucose level increased to a peak of 960 mg/dL and remained at a high level (720 mg/dL) at 90 min after glucose challenge. When compared with water control group, both low dosage and high dosage SR10 treatment groups did not show differences in blood glucose level at all time points after oral glucose intake. In positive control, metformin significantly inhibited the flux of blood glucose starting at 30 min after glucose challenge.



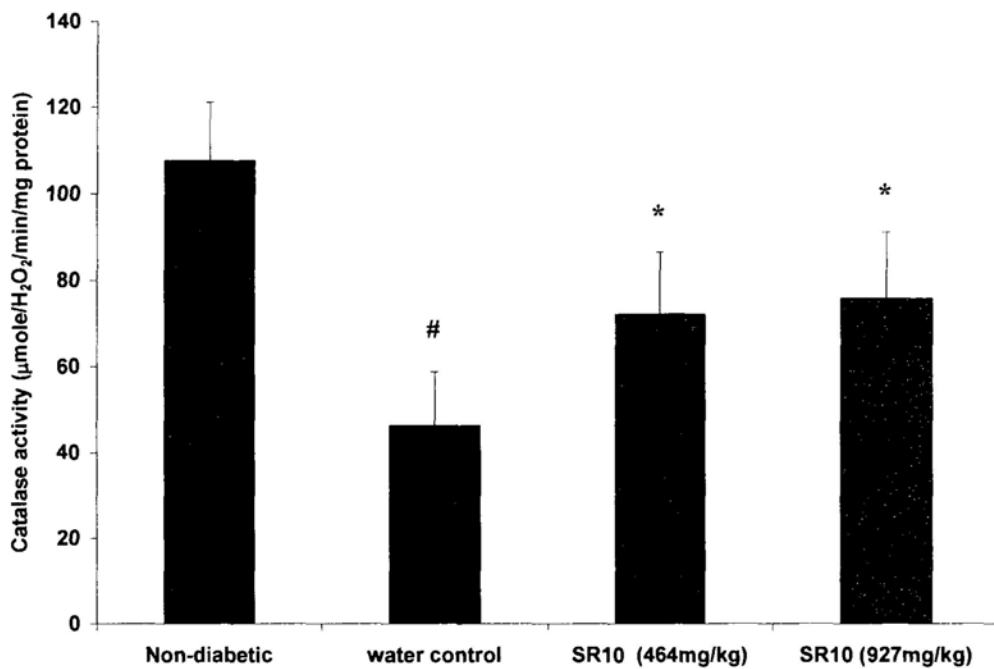
* $p < 0.01$ vs. water control on the same day

Figure 6-4 Effects of SR10 treatment on oral glucose tolerance test in *db/db* mice. All mice were challenged orally with glucose solution at dosage of 2 g/kg. For each group of mice ($n = 10$), the mean blood glucose concentrations were measured before SR10 oral administration (-30 min), before glucose challenge (0 min) as well as 30 min, 60 min and 90 min after glucose challenge. Data were expressed as Mean \pm S.D. P values were generated by One-way Analysis of Variance (ANOVA) using the Dunnett's Test for multiple comparisons to water control. Statistical significance was indicated by * $p < 0.05$ when compared to water control group at the same time point.

6.2.6 Increase of antioxidant enzyme activities in liver extracts and plasma by SR10 treatment

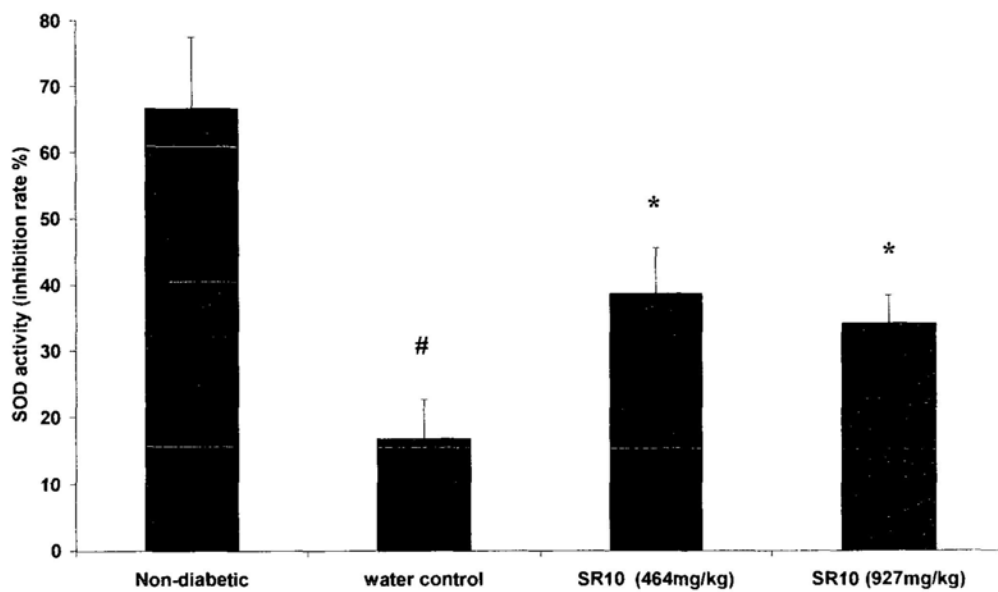
Catalase activities in both low dosage and high dosage SR10 groups were significantly higher than the water control group in both liver extract (Figure 6-5A) and plasma samples (Figure 6-5E). Significantly higher activities of SOD in both liver extract (Figure 6-5B) and plasma (Figure 6-5F) in high dosage group than in the water group were found, whereas in low dosage group, higher SOD activity was observed only in liver extract but not in plasma sample. Both tissue MDA and GSH did not show significant differences in liver extracts of both low and high dosage treatment groups when compared to water control group (Figure 6-5C & 6-5D). It should be noted that the catalase activities and SOD activities of the liver extracts in non-diabetic mice were significantly higher than those in diabetic mice (Fig. 6-5A & 6-5B), resulting in higher MDA and GSH levels (Fig. 6-5C & 6-5D). Similarly, the catalase activities and SOD activities in plasma of non-diabetic mice were significantly higher than those in diabetic mice (Fig. 6-5E & 6-5F).

(A)

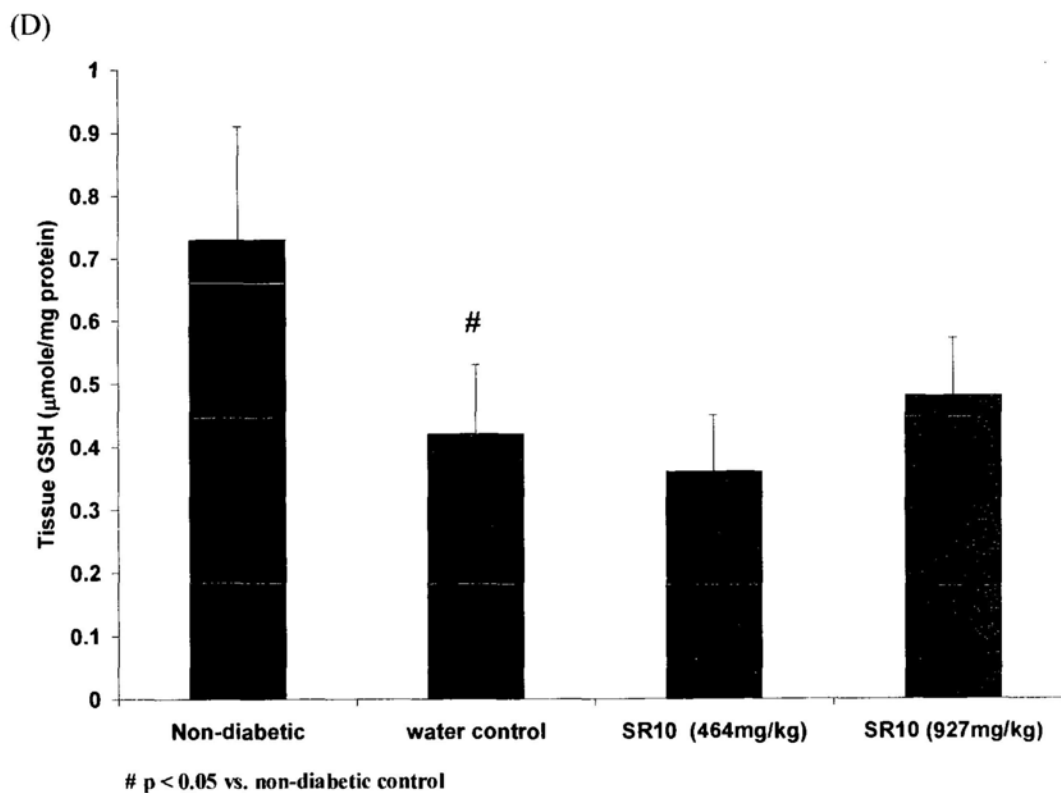
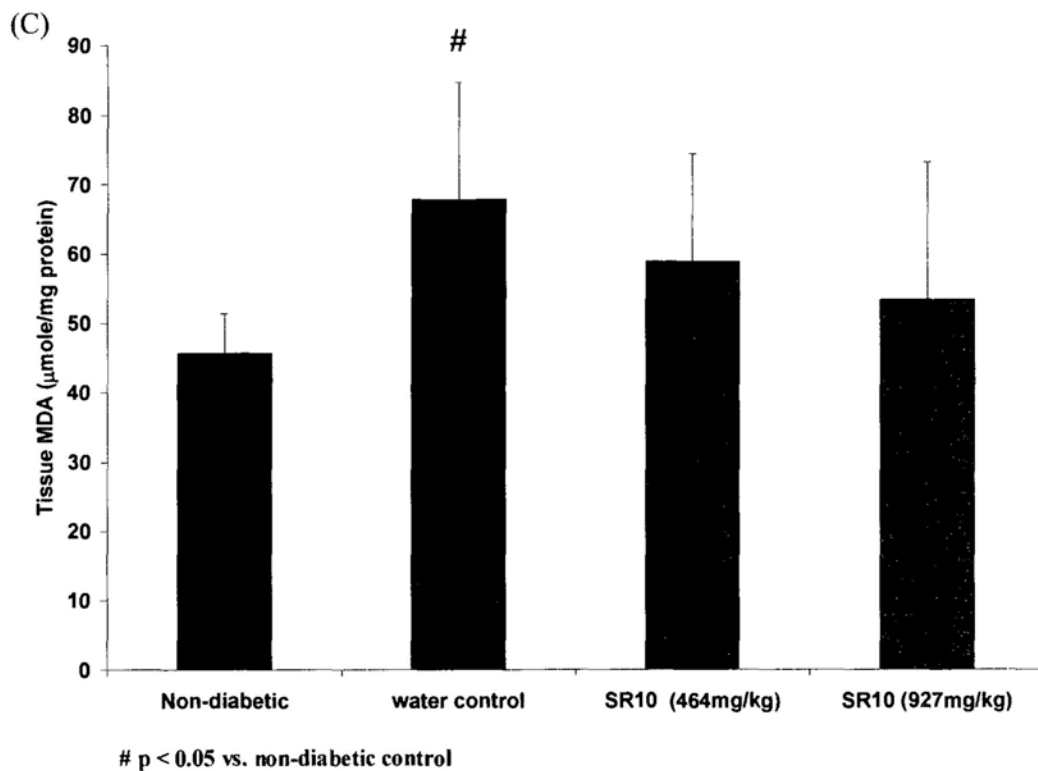


* p < 0.05 vs. water control
p < 0.05 vs. non-diabetic control

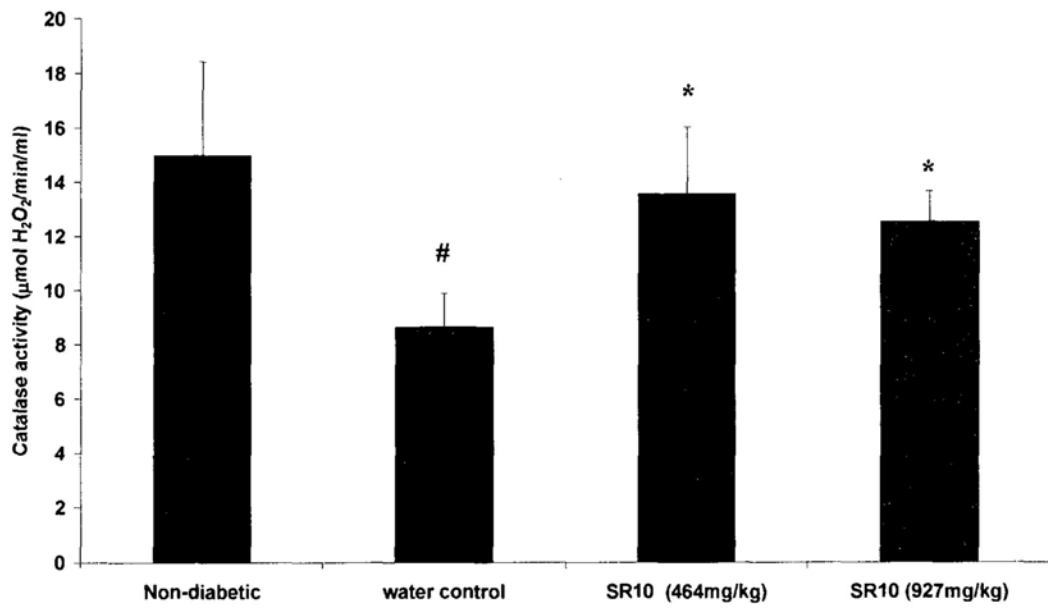
(B)



* p < 0.05 vs. water control
p < 0.05 vs. non-diabetic control



(E)



* $p < 0.05$ vs. water control

$p < 0.05$ vs. non-diabetic control

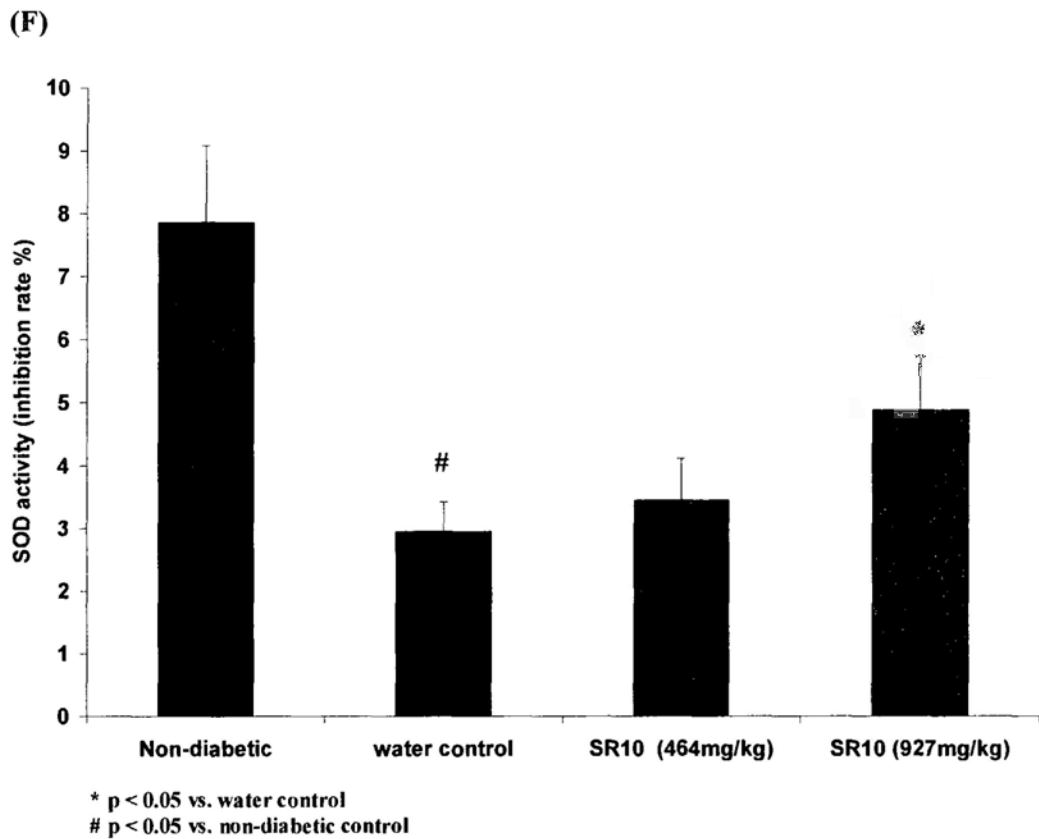


Figure 6-5 Effects of SR10 treatment on anti-oxidant enzyme activities in liver tissue and plasma of *db/db* mice. Activities of catalase (A) and superoxide dismutase (B), as well as amount of MDA (C) and GSH (D) in liver homogenates as well as plasma activities of catalase (E) and superoxide dismutase (F) were determined in *db/db* mice after 28 days of SR10 treatment. Data were expressed as Mean \pm S.D. of 24 determinants. *P* values were generated by One-way Analysis of Variance (ANOVA) using the Dunnett's Test for multiple comparisons. Statistical significance was indicated by # $p < 0.05$ when compared to non-diabetic control or * $p < 0.05$ when compared to water control.

6.2.7 Increase of antioxidant enzyme expression in islets of *db/db* mice by SR10

RNA from freshly isolated islets of *db/db* mice was quantified for the expression of catalase, superoxide dismutase (SOD) and glutathione peroxidase (GPx) by comparing with the housekeeping gene 18S (Table 6-2). There was significantly higher mRNA expression of catalase in high dosage SR10 group (2.18 folds) and that of SOD in both low and high dosage SR10 groups (2.10 folds and 2.52 folds, respectively) when compared to the water control group. However, for GPx, no significant difference was detected between SR10 treatment groups and water control group.

Table 6-2 Effects of SR10 treatment on mRNA expression of catalase, superoxide dismutase (SOD) and glutathione peroxidase (GPx) in the islets of *db/db* mice. The islets of mice treated with or without low and high dosages of SR10 were isolated from the pancreases after 28 days treatment period (n = 3 per group). RNA was prepared and real-time PCR was performed to examine the mRNA expression level. Each sample was done in triplicate for real-time PCR. Data were expressed as Mean \pm Standard Deviation. *P* values were generated by One-way Analysis of Variance (ANOVA) using the Dunnett's Test for multiple comparisons. Statistical significance was indicated by [#] *p* < 0.05 when compared to non-diabetic control or ^{*} *p* < 0.05 when compared to water control.

Relative change in mRNA expression				
Enzymes	Non-diabetic	Water control	SR10 (464 mg/kg)	SR10 (927 mg/kg)
Catalase	1	0.39 \pm 0.05 [#]	0.58 \pm 0.11	0.85 \pm 0.19 [*]
SOD	1	0.31 \pm 0.04 [#]	0.65 \pm 0.16 [*]	0.78 \pm 0.16 [*]
GPx	1	0.79 \pm 0.08 [#]	1.03 \pm 0.21	0.92 \pm 0.13

**Data was expressed as Mean \pm Standard Deviation
By One-way ANOVA with Dunnett's test,
^{*} *p* < 0.05 compared to water control
[#] *p* < 0.05 compared to non-diabetic control**

6.2.8 Activities of liver, heart and kidney specific enzymes in plasma of *db/db* mice treated with SR10

Plasma activities of creatine kinase (CK), aspartate transaminase (AST), alanine transaminase (ALT) and lactate dehydrogenase (LDH) as well as plasma level of creatinine were examined to determine the probable toxicities to the liver, heart and kidney of the animals. The results showed that no significant differences of these enzyme activities and creatinine level were detected between both SR10 treatment groups and water control group after 28 days treatment period (Figure 6-6).

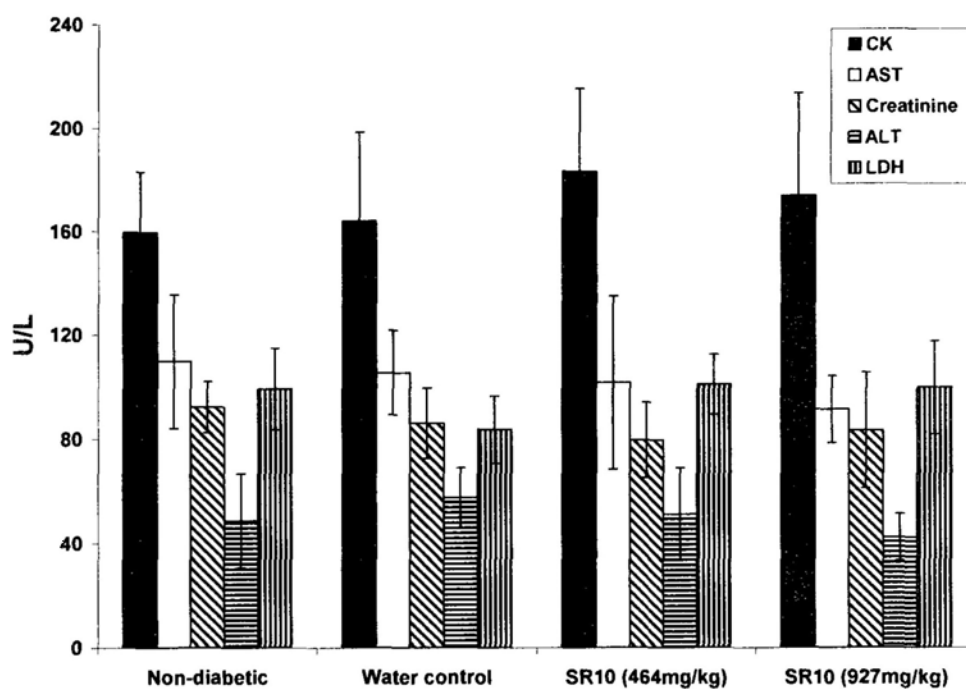


Figure 6-6 Effects of SR10 treatment on plasma enzyme activities in *db/db* mice. Plasma activities of creatine kinase (CK), aspartate transaminase (AST), alanine transaminase (ALT) and lactate dehydrogenase (LDH), as well as plasma level of creatinine were measured in different groups of mice (n = 24 for each group) after 28 days treatment period. Data were expressed as Mean \pm Standard Deviation.

6.3 Discussion

High glucose concentration impairs islet function by disturbing glucose metabolism in β cells mitochondria and induces apoptosis (Maedler *et al.*, 2001). In addition, it has been reported that high glucose concentration can enhance β cell vulnerability to toxic effects by increasing the expression of potential autoantigens on the cell membrane surface (Aguilar-Diosdado *et al.*, 1994). It has also been reported that chronic exposure to high glucose (for more than two days) leads to increased rat islet cell apoptosis (Piro *et al.*, 2002). In the current study, we firstly analyzed the protective effect of SR10 on rat β cell death in high glucose condition for 7 days. An increased percentage of β cell viability was observed when SR10 (12.5 $\mu\text{g/ml}$ to 50 $\mu\text{g/ml}$) was incubated with very high (33.3 mM) glucose concentrations in the medium (Figure 6-1). The results implied that SR10 not only inhibited STZ-induced β cell death but also protected from cell death induced by high glucose condition.

After confirming the effectiveness of SR10 in hyperglycemic condition, the anti-hyperglycemic effect of SR10 was investigated using diabetic mice model. C57BL/KsJ *db/db* mouse is an inbred strain with *db* gene mutation occurring spontaneously. The mice exhibit hyperglycemia, hyperinsulinemia and glucose intolerance that phenotypically resemble human type 2 DM. Since genetically diabetic *+db/+db* mice exhibit obesity, the body weights of *+db/+db* mice were significantly higher than normal non-diabetic mice (*m/+db*) and oral administration of SR10 did not affect body weight in both diabetic and non-diabetic mice (Figure 6-2). Fasting blood glucose levels were measured on Day 0, Day 7, Day 14, and Day 28 after daily oral administration of SR10 or water. The diabetic *+db/+db* mice exhibited its diabetic characteristics from 4 weeks of age and blood glucose

concentrations on 1st day of experiment (4-5 weeks of age) were similar in all groups. However, blood glucose levels of diabetic mice were markedly increased from Day 7 to Day 28 when compared to the normal non-diabetic mice, and SR10 intake (both low dosage and high dosage) significantly lowered the blood glucose levels. On Day 29, blood glucose levels in low dosage and high dosage SR10 fed *+db/+db* mice were 16.7% and 22.2% lower than those of water supplied *+db/+db* group, respectively. Blood insulin levels of diabetic mice were much higher than normal mice indicating insulin resistance in type 2 DM. Interestingly, SR10 oral administration also caused increases of insulin level in diabetic mice when compared with water control group, suggesting elevated insulin release in diabetic mice. The hypoglycemic effects of SR10 in type 2 diabetic mice model may be associated with the improvement of functions of pancreatic β cells.

Oxidative stress has been linked to the induction of β cell damage/apoptosis in the development of type 2 DM. Therefore, tissue anti-oxidant status is one of the major factors in determining the deterioration of diabetic condition (Bonfont-Rousselot *et al.*, 2000). Many anti-oxidant systems exist within cells to neutralize ROS. Superoxide anions are enzymatically converted to hydrogen peroxide by superoxide dismutase (SOD) within mitochondria. Hydrogen peroxide is then disposed of by the mitochondrial enzyme glutathione peroxidase (GPx). The inner mitochondrial membrane contains vitamin E, a powerful anti-oxidant. The intermembrane mitochondrial space contains the superoxide dismutase isozyme and cytochrome c, which also plays a role in control of ROS concentration and defense. Catalase, on the other hand, is the major hydrogen peroxide detoxifying enzyme found exclusively in peroxisomes (Sakurai *et al.*, 1988; Maritim *et al.*, 2003).

The protective mechanism of SR10 may contribute to its ROS scavenging activity. Therefore, SR10 administration may improve islet β cell function resulting in increased release of circulating insulin and thus, ameliorate hyperglycemia and delay the development of DM in these diabetic mice model. In the study, the protective effect of SR10 in *db/db* mice was evaluated. Liver is the tissue with highest anti-oxidant defense and its change in anti-oxidant status is easily detected when there is oxidative stress. Thus, we have examined the anti-oxidant status in the liver as well as in the plasma. The deleterious effects of superoxide anion and hydroxyl radicals can be counteracted by anti-oxidant enzymes catalase and SOD. The activities of these enzymes were detected in liver extracts and plasma, and they were found to be significantly lower in diabetic mice than the normal mice. These antioxidant enzymes were also found to be significantly up-regulated by treatment of SR10 for 4 weeks in diabetic mice (Figure 6-5A – Figure 6-5F). These results were further confirmed by mRNA expression level (Table 6-2). MDA, a by-product of lipid peroxidation as well as GSH, a marker of total anti-oxidant status, were detected in liver homogenate (the quantities of both markers were too low to be detected in plasma). However, no significant difference was found between SR10-treated diabetic mice and water control group (Figure 6-5C & 6-5D). As treatment of SR10 has lasted for 28 days, the probable toxic effects induced to the mice were examined by measuring the activities of heart-, liver- and kidney-specific enzymes. The results indicated that no toxicity was generated under the current treatment regimen of SR10.

CHAPTER 7

SUPPRESSION OF LOW DENSITY LIPOPROTEIN OXIDATION, VASCULAR SMOOTH MUSCLE CELL (VSMC) PROLIFERATION AND MIGRATION BY SR10

7.1 Introduction

Among different diabetic complications, atherosclerosis represents the major mortal threat to DM patients (Albright, 2008; Bessesen, 2008). Oxygen derived free radicals are very important mediators of cell injury. These free radicals include superoxide, hydrogen peroxide and nitric oxide. Collectively, the high reactivity of ROS determines chemical changes in virtually all cellular components, leading to DNA and protein modification and lipid peroxidation (Niedowicz *et al.*, 2005). Many studies have been carried out to find the association between diabetes and atherosclerosis. It was found that glucose enhanced low density lipoprotein (LDL) oxidation and glucose-mediated enhancement of LDL oxidation was partially blocked by superoxide dismutase (Vergès, 2005; Krentz, 2003). Oxidized LDL (ox-LDL) involved in atherogenesis by affecting cytokine production, endothelium-derived relaxing factor-mediated vascular reactivity and foam cell formation (Stewart *et al.*, 2005; Galle *et al.*, 2000). These findings explained how chronic hyperglycemia of diabetes accelerates lipoprotein oxidation, thereby promoting diabetic vascular disease.

In addition, excessive ROS in diabetes is thought to promote atherogenesis by affecting several steps. Firstly, it facilitates the recruitment of monocytes and macrophages. Secondly, it increases lipid deposition in the intimal layer. Thirdly, it promotes the proliferation and migration of smooth muscle cells (Stocker *et al.*, 2004). One of the principal regulators of mitogenesis in vascular smooth muscle cells

is platelet-derived growth factor-BB (PDGF-BB). The signaling pathway of PDGF-BB-induced mitogenesis involved the activation of extracellular regulated kinases 1 and 2 (ERK1/2) (Kingsley *et al.*, 2002). ERK1/2-mediated pathway is also shown to be important for PDGF-BB-induced cell cycle progression in vascular smooth muscle cells (VSMC). Within the arterial media, smooth muscle cells are mostly in quiescent stage (i.e. G₀/G₁ phase of the cell cycle). Upon vessel injury, smooth muscle cells migrate into the intima, where they transit through G₁ phase and re-enter into S phase.

In this part of study, the effect on oxidative resistance of human LDL which is an important step in initiating atherosclerosis was examined. Furthermore, the effect of SR10 in inhibiting PDGF-BB-induced rat vascular smooth muscle cell (A7r5) proliferation and migration was demonstrated.

7.2 Experimental results

7.2.1 Inhibition of AAPH-induced RBC hemolysis

2,2'-azo-bis-(2-amidinopropane) dihydrochloride (AAPH) is a well-known free radical generator. In the absence of AAPH, hemolysis of rat RBCs was negligible. When RBCs were incubated with 100 mM AAPH for 200 min, about 93% of hemolysis was detected (data not shown). However, percentage inhibition of hemolysis was increased when RBCs was incubated simultaneously with increasing concentrations of SR10. From Figure 7-1, SR10 was shown to inhibit up to 70% hemolysis at concentration 1 mg/ml, with IC_{50} value at 0.25 mg/ml. Ascorbic acid (vitamin C) was used as a positive control with IC_{50} value at 0.1 mg/ml.

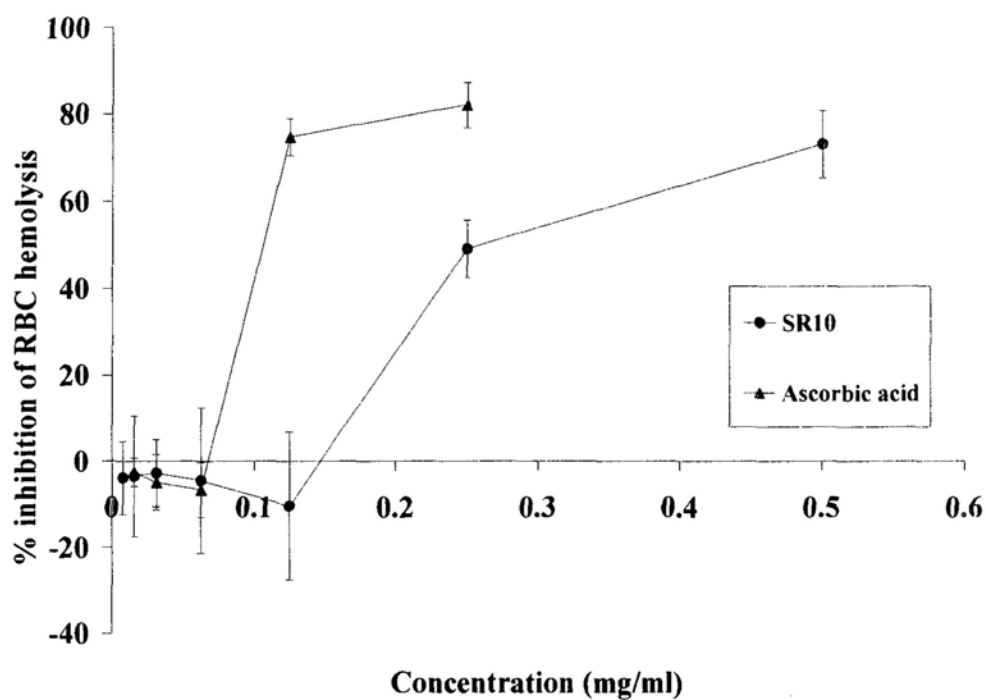
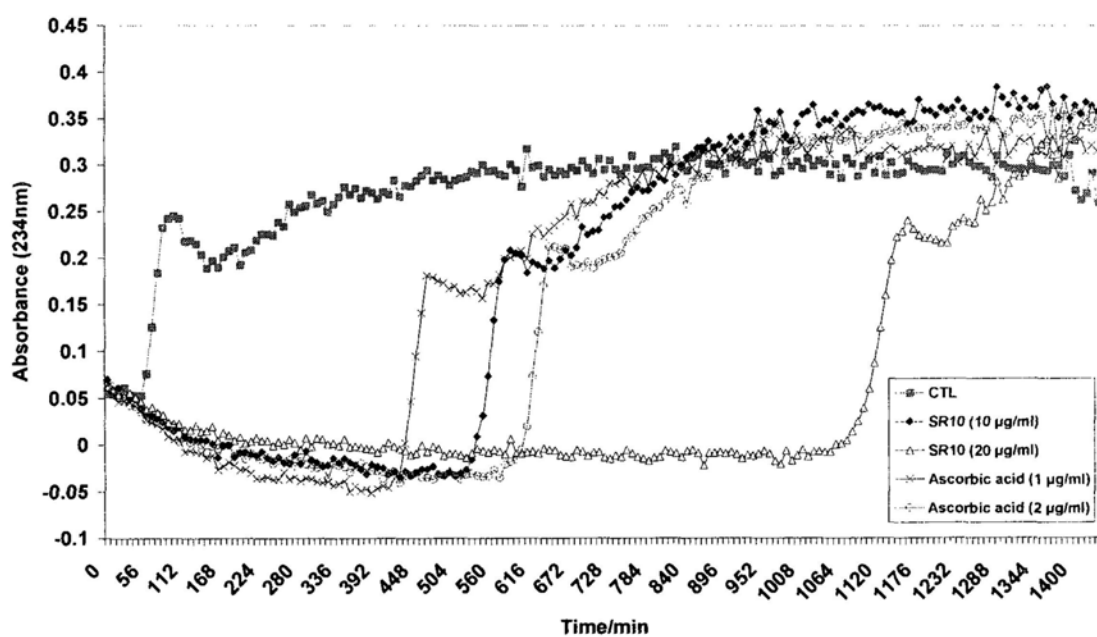


Figure 7-1 Effect of SR10 on AAPH-induced hemolysis in rat erythrocytes. Erythrocyte suspension was incubated with PBS (set as 0% inhibition), various concentrations of ascorbic acid (positive control) or SR10 in the presence of 100 mM AAPH for 200 min at 37°C. Data were expressed as Mean \pm S.D. of three independent experiments.

7.2.2 Prolongation of human LDL oxidation

Lag phase prolongation as calculated by $[\text{lag time}_{(\text{sample})} - \text{lag time}_{(\text{control})}]$ was used to measure the antioxidant property of the sample to protect from human LDL oxidation. Lag time was determined graphically as the X-intercept of the tangent to the propagation curve. Figure 7-2A showed the result of one representative trials. The data shown in Figure 7-2B was the average lag phase prolongation time of three independent trials. SR10 increased the lag time from 85 min (PBS control) to 480 min and 1000 min at concentrations 10 $\mu\text{g/mL}$ and 20 $\mu\text{g/mL}$, respectively. Ascorbic acid, as a positive control, increased the lag time to 370 min and 525 min at concentrations 1 $\mu\text{g/mL}$ and 2 $\mu\text{g/mL}$, respectively.

(A)



(B)

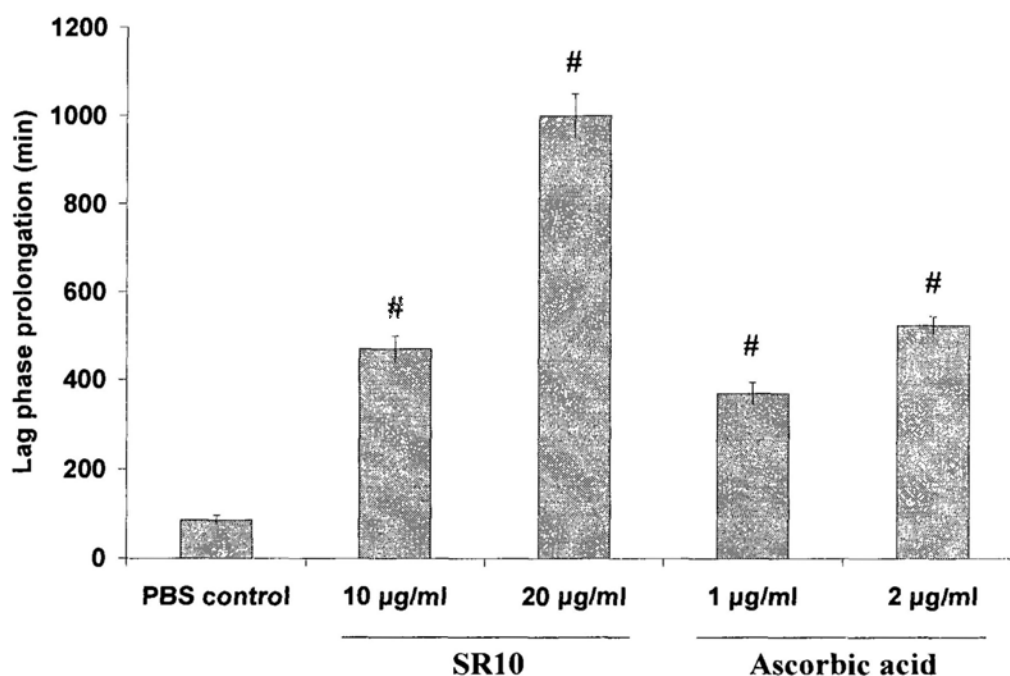


Figure 7-2 Effect of SR10 on prolongation of copper ion-induced human LDL oxidation. LDL in PBS was incubated with 5 μ M CuSO_4 at 37°C in the presence or absence of SR10, and ascorbic acid (positive control). Conjugated diene formation was measured by determining the absorbance at 234 nm at every 5 min for totally 24 h. A figure showing one representative experiment of three trials was shown in panel (A). Lag time was determined as the intercept of the slopes for the lag phase and propagation phase. Difference of lag time between treatment and control (PBS only) was defined as lag phase prolongation. Results of lag phase prolongation time from three independent trials was shown in panel (B). Data were expressed as Mean \pm S. D. for three independent experiments. By Mann-Whitney test, significant difference when compared to PBS control was indicated by # $p < 0.01$.

7.2.3 Inhibition of rat vascular smooth muscle cell (VSMC) proliferation

The effects of SR10 on rat vascular smooth muscle cell proliferation was evaluated. Rat VSMC, namely A7r5, were incubated with PDGF-BB in the absence or presence of SR10 for 24 hours. Then, the cell viability was examined by MTT assay. When A7r5 cells were stimulated with PDGF-BB for 24 h in the absence of SR10, cell growth (which is directly proportional to absorbance measured in MTT assay) was significantly increased. However, the addition of SR10 suppressed this PDGF-BB-stimulated proliferation in a concentration-dependent manner with significant effect found at concentrations 2.5 mg/mL and 5 mg/mL. This inhibition of cell proliferation was not due to toxicity of SR10 as evidenced by no significant change induced by SR10 without PDGF-BB (Figure 7-3).

The effect of SR10 on cell growth was also determined by measuring DNA synthesis. PDGF-BB highly increased ³H-thymidine incorporation into DNA but the increase was inhibited by co-treatment of SR10 in a concentration-dependent manner (Figure 7-4).

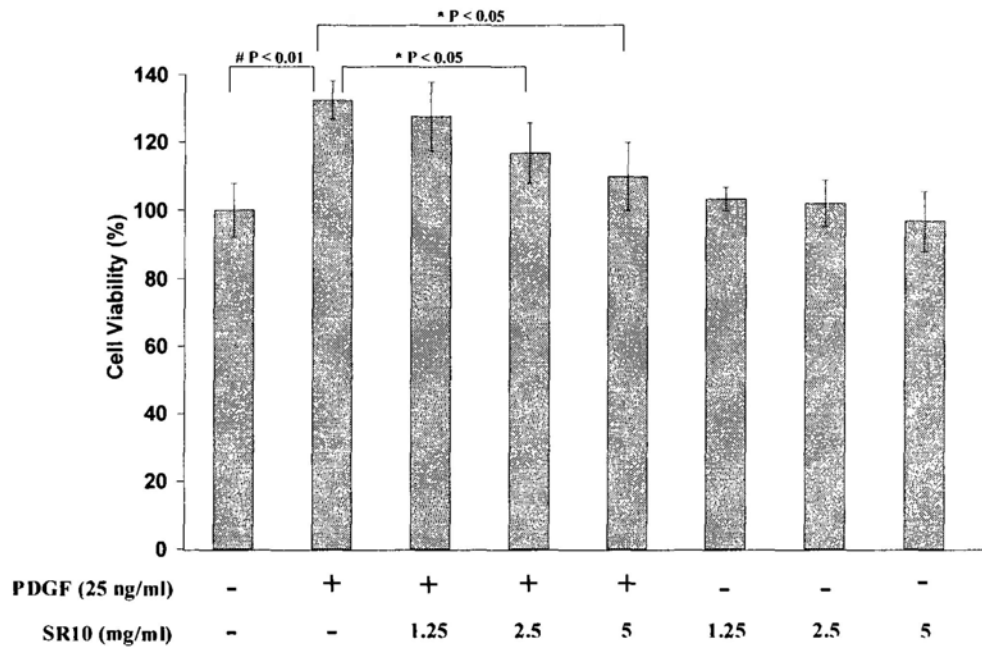


Figure 7-3 Effect of SR10 on PDGF-BB-stimulated proliferation of rat VSMCs. Cells were incubated with PDGF-BB (25 ng/mL) for 24 h in the absence or presence of various concentrations of SR10. Cells incubated with various concentrations of SR10 without PDGF-BB were used to indicate the cytotoxicity of SR10. After 24 h, MTT assay was performed to measure the cell viability in different treatments. Percentage viability of cells without treatment of PDGF-BB or SR10 was set as 100% (negative control). Percentage cell viability of other treatment groups was calculated against negative control. Data were expressed as Mean \pm Standard Deviation with 8 replicates for three independent experiments. By Mann-Whitney test, significant difference when compared to PDGF-BB alone was indicated by * $p < 0.05$ or # $p < 0.01$.

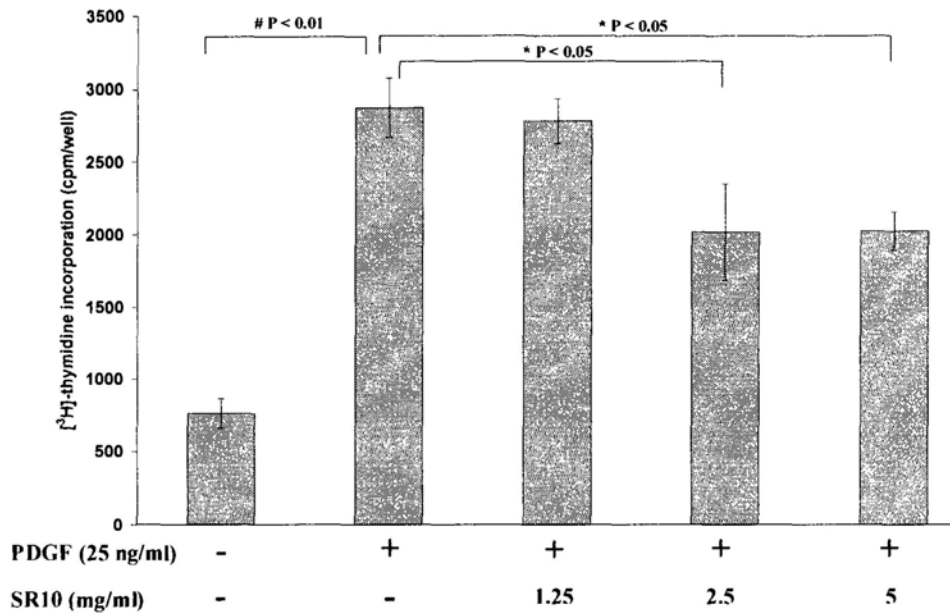


Figure 7-4 Effect of SR10 on PDGF-BB-induced ³H-thymidine incorporation in A7r5 cells. Cells were treated with PDGF-BB (25 ng/mL) for 24 h in the absence or presence of SR10 and incorporation of ³H-thymidine was measured. Data were expressed as Mean ± Standard Deviation with 6 replicates for three independent experiments. By Mann-Whitney test, significant difference when compared to PDGF-BB alone was indicated by * p < 0.05 or # p < 0.01.

7.2.4 Cell cycle arrest at G₀/G₁ and inhibition of expression of cyclin D1

The effect of SR10 on cell cycle progression in A7r5 cells was evaluated by staining with PI. In quiescent A7r5 cells, the populations in G₀/G₁, S and G₂/M phase were 69.52%, 10.56% and 19.93%, respectively. When the cells were stimulated by PDGF-BB for 24 h, cell cycle progression from G₀/G₁ to S and G₂/M phase was observed. However, treatment of various concentrations of SR10 blocked G₀/G₁-S phase transition. The population of G₀/G₁ phase was increased from 48.18% to 57.29%, 59.22% and 66.02% when PDGF-BB-stimulated was treated with SR10 at concentrations 1.25 mg/mL, 2.5 mg/mL and 5 mg/mL, respectively. Populations in S phase was decreased from 25.13% to 21.22%, 19.19% and 13.03%, respectively, while in G₂/M phase, the population was decreased from 26.69% to 21.48%, 21.59% and 20.95%, respectively (Figure 7-5).

As SR10 arrested cell cycle progression at G₀/G₁ phase, the expression of G₁ phase-regulated protein cyclin D1 was examined by Western blot. The results showed that SR10 mildly suppressed expression of cyclin D1 which was up-regulated by PDGF-BB (Figure 7-6).

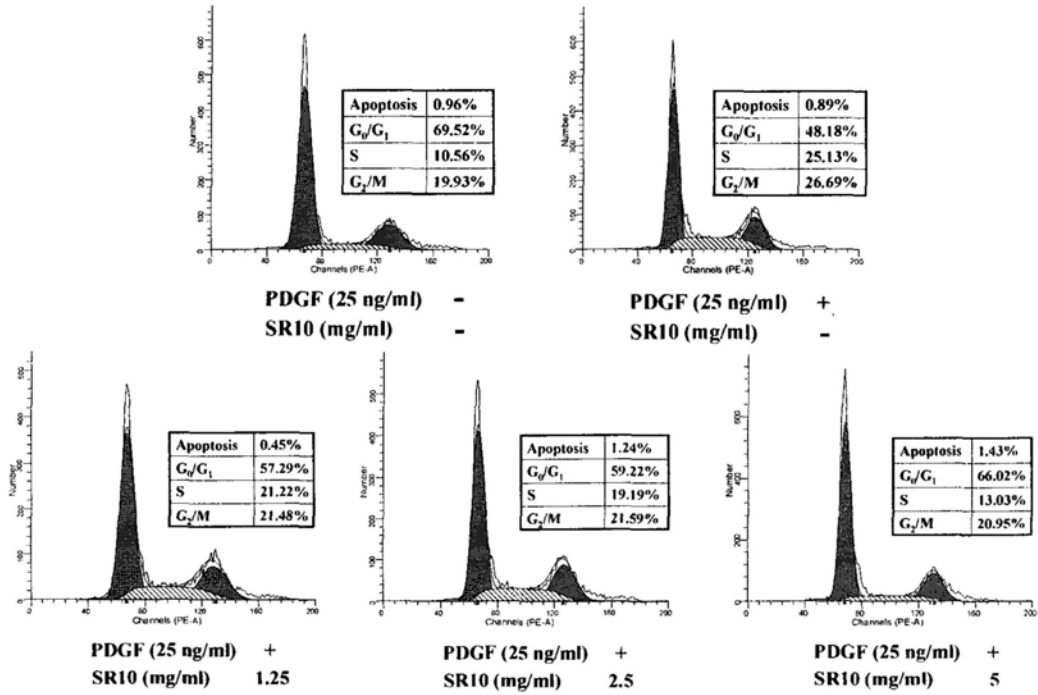


Figure 7-5 Effect of SR10 on cell cycle distribution of PDGF-BB-treated A7r5 cells. After starving with 1% FBS for 24 h, A7r5 cells were treated with PDGF-BB in the absence or presence of SR10 for 24 h. Then, the cells were stained with PI and cell cycle distribution was analyzed by flow cytometry. Three experiments were conducted and similar results were observed. This figure showed the results of one representative experiment.

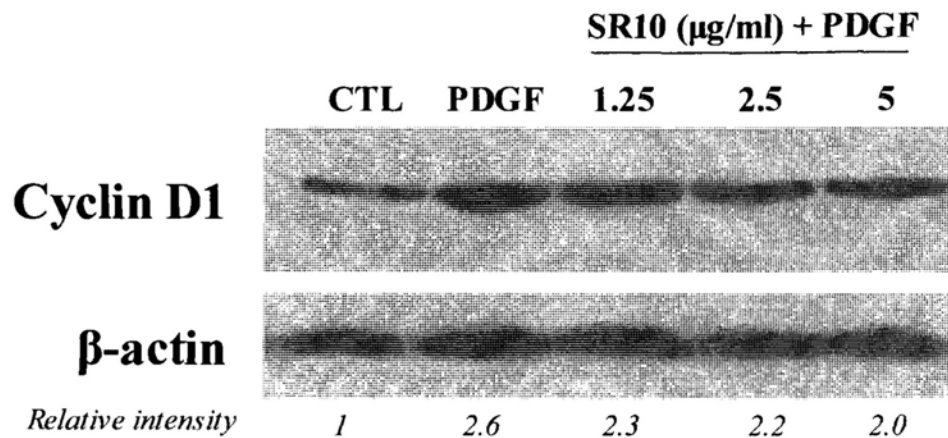
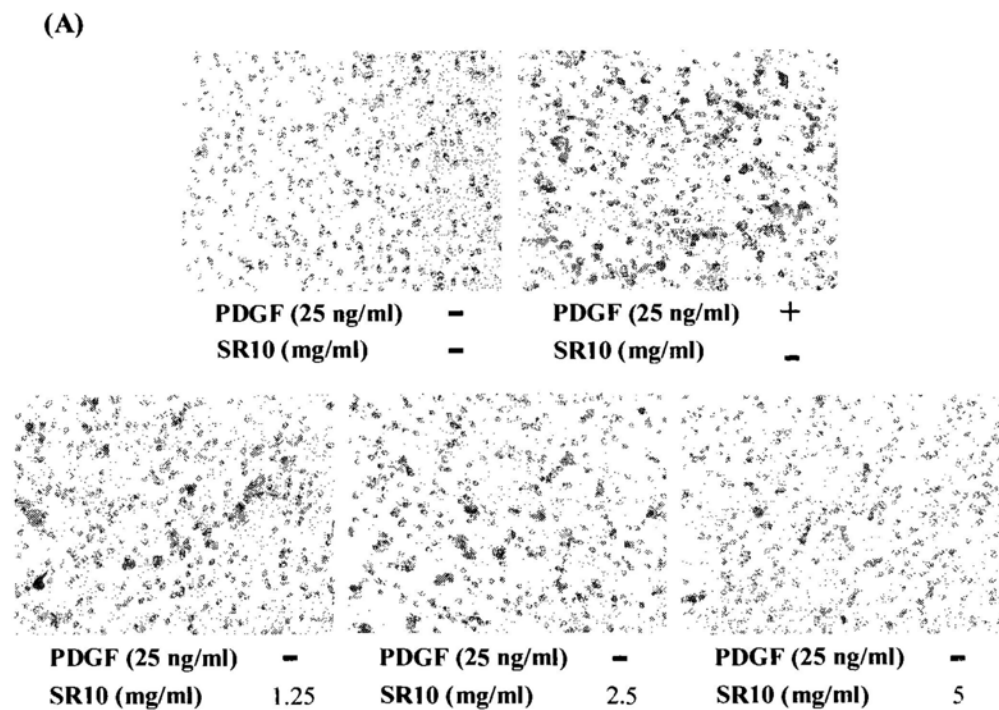


Figure 7-6 Effect of SR10 on expression of cyclin D1 on PDGF-BB-treated A7r5 cells. Cells without SR10 treatment were regarded as PDGF-BB control (Lane 2). Cells without the addition of both PDGF-BB (25 ng/mL) and SR10 were regarded as negative control (Lane 1). Other samples were treated by PDGF-BB with various concentrations of SR10. Then, the expression level of cyclin D1 was detected by Western blot.

7.2.5 Suppression of rat VSMC migration

Figure 7-7A showed the view of lower membrane after A7r5 cells migrated through the membrane. PDGF-BB greatly induced vascular smooth muscle cell migration. However, when SR10 was placed at the lower chamber with PDGF-BB, cell migration was inhibited significantly at all concentrations tested (Fig. 7-7B).



(B)

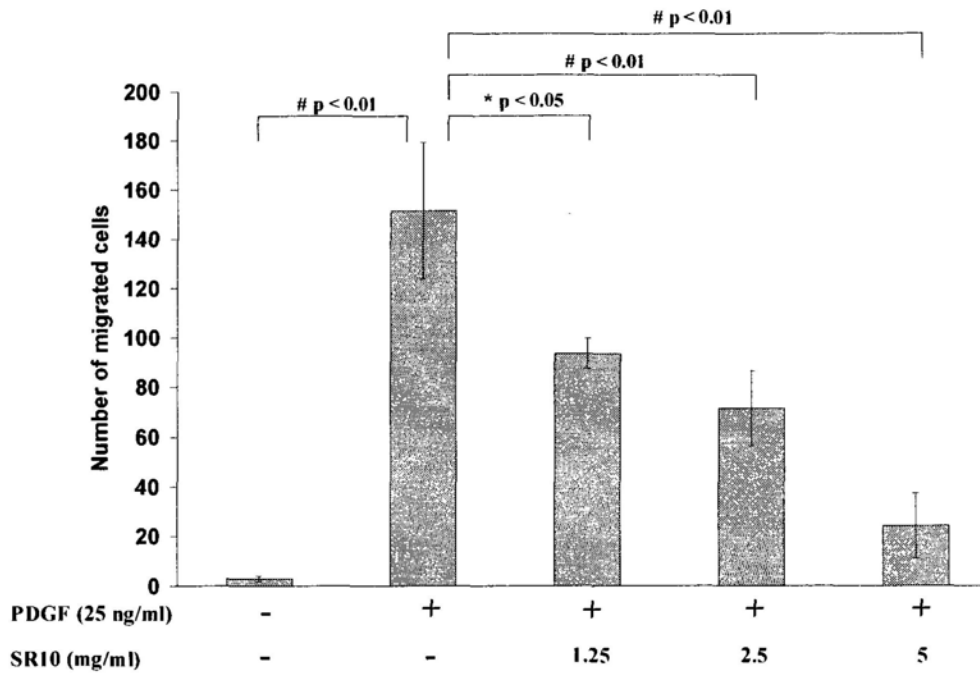


Figure 7-7 Effect of SR10 on PDGF-BB-induced migration of A7r5 cells in a transwell migration assay. A7r5 cells were loaded in the upper chamber while PDGF-BB (25 ng/mL) was loaded in the lower chamber in the absence or presence or various concentrations of SR10. After 3 h incubation, migrated cells were observed in the lower surface of the membrane (A). Number of migrated cells was counted for five regions per filter. Data were expressed as Mean \pm S.D. with 3 replicates of three independent trials. By Mann-Whitney test, significant difference when compared to PDGF-BB alone was indicated by * $p < 0.05$ or # $p < 0.01$ (B).

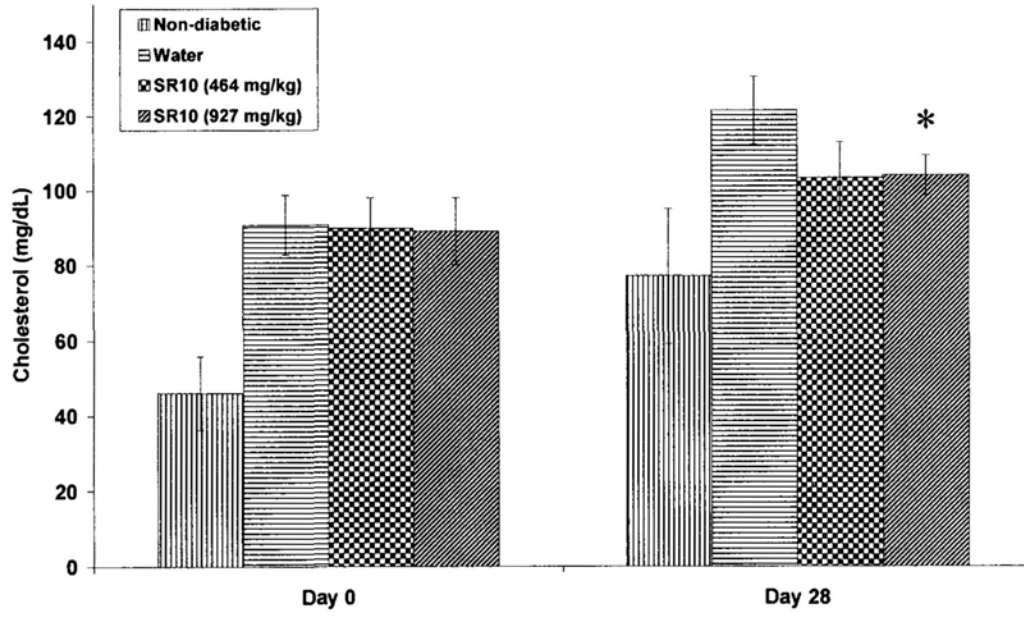
7.2.6 Plasma concentrations of total cholesterol, HDL-cholesterol (HDL-C), triglyceride, calculated LDL-cholesterol (LDL-C) and paraoxonase (PON) activity in *db/db* mice

In Chapter 6, diabetic mice model was used to examine the effect of SR10 on blood glucose. In this part, the effect of SR10 on plasma concentrations of total cholesterol, HDL-cholesterol, triglyceride, and paraoxonase (PON) activity were examined in non-diabetic *m/+db* mice and SR10-treated diabetic *+db/+db* mice. LDL-cholesterol of each mouse was calculated based on the following formula (Friedewald *et al.*, 1972):

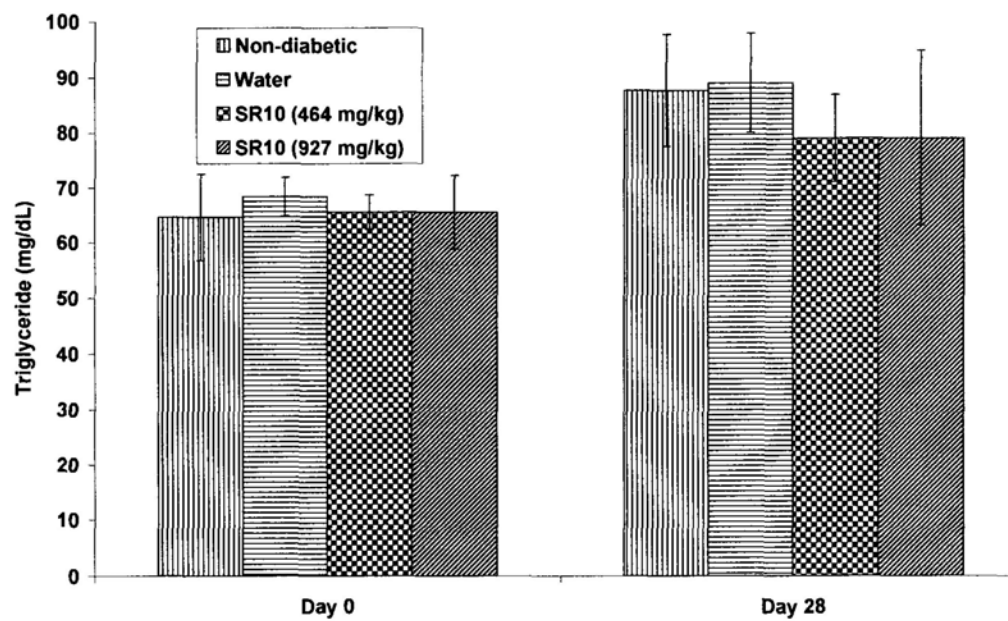
$$\text{LDL-C} = (\text{Total cholesterol}) - (\text{HDL-C}) - (\text{Triglyceride}/5)$$

From the results shown in Figure 7-8, it could be seen that total cholesterol was significantly decreased when diabetic mice were treated with SR10 (927 mg/kg) for 28 days (Figure 7-8A). For triglyceride, no difference was found between non-diabetic mice and diabetic mice, as well as between water-treated diabetic mice and SR10-treated diabetic mice (Figure 7-8B). HDL-cholesterol was found to be increased in SR10-treated mice after 28 day treatment but the difference was not statistically significant (Figure 7-8C). For calculated LDL-cholesterol, a significant decrease was found in both low dose and high dose SR10 treatment groups when compared to water control group (Figure 7-8D). PON activity was significantly lower in diabetic mice than in non-diabetic mice. After treatment with SR10, there was an increasing trend in PON activity in both high dosage and low dosage groups but the difference was not statistically significant (Figure 7-8E).

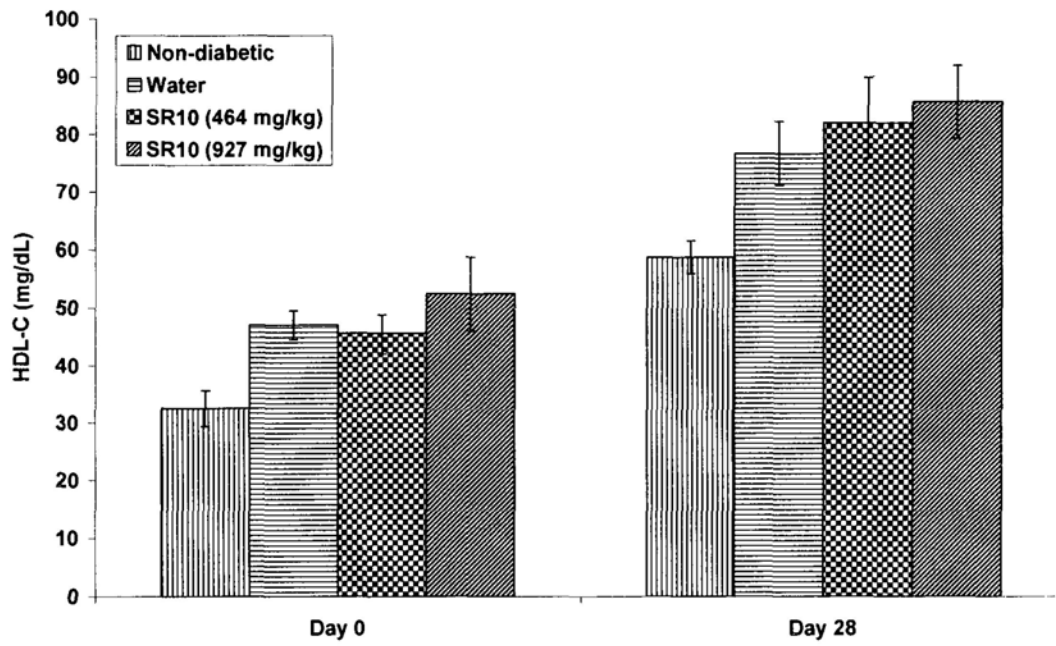
(A)



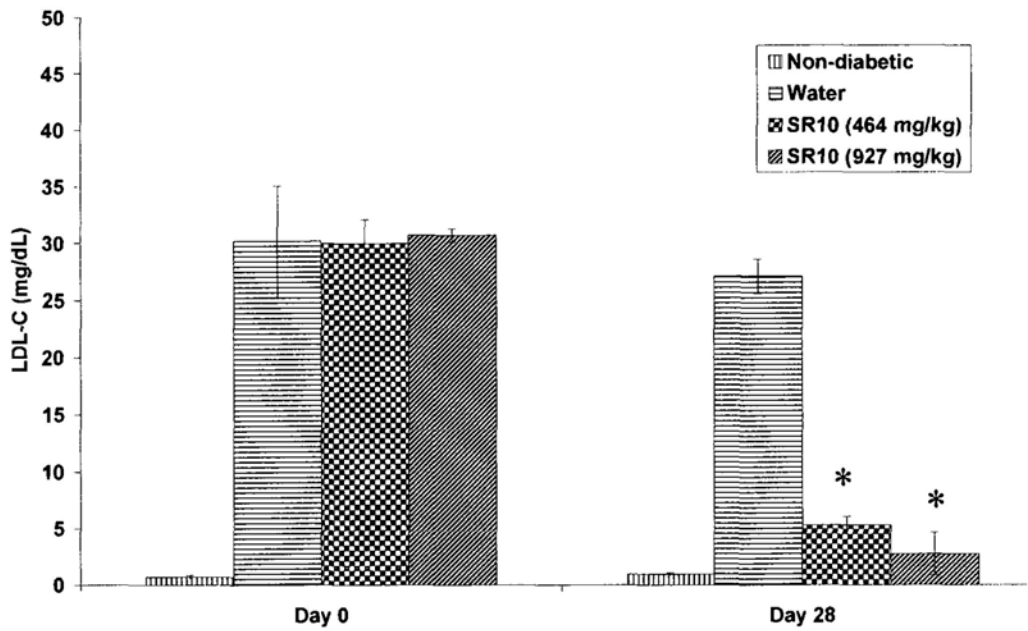
(B)



(C)



(D)



(E)

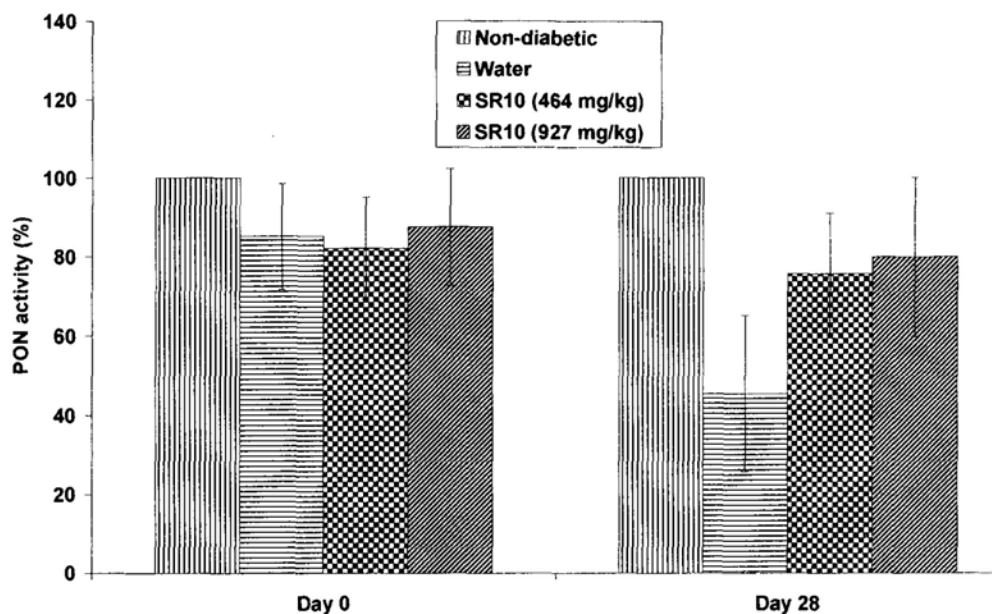


Figure 7-8 Effect of SR10 on plasma concentrations of total cholesterol, triglyceride, HDL-cholesterol, calculated LDL-cholesterol and PON activity in *db/db* mice. For all groups of mice ($n = 24$ in each group), the mean plasma concentrations of total cholesterol (A), triglyceride (B), HDL-cholesterol (C) and PON activity (E) were measured before and after 4 weeks treatment period of low and high dosages of SR10. LDL-cholesterol (D) was calculated from total cholesterol, HDL-cholesterol and triglyceride. Data were expressed as Mean \pm S.D. *P* values were generated by One-way Analysis of Variance (ANOVA) using the Dunnett's Test for multiple comparisons to water control. Statistical significance was indicated by * $p < 0.05$ when compared to water control group at the same time point.

7.3 Discussion

Proliferation and migration of VSMCs are the basic pathological changes in atherosclerosis, finally atherosclerotic plaque was formed. Oxidized LDL (ox-LDL) has been shown to be participated in the initiation and development of atherosclerotic plaques by initiating foam cell formation, promoting the recruitment of circulating monocytes into the intima as well as activating the proliferation of vascular smooth muscle cells (Lähteenmäki *et al.*, 1998). Oxidants for LDL oxidation include reactive oxygen species (ROS) such as superoxide anion and peroxynitrite, as well as peroxide and metal ions (Heinecke, 1998). Since ox-LDL was formed by oxidation of LDL, anti-oxidants that can prevent this process may decrease the development of atherosclerosis. Thus, in this part of study, the anti-oxidative activity of SR10 using AAPH-induced rat RBC hemolysis model and prolongation of human LDL oxidation were examined.

AAPH is a well-known free radical generator which induces lipid peroxidation on RBC membrane. Results demonstrated that SR10 inhibited AAPH-induced rat RBC hemolysis in a dose-dependent manner with IC_{50} found at 0.25 mg/mL. Vitamin C, as positive control, gave an IC_{50} value at 0.1 mg/mL. This showed that SR10 had anti-oxidative property. Therefore, the effect of SR10 on oxidative resistance of human LDL was determined. Measurement of conjugated diene formation in LDL by copper ion-mediated oxidation was used in the study. Lag time was obtained from the graph to measure the ability to inhibit LDL oxidation. Longer lag time represents stronger anti-oxidative activity to prolong LDL oxidation. Results demonstrated that SR10 inhibit LDL from being oxidized by copper ion. The results of both AAPH-induced and copper ion-induced lipid peroxidation indicated that SR10 is an anti-oxidant which could inhibit LDL oxidation.

Since LDL oxidation induces the initiation and development of atherosclerotic plaques, in the next step, the effects of SR10 in proliferation and migration of VSMC, which is an important stage strongly suggested in atherosclerotic plaque formation, were measured. Rat VSMCs, namely A7r5 cells, were used as cellular model. Vascular proliferation contributes to diffuse intimal thickening in arteries where the development of atherosclerosis occurred. Controlling vascular proliferation by regulating cell cycle progression is a new therapeutic strategy for atherosclerosis (Bicknell *et al.*, 2003). Many growth factors have been shown to function as mitogens for VSMC. One of the examples is PDGF-BB which is important in vascular repair after cellular injury and has been implicated in neointima formation. Inhibitors of PDGF-BB signal transduction have been shown to decrease the formation (Myllärniemi *et al.*, 1997). PDGF-BB was also found to trigger the production of extracellular matrix (ECM) and secretion of cytokines which lead to structural change of the media and allows the VSMC to migrate from media to the inflammatory site (Graf *et al.*, 1997). This part of study involved the use of PDGF-BB to induce A7r5 cell proliferation and migration, and investigated the inhibition of these processes by SR10. PDGF-BB induced A7r5 cell proliferation for 31%, which was suppressed by the addition of SR10 at concentrations 2.5 mg/mL and 5 mg/mL. The suppression was not due to cytotoxicity of SR10 because SR10 alone did not decrease cell viability when compared with negative control. Results of ³H-thymidine uptake assay also suggested that SR10 decreased DNA synthesis which is an indication of cell proliferation. The anti-proliferation of A7r5 cells by SR10 was further confirmed by cell cycle analysis. Cells are activated by entering from quiescent (G₀) stage to G₁ phase. To begin the DNA replication, the cell enter S phase for synthesis and then G₂/M phase for mitosis. Our results indicated that

PDGF-BB arrested the cells at S phase and G₂/M phase. This means that PDGF-BB activated cell proliferation. When SR10 was co-treated, cell population in G₀/G₁ phase was increased from 48.18% to 57.29%, 59.22% and 66.02%, respectively while that in S phase was decreased from 25.13% to 21.22%, 19.19% and 13.03%, respectively as well as that in G₂/M phase was decreased from 26.69% to 21.48%, 21.59% and 20.95%, respectively at concentrations 1.25 mg/mL, 2.5 mg/mL and 5 mg/mL when compared to PDGF-BB-treated control. The results demonstrated that SR10 suppressed PDGF-BB-induced VSMC proliferation by decreasing cell cycle arrest at S and G₂/M phase. Besides cell populations in difference phases, regulation on different cyclin-CDK complexes was also studied. Cyclin D-CDK4 and cyclin E-CDK2 complexes regulate G₁ and S phases transition while cyclin A-CDK2 and cyclin B-CDK1 regulate G₂/M phase transition (Schafer, 1998). The results of Western blot showed that PDGF-BB-induced expression of cyclin D1 was suppressed slightly by co-treatment of SR10 in a dose-dependent manner. The decrease in G₁ and S phases transition consolidated the result that SR10 inhibited PDGF-BB-induced S and G₂/M phase cell cycle arrest, and hence inhibited VSMC proliferation.

Besides cell proliferation, VSMC migration from media to intimal space is also important in development of atheroma. In the study, a transwell migration assay was applied to study the inhibitory effect of SR10 on VSMC migration. SR10 was shown to be inhibitory for A7r5 cell migration in a dose-dependent manner. Actually, VSMC proliferation and migration are two independent processes. As SR10 was found to be effective in inhibiting both processes, this means that it is a potential inhibitor of atherosclerosis.

HDL-C and LDL-C have long been identified as important risk factors for coronary heart disease (Castelli *et al.*, 1986; Miller *et al.*, 1975). In addition, HDL is believed to protect against atherosclerosis by inhibiting the oxidative modification of LDL and to attenuate the biological activity of oxidized LDL. These antioxidant and anti-atherogenic properties of HDL have been attributed to the various proteins associated with HDL. Paraoxonase (PON) is one of these proteins. In this part of study, plasma concentration of total cholesterol, HDL-C and triglyceride were determined. The results showed that SR10 decreased total cholesterol and lead to an increasing trend of HDL-C in diabetic mice. LDL-C has been related to total cholesterol, HDL-C and triglyceride by Friedewald equation (Friedewald *et al.*, 1972; Warnick *et al.*, 1990). Calculated LDL-C from the results indicated that SR10 highly decreased plasma concentration of LDL-C in diabetic *db/db* mice. Risk factor of coronary heart disease was found to be increased by LDL-C and decreased by HDL-C. Thus, the results of the study implied a potential effect of SR10 in anti-atherosclerosis. The conclusion was further supported by increased paraoxonase activity which has been shown to protect against copper-induced or cell-mediated LDL oxidation (Reddy *et al.*, 2001; Mackness *et al.*, 1993).

CHAPTER 8

INHIBITION OF LIPOPOLYSACCHARIDE-INDUCED INFLAMMATORY RESPONSES OF MACROPHAGES BY SR10

8.1 Introduction

The association between hyperglycemia and the development of diabetic complications is now well established (Brownlee, 2005). However, the actual underlying mechanisms that lead to the development of vascular complications are complex. Hyperglycemia, dyslipidaemia and altered levels of coagulation and anti-inflammatory factors directly contribute to an ongoing sub-chronic inflammatory and atherogenic state, which, when associated with vascular insulin resistance, leads to increased vascular endothelial free radical production in type 2 diabetic patients. It has also been demonstrated that chronic inflammatory state plays a crucial role in obesity-related pathologies such as cardiovascular diseases and type 2 DM (Xu *et al.*, 2003; Shoelson *et al.*, 2006). Recent studies have shown that activation of macrophages plays an important role in the initiation and propagation of inflammatory responses by the production of cytokines such as IL-1 β , IL-6, TNF- α , NO and other inflammatory mediators. Over-expression of the inflammatory mediators in macrophages is involved in many obesity-related diseases such as atherosclerosis (Weisberg *et al.*, 2006; Bruun *et al.*, 2005). Therefore, agents that can suppress macrophage activation may have the potential to prevent or delay the onset of, or ameliorate obesity-related diseases.

Lipopolysaccharide (LPS) is commonly used to model inflammation because of its ability to activate macrophages. Activated macrophages produce a variety of proinflammatory mediators, including interleukins, prostaglandin E₂ (PGE₂) and

nitric oxide (NO). The expression of genes encoding these mediators was regulated by nuclear factor kappa B (NF κ B) in macrophages (Fujiwara *et al.*, 2005).

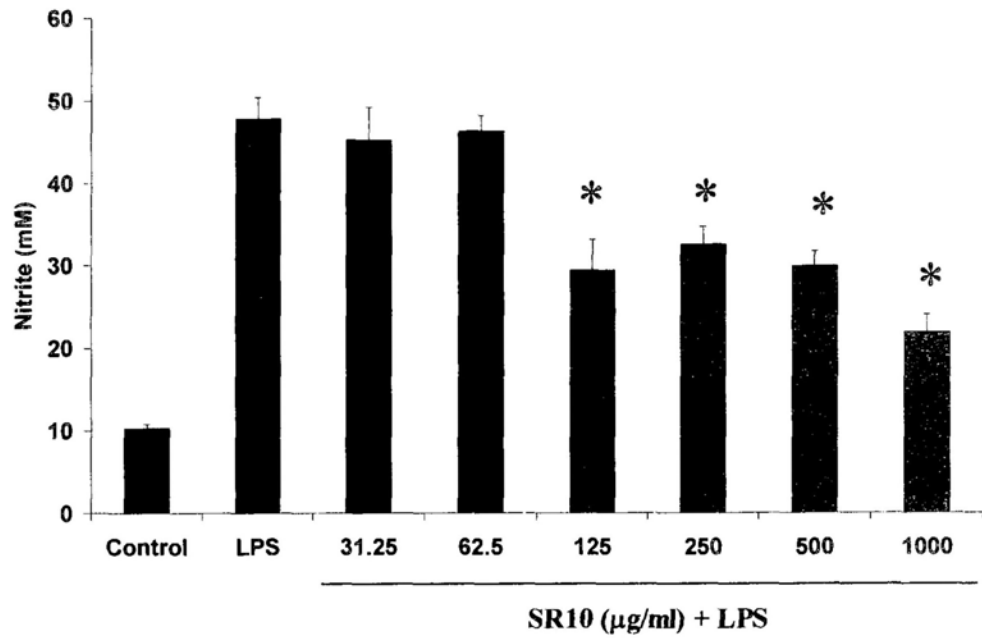
In this part of study, mouse macrophage cell line RAW264.7 was used to examine the effect of SR10 in inhibition of inflammatory responses induced by LPS. Release of cytokines IL-1 β , IL-6 and TNF- α , and proinflammatory mediators nitric oxide and prostaglandin E₂ was determined in culture supernatants. To confirm if the response is mediated by NF κ B through the activation of MAPK and Akt pathway, the expression of NF κ B and regulatory proteins in MAPK and Akt pathway were analyzed by Western blot.

8.2 Experimental results

8.2.1 Inhibition of nitric oxide release and nitric oxide synthase expression in macrophages

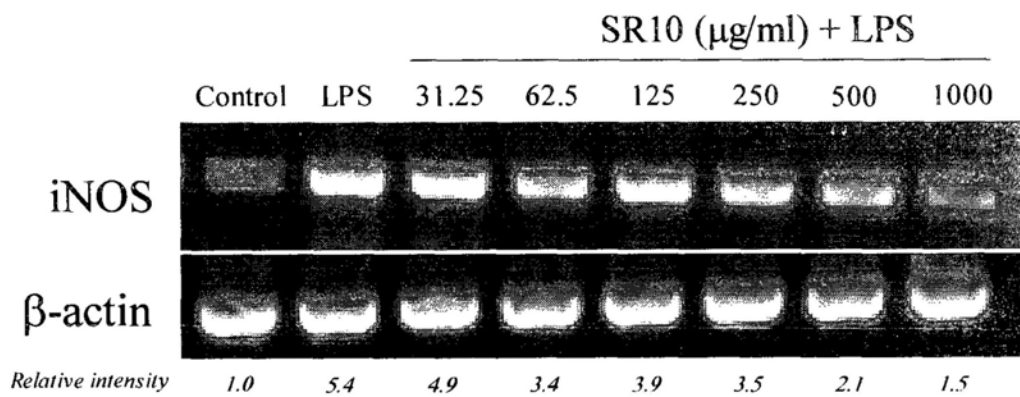
Mouse macrophage RAW264.7 cells were pre-treated with various concentrations of SR10 for 2 h before the addition of LPS (1 $\mu\text{g}/\text{mL}$). After further incubation for 24 h, culture medium was then collected and concentration of nitric oxide (NO) was determined. Results showed that LPS markedly induced NO release which was significantly inhibited by treatment of SR10 at concentrations ranged 125-1000 $\mu\text{g}/\text{mL}$ (Figure 8-1A). To examine the effects on inducible nitric oxide synthase (iNOS), mRNA and protein expression of iNOS were determined by RT-PCR and Western blot analysis, respectively. After normalization by housekeeping genes, obvious decreases in mRNA and protein expression of iNOS were observed at SR10 concentrations 250 $\mu\text{g}/\text{mL}$, 500 $\mu\text{g}/\text{mL}$ and 1000 $\mu\text{g}/\text{mL}$ when compared to LPS-treated control (Figure 8-1B & 8-1C).

(A)



* $p < 0.01$ vs. LPS

(B)



(C)

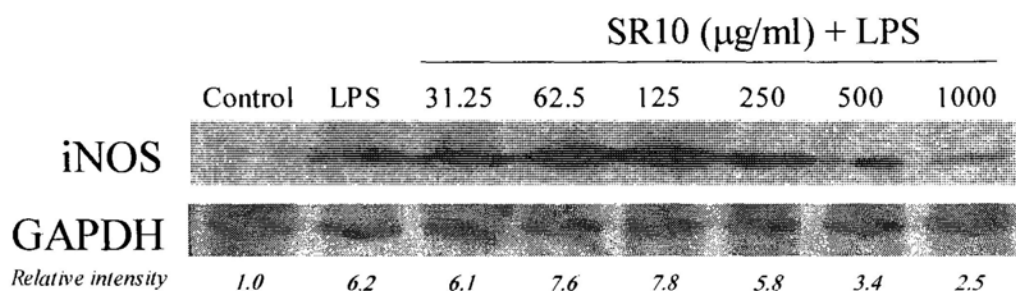


Figure 8-1 Effects of SR10 on nitric oxide release and expression of inducible nitric oxide synthase in mouse macrophages. RAW264.7 cells were pre-treated with various concentrations of SR10 for 2 h before the addition of LPS (1 $\mu\text{g/mL}$). After further incubation for 24 h, culture supernatant and cellular extract were collected. Cells treated with LPS and without SR10 pre-treatment were regarded as LPS control (Lane 2). Cells without the addition of both LPS and SR10 were regarded as negative control (Lane 1). The concentration of nitric oxide released in the medium was measured using Griess Reagent. Data were expressed as Mean \pm Standard Deviation with 4 replicates for each treatment. By Mann-Whitney test, significant difference when compared to LPS control was indicated by * $p < 0.05$ (A). The expression of iNOS was examined by RT-PCR (B) and Western blot analysis (C). Three independent trials were performed for each experiment. Representative figures of RT-PCR and Western blot were shown in Panel (B) and (C). Band intensity was measured using densitometer. Relative band intensity of each sample was calculated and compared to negative control which was set as 1.

8.2.2 Suppression of release and expression of IL-1, IL-6 and TNF- α

The level of pro-inflammatory cytokines is important in inflammation. Therefore, the effect of SR10 on the inhibition of IL-1, IL-6 and TNF- α was investigated. Cytokine released in the culture supernatant was detected by ELISA. Upon LPS treatment, cytokine released was markedly increased, 3.52 fold for IL-1, 7.23 fold for IL-6 and 32.65 fold for TNF- α , respectively. When SR10 was pre-treated, the increase of cytokine released was suppressed. Effective range for three cytokines was different but significant suppression could be found at 500-1000 $\mu\text{g/mL}$ (Table 8-1). mRNA expression of IL-1, IL-6 and TNF- α was detected by RT-PCR. Consistently, mRNA expression of these cytokines was obviously attenuated at concentrations 500-1000 $\mu\text{g/mL}$ when compared to LPS control (Figure 8-2).

Table 8-1 Fold of change in release of IL-1, IL-6 and TNF after treatment with LPS and SR10. RAW264.7 cells were pre-treated with various concentrations of SR10 for 2 h before the addition of LPS (1 $\mu\text{g}/\text{mL}$). After further incubation for 24 h, culture supernatants were collected. The amounts of cytokines in culture supernatant were determined using ELISA kit. Concentration of cytokine released in negative control (without LPS and SR10) was set to 1 and that of other treatments were interpreted as fold of change when compared to negative control. Three independent trials were carried out. Data were expressed as Mean \pm Standard Deviation with 3 replicates for each treatment. By Mann-Whitney test, significant difference when compared to LPS control was indicated by * $p < 0.05$ or # $p < 0.01$.

	Fold of change							
	Control	LPS	SR10 ($\mu\text{g}/\text{ml}$) + LPS					
			31.25	62.5	125	250	500	1000
IL-1	1	3.52 \pm 0.216	3.65 \pm 0.313	2.97 \pm 0.198 *	2.84 \pm 0.177 *	2.65 \pm 0.218 *	2.13 \pm 0.229 [#]	2.23 \pm 0.105 [#]
IL-6	1	7.23 \pm 1.28	7.33 \pm 1.35	5.97 \pm 0.78	5.78 \pm 0.59	4.76 \pm 0.46 *	3.25 \pm 0.23 [#]	3.69 \pm 0.5 [#]
TNF	1	32.65 \pm 2.69	31.52 \pm 3.55	31.25 \pm 3.69	25.66 \pm 2.65 *	27.84 \pm 2.35	23.65 \pm 3.09 *	20.87 \pm 2.52 [#]

* $p < 0.05$ compared with LPS

$p < 0.01$ compared with LPS

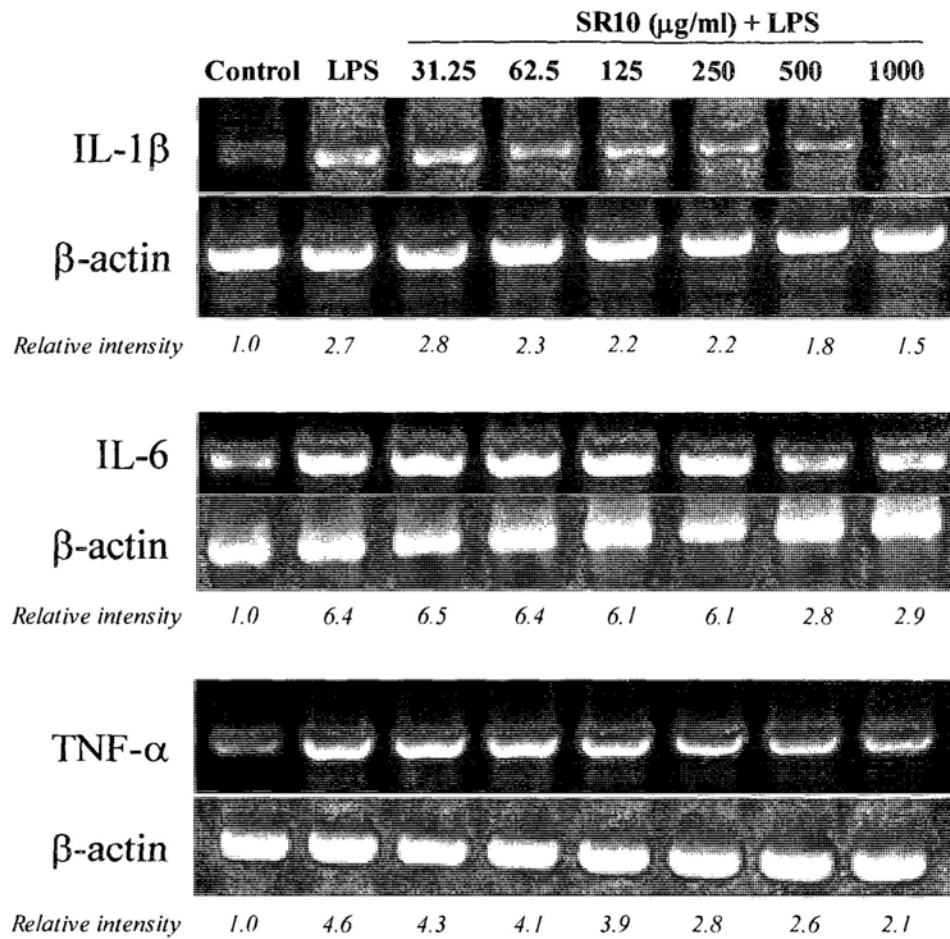
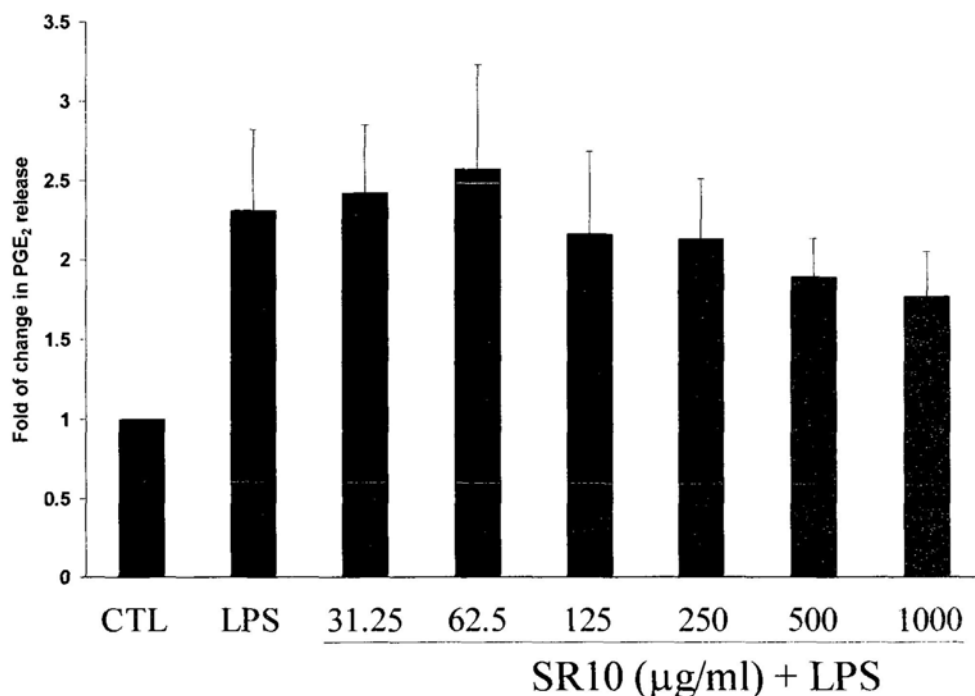


Figure 8-2 Effect of SR10 on mRNA expression of IL-1 β , IL-6 and TNF- α in mouse macrophages. RAW264.7 cells were pre-treated with various concentrations of SR10 for 2 h before the addition of LPS (1 $\mu\text{g/mL}$). After further incubation for 24 h, cellular extracts were collected. Then, mRNA expression levels of IL-1 β , IL-6 and TNF- α were detected by RT-PCR. Amount of RNA used in each sample was normalized by expression of β -actin. The figure is a representative of three independent trials. Band intensity was measured using densitometer. Relative band intensity of each sample was calculated and compared to negative control which was set as 1.

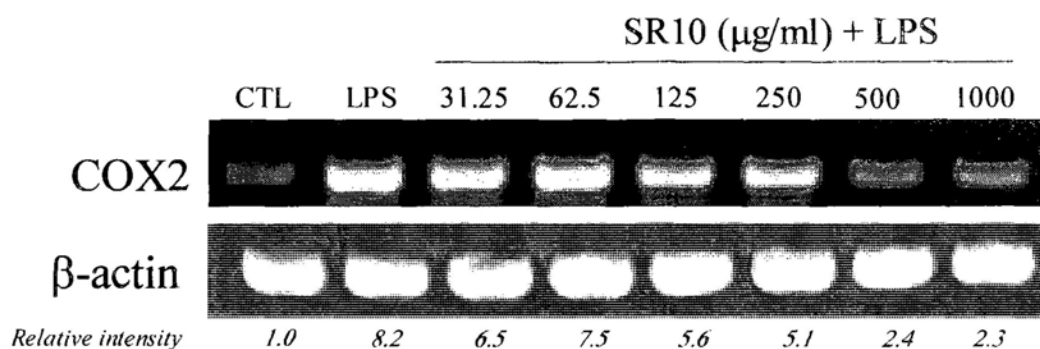
8.2.3 Decreased release of PGE₂ and expression of COX-2 in macrophages

Prostaglandin E₂ is an inflammatory mediator, whose secretion is regulated by COX-2. PGE₂ secreted in the medium is detected by ELISA kit. Results showed that LPS highly induced PGE₂ release and a trend of inhibition was observed when RAW264.7 cells were treated with SR10 (125 µg/mL to 1000 µg/mL) (Figure 8-3A). However, the difference did not show statistical significance. Expression of COX-2 was determined by both RT-PCR and Western blot (Figure 8-3B & 8-3C). Both results showed that decreasing expression of COX-2 was observed at increasing concentration of SR10. Significant inhibition of expression of COX-2 was found at concentrations 500 µg/mL and 1000 µg/mL.

(A)



(B)



(C)

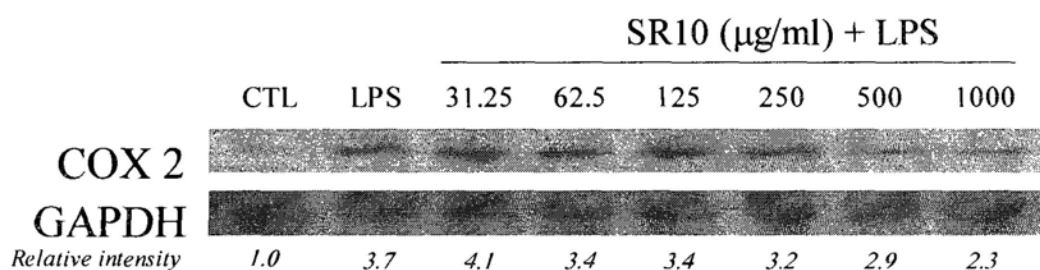


Figure 8-3 Effects of SR10 on PGE₂ release and expression of COX-2 in mouse macrophages. RAW264.7 cells were pre-treated with various concentrations of SR10 for 2 h before the addition of LPS (1 $\mu\text{g/ml}$). After further incubation for 30 min, culture supernatant and cellular extract were collected. Cells without SR10 pretreatment were regarded as LPS control (Lane 2). Cells without the addition of both LPS and SR10 were regarded as negative control (Lane 1). The concentration of PGE₂ released in the medium was determined using ELISA (A). The expression of COX-2 was examined by RT-PCR (B) and Western blot analysis (C). Three independent trials were performed for each experiment. Representative figures of RT-PCR and Western blot were shown in Panel (B) and (C). Band intensity was measured using densitometer. Relative band intensity of each sample was calculated and compared to negative control which was set as 1.

8.2.4 Effect of SR10 mediated by MAPK pathway in macrophages

MAPKs are comprised of three principal family members with distinct isoforms within each member: ERK, p38 and JNK. The expression of phosphorylated and total proteins (including both unphosphorylated and phosphorylated forms) of these three MAPK members were detected by Western blot in treated RAW264.7 cells. Results showed that higher expression level of phosphorylated form of ERK, p38 and JNK were detected when RAW264.7 cells were treated with LPS but the up-regulation was inhibited when the cells were pre-treated with SR10. Greater inhibition was observed when higher concentrations of SR10 were treated. However, total protein levels of these regulatory proteins (including both phosphorylated and unphosphorylated forms) did not show observable changes (Figure 8-4).

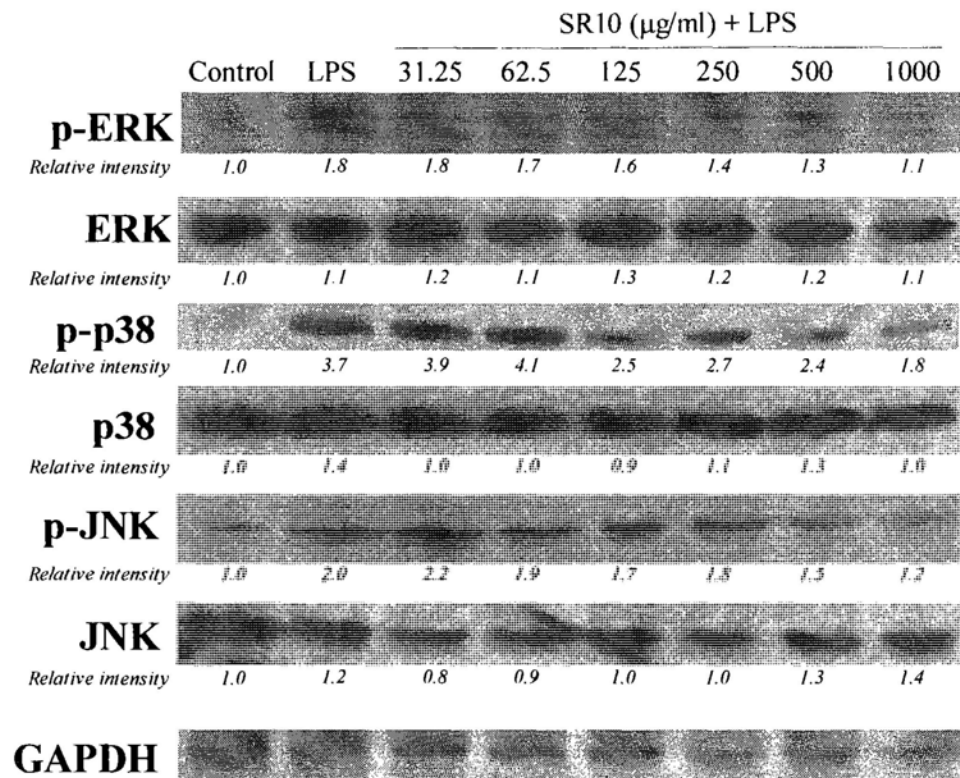


Figure 8-4 Effects of SR10 on protein expression levels of total and phosphorylated form of ERK, p38 and JNK in mouse macrophages. RAW264.7 cells were pre-treated with various concentrations of SR10 for 2 hours before the addition of LPS (1 $\mu\text{g/mL}$). After further incubation for 24 h, cellular extracts were collected. Then, expression levels of total ERK, p38 and JNK, and their phosphorylated forms (p-ERK, p-p38 and p-JNK) were detected by Western blot analysis. Protein content of each sample was normalized by GAPDH. Three independent trials were performed and this figure is a representative of three trials. Band intensity was measured using densitometer. Relative band intensity of each sample was calculated and compared to negative control which was set as 1.

8.2.5 Effect of SR10 mediated by Akt pathway in macrophages

Akt and I κ B- α are important regulatory proteins in Akt pathway. Results of Western blot analysis showed that there was a mild decrease in p-Akt expression when RAW264.7 cells were treated with SR10, when compared to LPS control. However, p-I κ B- α showed a significant inhibition upon SR10 treatment. Total proteins of Akt and I κ B- α did not show obvious changes under the normalization by GAPDH (Figure 8-5).

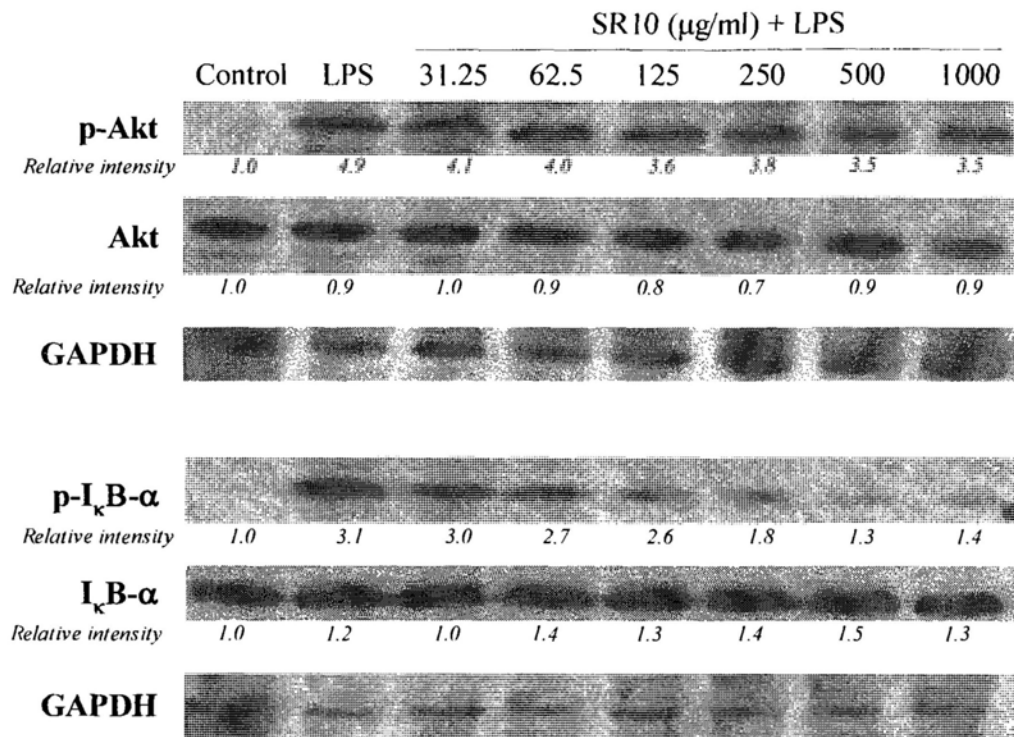


Figure 8-5 Effects of SR10 on protein expression levels of total and phosphorylated form of Akt and I κ B- α in mouse macrophages. RAW264.7 cells were pre-treated with various concentrations of SR10 for 2 hours before the addition of LPS (1 $\mu\text{g/ml}$). After further incubation for 24 h, cellular extract were collected. Expression levels of total Akt and I κ B- α , and their phosphorylated forms (p-Akt and p-I κ B- α) were detected and the result was normalized by GAPDH. Three independent trials were performed and this figure is a representative of three trials. Band intensity was measured using densitometer. Relative band intensity of each sample was calculated and compared to negative control which was set as 1.

8.2.6 Activation of NFκB translocation to nucleus in macrophages

NFκB is an important mediator linking Akt and MAPK pathway. It is a transcription factor that modulates the expression of variety of genes involved in immune and inflammatory responses, including iNOS, COX-2 and TNF-α. Under stimulation of inflammation, IκB-α becomes phosphorylated and is subsequently degraded, allowing NFκB to translocate into the nucleus. Proteins of nuclear fraction of RAW264.7 cells were prepared and expression of NFκB in this fraction was determined by Western blot. The results showed that NFκB level in nuclear fraction was highly up-regulated by LPS. However, the up-regulation was decreased by the treatment of SR10 (Figure 8-6).

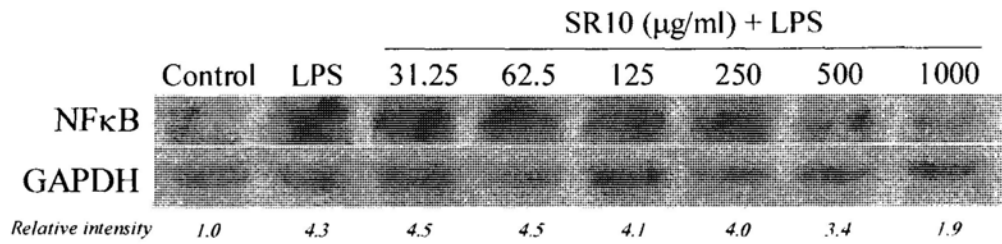


Figure 8-6 Effects of SR10 on NF κ B content in nuclear fraction of mouse macrophages. RAW264.7 cells were pre-treated with various concentrations of SR10 for 2 h before the addition of LPS (1 $\mu\text{g/mL}$). After further incubation for 24 h, nuclear protein fraction was prepared using commercially available cellular fractionation kit. Western blot analysis was then carried out to detect expression level of NF κ B in nuclear fraction. Total protein content in each sample was normalized by GAPDH. Three independent trials were performed and this figure is a representative of three trials with similar trend. Band intensity was measured using densitometer. Relative band intensity of each sample was calculated and compared to negative control which was set as 1.

8.3 Discussion

For many years atherosclerosis has been regarded as a lipid storage disease. More recently, substantial evidence has emerged to suggest that inflammation plays a paramount role in the dynamic process of initiation, progression and rupture of the atherosclerotic lesion. On the other hand, considerable interest has focused on establishing the role of inflammation in the pathogenesis of type 2 DM. Several lines of evidence suggest that inflammation not only predicts atherosclerosis but also the development of type 2 DM. Thus, there is accumulating evidence suggesting that inflammation is the bridging link between atherosclerosis and type 2 DM (Stern, 1995). High blood glucose in DM is a source of free radicals leading to oxidative stress in endothelial cells which in turn induces inflammatory response mediated by various signal pathways. The inflammatory response has been found to be involved in all stages of atherosclerosis, resulting in uncontrolled proliferation of vascular cells, production of foam cells and progressive vascular occlusion.

In Chapter 7, anti-atherosclerotic effects of SR10 were demonstrated by inhibiting rat VSMC proliferation and migration. As inflammation plays crucial roles in development of atherosclerosis, it is speculated that SR10 may affect inflammatory process. Thus, in this part of study, the effects of SR10 on inflammatory response induced by LPS were investigated.

Lipopolysaccharide (LPS) is the main component of endotoxin and is formed by lipid A linked to hydrophilic heteropolysaccharide (Rietschel *et al.*, 1994). LPS-induced macrophage activation was found to increase the production of cytokines such as IL-1 β , IL-6, TNF- α , NO and PGE2. SR10 inhibited inflammation induced by LPS by inhibiting the secretion of these mediators in mouse RAW264.7 cells. The

effects were further confirmed by decreased expression (both mRNA and protein) of their regulators, iNOS and COX-2, respectively.

Nitric oxide plays a dual role as a beneficial or detrimental molecule in the process of inflammation; namely, a small amount of NO produced by constitutive endothelial NOS (eNOS) and neuronal NOS (nNOS) is an important regulator of physiological homeostasis in reducing blood pressure, inhibition of platelet aggregation, and regulating neuronal transmission (MacMaking *et al.*, 1997; Liu *et al.*, 1995). However, high output production of NO by inducible nitric oxide synthase (iNOS) reacts with macrophage-derived superoxide to produce highly cytotoxic peroxynitrite, which contributes to a variety of diseases and inflammation (Moncada *et al.*, 1991; MacMaking *et al.*, 1997).

PGE₂ formation results from the release of arachidonic acid from cell-membrane phospholipids by phospholipase enzymes and is converted to PGE₂, via cyclooxygenase (COX) and PGE₂ synthase enzymes. LPS-induced release of arachidonic acid, the resulting up-regulation of COX-2 expression and PGE₂ formation, is mediated through toll-like receptor 4 in the RAW264.7 cells (Rhee *et al.*, 2000; Qi *et al.*, 2005).

The expression of genes encoding interleukins, COX and iNOS was regulated by NFκB in macrophages. NFκB is a dimer of members of the Rel family proteins, including p65, c-Rel and p50. In most unstimulated cells, NFκB covalently bound to inhibitor protein, IκB-α, which is sequestered in the cytoplasm (Ghosh *et al.*, 1998). Exposure of the cells to external stimuli, such as inflammatory cytokines and oxidative stress results in the activation of NFκB through the stimulation of the phosphorylation of IκB-α and its subsequent proteolytic degradation (Bours *et al.*, 2000; Wang *et al.*, 2002). The activated NFκB is then translocated to the nucleus,

where it binds to the cis-acting κ B enhancer element of target genes and regulates the expression of various inflammatory cytokines and proinflammatory mediators (Hayakawa *et al.*, 2003). The results of this study showed that SR10 activate NF- κ B accumulation in nuclear fraction. Therefore, in next step, the upstream signal pathway(s) leading to NF- κ B activation was investigated.

It has been shown that NF- κ B-activating stimuli such as IL-1 β and TNF- α were also down-regulated by inhibition of Akt activation, leading to decreased NO production. LPS-mediated phosphorylation and activation of Akt were blocked by pharmacological inhibitors of Akt. Events necessary for the activation of NF- κ B (such as I κ B degradation, nuclear translocation, and increased NF- κ B DNA binding) were all suppressed by inhibitors of Akt. These results place Akt upstream of NF- κ B activation in the sequence of signaling events, whereby activation of Akt up-regulates iNOS promoter activity, leading to transcription and translation of iNOS and increased NO production. The results of this study also showed that inhibition of lipopolysaccharide-induced Akt activation by SR10 led to down-regulation of NF- κ B activation, resulting in decreased iNOS expression and NO production.

On the other hand, LPS has also been shown to be a potent activator for the p38 mitogen-activated protein kinases (MAPK) which play an important role in the regulation of cell growth and differentiation, and in the control of cellular responses to cytokines and stresses. LPS activates all three types of MAPKs – ERK, p38 and JNK – in mouse macrophages (Chen *et al.*, 1999). The exact signalling pathways among the three types of MAPKs are still unclear; however, there is a cross-talk and signal convergence among the MAPKs. Many of the upstream kinases and downstream substrates are the same for each of the major cascades (Jordan *et al.*, 2000). Activation of p38 by LPS resulted in the stimulation of NF- κ B-specific DNA-

protein binding and the subsequent expression of inducible form of NO synthase and NO release in RAW 264.7 macrophages (Chen *et al.*, 1999). In this study, SR10 also decreased the phosphorylation level of p38 protein in LPS-stimulated cells in a concentration-dependent manner.

Results of this study demonstrated that SR10 inhibits the production of NO, interleukins and PGE₂ in LPS-stimulated macrophage cells, RAW264.7. This anti-inflammatory effect occurs by the down-regulation of iNOS and COX-2 expression via the suppression of NF- κ B activation, Akt and MAPK phosphorylation. The anti-inflammatory effects of SR10 in macrophages partly explain its anti-atherosclerotic effects.

CHAPTER 9

GENERAL DISCUSSION

9.1 Diabetes in Hong Kong

In Hong Kong, DM is getting more common. One in ten adults in Hong Kong suffer from DM and more than 20% of Hong Kong people above 65 years of age are diabetics. There is evidence that the incidence is increasing. Each year in Hong Kong, over 400 patients have diabetes associated kidney disease requiring dialysis and over 500 patients lost their vision because of diabetic eye complications. Approximately 30% of patients admitted to Hong Kong public Hospitals with stroke and heart attack were found to have co-existing DM (Department of Health, HKSAR, 2007).

Hong Kong people are generally living in an urbanized environment. Physical inactivity, diets high in fat and salt and low in fruit and vegetables, and great work-related stress are a few of the lifestyle factors associated with urbanization (Gu *et al.*, 2005). Obesity is a crucial risk factor of DM. In Hong Kong, with reference to two large-scale population-based studies, the prevalence of overweight ($\text{BMI} \geq 25 \text{ kg/m}^2$) increased from 28% to 38% in men, and from 28% to 34% in women in 1990 and 1995, respectively (Lee *et al.*, 2002). A prospective study on obese Hong Kong people found that obese people, after a mean follow-up of 2 years, had significantly higher rates of progression to diabetes (14.6% per year for people with $\text{BMI} \geq 28 \text{ kg/m}^2$) than their non-obese counterparts (8.4% per year) (Gary *et al.*, 2004).

Alongside with the rising prevalence of adult obesity in Hong Kong, the same phenomenon is also running rampant in children. According to a survey conducted by the Hong Kong Children Health Service, the obesity rates of Hong Kong primary and secondary school student boys and girls increased from 12.7% and 10.4% in 1998 to 14.7% and 12.4%, respectively, in 2001 (Department of Health, HKSAR,

2007). Another study showed a further increase of obesity rate to 15.9% (boys: 18.1%; girls: 13.9%) in Hong Kong adolescents in 2004 (Ko *et al.*, 2008). Obesity is associated with significant morbidity and mortality. Most obese children will grow up to become obese adults and most obesity related health problems are also applicable to children. The problem of obesity of Hong Kong adults and adolescents further leads to increasing DM cases.

Back to the worldwide situation, according to the World Health Organization (WHO), DM reduces life expectancy by 10-12 years, especially in young people (Roglic *et al.*, 2005). An estimate of 2.9 million deaths is directly attributable to DM each year, a figure comparable to that due to human immunodeficiency virus infection (Roglic *et al.*, 2005). The epidemic situation of DM leads to urgent need on promising therapeutic approaches.

9.2 Insulin dependent therapy: a nightmare for type 2 diabetic patients

DM is a complicated disease involving different pathologies. Type 1 DM is an immune-mediated diabetes. Up to now, therapy of type 1 DM is mainly dependent on exogenous insulin supply. Type 2 DM involved more complicated factors including genetics, environment and living style. At early stage of type 2 DM, most patients have no needs for medication. Most of them are non-insulin dependent. However, many cases of non-insulin dependent diabetes mellitus (NIDDM) will finally turn to insulin-dependent (IDDM) and insulin injection is required. From then, their lives will be highly affected.

How does the nightmare of IDDM appear in type 2 DM patients? In general, the development of type 2 DM is associated with pancreatic β cell dysfunction occurring together with insulin resistance. Normal β cells can compensate for insulin resistance

by increasing insulin secretion, but insufficient compensation due to abnormally high blood glucose concentration (especially after meal) leads to the onset of glucose intolerance. Once hyperglycemia becomes apparent, β cell function deteriorates progressively. Glucose-induced insulin secretion becomes further impaired and degranulation of β cells becomes evident, often accompanied by a decrease in the number of β cells (Porte, 1991; DeFronzo *et al.*, 1992; Yki-Jarvinen, 1992). The significance of hyperglycemia as a direct cause of these phenomena, i.e., glucose toxicity on β cell, has been demonstrated by various studies *in vivo* (Zangen *et al.*, 1997) and *in vitro* (Robertson *et al.*, 1992; Olson *et al.*, 1993; Sharma *et al.*, 1995; Poitout *et al.*, 1996; Moran *et al.*, 1997). The situation of how hyperglycemia become a secondary force that further damages the β cells is summarized in Figure 9-1. In general, this deterioration of cellular function caused by constant exposure to supraphysiologic concentrations of glucose is termed glucotoxicity (or glucose toxicity).

Further question is how chronic hyperglycemia induced β cell dysfunction. Under diabetic conditions, reactive oxygen species (ROS) are produced in various tissues mainly through the glycation reaction (Sakurai *et al.*, 1988; Hunt *et al.*, 1991), which may play a role in the development of complications in DM (Baynes, 1991). Although the induction of the glycation reaction in DM was originally found in neural cells and the lens crystalline, which are also known targets of diabetic complications, another target was recently shown to be the β cells (Kaneto *et al.*, 1996; Ihara *et al.*, 1999). It has been shown that advanced glycosylation end products (AGEs) were detectable in β cells kept under high glucose concentrations (Tajiri *et al.*, 1997), and the level of 8-hydroxy-2'-deoxyguanosine, a marker for oxidative stress, was increased in β cells of diabetic Goto-Kakizaki (GK) rats (Ihara *et al.*,

1999). Also, the expression of antioxidant enzymes, such as superoxide dismutase, catalase, and glutathione peroxidase, is known to be very low in islet cells compared with other tissues and cells (Tiedge *et al.*, 1997). Therefore, once β cells face oxidative stress, they may be rather sensitive to it, suggesting that glycation and subsequent oxidative stress may in part mediate the toxic effect of hyperglycemia. Studies also showed that glycation-mediated ROS production reduced insulin gene transcription (Matsuoka *et al.*, 1997) and also caused apoptosis of β cells.

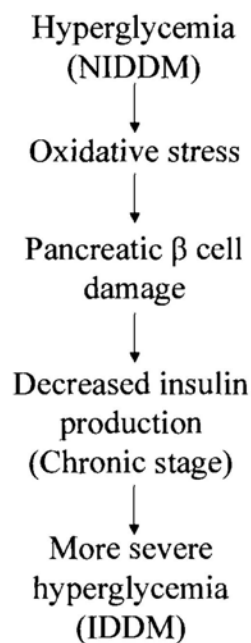


Figure 9-1 Proposed model for accelerated hyperglycemia when pancreatic β cells were damaged by oxidative stress. Many clinical studies suggested that patients with type 2 DM were subjected to oxidative stress. Free radicals when attacked our organs may result in various kinds of diseases. Pancreatic β cell is one of the cell types which are most easily attacked by free radicals due to its low level of intrinsic antioxidant defense. When β cells subjected to free radical damage, insulin production will further decrease, leading to more severe hyperglycemic situation.

How is oxidative stress increased in β cells of diabetic patients? Oxidative damage due to hyperglycemia contributes to the microvascular pathology of DM that occurs particularly in the retina, renal glomerulus, and peripheral nerves, causing blindness, renal failure, and peripheral neuropathy (West, 2000; Brownlee, 2001). Moreover, it has been suggested that increased mitochondrial ROS production during hyperglycemia may be central to much of the pathology of DM (Brownlee, 2001; Nishikawa *et al.*, 2000). Because β cell mitochondria play a central role in glucose-stimulated insulin secretion, damage to β cell mitochondrial will attenuate this response (Sakai *et al.*, 2003).

The mitochondrial respiratory chain is the major site of ROS production within the cells. Superoxide is thought to be produced continually as a byproduct of normal respiration through the one-electron reduction of molecular oxygen (Raha *et al.*, 2000). Superoxide itself damages iron sulfur center-containing enzymes such as aconitase (Vasquez-Vivar *et al.*, 2000) and can also react with nitric oxide to form the damaging oxidant peroxynitrite, which is more reactive than either precursor (Beckman *et al.*, 1990). The mitochondrial enzyme manganese superoxide dismutase (MnSOD) converts superoxide to hydrogen peroxide, which, in the presence of ferrous or cuprous ions, forms the highly reactive hydroxyl radical, which damages all classes of bio-molecules. Mitochondria have a range of defenses against oxidative damage. The antioxidant enzyme MnSOD converts superoxide to hydrogen peroxide (Forman *et al.*, 1997). The mitochondrial isoform of glutathione peroxidase and the thioredoxin-dependent enzyme peroxiredoxin III both detoxify hydrogen peroxide (Costa *et al.*, 2003).

Within the mitochondrial phospholipid bilayer, the fat-soluble antioxidants vitamin E and Coenzyme Q both prevent lipid peroxidation, while Coenzyme Q also recycles vitamin E and is itself regenerated by the respiratory chain (Maguire *et al.*, 1989). The mitochondrial isoform of phospholipid hydroperoxide glutathione peroxidase degrades lipid peroxides within the mitochondrial inner membrane (Costa *et al.*, 2003). There are also a range of mechanisms to repair or degrade oxidatively damaged lipid, protein, and DNA (Beckman *et al.*, 1998).

Due to the importance of β cell function in maintaining normal glycemia, an *in vitro* assay was selected in this study for screening the protective effects of different TCMs on β cell toxicity induced by STZ. STZ is a well-known diabetogenic agent. It has been widely reported that STZ induced the generation of NO in β cells which in turn damage the β cells by apoptosis (Murata *et al.*, 1999; Kaneto *et al.*, 1995)). Therefore, agents that can reduce NO production may reduce β cell damage in DM which in turn may decrease the shifting of NIDDM to IDDM.

Among 28 TCM selected, 3 TCMs (Radix Astragali, Radix Codonopsis and Cortex Lycii) showed potent effect against STZ induced apoptosis on pancreatic β cells. One of the reasons for having such protective effect may be the anti-oxidative property of this formula which will be discussed in the latter section. Antioxidant is potential therapeutic targets for several free radical-induced diseases including diabetes-accelerated atherosclerosis. Antioxidant intervention in animal and human studies will be discussed in the following section.

9.3 Antioxidant intervention in animal and human studies

The 'oxidation theory' of atherogenesis claims that it is the oxidation of LDL-derived lipids that is important in atherogenesis. Therefore, one important line of

research is to investigate and compare the role of antioxidants in lipid peroxidation and atherogenesis. In this study, the anti-oxidative activity of SR10 was demonstrated by inhibition of AAPH-induced hemolysis of rat RBC and prolongation of Cu^{2+} ion-induced human LDL oxidation, while the latter one is more representative in showing the anti-atherosclerotic effect of SR10.

Based on many different time-dependent analyses (Esterbauer *et al.*, 1992), the chronology of LDL oxidation by Cu^{2+} ions can be divided into three consecutive time phases: lag phase, propagation phase and decomposition phase. During the lag phase, LDL becomes progressively depleted of its antioxidants and only minimal lipid peroxidation occurs in LDL. When LDL is depleted of its antioxidants, the rate of lipid peroxidation rapidly accelerates to the maximum rate (propagation phase). Thereafter, the peroxide content of LDL starts to decrease again because decomposition reactions become predominant (decomposition phase). During the lag and propagation phase, the kinetics of the formation of lipid peroxides closely follow the diene content change versus time profile. Thus, a convenient and frequently used method monitoring the process of copper ion-induced LDL oxidation continuously, is to measure the change of the diene absorption at 234 nm (Esterbauer *et al.*, 1989). Copper ion-induced lipid peroxidation in LDL by binding to discrete sites of the apo B and forms centers for repeated free radical production similar to those proposed for other biological systems (Chevion, 1988). Any compounds that displace copper ions from the apo B-binding site should then inhibit or fully prevent LDL oxidation.

Other descriptive case-control and cohort studies have provided an early and influential indication that antioxidant has great potential in treating ox-LDL-induced atherosclerosis. These studies document that the regular intake of foods rich in fat-soluble antioxidants such as vitamin E is associated with a lower frequency of

clinical events and mortality due to coronary heart disease (CHD) (Gaziano, 1996). A large study that followed 19687 women without symptoms of cardiovascular disease who did not consume vitamin supplements for seven years, showed that the multivariate adjusted, relative risks for CHD decreased significantly from the lowest (≤ 4.9 IU/day) to highest quintile of vitamin E intake (≥ 9.6 IU/day) (Gey *et al.*, 1991). A combination of both vitamin C and E has been shown to be more effective than vitamin E alone in protecting LDL from becoming oxidized in vitro. Salonen *et al.* reported atherosclerotic progression was significantly reduced in men who were given the combination, while vitamin E alone was less effective (Salonen *et al.*, 2003).

Except for vitamin C and E, purified or synthetic compounds with anti-oxidative activities were reported to have anti-atherosclerotic effect. Among these antioxidants, probucol has been studied most extensively. The results obtained overall provide the strongest support for a beneficial effect of an antioxidant on atherosclerosis. Probucol inhibits atherosclerosis in hypercholesterolemic rabbits (Carew *et al.*, 1987; Kita *et al.*, 1987) and non-human primates (Sasahara *et al.*, 1994). In fact, the anti-atherogenic effect of probucol, which is independent of its hypolipidemic activity, is one of the cornerstones of the oxidation theory of atherosclerosis (Carew *et al.*, 1987). Probucol also reverses established plaques in rabbits (Nagano *et al.*, 1992) and xanthomas in humans (Kajinami *et al.*, 1996). Other studies on anti-atherosclerotic effects of synthetic antioxidants have been performed. N,N'-Diphenylphenylenediamine has been shown to reduce lesion development in both rabbits and mice, and to prolong the lag time in *ex vivo* oxidation of LDL induced by Cu^{2+} ions (Sparrow *et al.*, 1992; Tangirala *et al.*, 1995). Butylated hydroxytoluene (BHT) has also been reported to prevent atherosclerosis in rabbits (Björkhem *et al.*, 1991).

Results of this study showed that SR10 increased the activity of antioxidant enzymes in diabetic mice. Living organisms have developed defense mechanisms to protect against oxidative damage to their tissues. One line of defense includes antioxidant enzymes such as superoxide dismutase (SOD), catalase (CAT), and glutathione peroxidase (GPx). SOD catalyses the dismutation of superoxide radical to hydrogen peroxide. Hydrogen peroxide is removed by either CAT that is specific for hydrogen peroxide itself and by GPx that can also remove hydroperoxides. CAT has been implicated in the detoxification of H₂O₂ at high concentrations (mM range) whereas GPx is effective at much lower concentrations (μM range) of H₂O₂. The levels of these antioxidant enzymes were shown to be very low in pancreatic β cells. As SR10 could increase the enzyme activity directly in isolated islets, this may be one of the reasons that SR10 could decrease the deterioration of β cells which is evidenced by the inhibition of glycemic rise and increased insulin secretion in diabetic *db/db* mice.

9.4 Inflammation: A linkage between DM and atherosclerosis

The concept of atherosclerosis as an inflammatory disorder is supported by an ever-increasing body of pathologic, experimental, epidemiological and clinical evidence (Ross, 1999). The cellular elements involved in inflammation can be demonstrated to be present to variable degrees in multiple stages in the atherosclerotic process (Iiyama *et al.*, 1999; Fogelman *et al.*, 1981, Heinecke, 1999; Galis *et al.*, 1994):

1. Normal endothelium is not associated with significant adherence of inflammatory cells. Progressive expression of adhesion molecules on the dysfunctional endothelium provides the means for the recognition, binding and transmigration of circulating inflammatory cells.

2. LDL modified by processes such as oxidation or glycation are progressively internalized at a relatively rapid rate by macrophages and are associated with progressive lipid accumulation and the subsequent development of atherosclerosis.

3. Macrophages have the capacity to elaborate a variety of proteolytic enzymes that may be involved in the net balance between intraplaque matrix synthesis and degradation. Collagenases and gelatinase are matrix metalloproteinases that demonstrate the capacity to progressively degrade the stabilizing matrix protein constituents and result in a progressively increased risk for rupture due to reduction in the tensile strength of the plaque.

Inflammatory responses in macrophages have been found to be controlled via expression of multiple genes including signaling molecules such as NF κ B and ERK (Li *et al.*, 1999; Brownlee, 2005; Igarashi *et al.*, 1999). Under oxidative stress of hyperglycemia, over-expression of these genes may lead to endothelial dysfunction and ultimately to microvascular and macrovascular disease. High glucose can up-regulate expression of transcription factors, such as NF κ B and TNF- α (Guha *et al.*, 2000). Expression of TNF- α is mediated by the protein kinase p38 which is dependent on oxidative stress pathway. Several studies advocate the importance of the p38 pathway in DM (Igarashi *et al.*, 1999; Guha *et al.*, 2000). cAMP-dependent protein kinases (PKAs) can activate phosphorylation of substrate proteins and cross-talk with MAPK pathways and proteins involved in signal transduction pathways, leading to altered gene expression and modulation of physiological processes. cAMP is known to modulate cytokine production in a number of cell types (Reddy *et al.*, 2002; Ollivier *et al.*, 1996). This suggests that oxidative stress plays a key role in the regulatory pathway which progresses from elevated glucose to endothelial cell activation in the enhanced vascular inflammation of DM (Cardelli *et al.*, 2007; Singh

et al., 2005). Figure 9-2 proposed a model correlating the role of oxidative stress in diabetes and accelerated atherosclerosis. The results of this study showed that SR10 inhibited inflammatory responses of macrophages via the inaction of NFκB. One of the outcomes of this anti-inflammatory effect is inhibition of atherosclerosis which is further evidenced by attenuation of proliferation and migration of vascular smooth muscle cells. In addition, the lipid profile of diabetic mice showed a significant decrease in plasma total cholesterol level and calculated LDL-C level by treatment of SR10. Decreased HDL-C and increased LDL-C are well-established risk factors for cardiac disease in both non-diabetics and diabetics (Wilson *et al.*, 2008). In measuring the lipid profile of diabetic mice, LDL-C was not included because the quantification of LDL-C required relative large amount of plasma. However, the volume of plasma collected from each mouse is limited. Thus, the lipid profile does not measure LDL level directly but instead estimates it via the Friedewald Equation (Friedewald *et al.*, 1972) using levels of other cholesterol:

In mg/dL: LDL cholesterol = total cholesterol - HDL cholesterol - (0.20 × triglycerides)

This formula provides an approximation with fair accuracy for most people, assuming the blood was drawn after fasting for about 14 hours or longer. However, the concentration of LDL particles, and to a lesser extent their size, has far tighter correlation with clinical outcome than the content of cholesterol with the LDL particles, even if the LDL-C estimation is about correct.

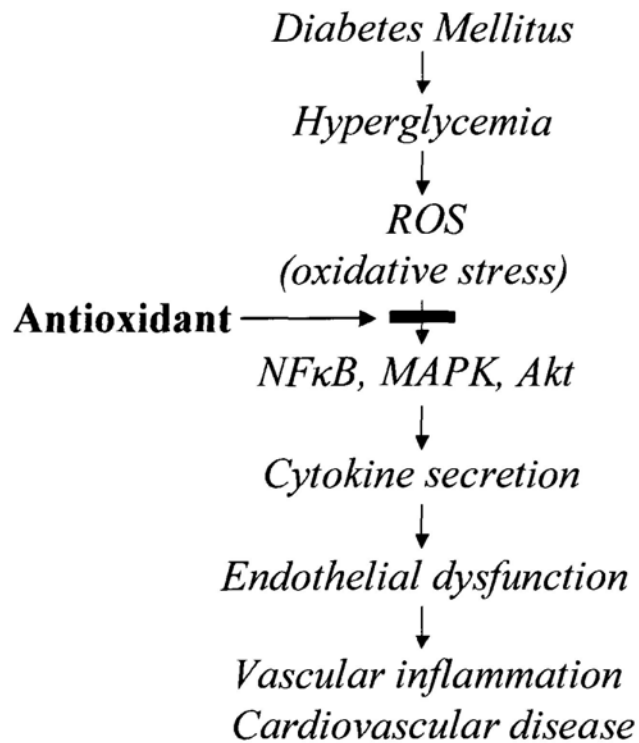


Figure 9-2 Proposed model for role of antioxidant supplementation in prevention of oxidative stress and vascular disease in diabetes.

9.5 Treatment of DM by Western medicine and Chinese medicine

In countries of modern world, Western medicine is the basic therapeutic approach supplemented with other ‘Alternative medicine’. In the concept of Western medicine, HbA1c is a good index for diabetic patients to reflect their progress of therapy. Practically, patients with HbA1c level lower than 7% are usually treated with therapeutic lifestyle measures. Those with HbA1c level of 7% to 8% are initially treated with single oral agents. Depending on motivation and adherence to therapeutic lifestyle changes, most patients with HbA1c level higher than 9% require therapy with two or more agents to reach glycemic goals. Of the oral agents, insulin

secretagogues produce the most rapid effect in reduction of blood glucose concentrations (Lebovitz, 2001; DeFronzo, 1999). Such therapy also reduces 'glucose toxicity'. After two oral drugs have failed to achieve the desired results, addition of a third class of oral agents can be considered (Yale *et al.*, 2001). In fact, the Food and Drug Administration of United States has approved oral triple therapy with a glitazone, metformin and a sulfonylurea. Virtually, all patients with type 2 DM ultimately become insulinopenic and require insulin therapy. One of the explanations is the damage of pancreatic β cell function by ROS, which has been mentioned in the previous section. Patients are often 'transitioned' to insulin with the use of a bedtime injection of intermediate or long acting insulin, retaining oral agents primarily for control during the day.

Knowledge to DM in China occurs early in the world. In the great medical book the *Yellow Emperor's Internal Classic* written in 400 B.C., there were already detailed descriptions on the disease. Diabetes in Western medicine is basically consistent with XiaoKeZheng (消渴症) in TCM according to their manifestations. XiaoKeZheng is a morbid state caused by improper diet and emotional disturbance and marked by polydipsia, polyphagia, polyuria and the urine of sweet taste. In Chinese medicine, pathogenesis of diabetes include dryness-heat due to *yin* deficiency, impairment of *yin* and *yang* due to *qi* and *yin* deficiency, blood stasis.

For a long time, herbal formulas have been used for the treatment of various diseases with different types of manifestations. The herbs Radix Astragali, Radix Codonopsis and Cortex Lycii in the formula SR10 have different roles in Chinese medicine. The characteristics of these three TCMs are described as follows:

Radix Astragali is of slightly 'warm' property. It is known for its vital-energy tonifying, skin-reinforcing, diuretic, abscess-draining and tissue generative actions. It

is, therefore, useful for palpitation with shortness of breath, spontaneous sweating, prostration, chronic diarrhea, prolapse of the uterus and rectum, chronic carbuncle and deep-rooted ulcer and persistent sores. Its pharmacological actions include enhancement of immunological functions, moderate diuretic action, antinephritis, protection of hepatitis and antibacterial effect. LD₅₀ of Radix Astragali in mice was determined to be 39.82 g/kg by oral administration.

Radix Codonopsis is mild in nature. It tonifies the vital-energy and the spleen and is chiefly used in shortness of breath with palpitation, lassitude and physical weakness, and watery stool with poor appetite. Its pharmacological actions include enhancement of animal motility, decrease of hypertension, antinephritis. LD₅₀ of Radix Codonopsis in mice was determined to be 79.21 g/kg by intraperitoneal injection.

Cortex Lycii has a 'cold' property. It is used to remove *heat* from the blood, with antipyretic and 'lung-heat' purgative actions. Moreover, it has hypoglycemic, anti-cholesterolemic, hypotension and antimicrobial action. LD₅₀ of the herb is determined to be 12.83 g/kg by intraperitoneal injection.

These three herbs have been included in different ancient and modern formulae for treating Xiaoke Syndrome or DM in Western medicinal terms. For ancient formulas, Radix Astragali have been included in Huangqi Tang (composed of **Radix Astragali**, Poria, Radix Ophiopogonis, Radix Rehmanniae, Radix Trichosanthis, Fructus Schisandrae and Radix Glycyrrhizae) and Buyang Huanwu Tang (composed of **Radix Astragali**, Radix Angelica sinensis, Radix Paeoniae lactiflorae, Radix Ligustici Chuanxiong, Semen Persicae, Flos Carthami Tinctorii and Lumbricus). Both Radix Astragali and Cortex Lycii are components of Lurong Wan (composed of **Radix Astragali**, Radix Ginseng, Radix Scrophulariae ningpoensis, Radix

Ophiopogonis, Fructus Schisandrae chinensis, Radix Rehmanniae Preparata, Fructus Corni officinalis, Cornu cervi Parvum, Fructus Psoraleae, Herba Cistanches, **Cortex Lycii**, Poria and Radix Achyranthis Bidentatae). Both Radix Astragali and Radix Codonopsis are components of Tangniaobing Fang (composed of **Radix Astragali**, Rhizoma Dioscoreae, Rhizoma Atractylodis, Radix Scrophulariae, Radix Rehmanniae, Radix Ophiopogonis, **Radix Codonopsis**, Fructus Schisandrae, Poria, Galla Chinensis, Concha Ostreae and Os Draconis Fossilla Osis Mastodi). Other commonly used herbal formulae for treating DM which have been reported in scientific journals are summarized in Table 9-1. From our studies, the optimal weight ratio of these three herbs, namely Radix Astragali, Radix Codonopsis and Cortex Lycii, at 3:3:1 in the formula SR10 in treating DM has been found out.

Herbal Formula	Components	Functions	Source of reference
Tang niabing Fang	Radix Astragalii Rhizoma Dioscoreae Rhizoma Atractylodis Radix Scrophulariae Radix Rehmanniae Radix Ophiopogonis Radix Codonopsis Fructus Schisandrae Poria Galia Chinensis Concha Ostreae	Nourishing yin Clearing away heat Invigorating the spleen and qi	The Journal of New Medicine and Pharmacy(1976) 5: 24
Huanglian Jiaolang San	Rhizoma Coptidis Radix Codonopsis Radix Trichosanthis Rhizoma Alismatis	Clearing away heat Supplementing qi Nourishing yin	Shandong Journal of Traditional Chinese Medicine (1983) 5: 15

Herbal Formula	Components	Functions	Source of reference
<p>Xiaosanduo Tang</p>	<p>Radix Ginseng Rhizoma Anemarrhenae Gypsum Fibrosum Rhizoma Coptidis Colla Corii Asini Radix Paeoniae Alba Radix Trichosanthis Rhizoma Dioscoreae Rhizoma Polygonati Radix Polygoni Multiflori Preparata Radix Ophiopogonis Cortex Lycii</p>	<p>Nourishing the liver-<i>yin</i> and the kidney-<i>yin</i> Moistening dryness Supplementing <i>qi</i> Clearing away heat Promoting the production of body fluid to quench thirst</p>	<p>Henan Traditional Chinese Medicine (1987) 5: 33</p>
<p>Shu Huafen Tang</p>	<p>Radix Astragali Rhizoma Dioscoreae Cortex Mori Radicis Cortex Lycii Herba Dendrobii Radix Trichosanthis</p>	<p>Supplementing <i>qi</i> Nourishing <i>yin</i> Promoting the production of body fluid to quench thirst</p>	<p>Shanghai Journal of Traditional Chinese Medicine (1983) 8: 28</p>

Herbal Formula	Components	Functions	Source of reference
Yuxiao Ling	<p>Radix Astragali Rhizoma Dioscoreae Rhizoma Polygonati Herba Dendrobii Radix Trichosanthis Radix Rehmanniae Radix Rehmanniae Preparata Lophatherum Cortex Lycii Bombax Batryriacatus, powdered</p>	<p>Nourishing yin Clearing away heat Supplementing qi Promoting the production of the body fluid Astringing qi Consolidating essence</p>	<p>The Encyclopedia of Proved Prescriptions of Contemporary Famous TCM Doctors in China</p>
Yiqi Xuanyin Yin	<p>Radix Astragali Radix Ginseng Radix Cnidii Rhizoma Polygonati Multiflori Radix Rehmanniae Rhizoma Dioscoreae Fructus Lycii Radix Asparagi Semen Cuscutae Fructus Ligustri Lucidi Radix Scrophulariae</p>	<p>Supplementing qi Nourishing yin</p>	<p>The Encyclopedia of Proved Prescriptions of Contemporary Famous TCM Doctors in China</p>

Herbal Formula	Components	Functions	Source of reference
Tangniaobing Fang	Radix Astragali Rhizoma Dioscoreae Rhizoma Atractylodis Radix Scrophulariae Radix Rehmanniae Radix Ophiopogonis Radix Codonopsis Fructus Schisandrae Poria Galla Chinensis Concha Ostreae	Nourishing yin Clearing away heat Invigorating the spleen and qi	The Journal of New Medicine and Pharmacy(1976) 5: 24
Huanglian Jiangtang San	Rhizoma Coptidis Radix Codonopsis Radix Trichosanthis Rhizoma Alismatis	Clearing away heat Supplementing qi Nourishing yin	Shandong Journal of Traditional Chinese Medicine (1983) 5: 15

Table 9-1 A table showing commonly used herbal formulae for treating diabetes in China

9.6 Future development of SR10

In this study, some biochemical aspects of anti-diabetic effects of SR10 were investigated. In future, studies concerning the following issues can be carried out:

1. In this study, biochemical approaches in examining the efficacy of SR10 was applied. The establishment of compound formula SR10 was performed instead of isolating active components from individual herbs. The strength in using crude herbal extracts rather than purified compounds includes (i) the toxicity and side effects of crude herbal extract are generally lesser than isolated compounds; (ii) the formula can be modified (such as the ratio between component herbs) upon the condition of individual patient; (iii) compound formula may affect the body as a whole but pure compound usually pinpoint to a specific action. However, the formula SR10 in this study is a novel one, it is of great significance if we can isolate the active components from the formula. The isolated compound can also be used as a marker for quality control of production of SR10.
2. Detailed toxicity tests (acute and chronic) can be performed to determine the maximum allowable dosage of SR10 in animals.
3. Nowadays, most diabetic patients were treated with Western drugs to control plasma glucose level. However, some DM patients may take TCM together with Western drugs. Therefore, the interaction of SR10 with commonly used anti-diabetic agents should be studied.
4. This study only gives preliminary results on anti-atherosclerotic effects of SR10 by *in vitro* assays. Further studies using animal models could provide clearer picture on the efficacy of SR10 in removing atherosclerotic plaque.
5. In this study, the anti-oxidative properties of SR10 were confirmed. It is of high clinical advantages as free radical-induced cellular damages have been found in

many diseases such as cancer, stroke, Alzheimer's disease, etc. Thus, SR10 is a potential herbal formula for clinical trial for ROS-related diseases.

6. In this study, many cell lines used are not human origin (e.g. RIN-m5F, A7r5 and RAW264.7). These non-human cell lines were used because they have been well characterized by the supplier (American Type Culture Collection) and have been long used as cellular models in certain aspects. For example, LPS induced inflammatory responses in RAW264.7 macrophages have been widely studied. Thus, it is beneficial to use the cell line for drug testing. In future, the responses of SR10 can be tested using human cell line when available.

7. In the study, the ratio of three herbs Radix Astragali, Radix Codonopsis and Cortex Lycii in SR10 was set to be 3:3:1. This ratio was fixed by changing the optimal ratio 30:30:1 found in screening (SR) to 30:30:10 (SR10), 30:30:20 (SR20) or 30:30:30 (SR30). After testing, SR10 was found to be the best among these four ratios. However, it is just an optimal range for using 1/7 ratio of Cortex Lycii in the formula. In future, the ratio of three herbs in the formula can be further fine-tuned to obtain better efficacies.

9.7 Conclusions

Twenty-eight TCMs commonly prescribed for treating DM were selected for screening their protective activity against pancreatic β cell toxicity induced by streptozotocin. Three TCMs, including Radix Astragali, Radix Codonopsis and Cortex Lycii, were found to increase the viability of rat pancreatic β cell line, RIN-m5F. By combining these three TCMs at a weight ratio of 3:3:1, a herbal formula namely SR10 was generated. The anti-diabetic effect of SR10 was examined *in vitro*. SR10 treatment resulted in significant enhancement in survival of streptozotocin-

treated rat pancreatic β cells, RIN-m5F cells. SR10 apparently reduced apoptosis of streptozotocin-treated β cells by decreasing DNA fragmentation, sub-G₁ peak area and percentage of apoptotic cells. Nitric oxide (NO) production in streptozotocin-treated cells was inhibited by SR10 via suppression of the expression of inducible nitric oxide synthase (iNOS). For *in vivo* study, investigation of the effect of SR10 on blood glucose level and anti-oxidant level in diabetic mice was carried out. *Db/db* mouse model is a useful animal model for investigating type 2 DM. Results showed that SR10 was effective in decreasing blood glucose level in chronic treatment by improving β cell function. The activities and expression of anti-oxidant enzymes, catalase and superoxide dismutase, were up-regulated when treated with SR10. Moreover, in this study, SR10 treatment did not exhibit any toxic effect to the kidney, liver and heart of the host. The body weight of diabetic *db/db* mice were not affected by SR10 administration.

Atherosclerosis is a major cause of death in developed world and LDL oxidation is an early event in atherosclerosis. In this study, the inhibitory effect of SR10 on LDL oxidation was investigated using AAPH-induced rat erythrocyte hemolysis model and copper ion-induced human LDL oxidation model. Since vascular smooth muscle cell (VSMC) proliferation and migration are important processes in atherogenesis, we also examined the effect of SR10 in inhibiting these events. Our results showed that SR10 inhibited rat erythrocyte hemolysis with IC₅₀ value at 0.25 mg/ml and significantly prolonged human LDL oxidation *in vitro*. SR10 attenuated PDGF-BB-induced VSMC proliferation by promoting cell cycle arrest at G₀/G₁ phase as well as inhibited VSMC migration.

More recently, substantial evidence has emerged to suggest that inflammation plays a paramount role in the dynamic process of initiation, progression and rupture of the

atherosclerotic lesion. On the other hand, considerable recent interest has focused on establishing the role of inflammation in the pathogenesis of type 2 DM. In this study, mouse macrophage cell line RAW264.7 was used to examine the effect of SR10 in inhibition of inflammatory responses induced by LPS. Release of cytokines IL-1 β , IL-6 and TNF- α , and proinflammatory mediators nitric oxide and prostaglandin E₂ were determined in culture supernatants. To confirm if the response is mediated by NF κ B through the activation of MAPK and Akt pathway, the expression of NF κ B and regulatory proteins in MAPK and Akt pathway were analyzed by Western blot. The present results in anti-hyperglycemic, anti-oxidative and anti-atherosclerotic effects of SR10 imply that SR10 is a potential prescription for treating diabetes and associated atherosclerosis.

REFERENCES

- Albright A. (2008) What is public health practice telling us about diabetes? *J Am Diet Assoc.* **108**, S12-S18.
- Aguilar-Diosdado M, Parkinson D, Corbett JA, Kwon G, Marshall CA, Gingerich RL, Santiago JV, McDaniel ML. (1994) Potential autoantigens in insulin dependent diabetes mellitus: Expression of carboxypeptidase H and insulin but not glutamate decarboxylase on the β cell surface. *Diabetes.* **43**, 418-425.
- Amiel SA, Dixon T, Mann R, Jameson K. (2008) Hypoglycaemia in Type 2 diabetes. *Diabet Med.* **25**, 245-254.
- Aminot-Gilchrist DV, Anderson HD. (2004) Insulin resistance-associated cardiovascular disease: potential benefits of conjugated linoleic acid. *Am J Clin Nutr.* **79**, 1159S-1163S.
- Asano T, Fujishiro M, Kushiya A, Nakatsu Y, Yoneda M, Kamata H, Sakoda H. (2007) Role of phosphatidylinositol 3-kinase activation on insulin action and its alteration in diabetic conditions. *Biol Pharm Bull.* **30**, 1610-1616.
- Baynes JW. (1991) Role of oxidative stress in development of complications in diabetes. *Diabetes.* **40**, 405-412.
- Beckman JS, Beckman TW, Chen J, Marshall PA, Freeman BA. (1990) Apparent hydroxyl radical production by peroxynitrite: implications for endothelial injury from nitric oxide and superoxide. *Proc Natl Acad Sci USA.* **87**, 1620-1624.
- Beckman KB, Ames BN. (1998) The free radical theory of aging matures. *Physiol Rev.* **78**, 547-581.
- Bessesen DH. (2008) Update on obesity. *J Clin Endocrinol Metab.* **93**, 2027-2034.
- Bicknell KA, Surry EL, Brooks G. (2003) Targeting the cell cycle machinery for the treatment of cardiovascular disease. *J Pharm Pharmacol.* **55**, 571-591.
- Björkhem I, Henriksson-Freyschuss A, Breuer O, Diczfalusy U, Berglund L, Henriksson P. (1991) The antioxidant butylated hydroxytoluene protects against atherosclerosis. *Arterioscler Thromb.* **11**, 15-22.
- Bonnefont-Rousselot D, Bastard JP, Jaudon MC, Delattre J. (2000) Consequences of the diabetic status on the oxidant/anti-oxidant balance. *Diabetes Metab.* **26**, 163-176.
- Boulton AJ. (2008) The diabetic foot: grand overview, epidemiology and pathogenesis. *Diabetes Metab Res Rev.* **24**, S3-S6.
- Bours V, Bonizzi G, Bentires-Alj M, Bureau F, Piette J, Lekeux P, Merville M. (2000) NF-kappaB activation in response to toxic and therapeutic agents: role in inflammation and cancer treatment. *Toxicol.* **153**, 27-38.

Brownlee M. (2001) Biochemistry and molecular cell biology of diabetic complications. *Nature*. **414**, 813-820.

Brownlee M. (2005) The pathobiology of diabetic complications: a unifying mechanism. *Diabetes*. **54**, 1615-1625.

Bruun JM, Lihn AS, Pedersen SB, Richelsen B. (2005) Monocyte chemoattractant protein-1 release is higher in visceral than subcutaneous human adipose tissue (AT): implication of macrophages resident in the AT. *J Clin Endocrinol Metab*. **90**, 2282-2289.

Buchanan TA, Xiang A, Kjos SL, Lee WP, Trigo E, Nader I, Bergner EA, Palmer JP, Peters RK. (1998) Gestational Diabetes: Antepartum Characteristics That Predict Postpartum Glucose Intolerance and Type 2 Diabetes in Latino Women. *Diabetes*. **47**, 1302-1310.

Carew TE, Schwenke DC, Steinberg D. (1987) Antiatherogenic effect of probucol unrelated to its hypocholesterolemic effect: evidence that antioxidants in vivo can selectively inhibit low density lipoprotein degradation in macrophage-rich fatty streaks and slow the progression of atherosclerosis in the Watanabe heritable hyperlipidemic rabbit. *Proc Natl Acad Sci USA*. **84**, 7725-7729.

Cardellini M, Andreozzi F, Laratta E, Marini MA, Lauro R, Hribal ML, Perticone F, Sesti G. (2007) Plasma interleukin-6 levels are increased in subjects with impaired glucose tolerance but not in those with impaired fasting glucose in a cohort of Italian Caucasians. *Diabetes Metab Res Rev*. **23**, 141-145.

Carvalho CR, Carvalheira JB, Lima MH, Zimmerman SF, Caperuto LC, Amanso A, Gasparetti AL, Meneghetti V, Zimmerman LF, Velloso LA, Saad MJ. (2003) Novel signal transduction pathway for luteinizing hormone and its interaction with insulin: activation of Janus kinase/signal transducer and activator of transcription and phosphoinositol 3-kinase/Akt pathways. *Endocrinol*. **144**, 638-647.

Castelli WP, Garrison RJ, Wilson PW, Abbott RD, Kalousdian S, Kannel WB. (1986) Incidence of coronary heart disease and lipoprotein cholesterol levels: the Framingham Study. *JAMA*. **256**, 2835-2838.

Chan ED, Riches DW. (2001) IFN-gamma + LPS induction of iNOS is modulated by ERK, JNK/SAPK, and p38(mapk) in a mouse macrophage cell line. *Am J Physiol Cell Physiol*. **280**, C441-450.

Chang L, Chiang SH, Saltiel AR. (2004) Insulin signaling and the regulation of glucose transport. *Mol Med*. **10**, 65-71.

Chen CC, Wang JK. (1999) p38 but not p44/42 mitogen-activated protein kinase is required for nitric oxide synthase induction mediated by lipopolysaccharide in RAW264.7 macrophages, *Mol Pharmacol*. **55**, 481-488.

Chen FC. (1987) Present advance in chemical and pharmacological research of natural products for anti-hyperglycemia. *Chin Trad Herb Drugs*. **18**, 39-44.

Chen SY, Li F, Diebschlag F. (1993) *A Clinical Guide to Chinese Herbs and Formulae*. Churchill Livingstone, New York, USA.

Chevion M. (1988) A site-specific mechanism for free radical induced biological damage: the essential role of redox-active transition metals. *Free Radic Biol Med.* **5**, 27-37.

Chinese Pharmacopoeia Editorial Committee (2000). *Chinese Pharmacopoeia 2000 edition*.

Coniff RF, Shapiro JA, Robbins D, Kleinfield R, Seaton TB, Beisswenger P, McGill JB. (1995) Reduction of glycosylated hemoglobin and postprandial hyperglycemia by acarbose in patients with NIDDM. A placebo-controlled dose-comparison study. *Diabetes Care.* **18**, 817-824.

Costa NJ, Dahm CC, Hurrell F, Taylor ER, Murphy MP. (2003) The interactions of mitochondrial thiols with nitric oxide. *Antioxid Redox Signal.* **5**, 291-305.

Dai BY. (2000) Present advance in therapeutical mechanism of diabetes in traditional Chinese medical system. *Chin J Inform Trad Chin Med.* **7**, 23-24.

Dalla Vestra M, Saller A, Mauer M, Fioretto P. (2001) Role of mesangial expansion in the pathogenesis of diabetic nephropathy. *J Nephrol.* **14**, S51-S57.

Deeks ED, Keam SJ. (2007) Rosiglitazone: a review of its use in type 2 diabetes mellitus. *Drugs.* **67**, 2747-2779.

Doggrell SA. (2008) Clinical trials with thiazolidinediones in subjects with Type 2 diabetes--is pioglitazone any different from rosiglitazone? *Expert Opin Pharmacother.* **9**, 405-420.

Dyck DJ, Heigenhauser GJ, Bruce CR. (2006) The role of adipokines as regulators of skeletal muscle fatty acid metabolism and insulin sensitivity. *Acta Physiol.* **186**, 5-16.

Esterbauer H, Gebicki J, Puhl H, Jürgens G. (1992) The role of lipid peroxidation and antioxidants in oxidative modification of LDL. *Free Radic Biol Med.* **13**, 341-390.

Esterbauer H, Striegl G, Puhl H, Rotheneder M. (1989) Continuous monitoring of in vitro oxidation of human low density lipoprotein. *Free Radic Res Commun.* **6**, 67-75.

Faure P. (2003) Protective effects of anti-oxidant micronutrients (vitamin E, zinc and selenium) in type 2 diabetes mellitus. *Clin Chem Lab Med.* **41**, 995-998.

Fineberg SE, Kawabata TT, Finco-Kent D, Fountaine RJ, Finch GL, Krasner AS. (2007) Immunological responses to exogenous insulin. *Endocr Rev.* **28**, 625-652.

Fioretto P, Mauer M. (2007) Histopathology of diabetic nephropathy. *Semin Nephrol.* **27**, 195-207.

- Fogelman AM, Haberland ME, Seager J, Hokom M, Edwards PA. (1981) Factors regulating the activities of the low density lipoprotein receptor and the scavenger receptor on human monocyte-macrophages. *J Lipid Res.* **22**, 1131-1141.
- Forman HJ, Azzi A. (1997) On the virtual existence of superoxide anions in mitochondria: thoughts regarding its role in pathophysiology. *FASEB J.* **11**, 374-375.
- Friedewald WT, Levy RI, Fredrickson DS. (1972) Estimation of the concentration of low-density lipoprotein cholesterol in plasma, without use of the preparative ultracentrifuge. *Clin Chem.* **18**, 499-502.
- Fujiwara N, Kobayashi K. (2005) Macrophages in inflammation. *Curr Drug Targets Inflamm Allergy.* **4**, 281-286.
- Galis ZS, Sukhova GK, Lark MW, Libby P. (1994) Increased expression of matrix metalloproteinases and matrix degrading activity in vulnerable regions of human atherosclerotic plaques. *J Clin Invest.* **94**, 2493-2503.
- Galle J, Lehmann-Bodem C, Hübner U, Heinloth A, Wanner C. (2000) CyA and OxLDL cause endothelial dysfunction in isolated arteries through endothelin-mediated stimulation of O₂(⁻) formation. *Nephrol Dial Transplant.* **15**, 339-346.
- Ganne S, Arora SK, Dotsenko O, McFarlane SI, Whaley-Connell A. (2007) Hypertension in people with diabetes and the metabolic syndrome: pathophysiologic insights and therapeutic update. *Curr Diab Rep.* **7**, 208-217.
- Garber AJ, Duncan TG, Goodman AM, Mills DJ, Rohlf JL. (1997) Efficacy of metformin in type II diabetes: results of a double-blind, placebo-controlled, dose-response trial. *Am J Med.* **103**, 491-497.
- Gaziano JM. (1996) Antioxidants in cardiovascular disease: randomized trials. *Nutrition.* **12**, 583-588.
- Gey KF, Puska P, Jordan P, Moser UK. (1991) Inverse correlation between plasma vitamin E and mortality from ischemic heart disease in cross-cultural epidemiology. *Am J Clin Nutr.* **53**, 326S-334S.
- Ghosh S, May MJ, Kopp EB. (1998) NF-kappa B and Rel proteins: evolutionarily conserved mediators of immune responses. *Annu Rev Immunol.* **16**, 225-260.
- Giorgino F, Laviola L, Leonardini A. (2005) Pathophysiology of type 2 diabetes: rationale for different oral antidiabetic treatment strategies. *Diabetes Res Clin Pract.* **68**, S22-S29.
- Graf K, Xi XP, Yang D, Fleck E, Hsueh WA, Law RE. (1997) Mitogen-activated protein kinase activation is involved in platelet-derived growth factor-directed migration by vascular smooth muscle cells. *Hypertension.* **29**, 334-339.

- Grimaud D, Levraut J. (2001) Acute postoperative metabolic complications of diabetes. *Minerva Anesthesiol.* **67**, 263-270.
- Gu D, Reynolds K, Wu X, Chen J, Duan X, Reynolds RF, Whelton PK, He J, InterASIA Collaborative Group. (2005) Prevalence of the metabolic syndrome and overweight among adults in China. *Lancet.* **365**, 1398-1405.
- Gu GY, Jian Y. (1997) A survey on anti-hyperglycemic constituents from plants. *World Phytomed.* **12**, 55-58.
- Gual P, Le Marchand-Brustel Y, Tanti JF. (2005) Positive and negative regulation of insulin signaling through IRS-1 phosphorylation. *Biochimie.* **87**, 99-109.
- Guha M, Bai W, Nadler JL, Natarajan R. (2000) Molecular mechanisms of tumor necrosis factor alpha gene expression in monocytic cells via hyperglycemia-induced oxidant stress-dependent and -independent pathways. *J Biol Chem.* **275**, 17728-17739.
- Guilherme A, Virbasius JV, Puri V, Czech MP. (2008) Adipocyte dysfunctions linking obesity to insulin resistance and type 2 diabetes. *Nat Rev Mol Cell Biol.* **9**, 367-377.
- Hadjivassiliou V, Green MH, James RF, Swift SM, Clayton HA, Green IC. (1998) Insulin secretion, DNA damage, and apoptosis in human and rat islets of Langerhans following exposure to nitric oxide, peroxynitrite, and cytokines. *Nitric Oxide.* **2**, 429-441.
- Hamer M, Chida Y. (2007) Intake of fruit, vegetables, and antioxidants and risk of type 2 diabetes: systematic review and meta-analysis. *J Hypertens.* **25**, 2361-2369.
- Hanefeld M, Schaper F. (2008) Acarbose: oral anti-diabetes drug with additional cardiovascular benefits. *Expert Rev Cardiovasc Ther.* **6**, 153-163.
- Harris, M. I. (2004) Definition and classification of diabetes mellitus and the criteria for diagnosis. In *Diabetes Mellitus - A Fundamental and Clinical Text*, eds. LeRoith, D., Taylor, S. I., and Olefsky, J. M., Lippincott Williams & Wilkins, Philadelphia, PN, USA. pp. 457-467.
- Hauer H. (2002) The mode of action of thiazolidinediones. *Diabetes Metab Res Rev.* **18**, S10-S15.
- Hayakawa M, Miyashita H, Sakamoto I, Kitagawa M, Tanaka H, Yasuda H, Karin M, Kikugawa K. (2003) Evidence that reactive oxygen species do not mediate NF-kappaB activation. *EMBO J.* **22**, 3356-3366.
- Heinecke JW. (1998) Oxidants and antioxidants in the pathogenesis of atherosclerosis: implications for the oxidized low density lipoprotein hypothesis. *Atherosclerosis.* **141**, 1-15.

- Heinecke JW. (1999) Mechanisms of oxidative damage by myeloperoxidase in atherosclerosis and other inflammatory disorders. *J Lab Clin Med.* **133**, 321-325.
- Henry RR. (1997) Thiazolidinediones. *Endocrinol Metab Clin North Am.* **26**, 553-573.
- Hong Kong SAR Government (2008) *Health Facts of Hong Kong*. Department of Health, Hong Kong SAR Government.
- Höppener JW, Lips CJ. (2006) Role of islet amyloid in type 2 diabetes mellitus. *Int J Biochem Cell Biol.* **38**, 726-736.
- Hotamisligil GS. (2005) Role of endoplasmic reticulum stress and c-Jun NH2-terminal kinase pathways in inflammation and origin of obesity and diabetes. *Diabetes.* **54**, S73-S78.
- Hunt JV, Smith CC, Wolff SP. (1991) Autoxidative glycosylation and possible involvement of peroxides and free radicals in LDL modification by glucose. *Diabetes.* **39**, 1420-1424.
- Igarashi M, Wakasaki H, Takahara N, Ishii H, Jiang ZY, Yamauchi T, Kuboki K, Meier M, Rhodes CJ, King GL. (1999) Glucose or diabetes activates p38 mitogen-activated protein kinase via different pathways. *J Clin Invest.* **103**, 185-195.
- Ihara Y, Toyokuni S, Uchida K, Odaka H, Tanaka T, Ikeda H, Hiai H, Seino Y, Yamada Y. (1999) Hyperglycemia causes oxidative stress in pancreatic β -cells of GK rats, a model of type 2 diabetes. *Diabetes.* **48**, 927-932.
- Iiyama K, Hajra L, Iiyama M, Li H, DiChiara M, Medoff BD, Cybulsky MI. (1999) Patterns of vascular cell adhesion molecule-1 and intercellular adhesion molecule-1 expression in rabbit and mouse atherosclerotic lesions and at sites predisposed to lesion formation. *Circ Res.* **85**, 199-207.
- Jordan JD, Landau EM, Iyengar R. (2000) Signaling networks: the origins of cellular multitasking. *Cell.* **103**, 193-200.
- Kabadi MU, Kabadi UM. (2003) Efficacy of sulphonylureas with insulin in type 2 diabetes mellitus. *Ann Pharmacother.* **37**, 1572-1576.
- Kadowaki T, Yamauchi T. (2005) Adiponectin and adiponectin receptors. *Endocrinol Rev.* **26**, 439-451.
- Kajinami K, Nishitsuji M, Takeda Y, Shimizu M, Koizumi J, Mabuchi H. (1996) Long-term probucol treatment results in regression of xanthomas, but in progression of coronary atherosclerosis in a heterozygous patient with familial hypercholesterolemia. *Atherosclerosis.* **120**, 181-187.
- Kaneto H, Fuji J, Seo HG, Suzuki K, Matsoka T, Nakamura M, Tatsumi H, Yamamsaki Y, Kamada T, Taniguchi N. (1995) Apoptotic cell death triggered by nitric oxide in pancreatic β -cells. *Diabetes.* **44**, 733-738.

- Kaneto H, Fujii J, Myint T, Miyazawa N, Islam KN, Kawasaki Y, Suzuki K, Nakamura M, Tatsumi H, Yamasaki Y, Taniguchi N. (1996) Reducing sugars trigger oxidative modification and apoptosis in pancreatic β -cells by provoking oxidative stress through the glycation reaction. *Biochem J.* **320**, 855-863.
- Kaneto H, Kawamori D, Nakatani Y, Gorogawa S, Matsuoka TA. (2004) Oxidative stress and the JNK pathway as a potential therapeutic target for diabetes. *Drug News Perspect.* **17**, 447-453.
- Kaneto H, Kawamori D, Matsuoka TA, Kajimoto Y, Yamasaki Y. (2005) Oxidative stress and pancreatic beta-cell dysfunction. *Am J Ther.* **12**, 529-533.
- Karihtala P, Soini Y. (2007) Reactive oxygen species and anti-oxidant mechanisms in human tissues and their relation to malignancies. *APMIS.* **115**, 81-103.
- Kim SH, Johnson VJ, Shin TY, Sharma RP. (2004) Selenium attenuates lipopolysaccharide-induced oxidative stress responses through modulation of p38 MAPK and NF-kappaB signaling pathways. *Exp Biol Med.* **229**, 203-213.
- Kingsley K, Huff JL, Rust WL, Carroll K, Martinez AM, Fitchmun M, Plopper GE. (2002) ERK1/2 mediates PDGF-BB stimulated vascular smooth muscle cell proliferation and migration on laminin-5. *Biochem Biophys Res Commun.* **293**, 1000-1006.
- Kita T, Nagano Y, Yokode M, Ishii K, Kume N, Ooshima A, Yoshida H, Kawai C. (1987) Probucol prevents the progression of atherosclerosis in Watanabe heritable hyperlipidemic rabbit, an animal model for familial hypercholesterolemia. *Proc Natl Acad Sci USA.* **84**, 5928-5931.
- Ko GT, Chan JC, Chow CC, Yeung VT, Chan WB, So WY, Cockram CS. (2004) Effects of obesity on the conversion from normal glucose tolerance to diabetes in Hong Kong Chinese. *Obes Res.* **12**, 889-895.
- Ko GT, Ozaki R, Wong GW, Kong AP, So WY, Tong PC, Chan MH, Ho CS, Lam CW, Chan JC. (2008) The problem of obesity among adolescents in Hong Kong: a comparison using various diagnostic criteria. *BMC Pediatr.* **8**, 10.
- Koda-Kimble MA, Carlisle BA. (2001) Diabetes mellitus. In *Applied Therapeutics: The Clinical Use of Drugs*, eds. Koda-Kimble, M. A. and Young, L. Y., Lippincott Williams & Wilkins, Philadelphia, PN, USA. pp. 59-78.
- Kraegen EW, Cooney GJ. (2008) Free fatty acids and skeletal muscle insulin resistance. *Curr Opin Lipidol.* **19**, 235-241.
- Krentz AJ. (2003) Lipoprotein abnormalities and their consequences for patients with type 2 diabetes. *Diabetes Obes Metab.* **5**, S19-S27.
- Kuchinski LM. (1999) *Controlling Diabetes Naturally with Chinese medicine*. Blue Poppy Press, Boulder, CO, USA. pp. 34-45.

Lähteenmäki TA, Korpela R, Tikkanen MJ, Karjala K, Laakso J, Solatunturi E, Vapaatalo H. (1998) Proliferative effects of oxidized low-density lipoprotein on vascular smooth muscle cells: role of dietary habits. *Life Sci.* **63**, 995-1003.

Le Marchand-Brustel Y, Gual P, Grémeaux T, Gonzalez T, Barrès R, Tanti JF. (2003) Fatty acid-induced insulin resistance: role of insulin receptor substrate 1 serine phosphorylation in the retroregulation of insulin signalling. *Biochem Soc Trans.* **31**, 1152-1156.

Lee WM. (2003) Drug-induced hepatotoxicity. *N Engl J Med.* **349**, 474-485.

Lee ZS, Critchley JA, Ko GT, Anderson PJ, Thomas GN, Young RP, Chan TY, Cockram CS, Tomlinson B, Chan JC. (2002) Obesity and cardiovascular risk factors in Hong Kong Chinese. *Obes Rev.* **3**, 173-182.

Lenzen S, Drinkgern J, Tiedge M. (1996) Low antioxidant enzyme gene expression in pancreatic islets compared with various other mouse tissues. *Free Radical Biol Med.* **20**, 463-466.

Levy AP, Blum S. (2007) Pharmacogenomics in prevention of diabetic cardiovascular disease: utilization of the haptoglobin genotype in determining benefit from vitamin E. *Expert Rev Cardiovasc Ther.* **5**, 1105-1111.

Li N, Karin M. (1999) Is NF-kappaB the sensor of oxidative stress? *FASEB J.* **13**, 1137-1143.

Li WL, Zheng HC, Bukuru J, De Kimpe N. (2004) Natural medicines used in the traditional Chinese medical system for therapy of diabetes mellitus. *J Ethnopharmacol.* **92**, 1-21.

Liang H, Yin B, Zhang H, Zhang S, Zeng Q, Wang J, Jiang X, Yuan L, Wang CY, Li Z. (2008) Blockade of tumor necrosis factor (TNF) receptor type I-mediated TNF-alpha signaling protected Wistar rats from diet-induced obesity and insulin resistance. *Endocrinol.* **149**, 2943-2951.

Liu RH, Hotchkiss JH. (1995) Potential genotoxicity of chronically elevated nitric oxide: A review. *Mutat Res.* **339**, 73-89.

Luo N, Liu SM, Liu H, Li Q, Xu Q, Sun X, Davis B, Li J, Chua S Jr. (2006) Allelic variation on chromosome 5 controls beta-cell mass expansion during hyperglycemia in leptin receptor-deficient diabetes mice. *Endocrinol.* **147**, 2287-2295.

Lupi R, Del Prato S. (2008) Beta-cell apoptosis in type 2 diabetes: quantitative and functional consequences. *Diabetes Metab.* **34**, S56-S64.

Mackness MI, Arrol S, Abbott, C, Durrington PN. (1993) Protection of low-density lipoprotein against oxidative modification by high-density lipoprotein associated paraoxonase. *Atherosclerosis.* **104**, 129-135.

MacMicking J, Xie QW, Nathan C. (1997) Nitric oxide and macrophage function. *Annu Rev Immunol.* **15**, 323-350.

Maedler K, Spinas GA, Lehmann R, Sergeev P, Weber M, Fontana A, Kaiser N, Donath MY. (2001) Glucose induces beta-cell apoptosis via upregulation of the Fas receptor in human islets. *Diabetes.* **50**, 1683-1690.

Maedler K, Sergeev P, Ris F, Oberholzer J, Joller-Jemelka HI, Spinas GA, Kaiser N, Halban PA, Donath MY. (2002) Glucose-induced beta cell production of IL-1beta contributes to glucotoxicity in human pancreatic islets. *J Clin Invest.* **110**, 851-860.

Maguire JJ, Wilson DS, Packer L. (1989) Mitochondrial electron transport-linked tocoferoxyl radical reduction. *J Biol Chem.* **264**, 21462-21465.

Maritim AC, Sanders RA, Watkins JB 3rd. (2003) Diabetes, oxidative stress, and anti-oxidants: a review. *J Biochem Mol Toxicol.* **17**, 24-38.

Matsuoka T, Kajimoto Y, Watada H, Kaneto H, Kishimoto M, Umayahara Y, Fujitani Y, Kamada T, Kawamori R, Yamasaki Y. (1997) Glycation-dependent, reactive oxygen species-mediated suppression of the insulin gene promoter activity in HIT cells. *J Clin Invest.* **99**, 144-150.

Mazzone T, Chait A, Plutzky J. (2008) Cardiovascular disease risk in type 2 diabetes mellitus: insights from mechanistic studies. *Lancet.* **371**, 1800-1809.

Meister B. (2000) Control of food intake via leptin receptors in the hypothalamus. *Vitam Horm.* **59**, 265-304.

Miller GJ, Miller NE. (1975) Plasma-high-density-lipoprotein concentration and development of ischaemic heart-disease. *Lancet.* **1**, 16-19.

Moncada S, Palmer RM, Higgs EA. (1991) Nitric oxide: Physiology, pathophysiology, and pharmacology. *Pharmacol Rev.* **43**, 109-142.

Moore T. (2004) Diabetic emergencies in adults. *Nurs Stand.* **18**, 45-52.

Moran A, Zhang H-J, Olson LK, Harmon JS, Poirout V, Robertson RP. (1997) Differentiation of glucose toxicity from beta cell exhaustion during the evolution of defective insulin gene expression in the pancreatic islet cell line, HIT-T15. *J Clin Invest.* **99**, 534-539.

Murata M, Takahashi A, Saito I, Kawanishi S. (1999) Site specific DNA methylation and apoptosis: Induction by diabetogenic streptozotocin. *Biochem Pharmacol.* **57**, 881-887.

Murata Y, Tsuruzoe K, Kawashima J, Furukawa N, Kondo T, Motoshima H, Igata M, Taketa K, Sasaki K, Kishikawa H, Kahn CR, Toyonaga T, Araki E. (2007) IRS-1 transgenic mice show increased epididymal fat mass and insulin resistance. *Biochem Biophys Res Commun.* **364**, 301-307.

Musi N, Goodyear LJ. (2006) Insulin resistance and improvements in signal transduction. *Endocrine*. **29**, 73-80.

Myllärniemi M, Calderon L, Lemström K, Buchdunger E, Häyry P. (1997) Inhibition of platelet-derived growth factor receptor tyrosine kinase inhibits vascular smooth muscle cell migration and proliferation. *FASEB J*. **11**, 1119-1126.

Nagano Y, Nakamura T, Matsuzawa Y, Cho M, Ueda Y, Kita T. (1992) Probucol and atherosclerosis in the Watanabe heritable hyperlipidemic rabbit--long-term antiatherogenic effect and effects on established plaques. *Atherosclerosis*. **92**, 131-140.

Nelson SE, Palumbo PJ. (2006) Addition of insulin to oral therapy in patients with type 2 diabetes. *Am J Med Sci*. **331**, 257-263.

Niedowicz DM, Daleke DL. (2005) The role of oxidative stress in diabetic complications. *Cell Biochem Biophys*. **43**, 289-330.

Nishikawa T, Edelstein D, Du XL, Yamagishi S, Matsumura T, Kaneda Y, Yorek MA, Beebe D, Oates PJ, Hammes HP, Giardino I, Brownlee M. (2000) Normalizing mitochondrial superoxide production blocks three pathways of hyperglycaemic damage. *Nature*. **404**, 787-790.

Ollivier V, Parry GC, Cobb RR, de Prost D, Mackman N. (1996) Elevated cyclic AMP inhibits NF-kappaB-mediated transcription in human monocytic cells and endothelial cells. *J Biol Chem*. **271**, 20828-20835.

Olson LK, Redmon JB, Towle HC, Robertson RP. (1993) Chronic exposure of HIT cells to high glucose concentrations paradoxically decreases insulin gene transcription and alters binding of insulin gene regulatory protein. *J Clin Invest*. **92**, 514-519.

Pataký Z, Vischer U. (2007) Diabetic foot disease in the elderly. *Diabetes Metab*. **33**, S56-S65.

Petersen KF, Shulman GI. (2002) Pathogenesis of skeletal muscle insulin resistance in type 2 diabetes mellitus. *Am J Cardiol*. **90**, 11G-18G.

Philbin TM, Berlet GC, Lee TH. (2006) Lower-extremity amputations in association with diabetes mellitus. *Foot Ankle Clin*. **11**, 791-804.

Piro S, Anello M, Di Pietro C, Lizzio MN, Patane G, Rabuazzo AM, Vigneri R, Purrello M, Purrello F. (2002) Chronic exposure to free fatty acids or high glucose induces apoptosis in rat pancreatic islets: possible role of oxidative stress. *Metabolism*. **51**, 1340-1347.

Poitout V, Olson LK, Robertson RP. (1996) Chronic exposure of bTC-6 cells to supraphysiologic concentrations of glucose decreases binding of the RIPE3b1 insulin gene transcription activator. *J Clin Invest*. **97**, 1041-1046.

Qi HY, Shelhamer JH. (2005) Toll-like receptor 4 signaling regulates cytosolic phospholipase A2 activation and lipid generation in lipopolysaccharide-stimulated macrophages. *J Biol Chem.* **280**, 38969-38975.

Raha S, Robinson BH. (2000) Mitochondria, oxygen free radicals, disease and ageing. *Trends Biochem Sci.* **25**, 502-508.

Reddy MA, Thimmalapura PR, Lanting L, Nadler JL, Fatima S, Natarajan R. (2002) The oxidized lipid and lipoxygenase product 12(S)-hydroxyeicosatetraenoic acid induces hypertrophy and fibronectin transcription in vascular smooth muscle cells via p38 MAPK and cAMP response element-binding protein activation. Mediation of angiotensin II effects. *J Biol Chem.* **277**, 9920-9928.

Reddy ST, Wadleigh DJ, Grijalva V, Ng C, Hama S, Gangopadhyay A, Shih DM, Lusis AJ, Navab M, Fogelman AM. (2001) Human paraoxonase-3 is an HDL-associated enzyme with biological activity similar to paraoxonase-1 protein but is not regulated by oxidized lipids. *Arterioscler Thromb Vasc Biol.* **21**, 542-547.

Reynolds A, Laurie C, Lee Mosley R, Gendelman HE. (2007) Oxidative stress and the pathogenesis of neurodegenerative disorders. *Int Rev Neurobiol.* **82**, 297-325.

Rhee SH, Hwang D. (2000) Murine TOLL-like receptor 4 confers lipopolysaccharide responsiveness as determined by activation of NF kappa B and expression of the inducible cyclooxygenase. *J Biol Chem.* **275**, 34035-34040.

Rietschel ET, Kirikae T, Schade FU, Mamat U, Schmidt G, Loppnow H, Ulmer AJ, Zähringer U, Seydel U, Di Padova F, Schreier M, Brade H. (1994) Bacterial endotoxin: molecular relationships of structure to activity and function. *FASEB J.* **8**, 217-225.

Robertson RP, Zhang H-J, Pyzdrowski KL, Walseth TF. (1992) Preservation of insulin mRNA levels and insulin secretion in HIT cells by avoidance of chronic exposure to high glucose concentrations. *J Clin Invest.* **90**, 320-325.

Robertson RP, Harmon J, Tran PO, Tanaka Y, Takahashi H. (2003) Glucose toxicity in beta-cells: type 2 diabetes, good radicals gone bad, and the glutathione connection. *Diabetes.* **52**, 581-587.

Robertson RP. (2004) Chronic oxidative stress as a central mechanism for glucose toxicity in pancreatic islet beta cells in diabetes. *J Biol Chem.* **279**, 42351-42354.

Robertson RP, Harmon JS. (2006) Diabetes, glucose toxicity, and oxidative stress: A case of double jeopardy for the pancreatic islet beta cell. *Free Radic Biol Med.* **41**, 177-184.

Roglic G, Unwin N, Bennett PH, Mathers C, Tuomilehto J, Nag S, Connolly V, King H.. (2005) The burden of mortality attributable to diabetes: realistic estimates for the year 2000. *Diabetes Care.* **28**, 2130-2135.

- Ross R. (1999) Atherosclerosis is an inflammatory disease. *Am Heart J.* **138**, S419-S425.
- Riccioni G, Bucciarelli T, Mancini B, Di Ilio C, Capra V, D'Orazio N. (2007) The role of the antioxidant vitamin supplementation in the prevention of cardiovascular diseases. *Expert Opin Investig Drugs.* **16**, 25-32.
- Risérus U. (2008) Fatty acids and insulin sensitivity. *Curr Opin Clin Nutr Metab Care.* **11**, 100-105.
- Sakai K, Matsumoto K, Nishikawa T, Suefuji M, Nakamaru K, Hirashima Y, Kawashima J, Shirotani T, Ichinose K, Brownlee M, Araki E. (2003) Mitochondrial reactive oxygen species reduce insulin secretion by pancreatic beta-cells. *Biochem Biophys Res Commun.* **300**, 216-222.
- Sakurai T, Tsuchiya S. (1988) Superoxide production from nonenzymatically glycation protein. *FEBS Lett.* **236**, 406-410.
- Salonen RM, Nyssönen K, Kaikkonen J, Porkkala-Sarataho E, Voutilainen S, Rissanen TH, Tuomainen TP, Valkonen VP, Ristonmaa U, Lakka HM, Vanharanta M, Salonen JT, Poulsen HE. (2003) Antioxidant Supplementation in Atherosclerosis Prevention Study. Six-year effect of combined vitamin C and E supplementation on atherosclerotic progression. Atherosclerosis Prevention (ASAP) Study. *Circulation.* **107**, 947-953.
- Sasahara M, Raines EW, Chait A, Carew TE, Steinberg D, Wahl PW, Ross R. (1994) Inhibition of hypercholesterolemia-induced atherosclerosis in the nonhuman primate by probucol. I. Is the extent of atherosclerosis related to resistance of LDL to oxidation? *J Clin Invest.* **94**, 155-164.
- Schafer KA. (1998) The cell cycle: a review. *Vet Pathol.* **35**, 461-478.
- Schena FP, Gesualdo L. (2005) Pathogenetic mechanisms of diabetic nephropathy. *J Am Soc Nephrol.* **1**, S30-S33.
- Schmidt AM, Hori O, Brett J, Yan SD, Wautier JL, Stern D. (1994) Cellular receptors for advanced glycation end products. *Arterioscl Thromb Vas.* **14**, 1521-1528.
- Scott LJ, Spencer CM. (2000) Miglitol: a review of its therapeutic potential in type 2 diabetes mellitus. *Drugs.* **59**, 521-549.
- Sharma A, Olson LK, Robertson RP, Stein R. (1995) The reduction of insulin gene transcription in HIT- T 1 5b cells chronically exposed to high glucose concentration is associated with loss of RIPE3b1 and STF-1 transcription factor expression. *Mol Endocrinol.* **9**, 1127-1134.
- Shoelson SE, Lee J, Goldfine AB. (2006) Inflammation and insulin resistance. *J Clin Invest.* **116**, 1793-1801.

- Singh R, Ramasamy K, Abraham C, Gupta V, Gupta A. (2008) Diabetic retinopathy: an update. *Indian J Ophthalmol.* **56**, 178-188.
- Singh U, Devaraj S, Jialal I. (2005) Vitamin E, oxidative stress, and inflammation. *Annu Rev Nutr.* **25**, 151-174.
- So WY, Chan JC, Yeung VT, Chow CC, Ko GT, Li JK, Cockram CS. (2002) Sulphonylurea-induced hypoglycaemia in institutionalized elderly in Hong Kong. *Diabet Med.* **19**, 966-968.
- Sowers JR, Epstein M, Frohlich ED. (2001) Diabetes, hypertension, and cardiovascular disease: an update. *Hypertension.* **37**, 1053-1059.
- Sparrow CP, Doebber TW, Olszewski J, Wu MS, Ventre J, Stevens KA, Chao YS. (1992) Low density lipoprotein is protected from oxidation and the progression of atherosclerosis is slowed in cholesterol-fed rabbits by the antioxidant N,N'-diphenylphenylenediamine. *J Clin Invest.* **89**, 1885-1891.
- Stern MP. (1995) Diabetes and cardiovascular disease. The "common soil" hypothesis. *Diabetes.* **44**, 369-374.
- Stewart CR, Tseng AA, Mok YF, Staples MK, Schiesser CH, Lawrence LJ, Varghese JN, Moore KJ, Howlett GJ. (2005) Oxidation of low-density lipoproteins induces amyloid-like structures that are recognized by macrophages. *Biochemistry.* **44**, 9108-9116.
- Stocker R, Keaney JF Jr. (2004) Role of oxidative modifications in atherosclerosis. *Physiol Rev.* **84**, 1381-1478.
- Student Health Service, Department of Health, Government of Hong Kong Special Administrative Region (2007).
- Stumvoll M, Goldstein BJ, van Haeften TW. (2005) Type 2 diabetes: principles of pathogenesis and therapy. *Lancet.* **365**, 1333-13346.
- Swarbrick MM, Havel PJ. (2008) Physiological, pharmacological, and nutritional regulation of circulating adiponectin concentrations in humans. *Metab Syndr Relat Disord.* **6**, 87-102.
- Tajiri Y, Moller C, Grill V. (1997) Long term effects of aminoguanidine on insulin release and biosynthesis: evidence that the formation of advanced glycosylation end products inhibits B cell function. *Endocrinology.* **138**, 273-280.
- Tangirala RK, Casanada F, Miller E, Witztum JL, Steinberg D, Palinski W. (1995) Effect of the antioxidant N,N'-diphenyl 1,4-phenylenediamine (DPPD) on atherosclerosis in apoE-deficient mice. *Arterioscler Thromb Vasc Biol.* **15**, 1625-1630.

- Tanti JF, Gual P, Grémeaux T, Gonzalez T, Barrès R, Le Marchand-Brustel Y. (2004) Alteration in insulin action: role of IRS-1 serine phosphorylation in the retroregulation of insulin signalling. *Ann Endocrinol.* **65**, 43-48.
- ter Steege JC, van de Ven MW, Forget PP, Brouckaert P, Buurman WA. (1998) The role of endogenous IFN-gamma, TNF-alpha and IL-10 in LPS-induced nitric oxide release in a mouse model. *Cytokine.* **10**, 115-123.
- Tiedge M, Lortz S, Drinkgern J, Lenzen S. (1997) Relation between antioxidant enzyme gene expression and antioxidative defense status of insulin-producing cells. *Diabetes.* **46**, 1733-1742.
- Tiedge M, Lortz S, Munday R, Lenzen S. (1998) Complementary action of antioxidant enzymes in the protection of bioengineered insulin-producing RINm5F cells against the toxicity of reactive oxygen species. *Diabetes.* **47**, 1578-1585.
- Tilig H, Moschen AR. (2008) Inflammatory mechanisms in the regulation of insulin resistance. *Mol Med.* **14**, 222-231.
- Vasquez-Vivar J, Kalyanaraman B, Kennedy MC. (2000) Mitochondrial aconitase is a source of hydroxyl radical. An electron spin resonance investigation. *J Biol Chem.* **275**, 14064-14069.
- Vergès B. (2005) New insight into the pathophysiology of lipid abnormalities in type 2 diabetes. *Diabetes Metab.* **31**, 429-439.
- Vu V, Riddell MC, Sweeney G. (2007) Circulating adiponectin and adiponectin receptor expression in skeletal muscle: effects of exercise. *Diabetes Metab Res Rev.* **23**, 600-611.
- Walker R. (2004) Diabetic retinopathy: protecting the vision of people with diabetes. *Br J Community Nurs.* **9**, 545-547.
- Wang T, Zhang X, Li JJ. (2002) The role of NF-kappaB in the regulation of cell stress responses. *Int Immunopharmacol.* **2**, 1509-1520.
- Warnick GR, Knopp RH, Fitzpatrick V, Branson L. (1990) Estimating low-density lipoprotein cholesterol by the Friedewald equation is adequate for classifying patients on the basis of nationally recommended cutpoints. *Clin Chem.* **36**, 15-19.
- Weisberg SP, McCann D, Desai M, Rosenbaum M, Leibel RL, Ferrante AW Jr. (2003) Obesity is associated with macrophage accumulation in adipose tissue. *J Clin Invest.* **112**, 1796-1808.
- West IC. (2000) Radicals and oxidative stress in diabetes. *Diabet Med.* **17**, 171-180.
- Wild S, Roglic G, Green A, Sicree R, King H. (2004) Global prevalence of diabetes: estimates for the year 2000 and projections for 2030. *Diabetes Care.* **27**, 1047-1053.

Wilson PW, Bozeman SR, Burton TM, Hoaglin DC, Ben-Joseph R, Pashos CL. (2008) Prediction of first events of coronary heart disease and stroke with consideration of adiposity. *Circulation*. **118**, 124-130.

Wolff SP, Jiang ZY, Hunt JV. (1991) Protein glycation and oxidative stress in diabetes mellitus and ageing. *Free Radical Biol Med*. **10**, 339-352.

Definition, Diagnosis and Classification of Diabetes Mellitus and its Complications. Report of a WHO Consultation. Part 1: Diagnosis and Classification of Diabetes Mellitus. (1999) World Health Organization, Geneva, Switzerland.

The World Health Report 2003. World Health Organization (2003), Geneva, Switzerland.

Wright D, Sutherland L. (2008) Antioxidant supplementation in the treatment of skeletal muscle insulin resistance: potential mechanisms and clinical relevance. *Appl Physiol Nutr Metab*. **33**, 21-31.

Wu SJ, Li DY. (1992) A survey on polysaccharides from plants for anti-hyperglycemia. *Chinese Traditional and Herbal Drugs*. **23**, 549-554.

Wu L, Nicholson W, Knobel SM, Steffner RJ, May JM, Piston DW, Powers AC. (2004) Oxidative stress is a mediator of glucose toxicity in insulin-secreting pancreatic islet cell lines. *J Biol Chem*. **279**, 12126-12134.

Xu H, Barnes GT, Yang Q, Tan G, Yang D, Chou CJ, Sole J, Nichols A, Ross JS, Tartaglia LA, Chen H. (2003) Chronic inflammation in fat plays a crucial role in the development of obesity-related insulin resistance. *J Clin Invest*. **112**, 1821-1830.

Xu LM, Lu RH 2000. Present advance in diabetic nephropathy in traditional Chinese medical system. *Chinese Journal of Information on Traditional Chinese Medicine* **7**, 10-12.

Yamagishi S, Nakamura K, Matsui T, Takenaka K, Jinnouchi Y, Imaizumi T. (2006) Cardiovascular disease in diabetes. *Mini Rev Med Chem*. **6**, 313-318.

Yee HS, Fong NT. (1996) A review of the safety and efficacy of acarbose in diabetes mellitus. *Pharmacotherapy*. **16**, 792-805.

Yin J, Chen MD (2000) Present advance in active constituents of Chinese medicinal herbs for anti-hyperglycemia. *Inform Chin Trad Med*. **6**, 12-13.

Yu J, Zhang Y, Sun S, Shen J, Qiu J, Yin X, Yin H, Jiang S. (2006) Inhibitory effects of astragaloside IV on diabetic peripheral neuropathy in rats. *Can J Physiol Pharm*. **84**, 579-587.

Zangen DH, Bonner-Weir S, Lee CH, Latimer JB, Miller CP, Habener JF, Weir GC. (1997) Reduced insulin, GLUT2, and IDX-1 in b-cells after partial pancreatectomy. *Diabetes*. **46**, 258-264.

Zick Y. (2005) Ser/Thr phosphorylation of IRS proteins: a molecular basis for insulin resistance. *Sci STKE*. **25**, 4.

Zimmerman BR. (1997) Sulphonylureas. *Endocrinol Metab Clin North Am*. **26**, 511-522.